4-11-2006

Investigation of Cretaceous Molluscan Shell Material for Isotopic Integrity: Examples and Implications from the Baculites compressus/ cuneatus Biozones (Campanian) of the Western Interior Seaway

Ashley da Silva
University of South Florida

Investigation of Cretaceous Molluscan Shell Material for Isotopic Integrity:

Examples and Implications from the *Baculites compressus/cuneatus* Biozones

(Campanian) of the Western Interior Seaway

by

Ashley da Silva

A thesis submitted in partial fulfillment
of the requirements for the degree of
Master of Science
Department of Geology
College of Arts and Sciences
University of South Florida

Major Professor: Peter J. Harries, Ph.D.
Gregory S. Herbert, Ph.D.
Eric A. Oches, Ph.D.

Date of Approval:
April 11, 2006

Keywords: Cretaceous, Campanian, epicontinental sea, paleoclimatology, paleooceanography, fossil preservation, mollusks, oxygen, carbon, minor elements

DEDICATION

I dedicate this Master's thesis to teachers of science. This is not because it is a study in science education, because it is not. This thesis is, however, part of the education of a science teacher. Experience with the scientific method and both the excitement and complications of scientific research should serve me well in communicating the nature of science to students. I hope that reading this document will help others who I do not formally teach to learn something about fossils, their preservation, and the paleooceanographic information they can contain.

I also dedicate this Master's thesis to teachers of science that I have been fortunate enough to learn from. Some of them have been in middle schools, high schools, and universities; others teach informally. These teachers have:

(1) Rewarded curiosity; the fundamental first step in scientific research

(2) Brought science home from research journals and newsmagazines into the classroom

(3) Defined science as a process undertaken by people, rather than a body of knowledge

Without support from exemplary teachers of science, I, and, I suspect, many students of science, would not be realizing their scientific curiosity with research.

ACKNOWLEDGMENTS

I would like to acknowledge the contributions of the University of South Florida Department of Geology, especially Dr. Peter Harries, for providing necessary facilities, fossil collection opportunities, and financial support. I would like to thank my committee members, Dr. Gregory S. Herbert and Dr. Eric A. Oches, for their valuable perspectives shared during this project. I would also like to acknowledge Dr. Terrence M. Quinn for use of his laboratory at the USF Marine Science campus in St. Petersburg, and to Ethan Goddard for running my samples on the ICP-OES and mass spectrometer there.

I would like to acknowledge the research of my colleagues, Dr. Neil Landman and Kathleen Sarg at the American Museum of Natural History, and Dr. Kirk Cochran at the State University of New York – Stonybrook. This investigation is a part of a National Science Foundation-funded grant, and I give thanks to the NSF for the financial support.

I would like to thank Neal Larson of the Black Hills Institute of Geological Research for the *Eutrephoceras* specimens used for sclerochronology. Likewise, I would like to thank William Cobban for samples of *Baculites* and *Didymoceras.*

I would like to acknowledge the Geological Society of America for allowing me to present this research at their 2005 annual meeting, and both the Southeastern Section of GSA and the USF Graduate Student Organization for providing travel reimbursement.

Lastly, I would like to thank my family for being supportive of my undertaking of a Master's degree and their patience with the time demands of my work.

TABLE OF CONTENTS

LIST OF TABLES	iv
LIST OF FIGURES	v
ABSTRACT	vii
1. INTRODUCTION	
1.1 An Introduction to the Western Interior Seaway	1
1.2 Biozones Selected for Study	2
1.3 Locations Selected for Study	5
1.4 Fossils Recovered	6
2. SHELL ALTERATION INVESTIGATION	
2.1 Previous Investigations of Molluscan Fossil Shell Alteration	13
2.2 Methods	19
2.3 Results	28
2.4 Discussion	67
3. SCLEROCHRONOLOGY INVESTIGATION	
3.1 Previous Investigations of Molluscan Sclerochronology	100
3.2 Methods	103
3.3 Results	108
3.4 Discussion	128
4. CONCLUSIONS	136
REFERENCES	140
APPENDICES	
Appendix A: Shell Alteration Mass Spectrometer Data	146
Appendix B: Shell Alteration ICP Data	156
Appendix C: Sclerochronology ICP Data	192
Appendix D: Sclerochronology Mass Spectrometer Data	208

LIST OF TABLES

TABLE 1—Upper Campanian Biozones for the Western Interior Seaway 4

TABLE 2—Fossil Genera Investigated in this Study 11

TABLE 3—Morphology of Ammonites Investigated in this Study 12

TABLE 4—Specimen Suites Used in Shell Alteration Investigations 22

TABLE 5—Detection Limits for ICP-OES System 25

TABLE 6—Summary Statistics for Mode of Preservation Suite 32

TABLE 7—Summary Statistics for "Shell Sampling Position" Suite 40

TABLE 8—Descriptive Names for Munsell Designations of Shell Color Classes 46

TABLE 9—Summary Statistics for 'Shell Color' Suite: Shell Opalescence 47

TABLE 10—Summary Statistics for 'Shell Color' Suite: Shell Color 48

TABLE 11—Colors for Unaltered Shell, by Genus 51

TABLE 12—Summary of Statistical Tests on Cemented and Uncemented Shell 60

TABLE 13—Statistical Tests for Kremmling Cements, Concretions, and Shell 64

TABLE 14—Statistical Tests for Game Ranch Concretions and Shell 65

TABLE 15—Statistical Tests for Trask Ranch Cements, Concretions, and Shell 66

TABLE 16—Statistics Comparing $\delta^{18}O$ of Pre-filter and Post-filter Datasets 95

TABLE 17—Statistics Comparing $\delta^{13}C$ of Pre-filter and Post-filter Datasets 97

TABLE 18—Paleoenvironmental Parameters Derived from Filtered Data 98

LIST OF FIGURES

FIGURE 1—Extent of the Western Interior Seaway During the *Baculites compressus/Baculites cuneatus* Biozones 9

FIGURE 2—Mode of Preservation Stable Isotope Cross-Plot 31

FIGURE 3—Sr/Ca and Mg/Ca Ratios for "Mode of Preservation" Suite 33

FIGURE 4—Radar Charts for Minor Element Concentrations in the "Mode of Preservation Suite" 34

FIGURE 5—Shell Sampling Position Stable Isotope Cross-Plot 39

FIGURE 6—Shell Sampling Position Sr/Ca-Mg/Ca Cross-Plot 41

FIGURE 7—Radar Charts for Minor Elements in "Shell Sampling Position" Specimens 42

FIGURE 8—Shell Color Stable Isotope Cross-Plot 49

FIGURE 9—Shell Color Sr/Ca-Mg/Ca Cross-Plot 50

FIGURE 10— Radar Charts for Minor Elements in Cemented and Uncemented Shell 57

FIGURE 11—Minor Element Content of "Cementation Suite Samples" 58/59

FIGURE 12—Comparison of Cements, Concretions, and Shell Material for Kremmling 61

FIGURE 13—Comparison of External Recrystallizations or Cements, Concretions, and Shell Material for Game Ranch 62

FIGURE 14—Comparison of Cements, Concretions, and Shell Material for Trask Ranch 63

FIGURE 15—Empirical Derivation of the Sr/Ca-Mg/Ca Filter 85-90

FIGURE 16—Stable Isotope Cross Plot for All Shell Samples 92/93

FIGURE 17—Isotope Cross-Plot For All Shell Samples, Filtered by Mg/Ca and Sr/Ca 106-107

FIGURE 18—Oxygen Isotope Range Chart 94

FIGURE 19— Carbon Isotope Range Chart 96

FIGURE 20—Stable Isotope Ranges for Genera in this Study and Prior Research 99

FIGURE 21—Specimens Used in Sclerochronology 97/98

FIGURE 22—Minor Element Ratios for Sclerochronology: Bivalves 111

FIGURE 23—Sclerochronology of *Inoceramus* Specimen I2 112

FIGURE 24—$\delta^{18}O$ Versus $\delta^{13}C$ for *Inoceramus* Specimen I2 113

FIGURE 25—Calculated Paleotemperature and Paleosalinity through "Ontogeny" in *Inoceramus* Specimen I2 114

FIGURE 26— Minor Element Ratios for Sclerochronology: *Baculites* 117

FIGURE 27—Sclerochronology of *Baculites* Specimen B7 118

FIGURE 28—Stable Isotope Sclerochronology of *Baculites* Specimen B7 119

FIGURE 29—$\delta^{18}O$ Versus $\delta^{13}C$ in *Baculites* Specimen B7 120

FIGURE 30—Calculated Paleotemperature and Paleosalinity in *Baculites* Specimen B7 121

FIGURE 31—Sclerochronology of *Eutrephoceras* Specimen E2 124

FIGURE 32—Stable Isotope Sclerochronology of *Eutrephoceras* Specimen E2 125

FIGURE 33—$\delta^{18}O$ Versus $\delta^{13}C$ in *Eutrephoceras* Specimen E2 126

FIGURE 34— Calculated Paleotemperature and Paleosalinity in *Eutrephoceras* Specimen E2 127

INVESTIGATION OF CRETACEOUS MOLLUSCAN SHELL MATERIAL FOR ISOTOPIC INTEGRITY: EXAMPLES AND IMPLICATIONS FROM THE *BACULITES COMPRESSUS/CUNEATUS* BIOZONES (CAMPANIAN) OF THE WESTERN INTERIOR SEAWAY

Ashley da Silva

ABSTRACT

Whether a global greenhouse interval is a distinct or distant future, it is important to understand the dynamics of a greenhouse system. During such intervals the oceans, in the absence of sizeable polar ice caps, flood the continental shelf. The stratification and circulation of these epicontinental seas are open to debate, because there are no Recent analogs. The carbon and oxygen stable isotope record of fossil molluscan shell from epicontinental seas has the potential to reveal their stratification and seasonal cycles.

As a study sample, mollusks from the *Baculites compressus* and *Baculites cuneatus* biozones of the Western Interior Seaway of North America were collected from three locations: Kremmling, Colorado; Trask Ranch, South Dakota; Game Ranch, South Dakota. These fossils date to the Campanian (Late Cretaceous). Taxa include ammonites, bivalves, gastropods, and nautiloids.

The first part of this investigation, described in Chapter 2, investigates the degree of alteration in these specimens. Elevated concentrations of minor elements such as magnesium and strontium reveal alteration from the original aragonite and/or calcite skeletons. Concentrations of these elements obtained by ICP-OES analysis are compared within several suites of specimens: mode of preservation, shell testing location, shell

color, cementation, appearance under light microscope, and appearance under scanning electron microscope. Each of these suites tests a hypothesis about optimal shell preservation. Shell was found to be preserved best in shale rather than concretions, ammonite phragmacone rather than septa, opalescent specimens rather that non-opalescent ones, and uncemented shells rather than cemented shells, especially those with second-order versus first-order cement. Salinity and temperature values were derived for the organisms in the Western Interior Seaway: while bivalves produced unusually low temperatures, the others were reasonable for an inland sea.

The second part of this study, described in Chapter 3, examines the isotopic record within exemplary mollusk shells, taken perpendicular to growth lines. The data for this investigation in sclerochronology documents the dominant isotopically enigmatic bottom-water habitat of the *Inoceramus*, the geochemical signature of the overlying water mass inhabited by *Baculites*, and short-term migrations between the two water masses in the nautiloid *Eutrephoceras*.

CHAPTER 1. INTRODUCTION

1.1 An Introduction to the Western Interior Seaway

The Western Interior Seaway, an epicontinental sea during the Cretaceous Period, has no modern analog. The seaway connected with open oceanic conditions in the north and south, unlike the restricted circulation of today's Hudson Bay, Persian Gulf, or North Sea. Reconstructing how these bodies of water affected global temperatures, water circulation, and biological migration and evolution patterns requires knowledge of the nature of water masses within these seaways. Several models for the structure of the Western Interior Seaway have been proposed. Of particular concern is the fate of the fresh water entering the basin from the east, as well as from the Sevier Orogenic Belt to the west. Wright (1987) argues, based on stable-isotope data from mollusk shells and whole-rock samples, that the intermediate waters in which most ammonites lived were cooler and less saline than the deep waters the bivalves inhabited. The models call for above-normal salinity in the bottom water due to coastal evaporation and subsequent sinking or below-normal salinity for the intermediate water due to high freshwater runoff rates, respectively. Tsujita and Westermann (1998) added a third layer – a "brachyhaline water cap" extending from the shoreline and tapering off towards the center of the seaway -- to explain their very light $\delta^{18}O$ values for *Placenticeras* ammonites. In contrast, Slingerland (1996) argues for greater estuarine circulation and mixing in the Western Interior Seaway, such that the salinity stratification only exists near the coasts where freshwater was input. It is certainly possible that at different times, the general

paleoceanographic circulation pattern of the Western Interior Seaway differed. For this study, two biozones in the Upper Campanian were selected. The sites in this investigation represent nearly synchronous deposits, so that any variation in circulation patterns with time is minimized, and included both nearshore and deeper-water environments.

Biozones Selected for Study

1.2.1 Selection of Biozones: The two biozones of the Upper Campanian that were selected were the *Baculites compressus* and *B. cuneatus* biozones. These zones are named for two common orthoconic heteromorph ammonites. The two biozones are often grouped together because of the uncertainty in the numeric date for the boundary between the two zones (Scott and Cobban, 1986) and the apparent stratigraphic overlap between the two ammonite species. Selection of the biozones was part of a larger study, funded by the National Science Foundation and in collaboration with the American Museum of Natural History, New York, to analyze molluscan oxygen, carbon, and strontium isotopes across the former Western Interior Seaway. The stratigraphic formation investigated is called the Pierre Shale in all sampling locations, although the lithologic characteristics of the unit differ between the Colorado and South Dakota locations. A summary of the basic lithologic characteristics of the Upper Campanian outcrops, including the *Baculites compressus* and *B. cuneatus* biozones, is presented in Table 1.

1.2.2 Fauna of the Biozones: The ammonites collected from these biozones consist of species within *Baculites, Solenoceras, Axonoceras, Anaklinoceras, Cirroceras, Didymoceras, Pachydiscus, Placenticeras, Hoploscaphites,* and *Jeletzkytes*. Except for the occassional *Pachydiscus* specimen, *Placenticeras* is the only planispiral ammonite represented; the remainder are all heteromorphic forms. The nautiloid *Eutrephoceras* occurs in the biozones. Bivalves include abundant *Inoceramus*, less frequent *Anomia*, and many other genera present in low abundances. Gastropods are uncommon and small in size.

1.2.3 Prior Research in the Baculites compressus *and* Baculites cuneatus *Biozones:* Because of the abundance of fossils in the *Baculites compressus*/*cuneatus* biozones, they have been used in previous paleooceanographic studies. One of the first studies on stable isotopes using fossil mollusks, by Tourtelot and Rye (1969), used the $\delta^{18}O$ ratio of *Baculites* specimens and belemnites to conclude that the Western Interior Seaway ranged from 21-33 ^{o}C, significantly warmer then the Atlantic coast, which was 17-23 ^{o}C at the time. The authors also found lighter oxygen isotopes and heaver carbon isotopes for their bivalve samples (inoceramids and oysters) than for their baculitid samples. This research is supported by Forester et al. (1977), who found an average $\delta^{18}O$ paleotemperature of 25 ^{o}C for the *Baculites compressus* biozone and 20 ^{o}C for the *Baculites cuneatus* biozone in southern Saskatchewan. He et al. (2005) disputed the difference in temperature between the two biozones using a more robust collection of baculitid specimens, from both the United States and Canada. They did, however, note a general trend toward heavier isotopic values coinciding with marine regression, which peaked during the biozones of interest. Their isotopic values for *Baculites* and

Inoceramus specimens are similar to those of Tourtelot and Rye (1969), but they add data points for the heteromorph ammonites *Didymoceras* and *Scaphites*, which fall between the *Inoceramus* and *Baculites* fields. Schmidt (1997) observed an overlap between epifaunal (primarily, bivalve) and nektonic (primarily, ammonite) stable isotope fields for the Western Interior Seaway. Tsujita and Westermann (1998) attempted to resolve paleotemperatures recorded by ammonites in the uppermost Campanian to the species level, but their intrageneric conclusions are hampered by a small dataset. They noted unrealisticly high paleotemperatures for *Inoceramus*, and also very light $\delta^{18}O$ (mean = -5.2‰ versus the Pee Dee Belemnite standard) in *Placenticeras*, which they attribute to low salinity in the uppermost part of the water column but which probably reflect diagenetically altered material (Landman, pers. comm., 2005)

Stable isotope sclerochronology has been performed on ammonites, bivalves, and the nautiloid *Eutrephoceras*. Because of their common occurrence, long generic stratigraphic ranges, and tendency to be preserved more completely than *Hoploscaphites* or *Placenticeras*, members of the genera *Baculites* and *Inoceramus* have been studied extensively. Tourtelot and Rye (1969) found a sinusoidal $\delta^{18}O$ curve in a *Baculites* section, with one minimum and two maxima. The $\delta^{18}O$ range of this baculitid was from -0.8‰ to -1.2‰, equivalent to a 1.5 ^{o}C temperature difference. The $\delta^{13}C$ curve for this specimen shows a direct relationship with age of the organism, and has superimposed maxima and minima paralleling the oxygen curve. Fatherree et al. (1998) show a slightly larger range (0.2‰ to -1.2‰) in a larger *Baculites* section. These authors note an inverse relationship between $\delta^{18}O$ and $\delta^{13}C$, consistent with temperature being the most significant variable reflected in the isotopic signatures. Along the first six and the last

eight centimeters of the shell, however, the $\delta^{13}C$ curve parallels the $\delta^{18}O$ curve. Likewise, Landman et al. (1983) document a positive correlation between $\delta^{13}C$ and $\delta^{18}O$ between the first nine septa in a Western Interior Seaway *Eutrephoceras*, after which the correlation becomes negative. Fatherree (1995) documents an inverse relationship between $\delta^{13}C$ and $\delta^{18}O$ in the bivalve *Artica ovata* and a direct relationship between them in another bivalve, *Inoceramus sagensis*. Tourtelot and Rye show an approximately parallel set of $\delta^{13}C$ and $\delta^{18}O$ maxima for their *Inoceramus* example. These investigations both calculate *Inoceramus* paleotemperatures above 30°C, a temperature that is at the upper limit for shell precipitation in Recent bivalves. Because inoceramids have no close living relatives, explanations from high-salinity environmental preferences to symbiotic bacteria have been generated to explain the unrealistic $\delta^{18}O$ paleotemperatures.

1.2 Locations Selected for Study

1.3.1 Kremmling, Colorado, Sampling Site: The Kremmling, Colorado, sampling site was located on the United States Bureau of Land Management Ammonite Preserve, north of the town of Kremmling, Colorado. Geographic coordinates were 40°14'N, 106°23 to 106°24'W. The outcrops, exposed on hilltops, were comprised of beige siltstone (Munsell color designations 2.5YR7/5 to 2.5YR7/6) with three stratigraphic horizons of concretions. The concretions, up to one meter in diameter, weathered to the same color as the siltstone, but were a light grey (5YR3/2) upon a fresh surface.

1.3.2 Game Ranch, South Dakota, Sampling Site: The Game Ranch, South Dakota site was located on a tall cutbank, within a private ranch on the southeastern rim of the Black Hills near the town of Farmingdale. Geographic coordinates were 43°55'N, 102°50'W. The lithology was a black, fissile shale (Munsell designation 5YR3/2 when dry) containing concretions and fossils preserved directly in the shale. Concretions were small, usually containing a single fossil, and had a reddish 10YR2/4 interior and an orange 10YR6/10 weathering rind. Concretionary horizons were obscured by shale erosion.

1.3.3 Trask Ranch, South Dakota, Sampling Site: The Trask Ranch, South Dakota, site was located on a private ranch, also on the southeastern side of the Black Hills. Geographic coordinates for this site were 44°14'N, 102°28'W. Large (25 cm to 1 m) concretions were dispersed in a riverbed; from these, numerous fossils were recovered. Some concretions contained mostly intact fossils, while others contained a "shell hash" of small broken fragments. Concretions at this site were 5YR3/2 to 5YR5/2 in color. Some showed veins of calcite crystals typical of septarian concretion, but ferrous weathering rinds were not well-developed as in the Game Ranch specimens.

1.4. Fossils Recovered

1.4.1 Fossils from Kremmling, Colorado: At the Kremmling, Colorado, site, large, numerous *Placenticeras* -- including mature macroconchs, mature microconchs, and juveniles -- were found (though most were internal and external molds with limited shell preservation). Classification for *Placenticeras* and other genera examined in this study is summarized in Table 2. One of the *Placenticeras* specimens had limpets of the

genus *Anisomyon* adhering to its shell, but these had little to no shell material preserved. Specimens of *Hoploscaphites* and *Baculites* were also relatively common. *Baculites* specimens appeared to be *Baculites compressus*, but many specimens were crushed, making evaluation of the amount of inflation, a key identification parameter, difficult. One *Axonoceras compressum* and two *Anaklinoceras gordiale* specimens were found, suggesting that the location is part of the *Baculites compressus* biozone. The morphology of these ammonites and others used in this investigation are described in Table 3. Unfortunately, the quantity of shell preserved on these tiny heteromorph ammonites did not allow for chemical analysis. Partial specimens of the nautiloid *Eutrephoceras* also had insufficicient shell material. Bivalves recovered included numerous *Inoceramus*, some preserved with calcitic and aragonitic layers together, but most with layers separated. *Anomia* was also represented, as were small (< 1 cm) bivalves and gastropods not identified in this study.

1.4.2 Fossils from Game Ranch, South Dakota: At the Game Ranch, South Dakota, site, *Hoploscaphites* was nearly absent. *Placenticeras*, *Baculites*, and *Inoceramus* were all present in both shale and concretions. Fossils did not appear to be compressed or otherwise deformed. Five *Nymphalucina* bivalves were discovered in the shale. In addition, two specimens each of *Anomia* and a scaphopod were collected. Only the bivalves were complete.

1.4.3 Fossils from Trask Ranch, South Dakota: At the Trask Ranch, South Dakota, *Placenticeras* was absent and *Hoploscaphites* fairly common. *Baculites* was the most common ammonite at the site. The most common bivalve was *Inoceramus,* and some concretions contained only specimens of this genus. Rarer genera, for which two to five specimens were collected, include the bivalve *Nymphalucina*, and the gastropods *Drepanocheilus* and *Anisomyon*. A single scaphopod was also found. Some fossils were partial or shattered, especially those in the "fossil hash" concretions, but many others appeared to be complete and undeformed. Two specimens of the nautiloid *Eutrephoceras* were collected from the site by Neal Larson, Black Hills Institute of Geological Research, and sent for the sclerochronology portion of this project.

1.4.4 Sampling Bias: The specimens collected at the three sampling locations are in no means an accurate, proportional sample of the Western Interior Seaway fauna from 73 Ma. Fossilization biases likely exist. Thin-shelled *Anomia*, for instance, may have been more common in the seaway than it is in the Kremmling deposits. Small specimens, such as the gastropods and bivalves, could easily have been overlooked during collection. Fossils with a large amount of preserved shell were preferentially collected. Lastly, generic variety was one of the goals in collection, so some specimens of common genera such as *Baculites* and *Inoceramus* were passed by in favor of less-common genera such as *Hoploscaphites*.

FIGURE 1—Extent of the Western Interior Seaway in the United States During the *Baculites compressus / Baculites cuneatus* Biozones.

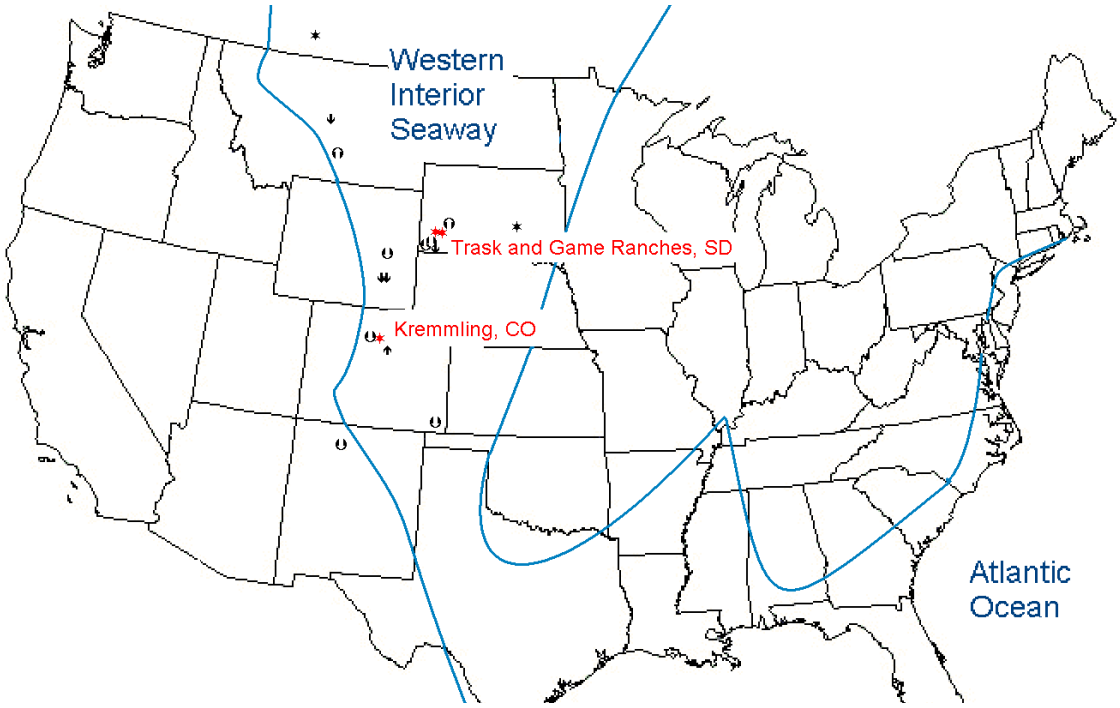

Key:

Lowermost Maastrichtian
Uppermost Upper Campanian
✶ Middle Upper Campanian (*B. compressus/B. cuneatus* biozones)
Lower Upper Campanian
Middle Cenomanian

The sample sites for this study are located in the western and central parts of the former Western Interior Seaway. Contemporaneous outcrops also occur in southern Saskatechewan, near the western shoreline of the seaway, and in east-central South Dakota, near the eastern shoreline. Shoreline taken from Larson et al., 1997; data for locations from the American Museum of Natural History (2005).

TABLE 1—Upper Campanian Biozones for the Western Interior Seaway

Ammonite biozone	Radiometric Ages from Bentonites (Larson et al., 1997)	Dominant Lithology, Kremmling, Colorado (Scott and Cobban, 1986)	Dominant Lithology, Trask Ranch and Game Ranch, South Dakota, (Larson et al., 1997)
Baculites jenseni	Upper boundary = 71.3 ± 0.5 Ma	Lower portion siltstone; upper portion sandstone with bentonitic shale beds; both bear ironstone concretions	Unconformity
Baculites reesidei		Shale with sparse ironstone concretions	Dark grey, fissile shale with septarian concretions
Baculites cuneatus		Shale with septarian concretions	Dark grey, fissile shale with septarian concretions
Baculites compressus	73.35 ±0.39 Ma	Siltstone and large dated bentonite bed in lower portion; shale in upper portion; both with septarian concretions	Dark grey, fissile shale with septarian concretions
Didymoceras cheyennense		Siltstone in lower portion, sandstone in upper portion; both with septarian concretions	Bentonitic shales
Exiteloceras jenneyi	74.6 ±0.72 Ma	Alternating sandstones and shales with septarian concretions	Dated bentonite, bentonitic shales
Didymoceras stevensoni		Alternating sandstones and shales with septarian concretions	Dark grey, fissile shale with septarian concretions
Didymoceras nebrascense		Alternating sandstones and bentonitic shales with septarian and ironstone concretions	Dark grey, fissile shale with septarian concretions

The lithology of the *Baculites compressus/Baculites cuneatus* biozones is dominated by dark grey, fissile shale in South Dakota. The Kremmling, Colorado, site also includes siltstones. Both locations contain septarian concretions. The *Baculites compressus* biozone has been dated to approximately 73.4 Ma.

TABLE 2–Fossil Genera Investigated in this Study

Phylum Mollusca
Class Bivalvia (Linnaeus, 1758) Subclass Heterodonta (Neumayr, 1884) Order Myoida (Goldfuss, 1820) Family Teredinidae (Rafinesque, 1815) *Teredo (Linnaeus, 1758)* Order Veneroida (H and A Adams, 1856) Family Lucinidae (Fleming, 1828) *Nymphalucina* (Speden, 1970) Subclass Pteriomorphia (Beurlen, 1944) Order Ostreoida (Férussac, 1822) Family Anomiidae (Rafenisque, 1815) *Anomia (*Linneaus, 1758*)* Order Pterioida (Newell, 1965) Family Inoceramidae[2] (Giebel, 1852) *Inoceramus* (J. Sowerby, 1814)
Class Cephalopoda[3] (Cuvier, 1797) Subclass Ammonoidea (Author unknown) Order Ammonitida (Hyatt, 1889) Family Baculitidae (Gill, 1871) *Baculites* (Lamarck, 1799) Family Nostoceratidae (Hyatt, 1894) *Cirroceras* (Conrad, 1868) *Didymoceras* (Hyatt, 1894) Family Placenticeratidae (Hyatt, 1900) *Placenticeras* (Meek, 1870) Family Scaphitidae (Meek, 1876) *Hoploscaphites* (Nowak, 1911) *Jeletzkytes* (Riccardi, 1983) Subclass Nautiloidea (Agassiz, 1847) Order Nautilida (Agassiz, 1847) Family Nautilidae (Blainville, 1825) *Eutrephoceras* (Hyatt, 1894)
Class Gastropoda[4] (Cuvier, 1797) Subclass Prosobranchia (Edwards,1848) Order Basommatophora (Schmidt, 1855) Family Siphonariidae (Gray, 1840) *Anisomyon* (Meek and Hayden, 1860) Order Mesogastropoda (Thiele, 1925) Family Aporrhaidae (Morch, 1852) *Drepanocheilus* (Meek, 1876)
[1] - Classification follows Speden (1970) [2] - Classification follows Walaszczyk and Cobban, 2000 [3] - Classification follows Besnosov and Michailova, 1991; Larson *et al.,* 1997 [4] - Classification follows Abdel-Gawad, 1986

TABLE 3—Morphology of Ammonites Investigated in this Study

	Protoconch & Neanoconch	**Juvenile**	**Adult**
Baculites	Planispiral	Orthoconic	Orthoconic
Hoploscaphites	Planispiral	Planispiral (moderately inflated)	J-shaped or U-shaped chamber
Anaklinoceras	Planispiral	Turritellid spire	Inverted U-shaped chamber (*A. gordiale*) or planispiral (*A. reflexum*)
Axonoceras	Planispiral	Planispiral (inflated), separated whorls	Planispiral (inflated), separated whorls
Placenticeras	Planispiral	Planispiral (compressed)	Planispiral (compressed)

Many of the types of ammonites found in the sampling sites for the *Baculites compressus* and *Baculites cuneatus* biozones exhibit vast changes in growth program across different growth stages. In others, the transition between growth stages is marked by changes in shell ornamentation alone.

CHAPTER 2. SHELL ALTERATION INVESTIGATION

2.1 Previous Investigations of Molluscan Fossil Shell Alteration

2.1.1. Rationale for Utilizing Minor Element Concentrations to Evaluate Shell Alteration:

Oxygen and carbon stable isotopes ratios recovered from mollusk shells are commonly used to reconstruct paleotemperature. Molluscan shells are used because they tend to be relatively common, are less susceptible to diagenetic alteration than bone apatite or bulk samples of rock because of their lower porosity (Constantz, 1986), generally secrete their shells in isotopic equilibrium with seawater (e.g., Bettencourt and Guerra, 1999; Ivany et al., 2003) and may be compared to Recent relatives or analogs to make paleoenvironmental inferences. In addition, the accretionary nature of molluscan growth makes sclerochronology, the focus of Chapter 3, possible. In mollusks, the $\delta^{18}O$ ratio is interpreted as a reflection of paleotemperature, once adjustments have been made to account for the $\delta^{18}O$ ratio of the ambient waters, which is a function of temperature, salinity, and, during icehouse intervals, the volume of water entrained in ice caps (Wright, 1987). Temperature decreases with heavier $\delta^{18}O$ ratios in aragonitic shell according to the equation:

$$T = 21.8 - 4.69(\delta^{18}O \text{ arag} - \delta^{18}O \text{ w}) \quad (1)$$

This equation uses isotopic ratios in terms of the Pee Dee Belemnite (PDB) standard (Grossman and Ku, 1986). The $\delta^{13}C$ ratio depends on temperature, salinity, and the isotopic composition of dissolved inorganic carbon in the system (Grossman and Ku, 1986). Dissolved inorganic carbon is isotopically heaviest near the surface, due to

preferential uptake of $\delta^{12}C$ by phytoplankton, and lightest in seafloor sediment pore waters. As temperature increases, the difference between the isotopic signatures of the molluscan shell and dissolved inorganic carbon (the carbon isotope enrichment) decreases in a linear fashion. Because the $\delta^{13}C$ ratio of dissolved inorganic carbon is isotopically heavier than the $\delta^{13}C$ ratios of molluscan shell, this means that at higher temperatures, heavier $\delta^{13}C$ ratios result (Grossman and Ku, 1986).

Carbon isotope ratios in molluscan shell may be modified from seawater $\delta^{13}C$ by exchange with metabolic CO_2, which tends to have an isotopic signature of -40‰ to -30‰, as evidenced by the trend toward lighter $\delta^{13}C$ ratios in the muscle scar regions of the *Nautilus* shell (Auclair et al., 2004). There has also been also a metabolic effect documented for mollusks with respect to $\delta^{18}O$, with greater variation in $\delta^{18}O$ for the surf clam *Spisula* (Ivany et al., 2003) during early ontogeny, and for the abalone *Haliotis* when rapidly repairing injured shell (Epstein et al., 1963). This effect may also be present in *Baculites* (Fatherree et al., 1998) and *Eutrephoceras* (Landman et al., 1983). A positive correlation between $\delta^{18}O$ and $\delta^{13}C$ suggests metabolic discrimination against heavier isotopes, while a negative correlation could indicate increased productivity due to higher temperatures (Mitchell et al., 1994). In some mollusks, such as *Strombus* and *Baculites*, with the onset of maturity, $\delta^{13}C$ and $\delta^{18}O$ trend simultaneously toward heavier values (Fatherree et al., 1998; Herbert, pers. comm., 2006). During spawning, shell precipitation slows (Elliot et al., 2003), so isotopic records are biased towards the temperatures of water when the organism is not spawning. Thus, a mollusk that spawns in summer may show mostly moderate and cold temperatures in its sclerochronologic record. A mollusk that spawns in summer but ceases precipitation of shell when

temperatures are below a certain threshold, which is reached in winter months, will show moderate temperatures.

When estimating paleoceanographic conditions from stable isotopes in fossil shell, it is imperative that the observed variation in the stable isotopes is due to paleoenvironment and/or metabolism, rather than post-depositional alteration. Defining "unaltered" shell presents a challenge to paleontologists and geochemists. Alteration may include dissolution and recrystallization. One sign of dissolution is the presence of holes in the individual crystals of the shell; another is the rounding of their edges (Buchardt and Weiner, 1981; Schmidt, 1997). Recrystallization produces a "blocky" crystal texture (Schmidt, 1997) or fusion of individual aragonitic platelets (Buchardt and Weiner, 1981). Mineralogical impurities may also grow upon or adsorb to the shell. Common mineralogical impurities include the calcite spar and gypsum crystals appearing on ammonite shell witnessed by Buchardt and Weiner (1981), the pyrite noted by Landman et al. (1983) in *Eutrephoceras* shell, and the chert and rhombohedral calcite crystals observed by Elorza and García-Garmilla (1996) in the void spaces of *Inoceramus* shell.

Minor element analysis measures the concentration of chemical elements within the shell. Some elements, such as Fe, Mg, Mn, and Sr, substitute into the crystal lattice of aragonite or calcite. Others, such as K and Na, either reside in interstitial spaces in the crystal lattice or adsorb to its exterior (Dodd, 1967). Analyses are usually performed on an electron microprobe or an ICP system. The electron microprobe detects X-ray radiation produced when electrons bombard a thin section, while the ICP-OES system detects the wavelength of radiation produced by interaction of a plasma beam with

cations in solution. Minor element analysis was selected for this study because:

1. Minor element analysis has the potential to reveal the source of alteration, such as exchange with meteoric water or precipitation of secondary cements;
2. The concentrations of minor elements, particularly Mg, K, Na, and Fe, may be altered in shells that show no evidence of recrystallization (Ragland et al., 1979);
3. A large body of molluscan minor element data exists for comparison (e.g., Brand, 1986; Pagani and Arthur, 1998;Dutton et al., 2002); and
4. The minor elements of Sr, Mg, and Na have experimentally determined relationships with temperature and salinity that may be applicable to this study.

Because the only elements of interest are cations that substitute into the aragonite crystal structure or form the cations of secondary minerals, the ICP-OES method was selected. Seven elements were then selected for, based upon prior research: aluminum, potassium, iron, manganese, magnesium, sodium, and strontium.

2.1.2. Studies Utilizing Minor Elements as a Proxy for Shell Alteration:

Concentrations of potassium and sodium are believed to reflect seawater compostion. White (1979) established that mollusks coprecipitate potassium and sodium in equilibrium with seawater (as cited in Brand, 1986). In the oyster *Crassostrea*, there is a statistically significant linear correlation between salinity and sodium concentration in the precipitated shell (Rucker and Valentine, 1961). Sodium content in *Crassostrea* valves is ~3000 ppm for seawater of normal salinity, but is ~2500 ppm for seawater with a salinity of 15‰. The salinity-sodium relationship is supported by the presence of similar Na/Ca ratios among different genera of ammonites that presumably lived in the same vertical level of the water column (Whittaker et al., 1986). However, whether the

Na/Ca ratio in cephalopod mollusks reflects true salinity may be debatable. There is no correlation between Na/Ca and stable isotopes in the Whittaker et al. (1986) study, which are influenced, albeit indirectly, by salinity. Of course, the study location (in the center-north of the Western Interior Seaway) may not have experienced sufficient salinity fluctuations to produce fluctuations in Na/Ca. Of more concern is a minor-element analysis of Recent *Nautilus* which found a discrimination factor of 2:1 for sodium, indicating a preference for sodium accumulation in the shell versus the concentration in seawater (Brand, 1983). These findings, however, have not been corroborated by study of other *Nautilus* species (Mann, 1992). Brand (1986) also describes a non-linear relationship between salinity and sodium in Recent and fossil aragonitic mollusks:

$$S = -5.769\ln(A) + 28.380 \quad (2)$$

Salinity S is given in parts per thousand ± 0.5, and A is the ratio of ppm Sr / ppm Na, or the geometric mean of such ratios. The use of strontium is empirically derived, and appears to correct for the genus-level variation in Na discrimination. Strontium and, to a lesser extent, sodium may be depleted during diagenesis; other elements which are typically enriched during diagenesis can be used to identify specimens that could produce questionable paleosalinities. The elements manganese, magnesium, and iron are all present in meteoric water at 2-4 times the level of seawater, so can be used as proxy for diagenetic alteration by exchange with meteoric water (Veizer and Fritz, 1976). For unaltered specimens, the covariance of magnesium with sulfur in the bivalve *Mytilus edulis* suggests that the organic matrix contains a significant amount of magnesium (Rosenburg and Hughes, 1991). Higher magnesium concentrations are also correlated with faster shell precipitation in this bivalve, suggesting variation of the element with

metabolism. The average concentrations of magnesium in molluscan shell vary significantly by taxonomic class (Turekian and Armstrong, 1960) and by species in *Nautilus* (Mann, 1992).

The strontium concentration of aragonitic molluscan shell has been correlated with many different environmental and physiological factors. A decrease in strontium, for instance, has been correlated with all of the following:

1) A decrease in salinity along an exponential relationship that can be approximated as linear above salinities of 20‰. This trend is based on values from a variety of Recent aragonitic bivalves and gastropods, compiled by Dodd and Crisp (1982).
2) An increase in salinity for individual *Neomidion* bivalves living in a Jurassic estuary (Holmden and Hudson, 2003).
3) A slowing of growth rate and/or metabolic effects in the Eocene bivalve *Venericardia* and gastropod *Clavilithes* (Purton et al., 1999).
4) Species-specific differences, rather than environmental or phylogenetic gradients, as in Recent *Nautilus*
5) A decrease in the $\delta^{18}O$ ratio, implying an increase in temperature and the potential utility of strontium in paleothermometry for the Antarctic Eocene bivalve *Cucullaea* (Dutton et al., 2002).
6) A decrease in visually assessed shell quality (Buchardt and Weiner, 1981), and percent aragonite (Hallam and Price, 1966),indicating alteration.

All of these trends are superimposed on a ~1:5 discrimination factor for strontium

concentrations in seawater versus strontium concentrations in the aragonite of bivalves, gastropods, and *Nautilus* (Turekian and Armstrong, 1960; Brand, 1983).

Very little research done has been on aluminum concentrations in molluscan shell, perhaps because the concentrations are low, approaching the detection limits of the analytical techniques (Brand, 1983). Brand (1983) found that *Nautilus* shell contains 0-30 ppm of aluminum. Unaltered inoceramid shell, according to Elorza and García-Garmilla (1996), is ~0.2% Al_2O_3. Given the paucity of information about aluminum, this study will significantly add to the existing data on this element. By far the most extensive data has been collected on magnesium and strontium concentrations, and these elements display complex, various relationships for different mollusks. With additional research, such complexities may be revealed for other minor elements included in molluscan shell.

2.2 Methods

2.2.1 Selection of Samples: Samples for the fossil shell alteration investigation were taken in groups, here called "suites," that each addressed particular multiple working hypotheses. The hypotheses, taken primarily from previous research on shell preservational issues in Western Interior Seaway fossils, are as follows:

(1) Shell preserved directly in shale will be more pristine than shell preserved in concretions, which may be chemically altered during the dissolution and precipitation associated with concretion formation. An alternative hypothesis is that shell preserved within concretions will be less altered than shell preserved in shale, because the concretion is impermeable to groundwater.

(2) Ammonite phragmacone will be less altered than ammonite septa, because of

the tendancy for cements to form in the interior of the ammonite shell. An alternative hypothesis is that ammonite phragmacone will be more altered, because it is on the exterior of the shell and could thus be exposed to more groundwater and/or surface water.

(3) Shell that is white to beige in color, with iridescent nacre, will be the most pristine. As in Recent molluscan shells, slight variation in color from that noted above may indicate optimal preservation for different genera.

(4) Molluscan shell will have distinct minor element and isotopic signatures from the surrounding matrix (shale, siltstone, or concretion), and from crystalline cements precipitated within the shell. Progressively more diagenetically altered shell material will have minor element and isotopic signatures intermediate between unaltered shell and the cement itself.

(5) Isotopic signatures will cluster by genus, and allow for a classification of mollusks as inhabiting deep-water, intermediate-water, or surface-water masses. Certain heteromorph ammonites may display two modes of life, changing habitat during ontogenetic changes in morphology.

(6) Isotopic signatures will display a shift between Kremmling, Colorado, specimens and Trask and Game ranches, South Dakota, specimens, due to differences in temperature and/or salinity.

To test hypothesis 1, a "Mode of Preservation" suite was developed. This suite included specimens of the same genus (*Placenticeras*, *Inoceramus*, *Baculites*, and *Nymphalucina*) preserved in shale and calcareous concretions. Shale-concretion pairs of *Baculites* and *Inoceramus* were selected from a single locality: the Game Ranch.

Limitations in the collected material meant that this was impossible for all genera, and lithologic pairs had to be constructed using multiple localities. One sample was taken from each of twenty specimens (ten shale-concretion pairs). Care was taken to select specimens for each pair that were similar in color and shell thickness, and sample these at the same point in ontogeny.

To address hypothesis 2, a "Shell Sampling Location" suite was developed. This suite included specimens of three ammonite genera (*Placenticeras, Baculites, and Hoploscaphites*). One sample was taken from a septum of each specimen and another from the adjacent phragmacone, for a total of twenty samples.

To investigate hypothesis 3, twenty specimens from each locality were analyzed, for a total of sixty specimens in the "Shell Color Suite". Genera represented included three ammonites (*Placenticeras*, *Baculites*, and *Hoploscaphites*), three bivalves (*Anomia*, *Nymphalucina*, and *Inoceramus*), and two gastropods (*Anisomyon* and *Drepanocheilus*). Two to five specimens of different shell colors were selected for each genus at each location, depending on available specimens. A single sample was taken from each specimen, at an equivalent point in ontogeny for specimens of each genus.

To test hypothesis 4, a 35-specimen "Cementation Suite" was assembled. Of this suite, specimens 1-10 were from Kremmling, specimens 11-15 were from Game Ranch, and the remainder were from Trask Ranch. Four types of samples were taken: ammonite phragmacone shell (from *Placenticeras*, *Baculites*, and *Hoploscaphites*), matrix (concretion or siltstone), cements precipitated in the cavities of the shell, and calcitic material found on the exterior of the shell. Each specimen contained two or more of these materials, with one sample taken of each material, for a total of 111 samples.

For hypotheses 5 and 6, the combined data set was used. As seen in Table 4, this includes over 100 ammonite samples: 59 *Baculites* samples, 24 *Placenticeras* samples, and 22 *Hoploscaphites* samples. The combined data set also contains bivalve samples (18 from *Inoceramus*, 6 from *Nymphalucina*, and 4 from *Anomia*) and gastropod samples (2 from *Anisonmyon* and 3 from *Drepanocheilus*).

2.2.2 Treatment of Samples: Three techniques were used to prepare samples for the shell-alteration investigation. Whenever possible, shell was removed intact, using laboratory tweezers and similar implements. Target sample size was the equivalent of a square 2-3 mm on each side. For particularly "promising" specimens – ammonites with clean, irridescent shell displaying growth lines and a total shell thickness of 0.5 mm or greater – a second, adjacent sample was taken and sent to the American Museum of Natural History for scanning electron microscopy and to SUNY Stony Brook for tstrontium isotopic analysis. When shell could not be removed intact, it was scaped from the specimen using a curved pick, with care taken to sample the entire thickness of shell. Different layers within a shell, due to differing crystal structures, different temperatures at the time of precipitation, and/or metabolic effects at time of deposition, may show different isotopic signatures. For example, the bivalve *Pecten* shows strongly depleted $\delta^{18}O$ and $\delta^{13}C$ in surficial samples relative to samples which included the entire thickness of the shell (Mitchell et al., 1994). In ammonites, differences in isotopic composition with respect to sampling location have been shown for *Baculites compressus* (Forester et al., 1977; Fatherree et al., 1998). Surficial recrystallization or cement samples were scraped from the shells they were preserved upon. Cement and concretion samples were taken using a Dremel® variable-speed drill fitted with a diamond-coated bit. All

specimens were ground into a uniform fine powder using a mortar and pestle, made of agate to minimize contamination.

2.2.3 Mass Spectrometer Analysis: Subsamples of 60-100 µg were measured on a microbalance into small glass vials. These specimens were dried in a laboratory oven at 70 ^{o}C for at least one week to remove moisture. The specimens were transferred to reaction vials for a target mass of 35-80 µg, which were then reacted with 100% phosphoric acid added to each reaction vial within the carbonate preparation device of the mass spectrometer. The mass spectrometer used in this study is a ThermoFinnigan Delta Plus XL dual inlet mass spectrometer with an in-line Kiel III Carbonate Preparation Device, and resides at the Center for at the College of Marine Sciences, University of South Florida, St. Petersburg, Florida. Six replicates of the NBS19 standard, taken as $\delta^{13}C = 1.95‰$ and $\delta^{13}C = -2.20‰$ with respect to PDB, were included in each mass spectrometer run to determine the analytic uncertainty. Analytical uncertainty, at the 95% confidence level, was ±0.03‰ for the $\delta^{13}C$ values and ±0.08‰ for the $\delta^{18}O$ values. Data from samples producing a signal of less than 600mv, which usually results from carbonate mass <20 µg, were discarded and, when possible, rereun. All values are reported with respect to the Pee Dee Belemnite.

2.2.4 ICP Analysis: Subsamples of 100-200 µg were placed directly into polyethylene tubes used for the analysis. Once all the samples were prepared, 2.0 mL of 2% HNO_3 was added and the samples were inverted to ensure the entire sample dissolved. The Perkin Elmer Optima 4300DV dual view ICP-OES, housed at the same facility as the mass spectrometer, was calibrated with a series of four serially diluted multi-element concentration standards, commercially available from SCP-Science. All

minor element samples were run as a single batch to minimize analytical uncertainty, which was better than 1% relative standard deviation for all values. Table 5 lists the detection limits for the elements focused upon in this study.

2.2.5 Data Processing: Minor element concentrations were received in parts per million (ppm) and converted to atomic ratios with respect to calcium. The ratios, given in mMol/Mol Ca, were obtained by dividing the weight percent of the minor element, divided by its atomic mass, by the weight percent of calcium, divided by its atomic mass. All statistical calculations were performed with the minor element ratios, but the concentrations of minor elements in ppm were needed for paleosalinity calculations using equation 2. This equation for paleosalinity, from Brand (1986), was selected because it was derived for both gastropod and bivalve mollusks, from a variety of habitats, fossil and Recent. A correction factor, derived from data on Recent Nautilus in the wild, was applied to the equation to compensate for the higher concentrations of sodium in cephalopods than bivalves or gastropods living in the same habitat (Dodd, 1967).

Stable isotope concentrations were received in per-mil notation, with respect to the Pee Dee Belemnite (PDB) standard. A value of $\delta^{18}O = -5‰$ means that the shell has a 5‰ lighter $\delta^{18}O$ ratio than the PDB standard; i.e., it has a greater proportion of $\delta^{13}C$ than the standard. Paleotemperature was calculatied using equation 1, Grossman and Ku's molluscan aragonite temperature correlation.after first applying to determine the $\delta^{18}O$ value of the waters surrounding the mollusk using Equation 3:

$$S_{(WIS)} = [1 - (\delta_{w(WIS)} - \delta_{w(ocean)}))/(\delta_f - \delta_{w(ocean)})] \times S_{(ocean)} \quad (3)$$

Constants for $\delta^{18}O$ of the open ocean were $\delta_{w(ocean)} = -1.22‰$ PDB and $S_{(ocean)} = 34.3$, values calculated from models of Earth without polar ice caps (Schmidt, 1997).

Grossman and Ku's equation is likewise appropriate because all molluscan shell samples used in this study, with the exception of calcitic *Anomia*, for which no unaltered specimens were found, were aragonitic. *Inoceramus*, which contains both a prismatic calcitic layer and aragonitic nacreous layer, was sampled only in the aragonite.

TABLE 4--Specimen Suites Used in Shell Alteration Investigations

	Mode of Preservation Suite	Shell Testing Location Suite	Shell Color Suite	Cementation Suite	Total Number of Samples
Baculites phragmacone	5	7	15	25	**52**
Baculites septa		7			**7**
Placenticeras phragmacone	6	2	10	4	**22**
Placenticeras septa		2			**2**
Hoploscaphites phragmacone		1	11	9	**21**
Hoploscaphites septa		1			**1**
Inoceramus shell	5		13		**18**
Nymphalucina shell	4		2		**6**
Anomia shell			4		**4**
Anisomyon shell			2		**2**
Drepanocheilus shell			3		**3**
Concretion				34	**34**
Cementation				33	**33**
Exterior Crystallization				6	**6**
Total Number of Samples	**20**	**20**	**60**	**111**	**211**

The 211 samples investigated in the shell alteration portion of this study are divided into four suits, each with its own hypothesis to test. Because the focus of most hypotheses is on ammonites, they are overrepresented in the dataset compared to *Inoceramus*, the only numerous bivalve genus for the sampling locations. Nonetheless, a variety of genera are represented by the combined dataset.

TABLE 5–Limits for ICP-OES System.

	Al	Ca	Fe	K	Mg	Mn	Na	Sr
Wavelength, nm	396.153	315.887	238.204	766.490	285.213	257.610	589.592	407.771
Detection Limit (ppm)	1.60	5.87	0.35	0.39	0.38	0.05	1.08	0.01
Limit of Quantitation (ppm)	5.35	19.56	1.17	1.29	0.68	0.16	3.53	0.03

Limits of quantitation for the ICP-OES system used in this study were approached for analyses of Fe, Mn, Mg, Sr, and Al. These values are the concentrations below which no numerical data analysis should be performed. All data with minor element concentions below the limit of quantitation were omitted from statistical analyses and regression trendlines. Limits of detection express how much of the element must be present in the sample to produce results. This threshold was crossed most frequently with Al.

2.3 Results

2.3.1 Mode of Preservation: Results for the "Mode of Preservation" suite were obtained for all twenty samples (see Appendices A and B). As Figure 2 displays, most of the samples cluster with $\delta^{18}O$ ratios ranging from 0.50‰ to 5.00‰, with respect to PDB. The $\delta^{13}C$ values range from -5‰ to 6‰. The *Nymphalucina* preserved in a Trask Ranch concretion is an exception with $\delta^{18}O$ = -9.07‰ and $\delta^{13}C$ = -13.0‰. Likewise, the *Placenticeras* samples from Kremmling, Colorado, concretions were anomalous with $\delta^{18}O$ ranging from -15‰ to -20‰ and $\delta^{13}C$ from -7.44‰ to -3.99‰.

In total, four of the five outliers were samples from concretions. A t-test of independent samples with level of significance = 0.05 reveals significantly lighter $\delta^{18}O$ in concretions and a strong relationship between concretions and lighter $\delta^{13}C$ values (Table 6). These statistical findings support the visual observation that, within the cluster of shell samples on the isotope cross-plot, there appears to be no pattern in the relative position of shale and concretion points. Within the cluster of stable isotope data, the *Inoceramus* samples show the isotopically heaviest carbon signature (mean $\delta^{13}C$ = 3.47 ± 2.44‰), along with the isotopically lightest oxygen signature (mean $\delta^{18}O$ = -3.38 ± 1.31‰). The *Inoceramus* found in Trask Ranch concretions had an isotopic signature closer to the *Inoceramus* found in Game Ranch shale than Game Ranch concretions. Conversely, the *Baculites* samples show the isotopically lightest carbon signature (mean $\delta^{13}C$ = -0.73 ± 1.30‰), along with the isotopically heaviest oxygen signature (mean $\delta^{18}O$ = -1.34 ± 1.09‰). The *Baculites* found in Trask Ranch concretions had isotopic signatures closer to the *Baculites* found in Game Ranch concretions than Game Ranch shale. The *Placenticeras* samples have similar carbon values (mean $\delta^{13}C$ = -1.43 ±

0.43‰) as the *Baculites*, but intermediate oxygen values (mean $\delta^{18}O$ = -2.58 ± 1.19‰) between the points for *Baculites* and *Inoceramus* specimens. While there are only two points for *Nymphalucina*, they are closest to the light-carbon, heavy-oxygen *Baculites*.

As in the isotopic data, in the minor element data, the outliers were from concretions. All minor element concentration data shown in Figures 3 and 4 is expressed in mMol/Mol ratios with calcium. The Kremmling *Placenticeras* and the Trask Ranch *Nymphalucina* represent outliers depleted in strontium and enriched in magnesium relative to Recent mollusks (Figure 3). An *Inoceramus* shell sample was slightly enriched in magnesium (3.44 mMol/Mol) and a *Baculites* sample from Trask Ranch was enriched in both strontium and magnesium relative to Recent aragonitic shell material (Buchardt and Weiner, 1981). Figure 4, a pair of radar charts, depicts minor element concentrations for all elements examined. Each axis of a chart records the concentration of an element, in mMol/Mol, with lines connecting all data points for a given sample. Enrichment outliers for aluminum, iron, manganese, and strontium were present for the concretion samples, but not for the shale samples (however, in the latter, no aluminum concentration data could be obtained due to concentrations below the analytical detection level). The outliers belong to four different samples, rather than to one sample that was highly altered. In both concretions and shale, the mean K/Ca ratio was ~0.8 mMol/Mol, Na/Ca ratio was ~16 mMol/Mol, and Sr/Ca ratio was ~3 mMol/Mol. The concretions had higher mean Fe/Ca ratios (8.3 ± 1.4 mMol/Mol vs. 1.12 ± 1.06 mMol/Mol), Mn/Ca ratios (5.1 ± 2.4 vs. 1.69 ± 1.23 mMol/Mol), and Mg/Ca ratios (6.2 ± 0.9 vs. 0.88 ± 0.94 mMol/Mol). The differences in magnesium and iron were the only statistically significant trends in the minor isotope ratios, as evaluated by one-tailed t-tests of

independent samples, 0.05 level of significance, reported in Table 2. The lower mean concentration of manganese in the shale samples was nearly significant, with t = -1.7 (critical t = -1.753) and the higher mean concretion of sodium in the shale samples was also nearly significant, with t = 1.4 (critical t = 1.746).

FIGURE 2—Mode of Preservation Stable Isotope Cross-Plot

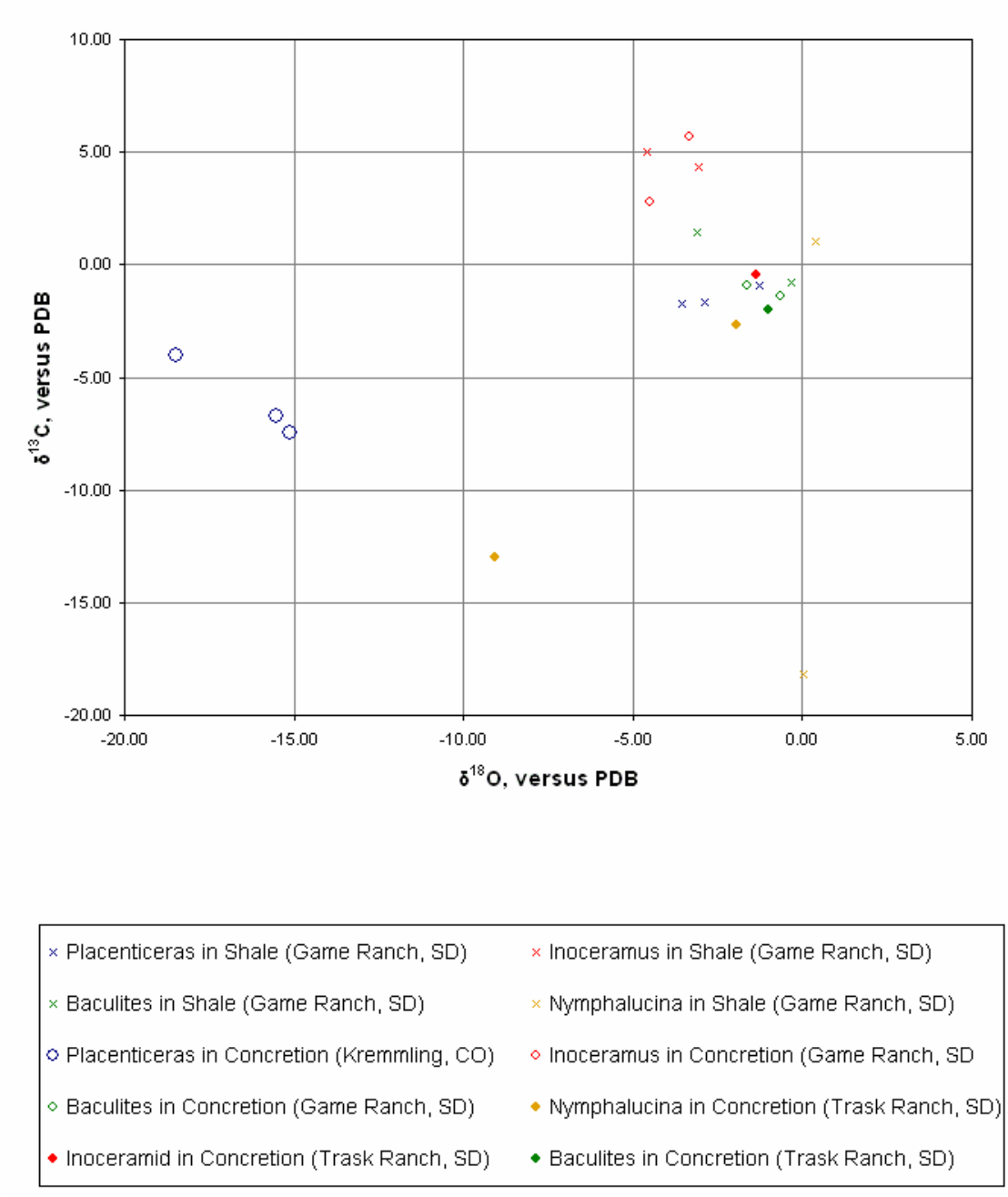

The plot of oxygen and carbon stable isotopes for the "Mode of Preservation" shell alteration suite, with color denoting genus and symbol type denoting location, clearly shows outlier data points for specimens preserved in concretions.

TABLE 6—Summary Statistics for Mode of Preservation Suite

Alternate Hypothesis	Type of Test	N	Mean, ± standard deviation	Calculated Value(s)	Critical Value (95% confidence)	Result
Significantly lighter mean $\delta^{13}C$ in concretions?	One-tailed t-test (independent samples)	9s, 11c	s: -1.28± 6.81 c: -2.74 ± 5.07	t = 1.35	t = 1.75	H_o retained
Significantly lighter mean $\delta^{18}O$ in concretions?	One-tailed t-test (independent samples)	9s, 11c	s: -2.04 ± 1.78 c: -6.60 ± 6.74	t = 4.76	t = 1.75	H_o rejected
Significantly lower mean Fe/Ca in shale?	One-tailed t-test (independent samples)	6s, 11c	s: 1.12 ± 1.06 c: 8.3 ± 1.4	t = -2.0	t = ±1.753	H_o rejected
Significantly lower mean K/Ca in shale?	One-tailed t-test (independent samples)	9s, 11c	s: 0.731 ± 0.855 c: 0.93 ± 0.20	t = -0.64	t = ±1.746	H_o retained
Significantly lower mean Mg/Ca in shale?	One-tailed t-test (independent samples)	9s, 11c	s: 0.88 ± 0.94 c: 6.2 ± 0.9	t = -2.8	t = ±1.746	H_o rejected
Significantly lower mean Mn/Ca in shale?	One-tailed t-test (independent samples)	6s, 11c	s: 1.69 ± 1.23 c: 5.1 ± 2.4	t = -1.7	t = ±1.753	H_o retained
Significantly higher mean Na/Ca in shale?	One-tailed t-test (independent samples)	9s, 11c	s: 17.2 ± 4.1 c: 14.0 ± 3.0	t = 1.4	t = ±1.746	H_o retained
Significantly higher mean Sr/Ca in shale?	One-tailed t-test (independent samples)	9s, 11c	s: 2.85 ± 1.69 c: 3.4 ± 0.74	t = -0.43	t = ±1.746	H_o retained

Summary statistics for the "Mode of Preservation" Suite show significantly lower Mg/Ca ratios in specimens preserved in shale and significantly lighter $\delta^{18}O$ in specimens preserved in concretions. The null hypothesis, that there is no significant difference in the mean between shale and concretion subsets, was retained for all other tests. All isotope ratios reported in ‰ versus PDB and all minor element ratios reported in mMol/Mol calcium.

FIGURE 3–Sr/Ca and Mg/Ca Ratios for "Mode of Preservation" Suite

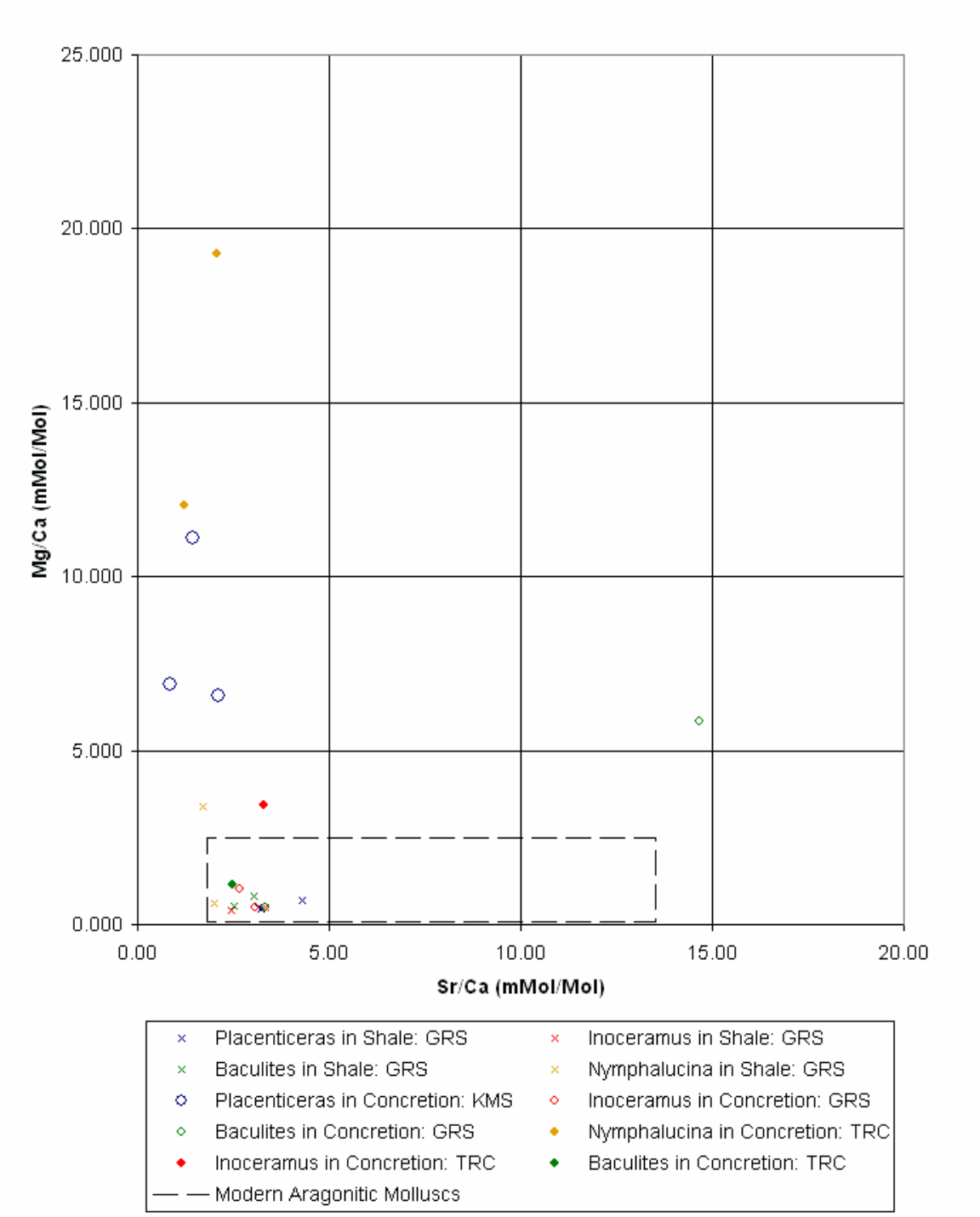

In the Sr/Ca-Mg/Ca minor element cross-plot, the majority of data points residing outside of the field for Recent aragonitic shell are from specimens in concretions. These points are enriched in magnesium relative to Recent aragonitic shell.

FIGURE 4–Radar Charts for Minor Element Concentrations in the "Mode of Preservation Suite"

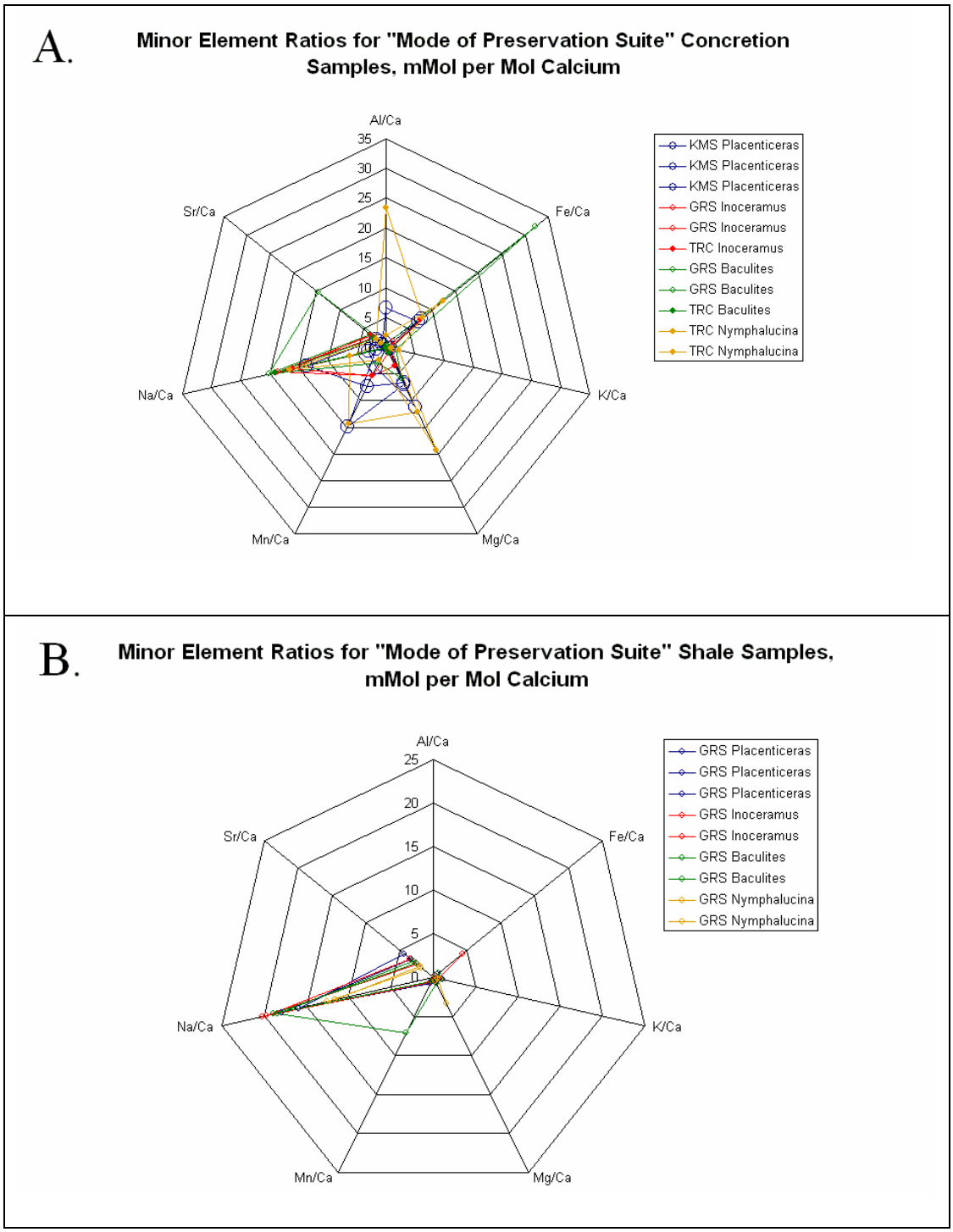

The minor element ratios for the concretion specimens show enrichment in iron, magnesium, and manganese relative to those taken from shale.

2.3.2 Shell Sampling Position: Minor element concentrations for the "Shell Sampling Position" suite were obtained for all twenty samples (ten phragmacone-septum pairs). Stable isotope results were obtained for eighteen of the samples (see Appendices A and B), with septum specimen 3S and phragmacone samples 2P unreliable, and therefore omitted, due to low mass spectrometer voltage, possibly from underweight samples. These results may be seen in tabular form within Appendices A and B.

In the stable isotope cross-plot (Figure 5), the data cluster by genus. The *Placenticeras* had the isotopically heaviest $\delta^{13}C$ and the isotopically lightest $\delta^{18}O$, with -3.71‰ and -3.74‰, for the septum, and -2.91‰ and -2.67‰ for the phragmacone, respectively. The *Hoploscaphites* had a similar $\delta^{18}O$, but lighter $\delta^{13}C$, with -3.69‰, -8.36‰ for the septum, and -3.64‰ and -7.46‰ for the phragmacone, respectively. The isotopic signatures of the *Baculites* samples vary greatly, with mean $\delta^{13}C$ and $\delta^{18}O$ values of -6.22 ± 4.13‰ and -1.36 ± 2.35‰, respectively.

The values recorded from each specimen often proved vastly different. Three phragmacone and septum pairs (the *Hoploscaphites* and two *Baculites* specimens from the Trask Ranch) do have similar isotopic values; the remaining seven do not. These pairs were analyzed using a statistical paired t-test for dependent samples, as shown in Table 7. At the 0.05 significance level, the difference in $\delta^{13}C$ between septum and phragmacone samples taken from the same specimen may be explained by random chance. The difference in mean $\delta^{18}O$ is significant at the 0.05 level, with $\delta^{18}O$ from the phragmacones lighter than those from the septa. It should be noted that the mean $\delta^{13}C$ value is influenced by a Trask Ranch *Baculites* phragmacone sample, at the bottom of Figure 6, which is a statistical outlier with respect to the other phragmacone samples.

When the septum-phragmacone pair containing this point is removed, the t-score for the $\delta^{13}C$ ratio increases, indicating a greater difference between phragmacone and septal samples, while the $\delta^{18}O$ ratio decreases below the 0.05 level of statistical significance. In addition, the $\delta^{13}C$ ratio of the phragmacone samples increases from -5.09 ± 4.41‰ to -3.72 ± 2.29‰ and the $\delta^{18}O$ ratio of the phragmacone samples increases from -7.03 ± 2.96‰ to -6.73 ± 3.07‰. While the statistical dependence of the samples upon each other precludes the ability to apply a t-test to the data subsets consisting of all phragmacone and all septal samples, it is clear from the means and the distribution of points in Figure 5 that the septal samples tend to have lower $\delta^{13}C$ values.

In the graph of Sr/Ca versus Mg/Ca ratios (Figure 6), only two data points fall within the limits established for Recent aragonitic shell. These points are both phragmacone samples: one a *Placenticeras* from Game Ranch and the other a *Hoploscaphites* from Trask Ranch. The septum of the aforementioned *Placenticeras* is an outlier strongly enriched in strontium (Sr/Ca = 16.4 mMol/Mol), while all other samples have Sr/Ca ratios between 2 and 5 mMol/Mol, values on the lower end of the range for Recent aragonitic shell. There is no difference between Sr/Ca ratios between corresponding septal and phragmacone samples to the 0.05 level of significance with a two-tailed t-test of dependent samples (Table 7). Likewise, there is no significant difference in Mg/Ca ratio, though in this instance the t-score is much higher (t = -1.9 versus critical t = ±2.262). The greater t-score is expected because of the high standard deviation of the Mg/Ca ratios within the "Shell Testing Location" suite and the large span of data points along the y-axis of Figure 6. Most of the data points in the suite are relatively enriched in magnesium, up to Mg/Ca = 48.9 mMol/Mol, without any statistical

outliers.

Statistical outliers do exist for the Fe/Ca, Na/Ca, and Sr/Ca ratios of the Kremmling, Colorado, *Placenticeras* sample, the first two ratios for both phragmacone and septum and the last ratio for the septum alone. Another outlier was the enriched Sr/Ca of the Game Ranch*Placenticeras* septum. These outliers may be seen graphically as the endpoints on the radar diagrams in Figure 7. Interestingly, the *Placenticeras* data that contain the statistical outliers also show the greatest mismatch between the chemical content of phragmacone and septal samples within a pair. All other pairs show similar chemical profiles, with peaks greater than 5 mMol/Mol for magnesium, sodium and, for the Colorado specimens and South Dakota *Hoploscaphites*, manganese. Small peaks, with concentrations less than or equal to 10 mMol/Mol Ca, also occur for iron in the South Dakota specimens. When the large Fe/Ca ratio of the Kremmling *Placenticeras* is removed from the data, a statistically significant difference in the Fe/Ca ratio for phragmacone-septum pairs emerges. Figure 7 reveals the difference to be a relative enrichment of iron for the septal samples.

Comparing the differences in isotopic ratios to the minor element data, several trends emerge. First, specimens with enriched magnesium and/or manganese -- such as the Game Ranch *Placenticeras* and the second, third, and fourth Trask Ranch *Baculites* – also had large differences between the isotopic signatures of their septa and phragmacones. However, the Trask Ranch *Hoploscaphites* specimen was enriched in magnesium but did not display a substantial difference between phragmacone and septal isotopic signatures and the fifth Trask Ranch *Baculites* specimen showed a fairly wide span of values on the isotope cross-plot without high magnesium or manganese

concentrations. The similarity in minor element distributions (overall shape of the radar chart polygon) is a better predictor of isotopic similarity than the numeric concentrations of minor elements. The best matches, as seen in Figure 7, are the Trask Ranch *Hoploscaphites* and the first and sixth Trask Ranch *Baculites*, and these are also the pairs that are closest together on the isotope cross-plot. The poorly-matched septal and phragmacone samples of the Game Ranch *Placenticeras* specimen correlate with a moderately high difference in $\delta^{13}C$ and $\delta^{18}O$. The Trask Ranch *Baculites* samples that were isotopically different had the same minor element distribution, with peaks in Fe, Mg, and Na, but the phragmacone and septal samples within a pair differed in their concentrations of these elements. Unfortunately, no isotopic data was available for the Kremmling specimens, which matched poorly in minor element distribution and would have provided useful comparisons.

FIGURE 5—Shell Sampling Position Stable Isotope Cross-Plot

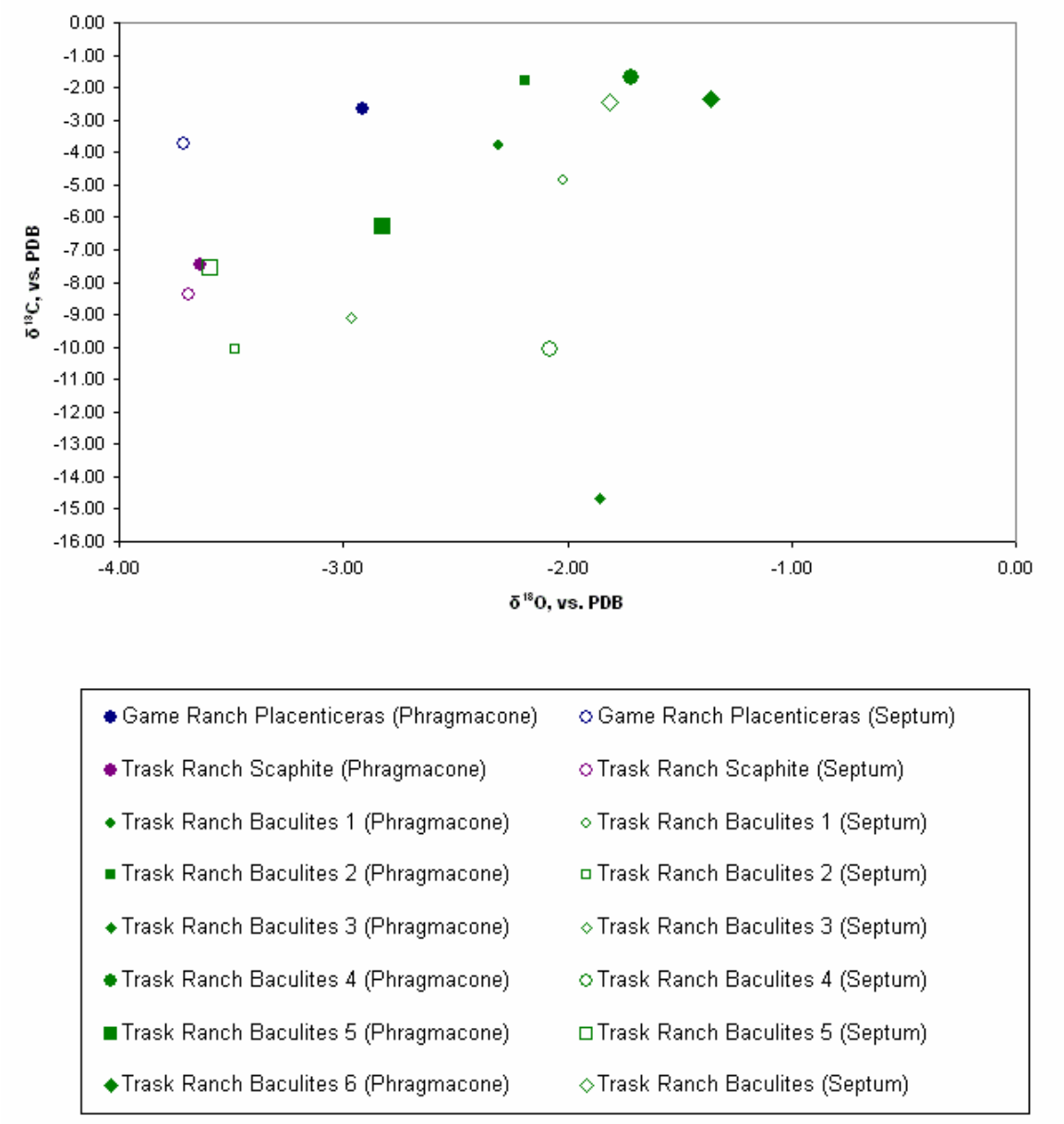

This plot shows oxygen and carbon stable isotopes for the "Shell Sampling Position" shell alteration suite, with color denoting genus, symbol shape denoting location, and symbol fill denoting septum versus phragmacone sampling. Quite frequently, phragmacone-septum pairs are isotopically different from each other.

TABLE 7 –Summary Statistics for "Shell Sampling Position" Suite

Alternate Hypothesis	Type of Test	N	Means, ± standard deviations	Calculated Value(s)	Critical Value (0.05)	Result
Difference in $\delta^{13}C$ values of septum-phragmacone pairs?	Paired t-test (dependent samples)	8s, 8p 6s, 6p	p: -5.09 ± 4.41 s: -7.03 ± 2.96 Without outlier: p: -3.72 ± 2.29 s: -6.73 ± 3.07	t = 1.21 t = 1.77	t = ± 2.365 t = ±2.571	H_o retained; H_o retained
Difference in $\delta^{18}O$ values of septum-phragmacone pairs?	Paired t-test (dependent samples)	8s, 8p 6s, 6p	p: -2.35 ± 0.74 s: -2.92 ± 0.82 Without outlier: p: -2.42 ± 0.77 s: -2.91 ± 0.89	t = 3.04 t = 2.02	t = ± 2.365 t = ±2.571	H_o rejected; H_o retained
Difference in Al/Ca of septum-phragmacone pairs?	Paired t-test (dependent samples)	8p, 8s 7s, 7p	p: 4.633 ± 4.579 s: 6.047 ± 6.200 Without outliers: p: 2.960 ± 1.921 s: 4.318 ± 2.428	t = -12.82 t = -7.590	t = ±2.365 t = ±2.447	H_o rejected; H_o rejected
Difference in Fe/Ca of septum-phragmacone pairs?	Paired t-test (dependent samples)	10p, 10s 8p, 8s	p: 6.1 ± 11.5 s: 8.6 ± 7.4 Without outliers: p: 2.80 ± 3.05 s: 5.64 ± 2.51	t = -1.3 t = 2.64	t = ±2.262 t = ±2.571	H_o retained; H_o rejected
Difference in K/Ca of septum-phragmacone pairs?	Paired t-test (dependent samples)	10p, 10s 8p, 8s	p: 0.07 ± 0.03 s: 0.1 ± 0.2 Without outliers: p: 0.07 ± 0.02 s: 0.07 ± 0.03	t = -1 t = 0.8	t = ±2.262 t = ±2.306	H_o retained; H_o retained
Difference in Mg/Ca of septum-phragmacone pairs?	Paired t-test (dependent samples)	10p, 10s 8p, 8s	p: 14.5 ± 13.9 s: 20.4 ± 10.5 Without outliers: p: 15.7 ± 14.8 s: 21.5 ± 10.5	t = -1.9 t = -1.5	t = ±2.262 t = ±2.306	H_o retained; H_o retained
Difference in Mn/Ca of septum-phragmacone pairs?	Paired t-test (dependent samples)	10p, 10s 8p, 8s	p: 4.3 ± 5.7 s: 5.5 ± 4.0 Without outliers: 3.5 ± 4.9 4.8 ± 4.2	t = -1.16 t = 1.81	t = ±2.262 t = ±2.306	H_o retained; H_o retained
Difference in Na/Ca of septum-phragmacone pairs?	Paired t-test (dependent samples)	10p, 10s 8p, 8s	p: 19.8 ± 12.6 s: 22.7 ± 11.9 Without outliers: p: 22.2 ± 12.7 s: 21.9 ± 12.4	t = -0.55 t = 0.050	t = ±2.262 t = ±2.306	H_o retained; H_o retained
Difference in Sr/Ca of septum-phragmacone pairs?	Paired t-test (dependent samples)	10p, 10s 8p, 8s	p: 2.69 ± 1. 21 s: 6.1 ± 6.5 Without outliers: p: 2.83± 1.14 s: 3.10 ± 1.04	t = 1.6 t = 0.855	t = ±2.262 t = ±2.306	H_o retained; H_o retained

Significant relationships exist for $\delta^{18}O$, Al/Ca, and Fe/Ca. For other tests, the null hypothesis of no difference in means between septa and phragmcones is retained. All isotope ratios reported in ‰ versus PDB; all minor element ratios reported in mMol/Mol.

FIGURE 6—Shell Sampling Position Sr/Ca-Mg/Ca Cross-Plot

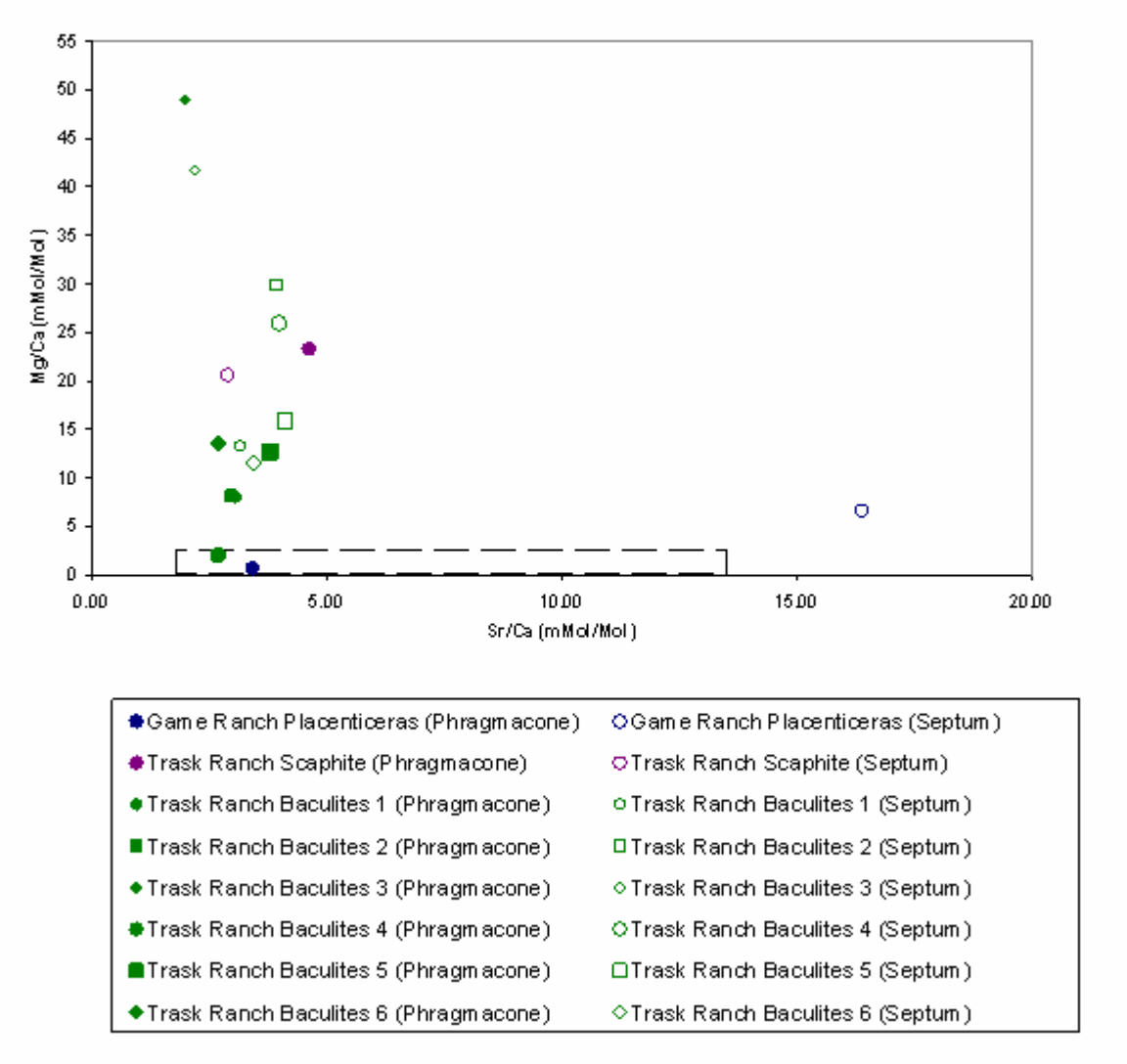

Very few of the samples for the "Shell Sampling Position" suite fall within the Mg/Ca and Sr/Ca limits for Recent aragonitic shell. As in the isotopic data, the phragmacone and septum samples may differ in their chemical composition.

FIGURE 7—Radar Charts for Minor Elements in "Shell Sampling Position" Specimens

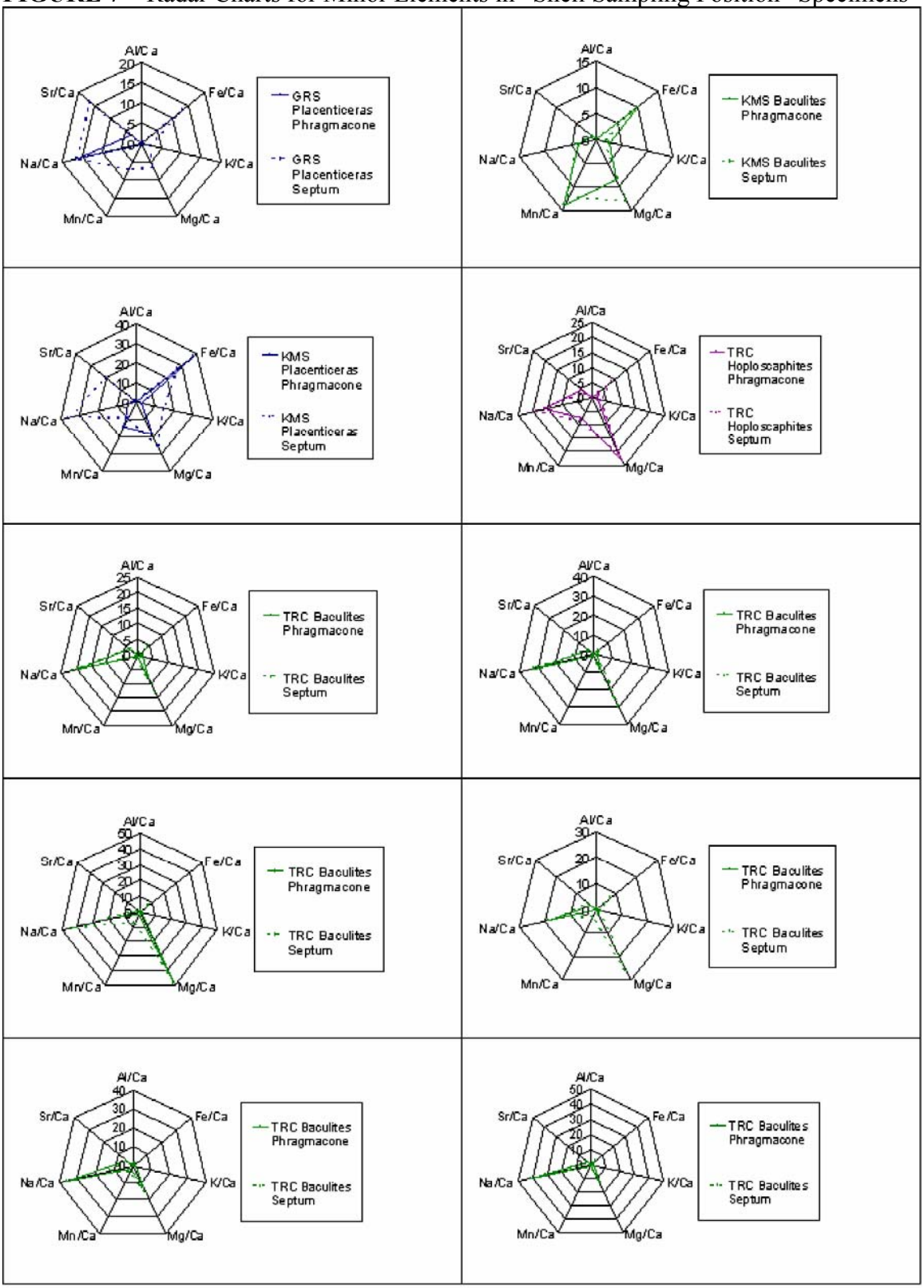

Most phragmacone-septum pairs share patterns in minor elements though amounts differ.

2.3.3 Shell Color Suite: Two aspects of shell color were investigated in this study: the presence or absence of an opalescent luster and the color of the shell. A suite of 60 specimens was assembled, with 20 samples per collection site and representatives of all genera (see Appendices A and B). For each genus at each location, specimens of at least two different colors were sampled. Twelve samples, including representatives of *Placenticeras*, *Baculites*, *Hoploscaphites*, and *Inoceramus*, could be classified as opalescent. These genera were also represented in non-opalescent shell, along with additional genera *Nymphalucina*, *Anomia*, *Drepanocheilus*, and *Anisomyon*. All genera in the study were thus represented in the "Shell Color" suite.

As Figure 8 illustrates, the majority of the samples from opalescent shells, including those from the opalescent 10YR3/6, opalescent 5Y8/9, opalescent 7.5YR6/7, and opalescent N9 color classes cluster between $\delta^{13}C$ values ranging from 5‰ to -5‰ and $\delta^{18}O$ values spanning 0‰ to -4‰ (See Table 8 for color designations). A single outlier is the Kremmling *Placenticeras* sample, with $\delta^{18}O$ and $\delta^{13}C$ values of -15.01‰ and -6.99‰, respectively. The non-opalescent shell samples show a greater range of values, but tend to cluster into two subsets as defined by $\delta^{18}O$. All of the members of the relatively $\delta^{18}O$-depleted cluster are from Kremmling (whereas only two members of the relatively $\delta^{18}O$-enriched cluster are). Therefore, the Colorado and South Dakota specimens were separated during statistical analysis (Tables 9 and 10). The $\delta^{13}C$ and $\delta^{18}O$ averages became heavier when the Kremmling points were removed, with an opalescent shell $\delta^{13}C$ average of -2.08 ± 2.47‰ (versus -3.43 ± 3.97‰ when including Kremmling data) and $\delta^{18}O$ average of -1.53 ± 1.95‰ (versus -2.27 ± 1.04‰). The non-

opalescent shell $\delta^{13}C$ average was -1.64 ± 5.71‰ (versus -3.07 ± 5.38‰ when including Kremmling data), and the $\delta^{18}O$ average was 3.61 ± 1.87‰ (versus -6.98 ± 5.22‰). In most instances, the standard deviation also decreases when the Kremmling data is removed, though this effect is more marked for the oxygen than carbon data. The one-tailed t-tests for independent samples calculated for the opalescent and non-opalescent shell reveal no significant differences in the $\delta^{18}O$ or $\delta^{13}C$ ratios. The extremely low $\delta^{13}C$ t-score (0.011) for the South Dakota data suggests that the variation in the data was caused by the difference between South Dakota and Colorado isotopic signatures. However, the t-score for $\delta^{18}O$ is greater, indicating that opalescent shell has heavier $\delta^{18}O$, but not at a level of statistical significance. Indeed, in Figure 8, the opalescent samples, designated by square boxes, tend to cluster towards heavier $\delta^{18}O$.

When examining the minor element ratios with respect to shell opalescence, few important results emerged. Using one-tailed t-tests at the 0.05 significance level, lower mean Mg/Ca, Mn/Ca, and Sr/Ca ratios were found for the opalescent shell of the full dataset. Another relatively strong relationship existed for higher Sr/Ca ratios in the opalescent shell. These conclusions were not true for the data subset containing only South Dakota collection sites so likely reflect the contribution of the Kremmling samples to the non-opalescent shell, which dominate the low-Sr/Ca, high-Mg/Ca region of the Sr/Ca-Mg/Ca plot shown as Figure 9. The opalescent shell instead resides below or near the Mg/Ca limit for Recent aragonitic shell, and shows little Sr/Ca depletion.

When the isotopic and minor element data are examined to see if groupings defined by shell color contributed to variation in the data, most null hypotheses cannot be statistically rejected, both in the complete and South Dakota datsets (Table 10). There

are statistically significant differences in mean K/Ca and Mn/Ca for the South Dakota dataset, and a difference in Mg/Ca for both datasets. Statistically insignificant but notable relationships include the differences in $\delta^{18}O$ (F = 1.94 versus critical F = 2.071), Al/Ca (F = 2.26 versus critical F = 2.477), and Sr/Ca (F = 1.59 versus critical F = 2.044), all for the complete datasets. Among the South Dakota specimens, the highest insignificant F-statistic was Na/Ca (F = 1.6 versus critical F = 2.321).

A graphical analysis of color with respect to genus is presented in Table 11. There is a degree of variability for colors in unaltered shell (with "unaltered" here defined as shell bearing Sr/Ca and Mg/Ca ratios analogous to Recent aragonitic shell). For instance, *Inoceramus* may display one of many colors (10YR8/1, 7.5YR8/2, opalescent N9, and 7.5YR9/2), whereas *Hoploscaphites* has a much narrower range of colors (10YR6/7, and sometimes 10YR7/8). Examining the isotope and minor element cross-plots, darker colors are associated with *Inoceramus* and *Hoploscaphites*, whereas lighter colors are associated with *Baculites* and *Placenticeras*. This observation suggests that the color of less-altered shell is influenced by a genus-level trait.

TABLE 8–Descriptive Names for Munsell Designations of Shell Color Classes

Descriptive Color Class Name	Munsell Designation
Dark Brown	10YR3/6
Cream	7.5Y9/4
Grey	10YR8/1
Light Grey-Tan	7.5YR8/2
Light Brown	10YR7/8
Orange	10YR7/11
Light Cream	7.5Y9/2
DarkTan	10YR6/7
Light Tan	5Y8/5
White	N9
Yellow	5Y8/9

The color descriptive terms used in this paper were selected because they create a more specific mental image of color than the color names associated with the Munsell designations listed above. Approximations of these colors may be seen in the data points in Figures 8 and 9.

TABLE 9–Summary Statistics for 'Shell Color' Suite: Shell Opalescence

Alternate Hypothesis	Type of Test	N	Means, ± std. dev.s	Calculated Value(s)	Critical Val. (0.05 sig.)	Result
Lower mean $\delta^{13}C$ in non-opalescent shell?	One-tailed t-test of independent samples	11o, 44n	o: -2.08 ± 2.47 n: -2.82 ± 4.54	t = 0.149	t = 1.674	H_o retained
			South Dakota only:			
		10o, 28n	o: -1.58 ± 1.95 n: -1.64 ± 5.71	t = 0.011	t = 1.688	H_o retained
Lower mean $\delta^{18}O$ in non-opalescent shell?	One-tailed t-test of independent samples	11o, 44n	o: -3.43 ± 3.97 n: -6.98 ± 5.22	t = 0.765	t = 1.674	H_o retained
			South Dakota only:			
		10o, 28n	o: -2.27 ± 1.08 n: -3.61 ± 1.87	t = 0.877	t = 1.688	H_o retained
Lower mean Al/Ca in opalescent shell?	One-tailed t-test of independent samples	5o, 28n	o: 3.47 ± 2.14 n: 5.8 ± 6.2	t = -0.73	t = -1.696	H_o retained
			South Dakota only:			
		5o, 15n	o: 2.78 ± 2.52 n: 3.0 ± 2.6	t = -0.17	t = -1.734	H_o retained
Lower mean Fe/Ca in opalescent shell?	One-tailed t-test of independent samples	12o, 48n	o: 8.5 ± 11.8 n: 10.5 ± 20.1	t = -0.32	t = -1.672	H_o retained
			South Dakota only:			
		11o, 29n	o: 9.3 ± 12.3 n: 9.0 ± 24.9	t = 0.039	t = -1.686	H_o retained
Lower mean K/Ca in opalescent shell?	One-tailed t-test of independent samples	12o, 48n	o: 0.07 ± 0.05 n: 0.08 ± 0.07	t = -0.5	t = -1.672	H_o retained
			South Dakota only:			
		11o, 29n	o: 0.07 ± 0.05 n: 0.06 ± 0.03	t = 0.6	t = -1.686	H_o retained
Lower mean Mg/Ca in opalescent shell?	One-tailed t-test of independent samples	12o, 48n	o: 6.1 ± 8.1 n: 14.1 ± 12.3	t = -2.1	t = -1.672	H_o rejected
			South Dakota only:			
		11o, 29n	o: 6.6 ± 8.5 n: 13.5 ± 16.4	t = -1.3	t = -1.686	H_o retained
Lower mean Mn/Ca in opalescent shell?	One-tailed t-test of independent samples	12o, 46n	o: 3.4 ± 3.4 n: 7.0 ± 5.5	t = -2.1	t = -1.673	H_o rejected
			South Dakota only:			
		10o, 28n	o: 4.087 ± 10.065 n: 4.483 ± 4.757	t = -0.24	t = -1.688	H_o retained
Higher mean Na/Ca in opalescent shell?	One-tailed t-test of independent samples	12o, 48n	o: 18.3 ± 14.0 n: 16.0 ± 27.0	t = 0.278	t = 1.672	H_o retained
			South Dakota only:			
		11o, 29n	o: 19.9 ± 11.4 n: 20.1 ± 31.6	t = -0.018	t =1.686	H_o retained
Higher mean Sr/Ca in opalescent shell?	One-tailed t-test of independent samples	12o, 48n	o: 3.28 ± 0.75 n: 2.35 ± 2.60	t = 1.9	t = 1.672	H_o rejected
			South Dakota only:			
		11o, 29n	o: 3.57 ± 0.62 n: 3.23 ± 1.62	t = 0.68	t = 1.686	H_o retained

The null hypothesis, that there is no difference in the means of the opalescent and non-opalescent data sets, holds for most tests in this sampling suite. All isotope ratios reported in ‰ versus PDB and all minor element ratios reported in mMol/Mol calcium.

TABLE 10– Summary Statistics for 'Shell Color' Suite: Shell Color

Alternate Hypothesis	Type of Test	N	Overall means, ± average standard deviations	Calculated Value(s)	Critical Value (0.05 significance)	Result
Difference in mean $\delta^{13}C$ among shell hue classes?	F-statistic	52 34	-3.04 ± 5.45 South Dakota only: -1.63 ± 5.83	F = 0.495 F = 0.443	F= 2.071 F = 2.337	Ho retained Ho retained
Difference in mean $\delta^{18}O$ among shell hue classes?	F-statistic	52 34	-6.92 ± 4.40 South Dakota only: -3.65 ± 1.43	F = 1.940 F = 1.345	F= 2.071 F = 2.337	Ho retained Ho retained
Difference in mean Al/Ca among shell hue classes?	F-statistic	28 15	6.46 ± 4.25 South Dakota only: 4.30 ± 3.95	F = 2.26 F = 1.62	F = 2.477 F = 3.478	Ho retained Ho retained
Difference in mean Fe/Ca among shell hue classes?	F-statistic	57 35	9.8 ± 9.9 South Dakota only: 15.4 ± 12.1	F = 0.42 F = 0.674	F = 2.044 F = 2.321	Ho retained Ho retained
Difference in mean K/Ca among shell hue classes?	F-statistic	57 35	1.89 ± 1.24 South Dakota only: 3.33 ± 2.59	F = 0.977 F = 8.25	F = 2.044 F = 2.321	Ho retained Ho rejected
Difference in mean Mg/Ca among shell hue classes?	F-statistic	57 35	14.5 ± 10.3 South Dakota only: 21.9 ± 10.0	F = 3.21 F = 7.78	F = 2.044 F = 2.321	Ho rejected Ho rejected
Difference in mean Mn/Ca among shell hue classes?	F-statistic	55 34	6.8 ± 4.4 South Dakota only: 10.3 ± 5.9	F = 1.3 F = 6.9	F = 2.054 F = 2.337	Ho retained Ho rejected
Difference in mean Na/Ca among shell hue classes?	F-statistic	57 35	15.9 ± 9.2 South Dakota only: 25.2 ± 8.9	F = 1.3 F = 1.6	F = 2.044 F = 2.321	Ho retained Ho retained
Difference in mean Sr/Ca among shell hue classes?	F-statistic	57 35	2.47 ± 1.26 South Dakota only: 4.11 ± 2.76	F = 1.59 F = 1.01	F = 2.044 F = 2.321	Ho retained Ho retained

Mean Mg/Ca and Mn/Ca statistically differs with respect to shell color. For all other elements, the null hypothesis, that the mean values do not differ by color grouping, holds. All isotope ratios reported in ‰ vs. PDB; all minor element ratios reported in mMol/Mol.

FIGURE 8—Shell Color Stable Isotope Cross-Plot

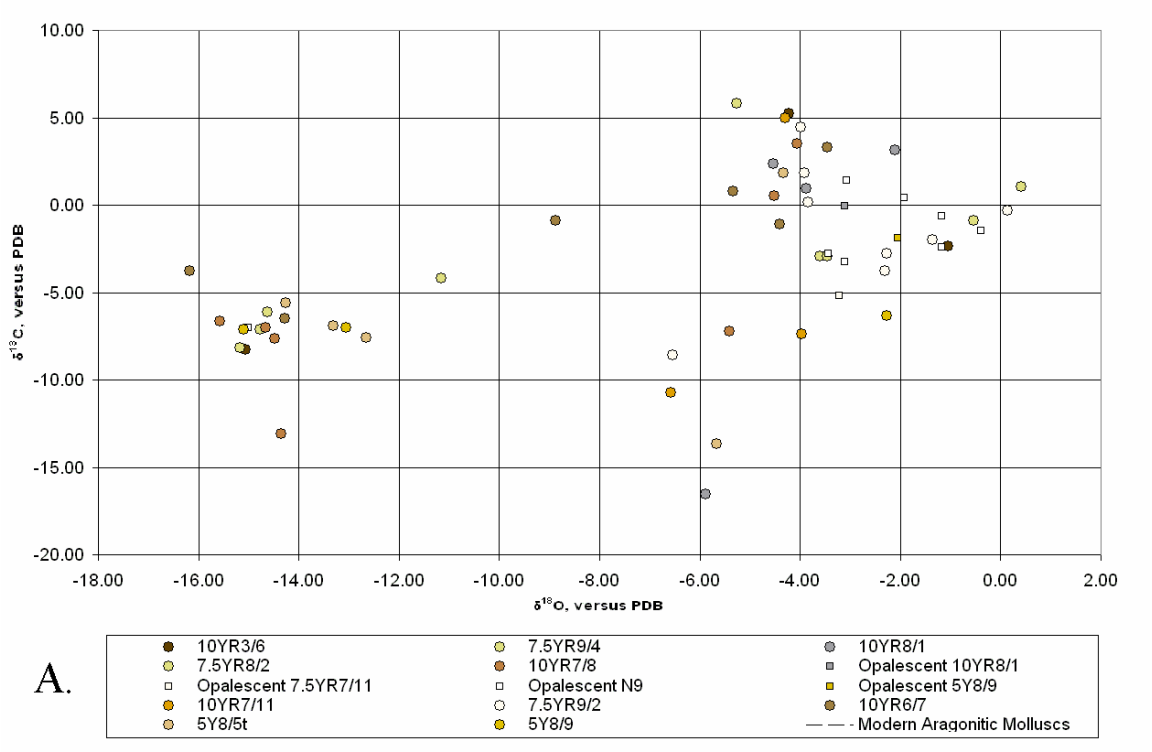

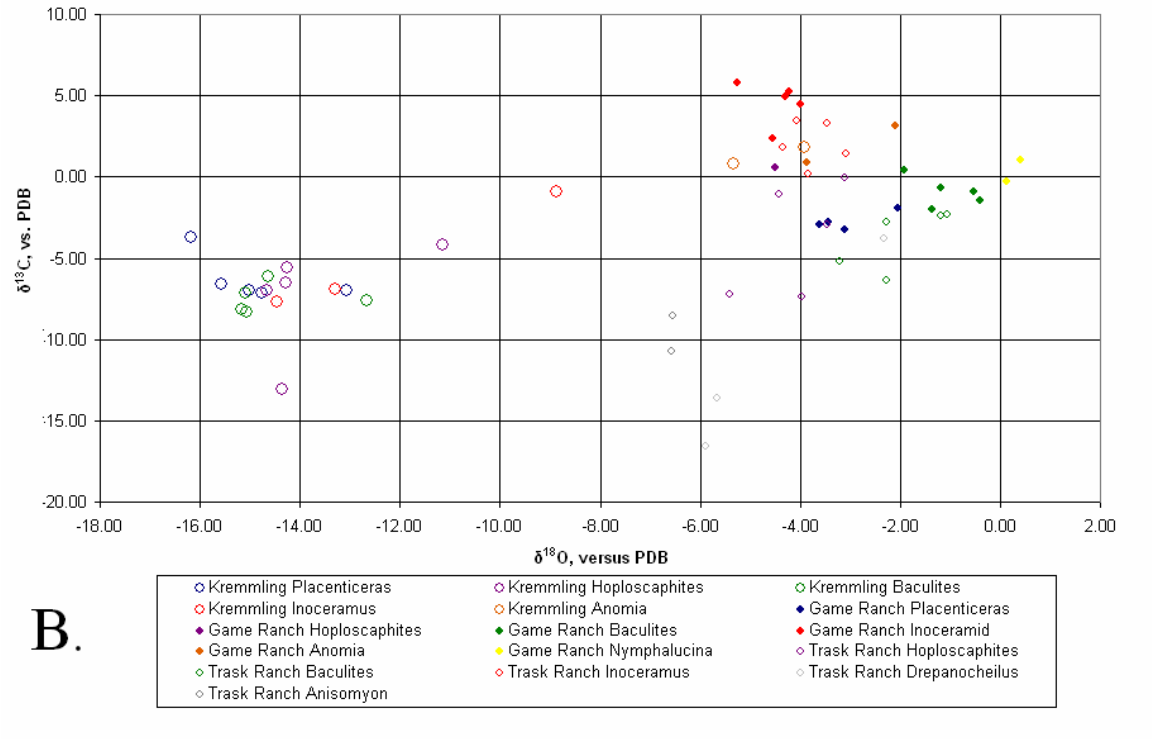

The opalescent shell clusters at isotopically heavy $\delta^{18}O$ and intermediate $\delta^{13}C$ relative to other shell. No clearly-defined pattern exists in relation to shell color and isotopes.

FIGURE 9—Shell Color Sr/Ca-Mg/Ca Cross-Plot

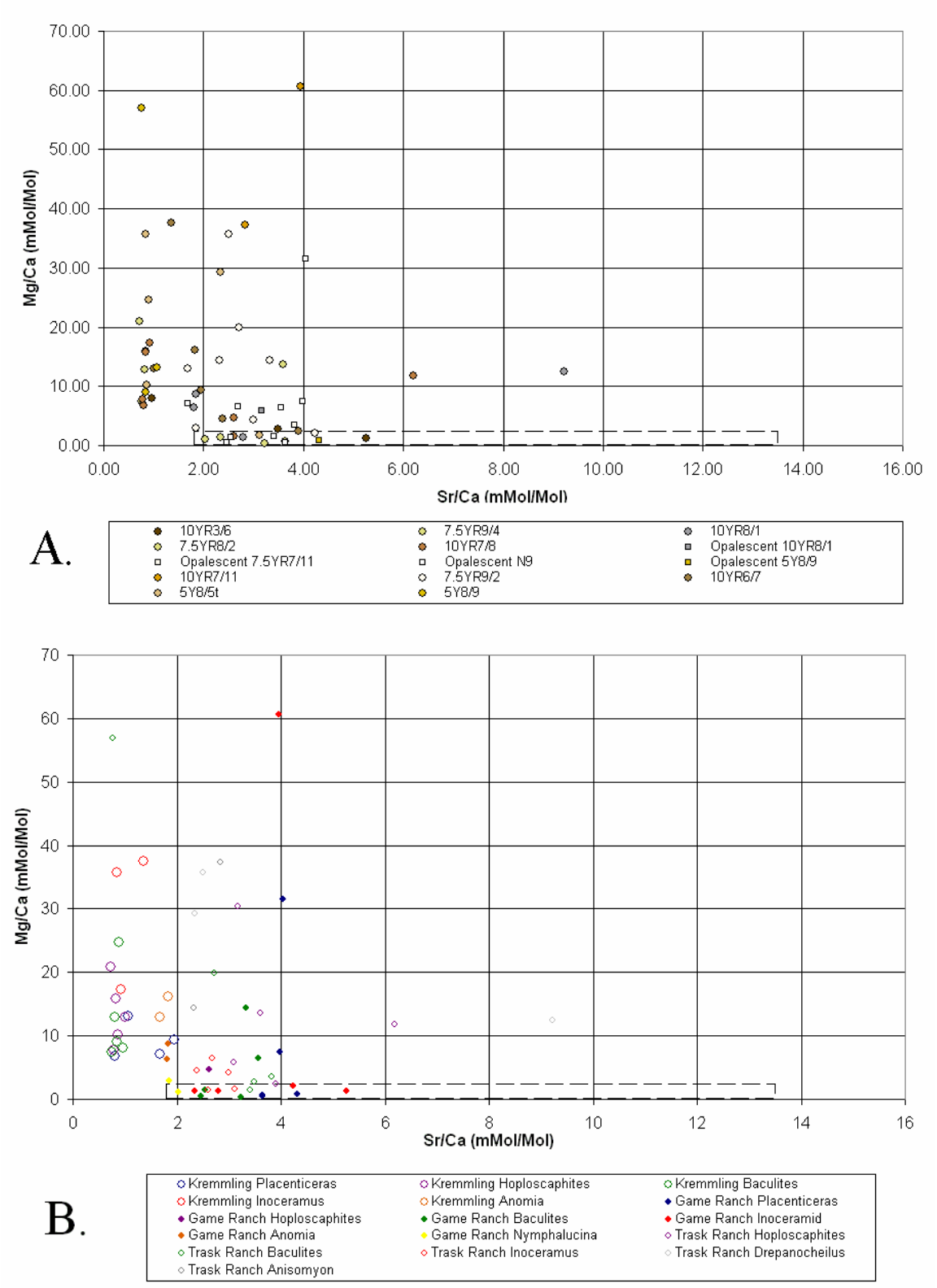

Samples from specimens with a light color, without yellow tones, have low Mg/Ca ratios.

TABLE 11—Colors for Unaltered Shell, by Genus

	Placenticeras	*Hoploscaphites*	*Baculites*	*Inoceramus*	*Anomia*	*Nymphalucina*	*Anisomyon*	*Drepanocheilus*
10YR3/6			o	+				
7.5Y9/4	-	-	-			+		
10YR8/1				+	-			-
7.5YR8/2	+	-	+	+				
10YR7/8	-	o		o				
Opalescent 10YR8/1		-						
Opalescent 7.5Y9/2			+					
Opalescent N9	-		+	+				
Opalescent 5Y8/9	+							
10YR7/11		-		-			-	
7.5Y9/2			-	+	-	+	-	-
5Y8/5	-	+			-			
N9		-	-	o				-
5Y8/9	-		-					

Key: + = majority of samples fell within Sr/Ca and Mg/Ca ranges for Recent molluscs
- = majority samples fell outside of Sr/Ca and Mg/Ca ranges for Recent molluscs
o = equal number of samples within and outside of ranges

Based on the Mg/Ca and Sr/Ca ranges for Recent aragonitic (and, in the case of *Anomia*, calcitic) shell, unaltered shell may come in several colors. The colors for unaltered shell depend in part on genus, with some genera, such as *Inoceramus*, having many colors for unaltered shell, while others, like *Placenticeras*, having fewer.

2.3.4 Cementation Suite: In the cementation suite, two questions pertaining to shell alteration were addressed. The first of these is whether the presence of cement, crystals precipitated within the phragmacone or growing upon the septa of ammonite shells, mirrors altered minor element concentrations and/or isotopic signatures. The second question is whether, for each sample site investigated, there is a difference between the minor element concentrations and/or isotopic signatures for cements, concretions, and shell. Significant differences in mean isotopic and/or minor element values among the cements, concretions, and shell could serve as indicators for sample contamination. For instance, if samples were taken from a *Hoploscaphites* for sclerochronology, and one showed minor element concentrations intermediate between unaltered shell samples and the concretion, concretion material was likely contaminating the sample and the isotopic data should therefore be disregarded.

A pair of radar charts showing the concentrations of minor elements (Figure 10), in mMol/Mol calcium, shows that shell taken from cemented specimens may have higher concentrations of iron, magnesium, and sodium than shell taken from uncemented samples. The greatest Mg/Ca and Fe/Ca ratios are for the Game Ranch specimens, with Trask Ranch specimens having the greatest Na/Ca ratio and the second-highest Mg/Ca and Fe/Ca ratios. As Figure 11A shows, the average minor element compostion of the cement at the Game Ranch is highly enriched in iron and magnesium relative to the average shell from that location. The cement in the Trask Ranch, however, has a lower concentration of sodium than the average for the shell (Figure 11B). Kremmling cements show a relatively low concentration of all minor elements.

Shell material for samples that were not in the "Cementation Suite" were selected

from shells that were not infilled with cement. These shell samples were added to the "Cementation Suite" data to statistically evaluate the differences between cemented and uncemented shell material. The only statistically significant difference with respect to minor element concentrations was the lower mean Mg/Ca concentration in uncemented specimens (Table 12). Other moderately strong relationships, using a one-tailed t test at 0.05 significance, were the lower Al/Ca ratio in uncemented specimens (t = 0.93 versus critical t = 1.663) and lower Na/Ca ratio in uncemented samples (t = 0.96 versus critical t = 1.656). Isotopically, there was a significant difference in the $\delta^{13}C$ ratio of shell with and without cementation, with lower average $\delta^{13}C$ values for the cemented shells. At t = 3.80 versus critical t = 1.656, this is the strongest relationship in the examination of cemented and uncemented shell. The oxygen isotope ratio produced the weakest statistical relationship and was, therefore, significantly not affected by cementation.

Figures 12, 13, and 14 display the Sr/Ca-Mg/Ca and $\delta^{18}O$ - $\delta^{13}C$ cross-plots for the Kremmling, Game Ranch, and Trask Ranch sites, respectively. In the Kremmling, plot (Figure 12), the samples from cemented specimens seen directly to the right of the cement samples are the shells lowest in Sr/Ca and, thus, furthest from the limit for Recent aragonitic shell. These points have lower $\delta^{18}O$ and higher $\delta^{13}C$ than the uncemented samples. Their $\delta^{13}C$ is comparable with that for cement, whereas their $\delta^{18}O$ values are intermediate between the cement and samples from uncemented shells. For the Game Ranch site, isotopic data for the cement samples was not available due to low voltage on the mass spectrometer. Therefore, comparisons can only be made with respect to external crystallization. Shells with external recrystallization or cement had lower $\delta^{13}C$ values than the samples from uncemented shell and $\delta^{18}O$ values among the lowest for

shell (Figure 13). Two of three samples from shells bearing external recrystallization or cement had Sr/Ca-Mg/Ca profiles identical to shell without such precipitation; the third had a Sr/Ca-Mg/Ca profile similar to the concretions. The Trask Ranch data shows the samples from cemented and uncemented shell intermixed on the Sr/Ca-Mg/Ca plot (Figure 14). On the other hand, the isotope cross-plot clearly shows the samples from shell with cement intermediate between samples from uncemented shell and the subset of cement samples that are low in $\delta^{13}C$. The samples from cemented shell appear to be dispersed along a line extending from the cluster of uncemented shell to the low $\delta^{18}O$ and $\delta^{13}C$ ratios of the cement. A linear fit of $y = 0.892x - 4.286$ links both cement and cemented shell with an $r^2 = 0.730$.

In order to properly compare samples from cemented shell, cement, and concretions, it must be determined if a significant difference exists between for each sampling location. A series of paired t-tests for dependent samples, reported in Tables 13-15, seeks to address this issue. All samples are from specimens that contained shell, concretion, and cement (or, in the case of the Game Ranch, externally precipitated cement or recrystallization). Al/Ca was omitted from the analysis of the Kremmling site because of scarce data.

Partly because the standard deviations are relatively low, within the Kremmling data, the difference in the means of K/Ca and Mn/Ca ratios seen in Figure 11B are statistically significant. The smaller difference in means for Sr/Ca of the shell and cement samples implies that, while positioned completely to the right (higher Sr/Ca) of the cement in Figure 12, the shell samples are not statistically distinct. The $\delta^{13}C$ values for shell were significantly heavier than those for cement. When comparing shell to

concretion, the shell was significantly lower in Fe/Ca, K/Ca, Mg/Ca, and significantly higher in Na/Ca and Sr/Ca. Thus, on the Figure 12 Sr/Ca-Mg/Ca cross-plot, the concretions appear as a cluster with higher Mg/Ca and lower Sr/Ca than any of the shell samples. The remainder of the elements can be visually compared using Figure 11B; although this graph shows only the mean values, differences can be easily noted for all statistically significant minor element concentrations except the Na/Ca ratio. There was no significant difference between the isotopic signature of shell and concretion for Kremmling, as can be seen by the intermixed data points in Figure 12.

The only statistically significant difference between and shell and concretion for the Game Ranch, South Dakota, data is lower $\delta^{13}C$ for the concretions. This can be seen in Figure 13 where the data points for the three concretion samples reside clearly below the shell data points. These points are isotopically heavier in $\delta^{18}O$ than the majority of the shell samples, so a fairly high t-score ($t = 1.54$ versus critical $t = 2.132$) results. Other strong relationships include lower Fe/Ca ($t = -2.0$), K/Ca ($t = -1.80$), Mg/Ca ($t = -2.13$), and Mn/Ca ($t = -1.5$) in shell, all with critical $t = -2.13$. The samples of external recrystallization or cement and interior cement compare with both concretions and shell by having much higher mean minor element concentrations, especially Fe/Ca, K/Ca, and Mg/Ca (Figure 11A).

Specimens recovered from Trask Ranch show two types of cements. For simplicity, these will be referred to as the Cement-1 and Cement-2 subsets. Cement-2 samples have lower Al/Ca and Mg/Ca, but higher Sr/Ca, than Cement-1 samples, and appear along the regression line with shell in the isotope cross-plot in Figure 14. A shift towards isotopically lighter $\delta^{13}C$ values is accompanied by a shift towards lighter $\delta^{18}O$ values. Cement-1 samples appear with concretion samples on the aforementioned graph. For these samples, a shift toward isotopically lighter $\delta^{13}C$ values is not correlated with any change in $\delta^{18}O$. Cement-1 samples cannot be distinguished by appearance in hand sample, and use of thin sections would be advantageous for futher study. Using paired t-tests for dependent samples, 0.05 level of significance, cemented shell shows significantly higher Na/Ca and Sr/Ca than Cement-1, as well as lighter $\delta^{18}O$. This shell also has significantly lighter $\delta^{13}C$. Though not statistically significant, the Mn/Ca values were lower for shell ($t = -1.9$ versus critical $t = 2.132$). When compared instead to Cement-2, shell has significantly lower Fe/Ca, Mg/Ca, and Mn/Ca, and higher Na/Ca and Sr/Ca. Other strong relationships include Al/Ca ($t = 1.1$ versus critical $t = 1.860$), which is higher in shell, and Mg/Ca ($t = -1.72$ versus critical $t = -1.860$), which is lower. Isotopically, as shown in Figure 16, shell is significantly heavier than Cement-2 with respect to carbon but shows no significant difference with respect to oxygen ($t = 1.25$ versus critical $t = 1.895$). Lastly, comparing shell from the cemented samples with their concretions, it has lighter $\delta^{13}C$ and heavier $\delta^{18}O$ (as visible in Figure 14); lower Al/Ca, Fe/Ca, K/Ca, Mg/Ca, Mn/Ca; and higher Na/Ca and Sr/Ca. The results for all of these comparisons, with the exception of Sr/Ca, are statistically significant.

FIGURE 10— Radar Charts for Minor Elements in Cemented and Uncemented Shell

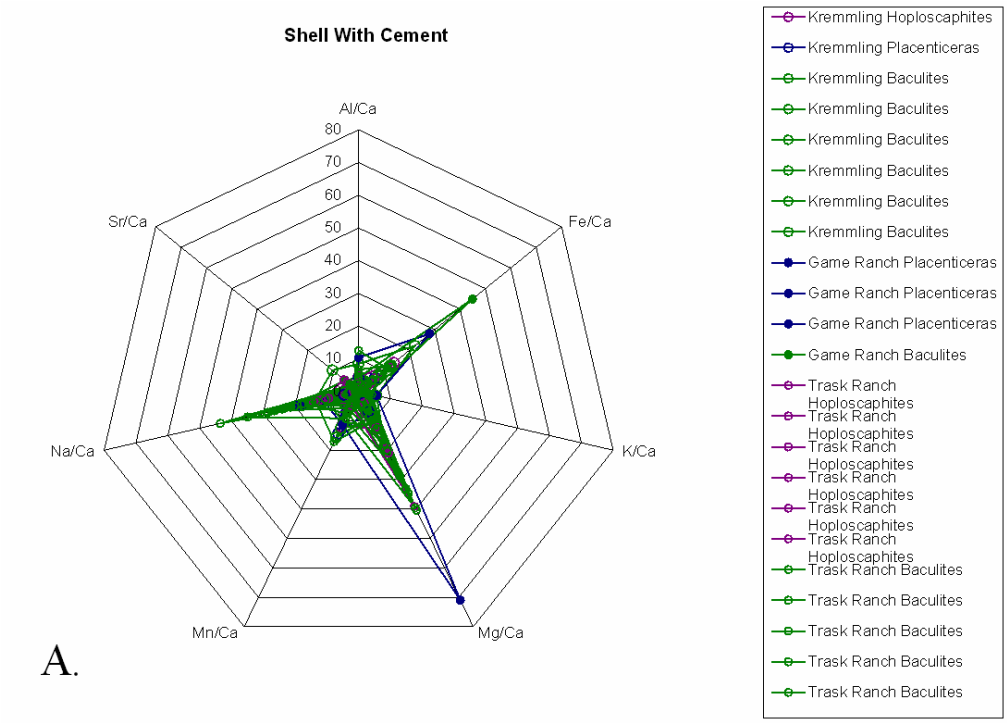

A.

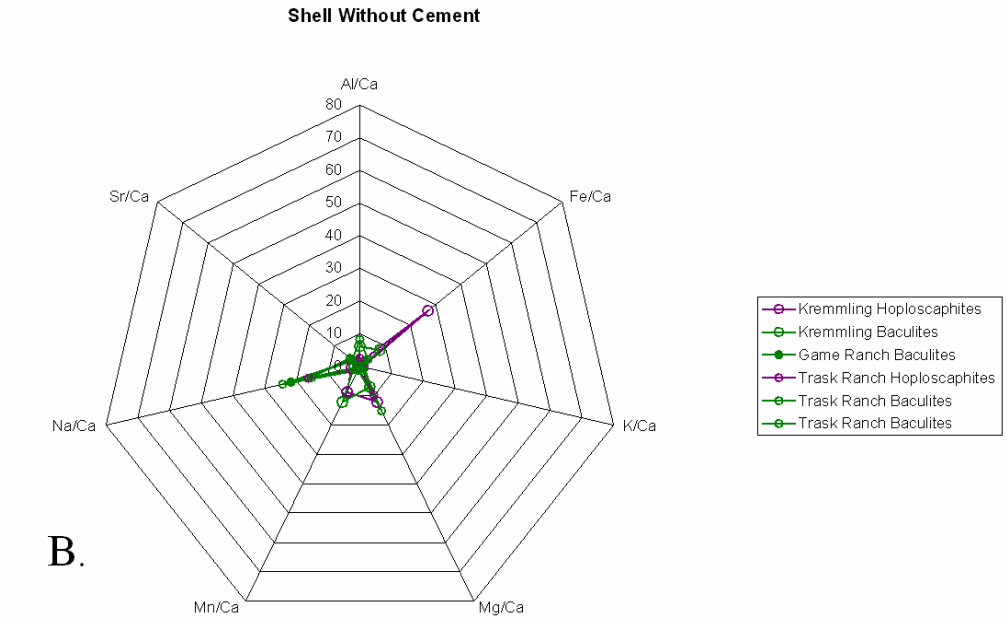

B.

Cemented shell appears to have higher possible concentrations of Fe, Mg, and Na. However, because n = 7 for the uncemented specimens in the "Cementation" suite, the dataset must be expanded into other suites to make more robust comparisons.

FIGURE 11—Minor Element Content of "Cementation Suite" Samples

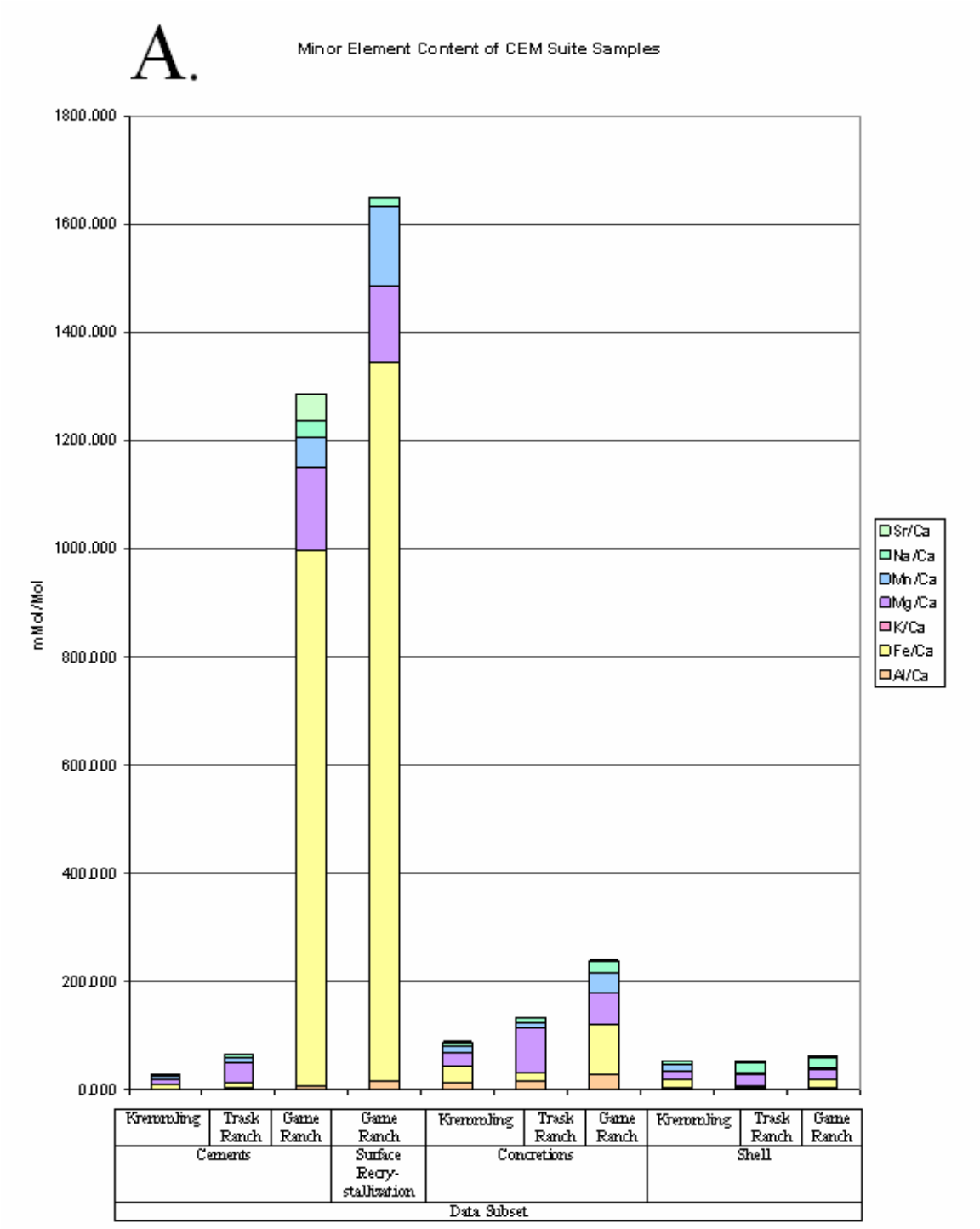

Figure 11A shows a very large enrichment in Fe/Ca, Mg/Ca, and Mn/Ca ratios for cements and external recrystallization or cement from the Game Ranch locality.

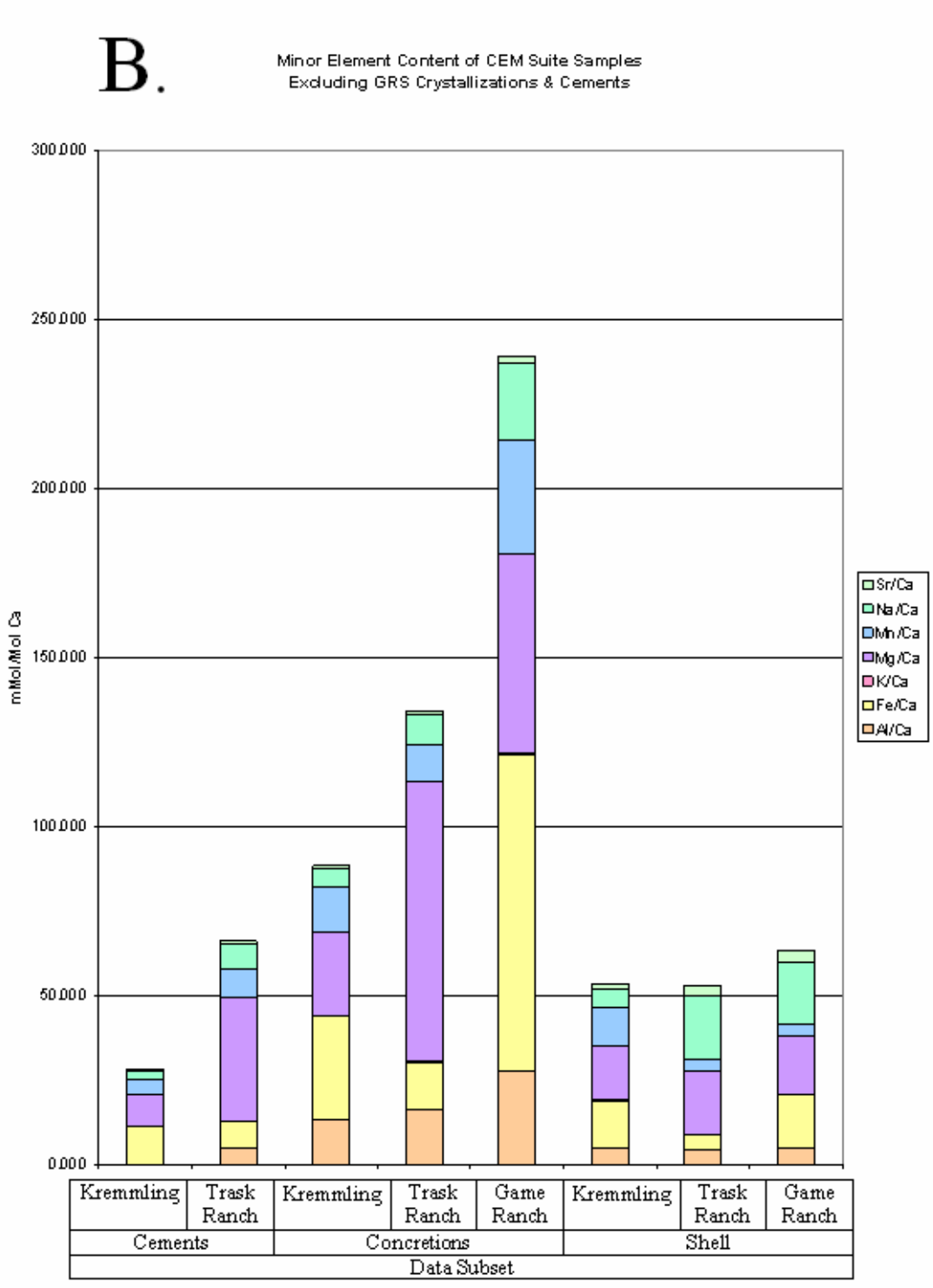

Figure 11B eliminates the Game Ranch interior cement and external recrystallization or cement samples, so the minor element ratios of the other cementation suite materials become apparent. There are higher Mg/Ca ratios, and sometimes Fe/Ca ratios, in concretions than in shell.

TABLE 12—Summary of Statistical Tests on Cemented and Uncemented Shell

Alternate Hypothesis	Type of Test	N	Means, ± standard deviations	Calculated Value(s)	Critical Value (0.05 significance)	Result
Lighter mean $\delta^{13}C$ in cemented shells?	one-tailed t test	100u, 30c	u: -3.45 ± 4.85 c: -7.065 ± 3.410	t = 3.80	t = 1.656	H_o rejected
Lighter mean $\delta^{18}O$ in cemented shells?	one-tailed t test	100u, 30c	u: -5.80 ± 5.27 c: -5.62 ± 5.00	t = -0.169	t = 1.656	H_o retained
Lower mean Al/Ca in uncemented specimens?	one-tailed t test	59u, 27c	u: 5.4 ± 5.9 c: 4.2 ± 3.1	t = 0.93	t = -1.663	H_o retained
Lower mean Fe/Ca in uncemented specimens?	one-tailed t test	101u, 36c	u: 8.8 ± 15.5 c: 8.1 ± 9.2	t = 0.2	t = -1.656	H_o retained
Lower mean K/Ca in uncemented specimens?	one-tailed t test	106u, 37c	u: 1.76 ± 1.82 c: 1.89 ± 1.34	t = -0.41	t = -1.656	H_o retained
Lower mean Mg/Ca in uncemented specimens?	one-tailed t test	106u, 37c	u: 11.5 ± 12.4 c: 18.1 ± 15.2	t = -2.63	t = -1.656	H_o rejected
Lower mean Mn/Ca in uncemented specimens?	one-tailed t test	101u, 37c	u: 5.5 ± 5.2 c: 6.0 ± 5.2	t = -0.48	t = -1.656	H_o retained
Higher mean Na/Ca in uncemented specimens?	one-tailed t test	106u, 37c	u: 16.9 ± 9.9 c: 15.1 ± 9.5	t = 0.96	t = 1.656	H_o retained
Higher mean Sr/Ca in uncemented specimens?	one-tailed t test	106u, 37c	u: 3.0 ± 2.8 c: 2.8 ± 1.9	t = 0.36	t = 1.656	H_o retained

The cemented shell shows lighter $\delta^{13}C$ and higher Mg/Ca ratios than uncemented shell. For all other tests, the null hypothesis of no significant difference in mean minor element concentrations or isotopic values between cemented and uncemented shell must be retained. Beyond the level of statistical significance, cemented shell shows lower Na/Ca and higher Al/Ca than uncemented shell. All isotope ratios reported in ‰ versus PDB and all minor element ratios reported in mMol/Mol calcium.

FIGURE 12—Comparison of Cements, Concretions, and Shell Material for Kremmling

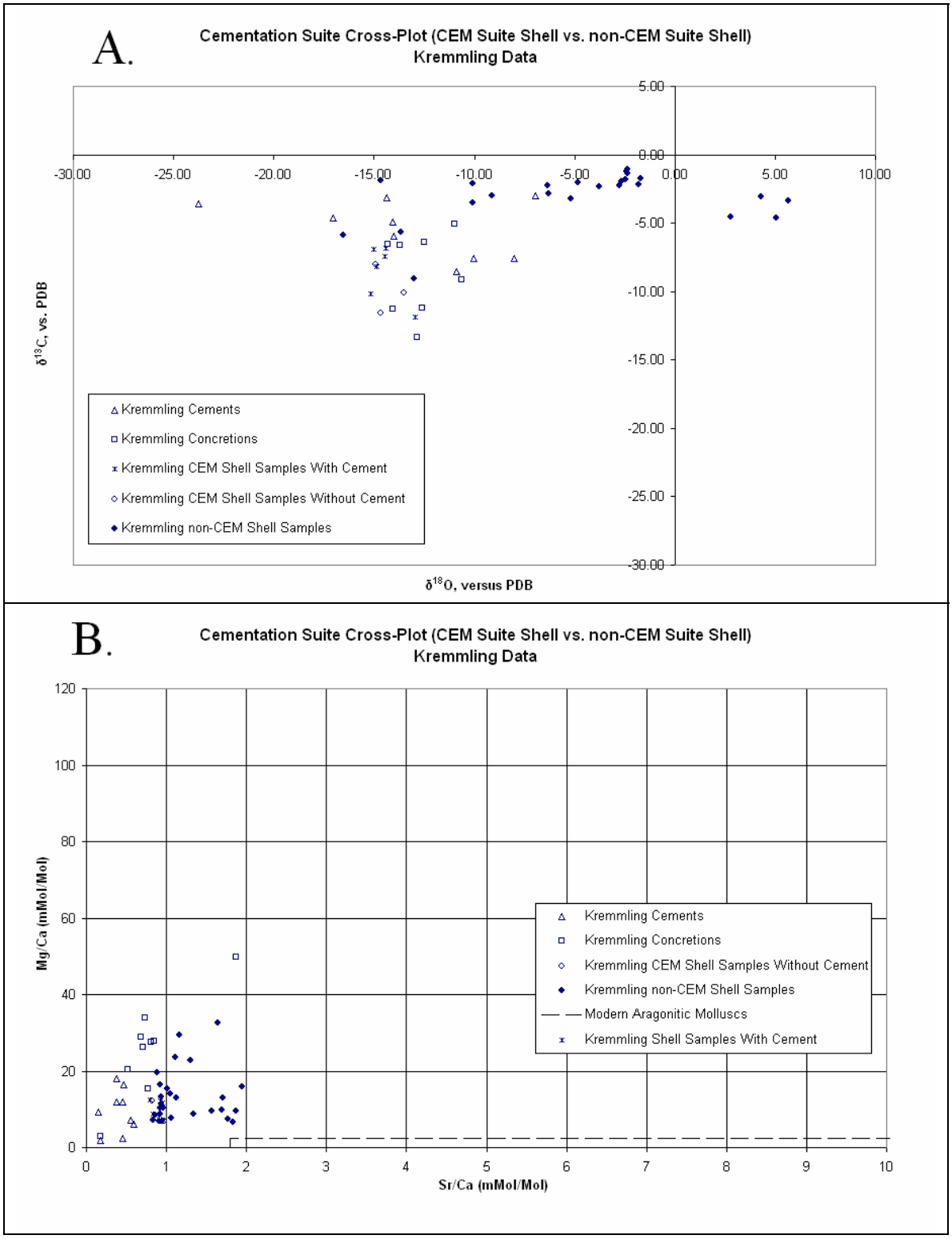

FIGURE 13—Comparison of External Recrystallizations or Cements, Concretions, and Shell Material for Game Ranch

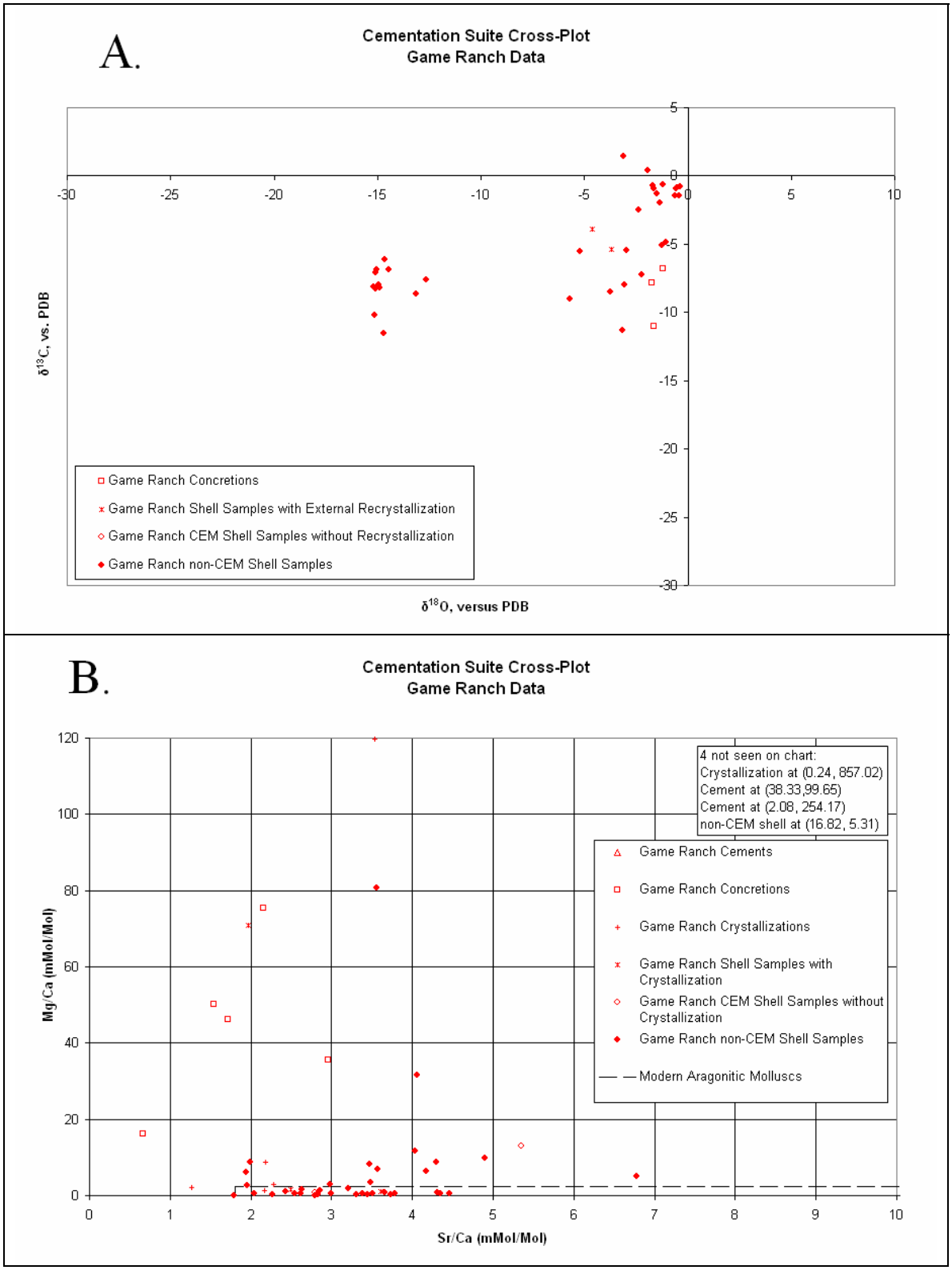

FIGURE 14—Comparison of Cements, Concretions, and Shell Material for Trask Ranch

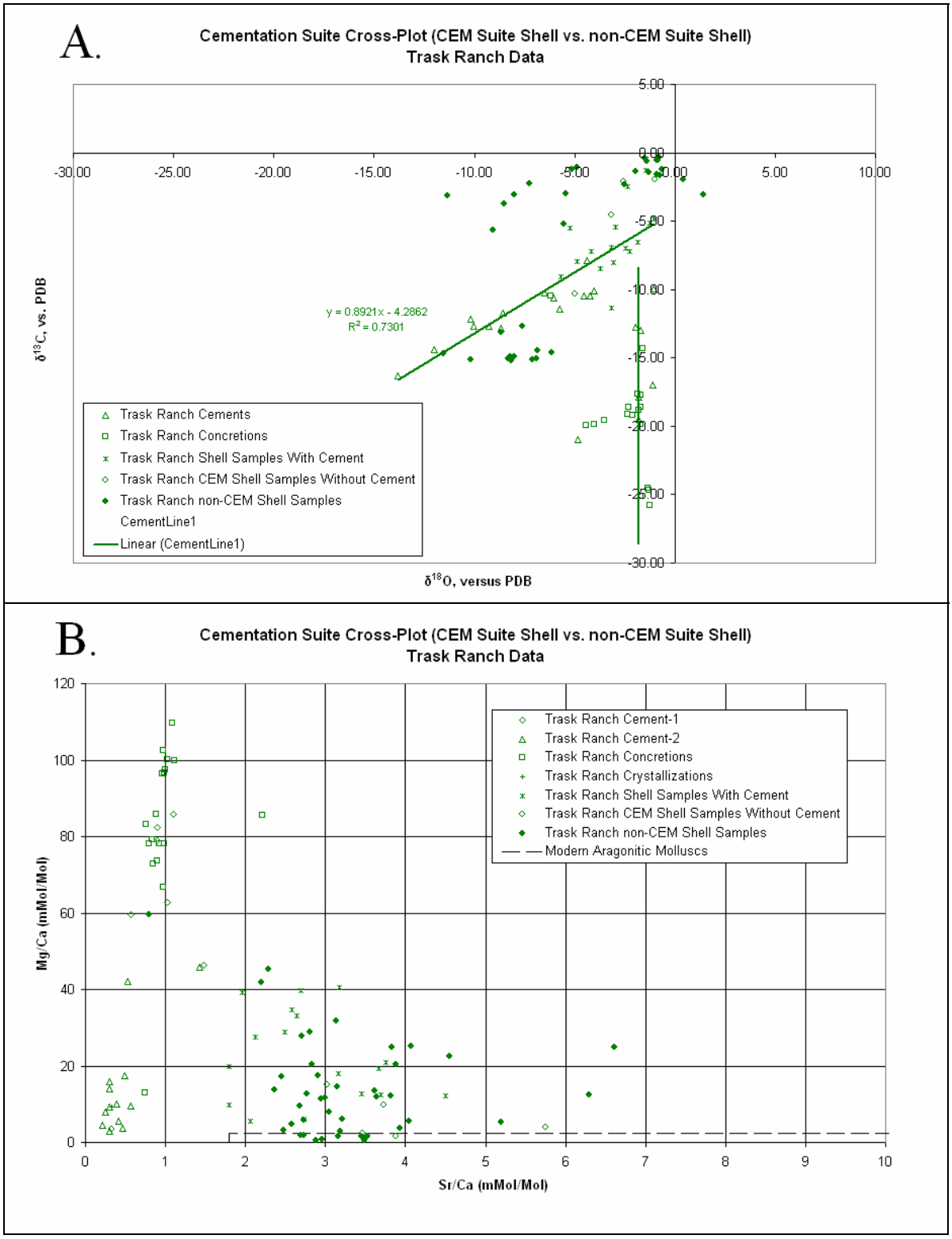

TABLE 13—Statistical Tests for Kremmling Cements, Concretions, and Shell

Alternate Hypothesis	Type of Test	N	Means, ± standard deviations	Calculated Value(s)	Critical Value (0.05 signif.)	Result
Heavier mean $\delta^{13}C$ in shell?	paired t-tests (dependent samples)	8s, 8co, 8ce	s: -5.45 ± 2.03 co: -9.01 ± 3.01 ce: -8.64 ± 1.99	t(s-co) = -0.433 t(s-ce) = -3.11	t(s-co) = -1.895 t(s-ce) = -1.895	H_o retained H_o rejected
Heavier mean $\delta^{18}O$ in shell?	paired t-tests (dependent samples)	8s, 8co, 8ce	s: -13.52 ± 5.74 co: -12.49 ± 1.28 ce: -13.00 ± 3.83	t(s-co) = -0.909 t(s-ce) = -0.476	t(s-co) = -1.895 t(s-ce) = -1.895	H_o retained H_o retained
Lower mean Fe/Ca in shell?	paired t-tests (dependent samples)	8s, 8co, 8ce	s: 12.9 ± 6.4 co: 19.4 ± 10.6 ce: 11.5 ± 5.1	t(s-co) = -2.8 t(s-ce) = -0.49	t(s-co) = -1.895 t(s-ce) = -1.895	H_o rejected H_o retained
Lower mean K/Ca in shell?	paired t-tests (dependent samples)	8s, 8co, 8ce	s: 0.67 ± 0.12 co: 4.58 ± 2.11 ce: 1.78 ± 1.63	t(s-co) = -3.6 t(s-ce) = 2.0	t(s-co) = -1.895 t(s-ce) = -1.895	H_o rejected H_o rejected
Lower mean Mg/Ca in shell?	paired t-tests (dependent samples)	8s, 8co, 8ce	s: 10.4 ± 5.3 co: 21.3 ± 9.8 ce: 11.2 ± 3.5	t(s-co) = -2.8 t(s-ce) = 0.48	t(s-co) = -1.895 t(s-ce) = -1.895	H_o rejected H_o retained
Lower mean Mn/Ca in shell?	paired t-tests (dependent samples)	8s, 8co, 8ce	s: 4.4 ± 1.5 co: 11.7 ± 3.2 ce: 11.20 ± 4.57	t(s-co) = -0.33 t(s-ce) = 4.8	t(s-co) = -1.895 t(s-ce) = -1.895	H_o retained H_o rejected
Higher mean Na/Ca in shell?	paired t-tests (dependent samples)	8s, 8co, 8ce	s: 2.4 ± 0.6 co: 4.24 ± 1.52 ce: 5.47 ± 4.35	t(s-co) = 4.4 t(s-ce) = 2.1	t(s-co) = 1.895 t(s-ce) = 1.895	H_o rejected H_o rejected
Higher mean Sr/Ca in shell?	paired t-tests (dependent samples)	8s, 8co, 8ce	s: 0.4 ± 0.1 co: 0.65 ± 0.22 ce: 2.08 ± 3.32	t(s-co) = 3.3 t(s-ce) = 1.4	t(s-co) = 1.895 t(s-ce) = 1.895	H_o rejected H_o retained

At the Kremmling site, significant differences were found between concretions and shell, or cement and shell, for most minor elements. The only statistically significant difference in stable isotopes was heavier $\delta^{13}C$ in shell versus cement. The null hypothesis, that there is no significant difference between shell and concretion, and between shell and cement, was retained for all other isotopic comparisons and some minor element comparisons. All isotope ratios reported in ‰ vs.PDB; all minor element ratios reported in mMol/Mol.

TABLE 14—Statistical Tests for Game Ranch Concretions and Shell

Alternate Hypothesis	**Type of Test**	**N**	Means, ± standard deviations	**Calculated Value(s)**	**Critical Value (0.05 significance)**	**Result**
Heavier mean $\delta^{13}C$ in shell?	paired t-tests (dependent samples)	5s, 5co	s: -1.91 ± 1.67 co: -10.85 ± 4.93	t(s-co) = -2.51	t(s-co) = -2.132	H_o rejected
Heavier mean $\delta^{18}O$ in shell?	paired t-tests (dependent samples)	5s, 5co	s: -2.68 ± 0.82 co: -1.56 ± 0.25	t(s-co) = 1.54	t(s-co) = -2.132	H_o retained
Lower mean Al/Ca in shell?	paired t-tests (dependent samples)	2s, 2co	s: 5.4 ± 7.0 co: 21.9 ± 21.4	t(s-co) = -1.8	t(s-co) = -6.314	H_o retained
Lower mean Fe/Ca in shell?	paired t-tests (dependent samples)	5s, 5co	s: 8.1 ± 13.3 co: 80. ± 72	t(s-co) = -2.0	t(s-co) = -2.132	H_o retained
Lower mean K/Ca in shell?	paired t-tests (dependent samples)	5s, 5co	s: 2.21 ± 2.31 co: 12.3 ± 10.5	t(s-co) = -1.80	t(s-co) = -2.132	H_o retained
Lower mean Mg/Ca in shell?	paired t-tests (dependent samples)	5s, 5co	s: 18.6 ± 34.9 co: 51.9 ± 16.9	t(s-co) = -2.13	t(s-co) = -2.132	H_o retained
Lower mean Mn/Ca in shell?	paired t-tests (dependent samples)	5s, 5co	s: 3.5 ± 5.2 co: 22.0 ± 14.3	t(s-co) = -1.5	t(s-co) = -2.132	H_o retained
Higher mean Na/Ca in shell?	paired t-tests (dependent samples)	5s, 5co	s: 17.4 ± 4.4 co: 18.7 ± 12.2	t(s-co) = -0.39	t(s-co) = 2.132	H_o retained
Higher mean Sr/Ca in shell?	paired t-tests (dependent samples)	5s, 5co	s: 2.71 ± 0.69 co: 2.09 ± 0.63	t(s-co) = -0.89	t(s-co) = 2.132	H_o retained

Among the Game Ranch samples, no significant differences were found between concretions and shell for minor elements. Several minor elements, however, approached statistical significance: Al/Ca, Fe/Ca, K/Ca, Mg/Ca, and Mn/Ca, all of which were higher in concretions. Heavier $\delta^{13}C$ occurred in shell versus concretions. The remainder of comparisons did not allow for the statistical rejection of the null hypothesis, no difference between isotopic values and minor element concentrations between shell material and concretions. All isotope ratios reported in ‰ versus PDB and all minor element ratios reported in mMol/Mol calcium.

TABLE 15—Statistical Tests for Trask Ranch Cements, Concretions, and Shell

Alternate Hypothesis	Type of Test	N	Means, ± std. deviations	Calculated Value(s)	Critical Value (0.05 signif.)	Result
Heavier mean $\delta^{13}C$ in shell?	paired t-tests (dep. samples)	14s, 14co, 5ce1, 8ce2	s: -7.96 ± 3.15 co: -19.85 ± 4.11 ce1: -12.12 ± 3.96 ce2: -13.28 ± 3.63	t(s-co) = 2.72 t(s-ce1) = 2.18 t(s-ce2) =1.25	t(s-co) = 1.771 t(s-ce1) = 2.132 t(s-ce2) = 1.895	H_o rejected H_o rejected H_o retained
Heavier mean $\delta^{18}O$ in shell?	paired t-tests (dep. samples)	14s, 14co, 5ce1, 8ce2	s: -3.21 ± 1.04 co: -2.59 ± 1.53 ce1: -5.29 ± 3.88 ce2: -4.63 ± 3.48	t(s-co) = -1.85 t(s-ce1) = 1.41 t(s-ce2) = 0.33	t(s-co) = 1.771 t(s-ce1) = 2.132 t(s-ce2) = 1.895	H_o rejected H_o retained H_o retained
Lower mean Al/Ca in shell?	paired t-tests (dep. samples)	14s, 14co, 5ce1, 9ce2	s: 4.0 ± 3.3 co: 15.4 ± 8.4 ce1: 5.6 ± 8.4 ce2: 2.2 ± 2.7	t(s-co) = -3.7 t(s-ce1) = 0.49 t(s-ce2) = 1.1	t(s-co) = -1.771 t(s-ce1) = -2.132 t(s-ce2) = -1.860	H_o rejected H_o retained H_o retained
Lower mean Fe/Ca in shell?	paired t-tests (dep. samples)	15s, 15co, 5ce1, 9ce2)	s: 4.4 ± 3.5 co: 13.7 ± 3.1 ce1: 7.3 ± 4.9 ce2: 8.0 ± 4.1	t(s-co) = -4.2 t(s-ce1) = -0.48 t(s-ce2) = -1.9	t(s-co) = -1.761 t(s-ce1) = -2.132 t(s-ce2) = -1.860	H_o rejected H_o retained H_o rejected
Lower mean K/Ca in shell?	paired t-tests (dep. samples)	15s, 15co, 5ce1, 9ce2	s: 1.78 ± 1.00 co: 4.98 ± 1.58 ce1: 1.60 ± 1.87 ce2: 1.55 ± 0.81	t(s-co) = -4.0 t(s-ce1) = 0.50 t(s-ce2) = 0.33	t(s-co) = -1.761 t(s-ce1) = -2.132 t(s-ce2) = -1.860	H_o rejected H_o retained H_o retained
Lower mean Mg/Ca in shell?	paired t-tests (dep. samples)	15s, 15co, 5ce1, 9ce2	s: 23.0 ± 12.8 co: 79 ± 24 ce1: 29.6 ± 35.0 ce2: 32.0 ± 23.7	t(s-co) =-4.73 t(s-ce1) = 0.05 t(s-ce2) = -1.72	t(s-co) = -1.761 t(s-ce1) = -2.132 t(s-ce2) = -1.860	H_o rejected H_o retained H_o retained
Lower mean Mn/Ca in shell?	paired t-tests (dep. samples)	15s, 15co, 5ce1, 9ce2	s: 3.53 ± 2.56 co: 11.2 ± 7.2 ce1: 10.0 ± 6.7 ce2: 6.9 ± 4.1	t(s-co) = -3.1 t(s-ce1) = -1.9 t(s-ce2) = -4.4	t(s-co) = -1.761 t(s-ce1) = -2.132 t(s-ce2) = -1.860	H_o rejected H_o retained H_o rejected
Higher mean Na/Ca in shell?	paired t-tests (dep. samples)	15s, 15co, 5ce1, 9ce2	s: 18.7 ± 10.0 co: 9.4 ± 3.9 ce1: 5.99 ± 3.03 ce2: 11.25 ± 13.81	t(s-co) = 3.5 t(s-ce1) = 2.55 t(s-ce2) = 2.22	t(s-co) = 1.761 t(s-ce1) = 2.132 t(s-ce2) = 1.860	H_o rejected H_o rejected H_o rejected
Higher mean Sr/Ca in shell?	paired t-tests (dep. samples)	14s, 14co, 5ce1, 9ce2	s: 3.27 ± 0.97 co: 0.89 ± 0.09 ce1: 0.50 ± 0.35 ce2: 0.59 ± 0.39	t(s-co) = -0.60 t(s-ce1) = 20. t(s-ce2) = 7.5	t(s-co) = 1.771 t(s-ce1) = 2.132 t(s-ce2) = 1.860	H_o retained H_o rejected H_o rejected

Statistically significant differences for the Trask Ranch site include Sr/Ca for the shell versus cements, $\delta^{13}C$ and $\delta^{18}O$ for the shell versus concretions, and Na/Ca for both. Most other comparisons resulted in the retention of the null hypothesis, no significant difference in the mean isotopic value or minor element concentration between shell and concretion or shell and cement. All isotope ratios reported in ‰ versus PDB and all minor element ratios reported in mMol/Mol calcium.

2.4 Discussion

2.4.1 Review of Sample Suites: In the "Mode of Preservation" suite, enrichment outliers in aluminum, iron, manganese, and strontium were present in the shell material found within the concretions. Furthermore, the concretions had statistically significant higher mean Fe/Ca and Mg/Ca, with a strong (but not statistically significant) relationship between mode of preservation and Mn/Ca ratio. Enrichment in Fe/Ca and Mn/Ca is a diagenetic signature indicative of interaction with meteoric waters (Veizer and Fritz, 1976) or cementation associated with methane seeps (Krause et al., 2003). Therefore, the ammonite specimens preserved in shale are less altered. Buchardt (1977) explains the superior preservation in shale as due to retention of the organic matrix in the low-permeability, chemically reducing environment. Another idea is that the formation of the concretion, itself a chemical phenomenon, sometimes significantly alters the shell that it precipitates around, partially dissolving the shell and reprecipitating the calcium carbonate as calcite within the shell microstructure. The precipitated calcite would have a minor element and isotopic signature between that of pure shell and that of the diagenetic fluid. Thus, taking samples only from the interior of concretions may minimize the effect of chemical weathering when concretions are exposed at the surface, but can do nothing to address early diagenetic alteration. Veizer and Fritz (1976) offer a manganese-based alteration equation to estimate the "degree of alteration" from diagenesis:

$$\text{Degree of alteration (\%)} = \frac{(Mn_{shell} - Mn_{equilibrium}) \times 100}{Mn_{enclosing\ rock\ carbonate} - Mn_{equilibrium}} \quad (4)$$

Using this equation, the average degree of alteration for the samples taken from shell

preserved in concretions was 33.3% ± 37.4%, whereas the average degree of alteration for shell preserved in shale was 5.6% ± 9.1%. These figures should be regarded as general estimates because the "Mode of Preservation" suite did not contain samples of the concretions themselves, so an average Mn/Ca values for each locality, calculated from the "Cementation" suite data, was used. The effect of such alteration on isotopic signals is statistically significant for $\delta^{18}O$, and nearly so for $\delta^{13}C$. Therefore, shale should be the preferred source for shell material used in $\delta^{18}O$ paleotemperature and $\delta^{13}C$ productivity/diet calculations. A third idea, supported by further data in the "Cementation" suite, is that cements found in the concretions are formed by the same diagenetic fluids that cause shell alteration. There was no statistically significant difference in the mean concentrations of Na/Ca (~16 mMol/Mol), K/Ca (~0.8 mMol/Mol) or Sr/Ca (~3mMol/Mol) with respect to mode of preservation. The independence of concentrations of these elements from lithology suggests that shell from both concretions and shale could be used in paleosalinity calculations.

In the "Shell Sampling Location" suite, ammonite septa and adjacent phragmacone were found to commonly display very different isotopic signatures. The $\delta^{18}O$ values of the septum-phragmacone pairs were significantly different at the 0.05 significance level, whereas the $\delta^{13}C$ values were not. With a sample size of only ten pairs available, clearly, a larger sample size is needed to resolve this issue. Mann (1992) found greater concentrations of Mg/Ca and Sr/Ca in *Nautilus* septa than in phragmacone. If true for the ammonite samples, this could indicate the influence of mineral-rich extrapallial fluid in shell precipitation. Alternately, higher Mg/Ca but lower Sr/Ca in the septa could indicate diagenetic alteration. The septa of ammonites are frequently

cemented to a greater degree than the phragmacone, and these cements, as Figures 12 and 14 illustrate, are lighter in $\delta^{18}O$ than the shell they precipitate upon. Differences in the minor element compostion of septa versus phragmacone shell, however, are minimal, so neither extrapallial fluid nor cementation is likely the cause of the isotopic disparity in this dataset. Paleosalinity calculations could therefore be performed on septa or phragmacone samples. Nearly all septa – in *Placenticeras, Hoploscaphites*, and *Baculites* – have isotopically lighter $\delta^{18}O$ than the phragmacone samples. The depression of $\delta^{18}O$ along the septum is consistent with the highly negative $\delta^{18}O$ signature of *Nautilus* metabolic CO_2, which contributes 0-10% of shell carbonate in Recent mollusks (Auclair et al., 2004). However, in a study of aquarium-raised *Nautilus*, Landman et al. (1994) demonstrated that temperatures coincident with the temperature range of the aquarium could be derived from the shell $\delta^{18}O$ signature. Another suggestion is the time averaging inherent in the formation of a septum. A septum in wild, immature *Nautilus* may take from 23 to 75 days to precipitate (Cochran et al., 1981), while 0.2 mm of shell takes 17 to 30 days (Saunders, 1983). The onset of septal formation, coincident with the phragmacone samples in this study, could be at times of relatively lower temperature than the average temperature during the spans of time over which the septa were precipitated. Isotopically light $\delta^{13}C$ could also be a sign of metabolism, as ontogenetically young, small mollusks with a high metabolic rate accumulate more of the lighter isotope derived from food (Mitchell et al., 1994). Because $\delta^{13}C$ does not vary between septa and phragmcone, however, it may be possible to extract reasonable productivity/food source data from septa.

In the "Shell Color" suite, the assertations of researchers (e.g., Forester et al.,

1977; Tsujita and Westermann, 1998) who advocate a preference for opalescent shell were supported slightly. Opalescent shell did tend to possess a lower Mg/Ca ratio, with magnesium being an indicator of the presence of secondary calcitic cement, while non-opalescent shell often was depleted in strontium. Strontium depletion will lead to erroneous paleosalinity values, so should be avoided in studies that include paleosalinity using the equation of Brand (1986). Opalescent shell also had isotopically heavier $\delta^{18}O$, which might be less altered because both diagenetic cement and meteoric water have lighter $\delta^{18}O$ than shell material. However, neither of these findings is statistically significant, despite n = 55 (all locations) and n = 38 (South Dakota locations only). Only when Colorado data was removed did the differences in K/Ca and Mn/Ca ratios relate to color class. The only element to vary significantly with color, regardless of collection site, was magnesium (see Figure 9), which tends to be found at higher relative concentrations in yellow, orange, and brown shell material. In particular, the relationship between color class and $\delta^{13}C$ was weak, suggesting that any color of shell could be used in productivity/food source studies.

In the "Cementation" suite, a comparison of cemented and uncemented shell material revealed a significant difference in only $\delta^{13}C$. Cemented shell, therefore, may be used in paleosalinity and paleotemperature reconstructions, but not productivity/food source ones. At the Trask Ranch site, the isotopic signature of the cements which form a linear trend with the altered shell is consistant with second-order cements, having formed by waters of meteroric origin late after deposition (Wright, 1987). These findings conflict directly with the shell alteration model of Veizer and Fritz (1976), which uses the carbonate fraction of the rock (i.e., the concretion) as the composition of the diagenetic

fluid which determined manganese and/or iron enrichment. Therefore, for this locality, the shell alteration equation of Veizer and Fritz (1976) should be modified:

$$\text{Degree of alteration (\%)} = \frac{(Mn_{shell} - Mn_{equilibrium}) \times 100}{Mn_{second\ order\_cement} - Mn_{equilibrium}} \quad (5)$$

Application of this modified equation, with $Mn_{equilibrium}$ = 15 ppm for seawater, to Trask Ranch shell data which have associated secondary cement and concretion values, yields a higher average percent altered (57%) for the cement calculation than for the concretion calculation (43%). Because this figure is an estimation of the percent secondary calcite present in a shell sample, it can be correlated with the actual percentage of calcite, as determined by X-ray diffraction, as part of a future study. The isotopic signature of the other cements at the Trask Ranch is consistent with first-order cements, formed by marine waters during early diagenesis (Brand, 1994). The first-order cements, which have the same $\delta^{18}O$ and $\delta^{13}C$ signatures as the concretions and a marine isotopic signature, do not appear to have altered shell associated with them. The matrix within the Trask Ranch concretions has slightly negative $\delta^{18}O$ values and very negative $\delta^{13}C$ values (-14 to -25‰), similar to those documented for ammonite-bearing concretions from the Late Cretaceous of eastern Siberia (Teys et al., 1978). The values are also similar to those of cements precipitated under conditions of methane oxidation and sulfate reduction for the Gulf of Mexico during the Pleistocene (Howard et al., 2005), and are similarly high in magnesium and iron. The concretions and cements of the Game Ranch locality are even higher in iron and magnesium, enough to classify them as very-high-magnesium or iron-calcites (Howard et al., 2005). Again, this is characteristic of depositional environments where methane is being oxidized and sulfate reduced. More

shell material with cementation is also needed, as cementation was an uncommon phenomenon (n = 2 for n = 40 shell samples) in Game Ranch specimens. Exterior crystallization upon the shells had the same minor element and oxygen isotope signature as shell, and thus likely represented recrystallization of the shell rather than a secondary calcite precipitated from a late diagenetic fluid. Concretions had isotopic signatures of -6‰ to -11‰ and -1‰ to -2‰ for $\delta^{18}O$ and $\delta^{13}C$, respectively. The $\delta^{18}O$ values, heavier than those for Trask Ranch, were equivalent to those reported for a Turonian Western Interior Seaway dataset (Pagani and Arthur, 1998).

Conceivably, the South Dakota concretions were formed from sediment and shell at the bottom of the Western Interior Seaway, perhaps initiated by the interface between an isotopically unusual bottom water and the slightly brackish but isotopically normal seawater above. Because of low oxygen, the presence of methane and sulfur, and rapid sedimentation vertebrate and crustacean predators did not disturb the organisms' remains. Instead, an anaerobic bacterial community, drawn to the organic matter accumulation, thrived. These bacteria produced methane and sulfur compounds. The isotopic signatures of the cements are clearly marine, so the effect from bacterial metabolism on the $\delta^{18}O$ value of the cement and concretions is likely negligible. The low carbon values of the concretions and infaunal organisms (*Drepanocheilus* and *Anisomyon*) are consistent with the accumulation of methane in the sediment pore spaces. A study of the sulfur present in shell, concretion, and cement, which is not possible with the ICP-OES system but could be performed by electron microprobe, could help establish the dynamics of such an ecosystem, as would observation of Recent anaerobic communities. There was, at least occasionaly, a large amount of sulfur in the Western Interior Seaway

because of large pyrite crystals and pyrite-replaced ammonites found in the Pierre Shale in Colorado. Regardless of the proportion of each bacterial type on the seafloor of the Western Interior Seaway, the products from the oxidation of methane and the reduction of sulfate are acidic, and could begin dissolving shell and reprecipitating it as cement to form the start of a concretion. Once the concretion begins growing, it could incorporate calcite from surrounding pore water, producing the characteristic isotopic values. However, this microbially favorable environment came to an end with the Western Interior Seaway, the shale containing concretions was exposed to meteoric water, and diagenetic fluids derived from it penetrated the concretions along planes of weakness, such as dewatering cracks and the fossils themselves. Under this hypothesis, the "septarian" calcites which cross through the concretions should return signatures as Cement-2, influenced by meteoric water.

Lastly, at Kremmling, Colorado, the concretions had a $\delta^{18}O$ signature similar to the Game Ranch concretion specimens, along with an isotopically light $\delta^{13}C$ signature (-5‰ to -15‰) on the order of that in meteoric water. Because the isotopic signature of the Kremmling, Colorado, cements is identical to that of the concretions, the cement is likely first-order and thus precipitated from the same fluids that cemented the concretions. Shell material was similar to both concretions and cements in terms of isotopic composition, and appears to follow a J-shaped curve characteristic of alteration by meteoric water. Because Kremmling, Colorado, was a nearshore environment, continued regression during or slightly after the *Baculites compressus/cuneatus* biozones could have exposed the seafloor, even before the concretions fully lithified. This would explain the consistent, thorough alteration of the shell, especially the depletion in Sr/Ca

and Na/Ca, which are present in much smaller concentrations in freshwater than in saltwater. The shell nonetheless differed from concretions and cement in its minor element composition, with significantly lower Fe/Ca, K/Ca, and Mg/Ca ratios than cement, higher Na/Ca and Sr/Ca ratios than cement, and lower K/Ca and Mn/Ca, and higher Na/Ca ratios than concretions. In summary, the variety of isotopic signatures of concretions and cements across the *Baculites compressus/cuneatus* biozones suggest localized diagenetic environments. In terms of minor elements, second-order cementation appears to have the strongest influence on shell light stable isotope chemistry, whereas concretion formation and first-order cements also influence the minor element concentration but appear to have less of an effect on isotopic signature of the shell material.

2.4.2 Utility of a Minor Element Alteration Indicator:

With data from all four suites, an evaluation of the utility of a minor-element alteration indicator may be established. Appropriate minor elements to select should be those that, above or below a certain limit, correlate with unusually light isotopic values. The only minor element ratio that does so for both $\delta^{18}O$ and $\delta^{13}C$ is Mg/Ca. The Mg/Ca dataset has the added advantage of being more complete than the Fe/Ca and Mn/Ca datasets. For the $\delta^{18}O$ data, the Sr/Ca ratio also produces a fairly clear fit, among the minor elements that appear be linked to unusually light isotopes (Figure 15). Therefore, a Sr/Ca-Mg/Ca filter is proposed. The use of Sr/Ca was also proposed by Elorza and García-Garmilla (1996) in their study of aragonitic and calcite layers of *Inoceramus* specimens from Spain. For the Western Interior Seaway, the data of Pagani and Arthur (1998) support the use of magnesium as an indicator of alteration. Their figures comparing minor element ratios with visually assessed shell preservation compared to Recent *Nautilus*, show Mg/Ca as the best discriminator between well-preserved and poorly-preserved shell. In contrast, the fields for Fe/Ca and Mn/Ca content show significant proportions of the better-preserved shell outside the limits defined by *Nautilus* (Pagani and Arthur, 1998). Limits for these could be more conservatively based on the full spectrum of Recent aragonitic shell—including habitats worldwide and representatives of Bivalvia, Gastropoda, and Cephalopoda—as given in Buchardt and Weiner (1981), instead of only *Nautilus*, which lives, at least for part of its life, in a deep-water habitat that was nonexistent in the Western Interior Seaway. It is unlikely that Western Interior Seaway mollusks secreted shell with higher minor element concentrations than mollusks today. In life, mollusks discriminate against both Mg and

Sr in proportion with the concentration of these elements in seawater (Dodd, 1967). The chemistry of first-order marine cements in this study is unusual for the Late Cretaceous, which, based on oolitic limestones and first-order marine cements worldwide, generally had a high overall concentration of Ca in the water and low Mg/Ca ratios (Stanley and Hardie, 1998). Using halites, Trimofeff et al. (2006) demonstate that the Mg/Ca ratios in seawater were low in the Late Cretaceous compared to the present, though the authors calculate that the Early Cretaceous concentrations were even lower. Also, the geochemistry of waters formed under different oxygenation conditions would have influenced shell geochemistry. The Western Interior Seaway, at least in proximity to the sediment-water interface, was often dysoxic, as evidenced by the predominance of black shales. Therefore, the minor element concentrations of the concretions and cements may reflect unique geochemical conditions within the sediments at the bottom of the Western Interior Seaway. Because of this, an empirical filter based on observations of anomalous $\delta^{18}O$ signatures, derived from Figure 15, is used. These values appear for Mg/Ca > 6.5 mMol/Mol, above the 2.5 mMol/Mol limit for Recent aragonitic molluscan shell material and Sr/Ca < 1.8 mMol/Mol, equivalent to the lower limit for Recent aragonitic molluscan shell (Buchardt and Weiner, 1981). Because higher Mg/Ca ratios than Recent shells are unlikely for the Late Cretaceous, the Mg/Ca acceptability level most likely represents a threshold above which the shell has interacted with mineral-rich diagenetic fluids enough to be isotopically altered and a most-conservative range for the possible minor-element ratios for Cretaceous shell material.

After applying the modified minor element filter described above to all data, when comparing the unfiltered isotopic data (Figure 16) with the filtered isotopic data (Figure 18A), several observations can be made. The first is that the filter eliminates the vast majority of data points, including the entire suite of Kremmling, samples. Data points for both $\delta^{18}O$ and $\delta^{13}C$ isotopically lighter than -6‰ are rejected by the filter, although the filter was created looking at values in the -10 to -15‰ range. Fields emerge for *Baculites*, *Inoceramus*, and *Placenticeras*, with a *Hoploscaphites* point and four *Nymphalucina* points represented as well (two of these are outliers not included in the graph). All of the gastropods specimens from the genera *Anisomyon* and *Drepanocheilus*, as well as the bivalve *Anomia*, were excluded based on their minor-element ratios. However, further research is needed to determine if this loss is an effect of sample size (i.e., with a larger dataset of these fossils, less-altered specimens would be present) or whether the taxa do tend to contain higher concentrations of Mg/Ca and lower concentrations of Sr/Ca. If the latter is true, the accuracy of isotopic signals from these genera needs to be determined.

Figure 18B replicates the filtered isotopic data, with 90% confidence intervals surrounding the mean ($\delta^{18}O$, $\delta^{13}C$) data point for each data subset. At the Game Ranch, the overlap of fields for *Placenticeras* and *Baculites* suggests that their habitats in life overlapped. Because of its shell morphology, *Placenticeras* had the most shallow implosion depth of any Western Interior Seaway ammonite, calculated by Tsujita and Westermann (1998) to be ~40 m. However, the total depth of the Western Interior Seaway during the *Baculites compressus/cuneatus* biozones (Harries, pers. comm., 2004), was likely shallower. Based on facies distribution patterns, Batt (1989) proposes

that *Baculites* were planktic but living at a slightly greater average depth than *Placenticeras*. The position of *Jeletskytes* near the *Placenticeras* data points suggests a habitat in the upper water column, consistent the analysis of its mobility by Westerman (1996). The values for *Inoceramus* at the Game Ranch site are distinct, suggesting a different habitat from the ammonites. This benthic habitat must have had a different $\delta^{18}O$ signature, perhaps influenced by freshwater or by the unique chemical conditions at the bottom of a dysoxic sea. The separation of benthic epifaunal *Inoceramus* from the nektic ammonites is consistent with all other studies for the Western Interior Seaway reviewed in this paper. The overlap in ranges for the Trask Ranch site could indicate a less stratified water column at the time and location the organisms lived. Neither the relative nor the absolute timing, and neither the relative nor absolute depth, of the Trask Ranch and Game Ranch localities within the *Baculites compressus* biozone is known, and instability (with periodic seafloor dysoxia, which could also explain the abundant black shales) is likely in the Western Interior Seaway. Along with the salinity levels below normal-marine, the dysoxia explains the scarcity of echinoderms, corals, and rudist bivalves in the Western Interior Seaway deposits. Therefore, it is not unreasonable to conclude that the isotopic composition of the water could have varied on a short time scale. On the other hand, the overlap could be due to insufficient data or misapplication of minor-element filters. An important observation that should be made when comparing the $\delta^{18}O$ and $\delta^{13}C$ ranges for each genus (Figures 18 and 19, respectively) with statistical data taken for each genus at each location (Tables 16 and 17, respectively), is that the minor element filter is effective at identifying localities that possess shell alteration. In selecting unaltered samples within each locality, the minor element filter discards many

samples that, nevertheless, yield reasonable $\delta^{18}O$ and $\delta^{13}C$ values. Of course, a value may be within the range of "reasonable" values yet still not reliably record of the original paleoceanographic signals. The difference in mean isotopic composition between filtered and unfiltered data is not significant for any of the genus-location subsets at the 0.05 significance level, though the increase in $\delta^{18}O$ ratio of the Trask Ranch baculitids after the application of the filter points to a strong relationship, with t = -1.44 versus critical t = -1.69. The standard deviations for the data subsets do not decrease with the application of the filter. This suggests that despite the possibility of alteration as indicated by minor-element proxies, many specimens with Mg/Ca > 6 mMol/Mol or, to a lesser extent, Sr/Ca < 1.8 mMol/Mol, carry isotopic signatures no different than the "more pristine" shell and that the isotopic signatures contained within shell material may be more robust than generally assumed. Why some fossil shell with increased Mg/Ca ratios and decreased Sr/Ca ratios relative to Recent aragonitic shell is isotopically identical to shell unaltered with respect to these chemicals is a topic that should be explored further. X-ray diffraction could deduce the percentage of calcite in the specimens, and any other minerals contributing to the minor element composition of the shell. Then, scanning electron microscopy of the specimens could reveal if the minerals are replacing aragonite or adhering to it, and if it is the latter, removal of the minerals could restore normal isotopic composition for samples (Cochran et al., 2005).

The values obtained in this study for agree well with prior research in the Western Interior Seaway, though the ranges are greater (Table 19). This study does document a larger $\delta^{13}C$ range than He et al. (2004) do for *Inoceramus*, extending the bivalve's $\delta^{13}C$ signature towards heavier values, though the average remains an isotopically heavy 3.06 ± 1.94‰. The *Hoploscaphites* value is heavier in $\delta^{13}C$ and lighter in $\delta^{18}O$ than their scaphite, though conclusions should not be overextended from a single data point. Differences may be due to taxonomic effect, as the other studies used other genera of scaphites, or to actual environmental variability. Lastly, the Placenticeras samples in this study, while isotopically light compared to contemporaneous ammonites, did not show the extremely light (-3.4‰ to -7.0‰) values documented by Tsujita and Westermann (1998), because their specimens were likely diagenetically altered.

2.4.3 Salinity and temperature calculations: Several authors (e.g., Rucker and Valentine, 1961; Dodd and Crisp, 1982; Rosenberg and Hughes, 1991) support a positive correlation between salinity and the concentration of sodium within molluscan shell. Brand (1986) found a positive relationship for a large dataset of bivalve and gastropods, both fossil and Recent, the empirically derived equation for which is:

$$S = -5.769\ln(A) + 28.380 \quad (2)$$

Salinity S is given in parts per thousand ± 0.5, and A is the ratio of ppm Sr / ppm Na, or the geometric mean of such ratios. Salinity has little to no correlation with Sr/Ca in molluscan shell (Purton et al., 1999), so Na is the measure of salinity, as advocated by Dodd (1967), and Sr/Ca corrects for taxonomic effects in minor element discrimination. Turekian and Armstrong (1960) show that the concentration of strontium in molluscan shell varies primarily by genus. This is likely because of intergeneric differences in

metabolic rate, which in turn determines the strontium concentrations of molluscs (Rosenberg and Hughes, 1991). Strontium concentrations are significantly higher in Recent cephalopods than in Recent bivalves and gastropods (Dodd, 1967), so the salinity-Sr/Na equation should not be applied directly to cephalopods, as it will overestimate the salinity. Using strontium and salinity data from Brand (1983) and Mann (1992), an adjustment factor of -1.5‰ was derived for the salinity of *Nautilus*. The adjustment is approximate because it was derived from the average Sr/Ca values and environmental salinity for individuals of *Nautilus* found in prior research. This adjustment factor was then applied to the results of the equation on the ammonite specimens in the dataset. The resulting salinities ranged from 27.7 ± 9.6‰ to 31.6 ± 0.6‰ for the filtered dataset (Table 18). The lowest salinities were found in *Placenticeras* and *Hoploscaphites* and the highest were found in *Inoceramus*, consistent with a seaway with denser, more saline water at the bottom.

To calculate the mean $\delta^{18}O$ of the Western Interior Seaway seawater, the following equation, from Wright (1987), was used:

$$S_{(WIS)} = [1 - (\delta_{w(WIS)} - \delta_{w(ocean)}))/(\delta_f - \delta_{w(ocean)})] \times S_{(ocean)} \quad (3)$$

Constants for $\delta^{18}O$ of the open ocean were $\delta_{w(ocean)}$ = -1.22‰ PDB and $S_{(ocean)}$ = 34.3, values calculated from models of Earth without polar ice caps (Schmidt, 1997). The mean $\delta^{18}O$ (WIS) was calculated at ~-1.27‰, only slightly lighter than the oceanic value and comparable to the data of Schmidt (1997). Slingerland et al. (1996) advocate using freshwater cements as an indicator of freshwater $\delta^{18}O$ values, noting their general agreement with values from kaolinitic clay from the eastern shore of the Western Interior Seaway. A freshwater value of $\delta^{18}O$ = -12.72‰, equivalent to the freshwater first-order

cements/concretions at Kremmling, was used in calculations because this meteoric-water-derived freshwater was likely present shortly after the deposition of the fossils. It should be noted, however, that using the value of -20 to -25‰ advocated by Dettman and Lohman, produces $\delta^{18}O$ (WIS) values that are only 0.02‰ lower.

Lastly, paleotemperature was calculated with Grossman and Ku's (1986) equation for aragonitic shell:

$$T(^{o}C) = 21.8 - 4.69(\delta_c - \delta_w). \quad (5)$$

All *Inoceramus* specimens were from the inner nacreous aragonitic layer, rather then the outer prismatic calcitic layer, so the calcite paleotemperature equation of Epstein et al. (1953) was not needed. For this equation, δ_c= the $\delta^{18}O$ value of the shell and both this value and the δ_w value are expressed relative to PDB (1986). Using Bettman and Lohman's freshwater signature, paleotemperatures are higher by 0.1 ^{o}C.

The resulting values for *Baculites* agree with values given by He et al. (2005), Tsujita and Westermann (1998), Schmidt (1997), and Fatherree et al. (1998). The Game Ranch values are also equivalent to the *Baculites* values given by Zakharov et al. (2005) for Cretaceous material from the continental shelf of eastern Siberia, though these values are from an earlier time period, the Coniacian. The temperature equivalence implies that the genus *Baculites* lived in habitats of similar temperature across its geographic and stratigraphic range.

For *Placenticeras*, a paleotemperature of 28.1 ± 1.1 ^{o}C suggests that these ammonites lived in warm upper waters. This value is at the low end of the range Tsuijita and Westermann calculated, but, as stated previously, their isotopically light $\delta^{18}O$ values likely come from diagenetically altered material. The high (36 ^{o}C) paleotemperature for *Hoploscaphites* is slightly higher than values found for the scaphite *Jeletskytes* by Tsujita and Westermann (1998) and for *Scaphites* by Whittaker, Kyser, and Caldwell (1986). However, the value is at the high end of their range and is approximately at the boundary for cessation of shell precipitation for Recent aragonitic mollusks (Elliot et al., 2003). More unaltered specimens must be examined to determine if the mean shell precipitation is, in fact, closer to the average of 25^{o}C found by Tsujita and Westermann (1998). The $\delta^{13}C$ value for the *Hoploscaphites* (Figure 20) is within the range of other ammonites, suggesting that the organism lived in a similar habitat.

The *Baculites* specimens examined in this study yielded a paleotemperature of 20.9 ± 4.9 ^{o}C for Game Ranch and 24.7 ± 4.2 ^{o}C for Trask Ranch. However, as depicted in Figure 20, the isotopic ranges for *Baculites* specimens were quite wide. This could be a reflection of the temperature-induced natural variability in *Baculites*, water-mass migration, short-term climate fluctuations, or an imperfect filter. It is possible that the differences in $\delta^{18}O$ between Tourtelot and Rye's (1969) *Baculites* data and Forester et al.'s (1977) *Baculites* data do not represent real temperature differences between the two locations, but are instead within the range of variability for *Baculites* from a single location. The $\delta^{13}C$ range for the *Baculites* specimens is comparable to both prior research and the $\delta^{13}C$ range for *Placenticeras*.

While data for *Placenticeras* and *Hoploscaphites* are sparse, numerous studies provide comparative stable isotope and paleotemperature data for *Inoceramus*. The range of values produced in this investigation, for both $\delta^{18}O$ and $\delta^{13}C$, was comparable to prior research. For each of these isotopes, the range produced by this study is greater than any of the other ranges, but this could be an artifact of the greater amount of data examined. Tsujita and Westermann (1998) and Wright (1987) also obtain anomalously high paleotemperature values for *Inoceramus*. The authors invoke the presence of highly saline bottom water to explain the values. An argument against this explanation, along with further discussion on the paleobiotic implications of these paleotemperatures, is presented in Chapter 3, Section 3.

FIGURE 15—Empirical Derivation of the Sr/Ca-Mg/Ca Filter

A. $\delta^{13}C$ vs. Mg/Ca

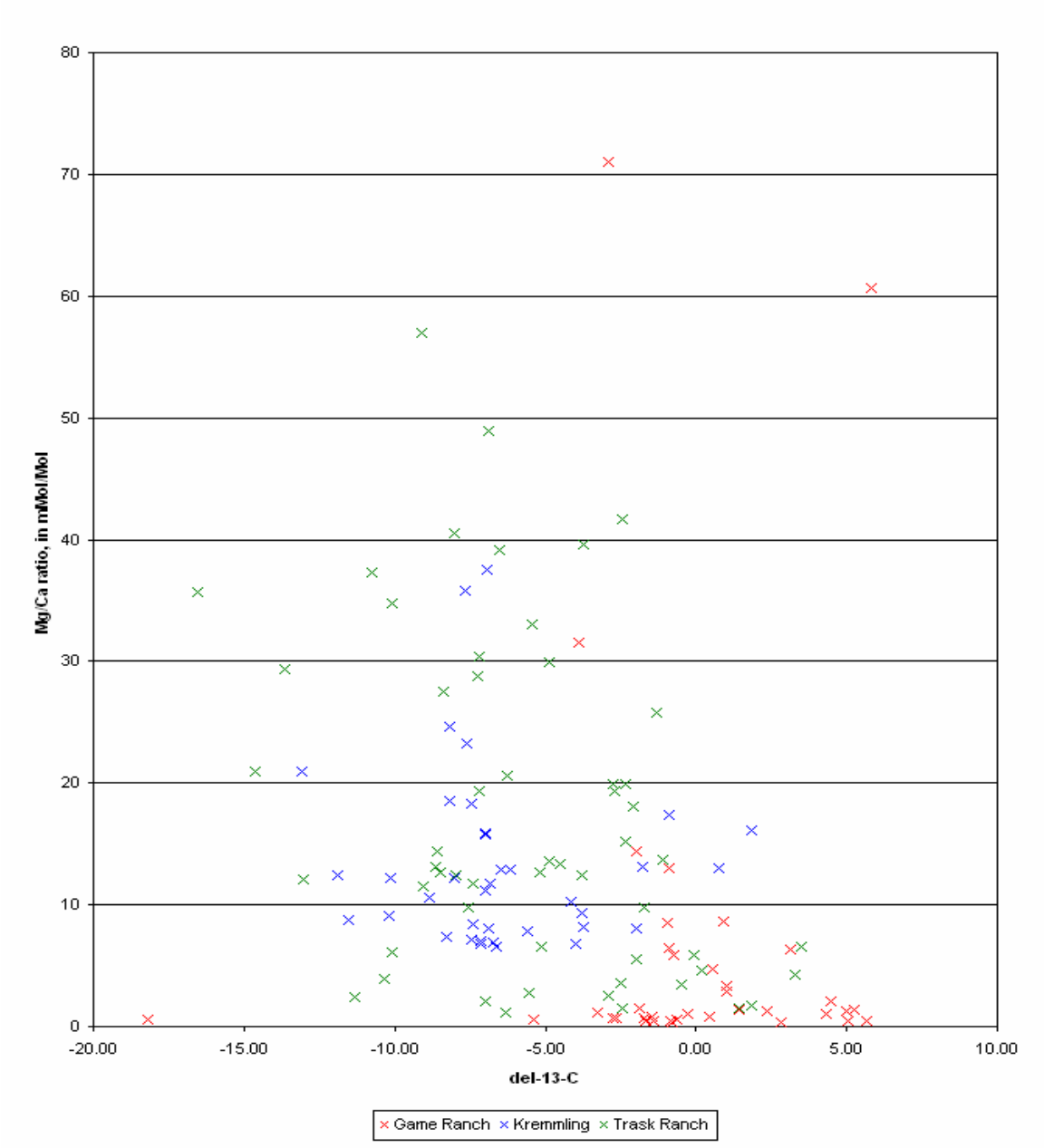

Above approximately 7 mMol/Mol, a greater number of unrealistic (10-20‰, versus PDB) $\delta^{13}C$ values emerge for the Kremmling dataset. Isotopic outliers for Trask Ranch occur at the same level.

FIGURE 15—Empirical Derivation of the Sr/Ca-Mg/Ca Filter (continued)

B. $\delta^{18}O$ vs. Fe/Ca

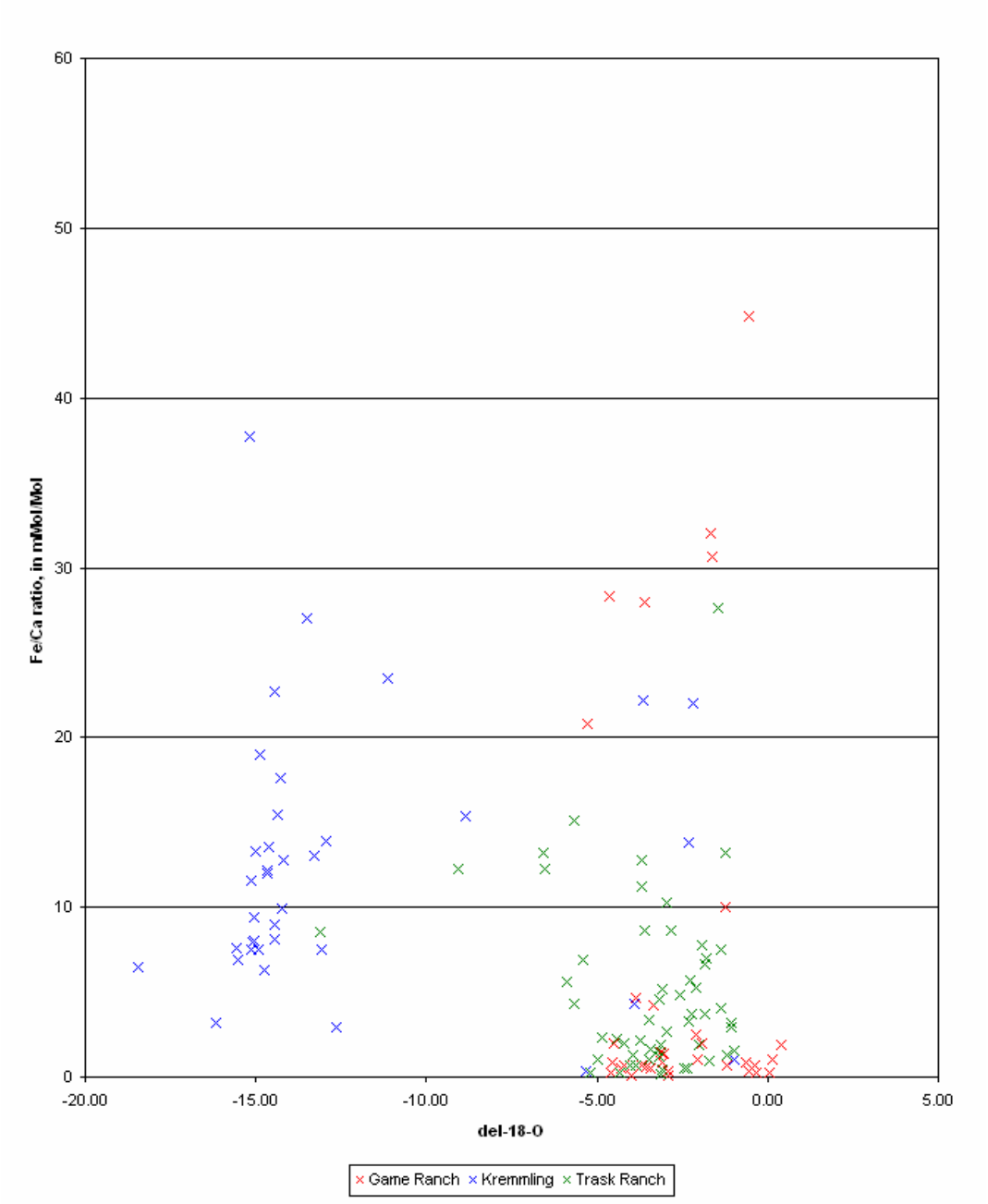

Above approximately 7 mMol/Mol Fe/Ca, very negative $\delta^{18}O$ values emerge for the Kremmling dataset. Isotopic outliers for Trask Ranch occur above 9 mMol/Mol.

FIGURE 15—Empirical Derivation of the Sr/Ca-Mg/Ca Filter (continued)

C. $\delta^{18}O$ vs. Mg/Ca

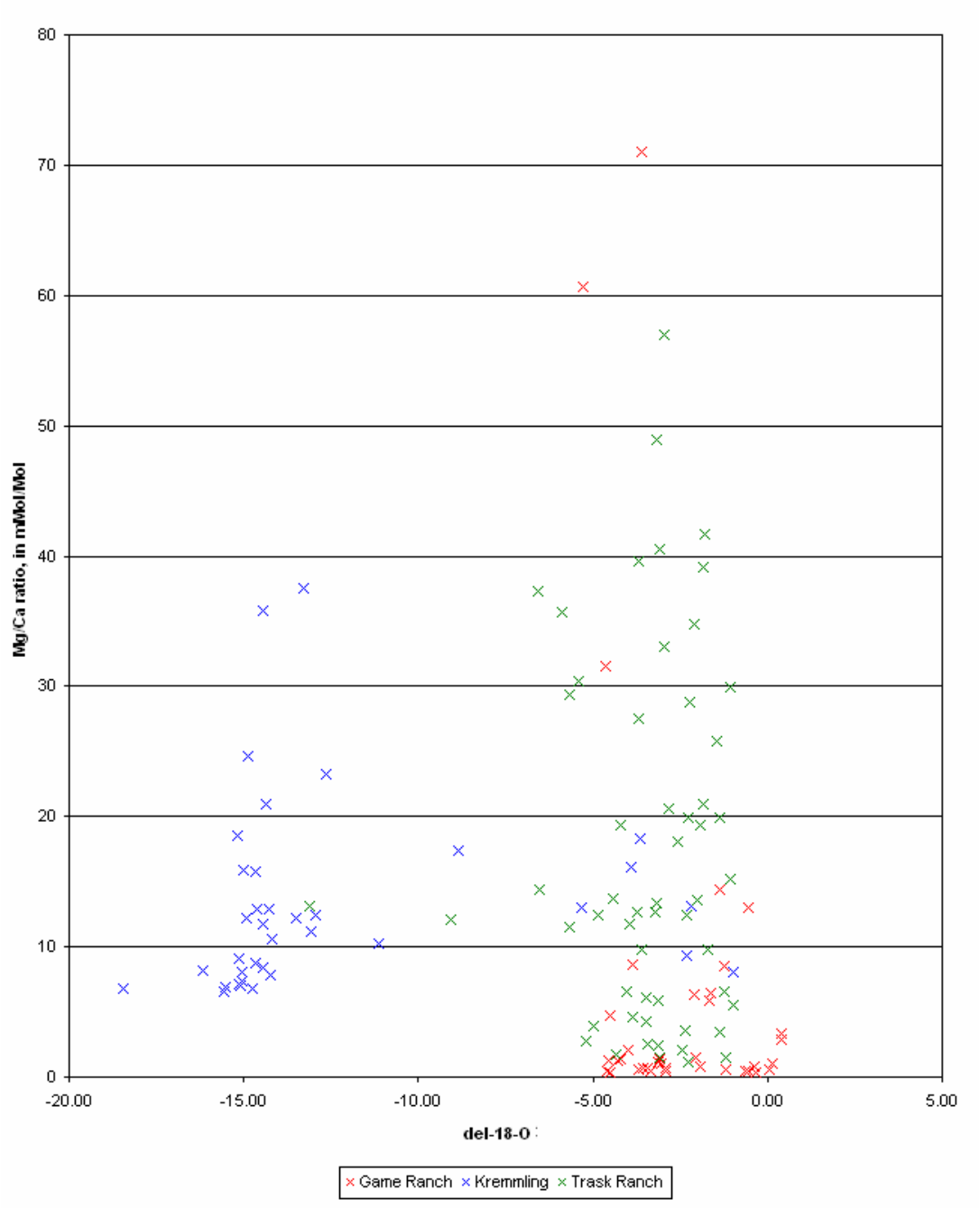

Above approximately 6.5 mMol/Mol Mg/Ca, a greater number of unrealistic (10-20‰, versus PDB) $\delta^{18}O$ values emerge for the Kremmling dataset. Isotopic outliers for Trask Ranch occur above 12 mMol/Mol.

FIGURE 15—Empirical Derivation of the Sr/Ca-Mg/Ca Filter (continued)
D. $\delta^{18}O$ vs. Mn/Ca

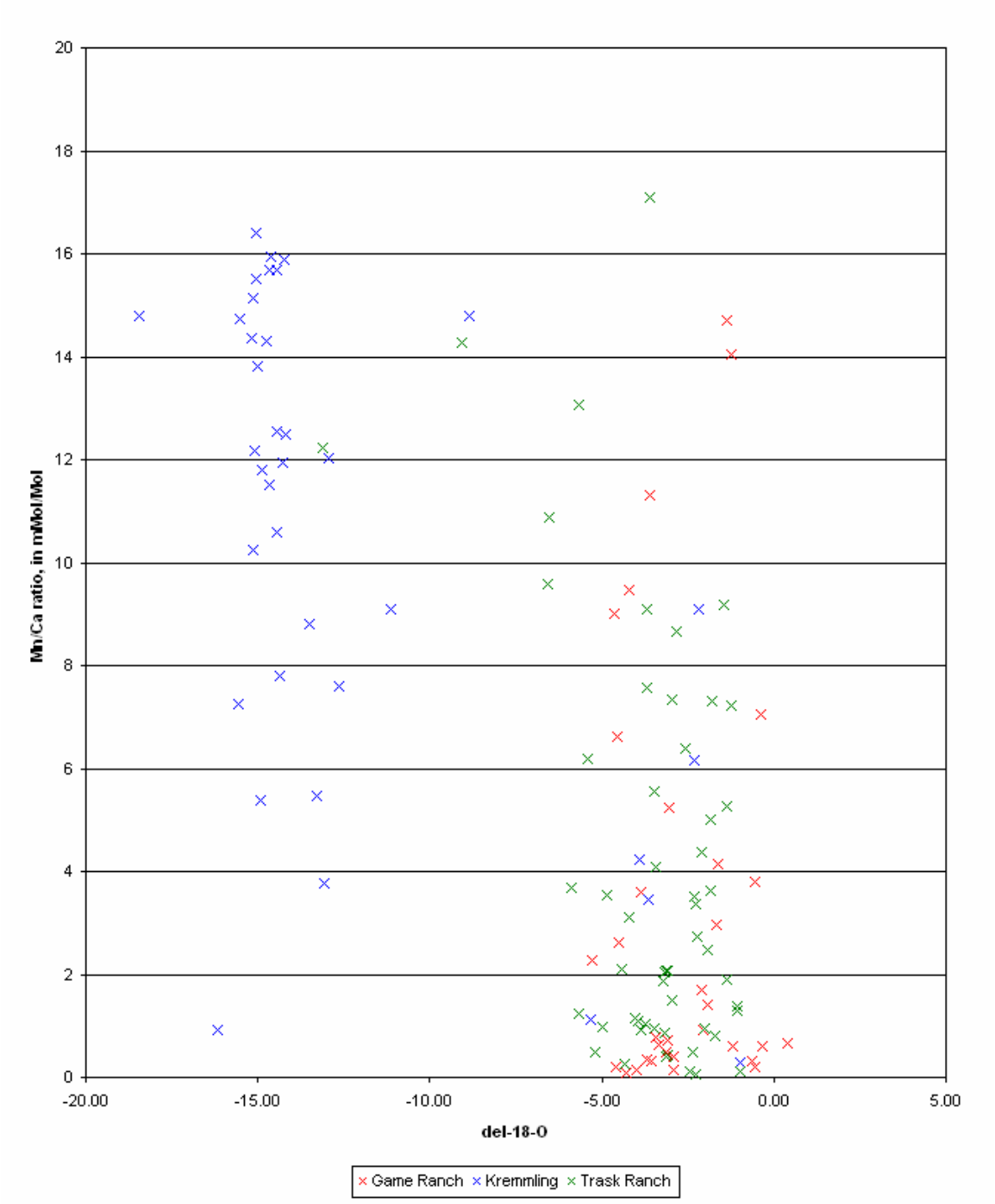

Above approximately 11 mMol/Mol Mn/Ca, very negative $\delta^{18}O$ values emerge for the Kremmling dataset. Isotopic outliers for Trask Ranch occur above 12 mMol/Mol.

FIGURE 15—Empirical Derivation of the Sr/Ca-Mg/Ca Filter (continued)
E. $\delta^{18}O$ vs. Na/Ca

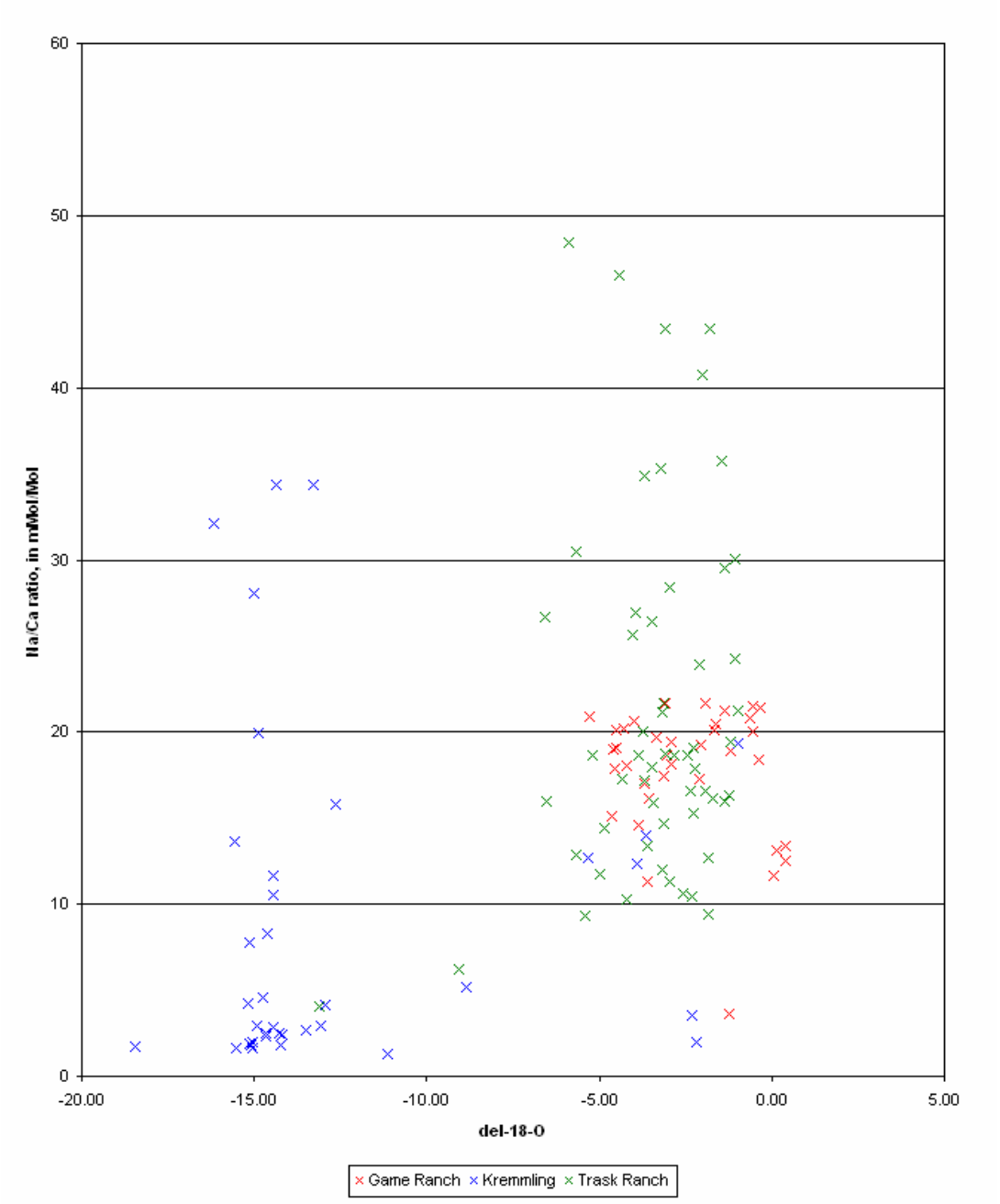

Below approximately 10 mMol/Mol Na/Ca, very negative $\delta^{18}O$ values emerge for the Kremmling dataset. Isotopic outliers for Trask Ranch occur below 9.5 mMol/Mol.

FIGURE 15—Empirical Derivation of the Sr/Ca-Mg/Ca Filter (continued)

F. $\delta^{18}O$ vs. Sr/Ca

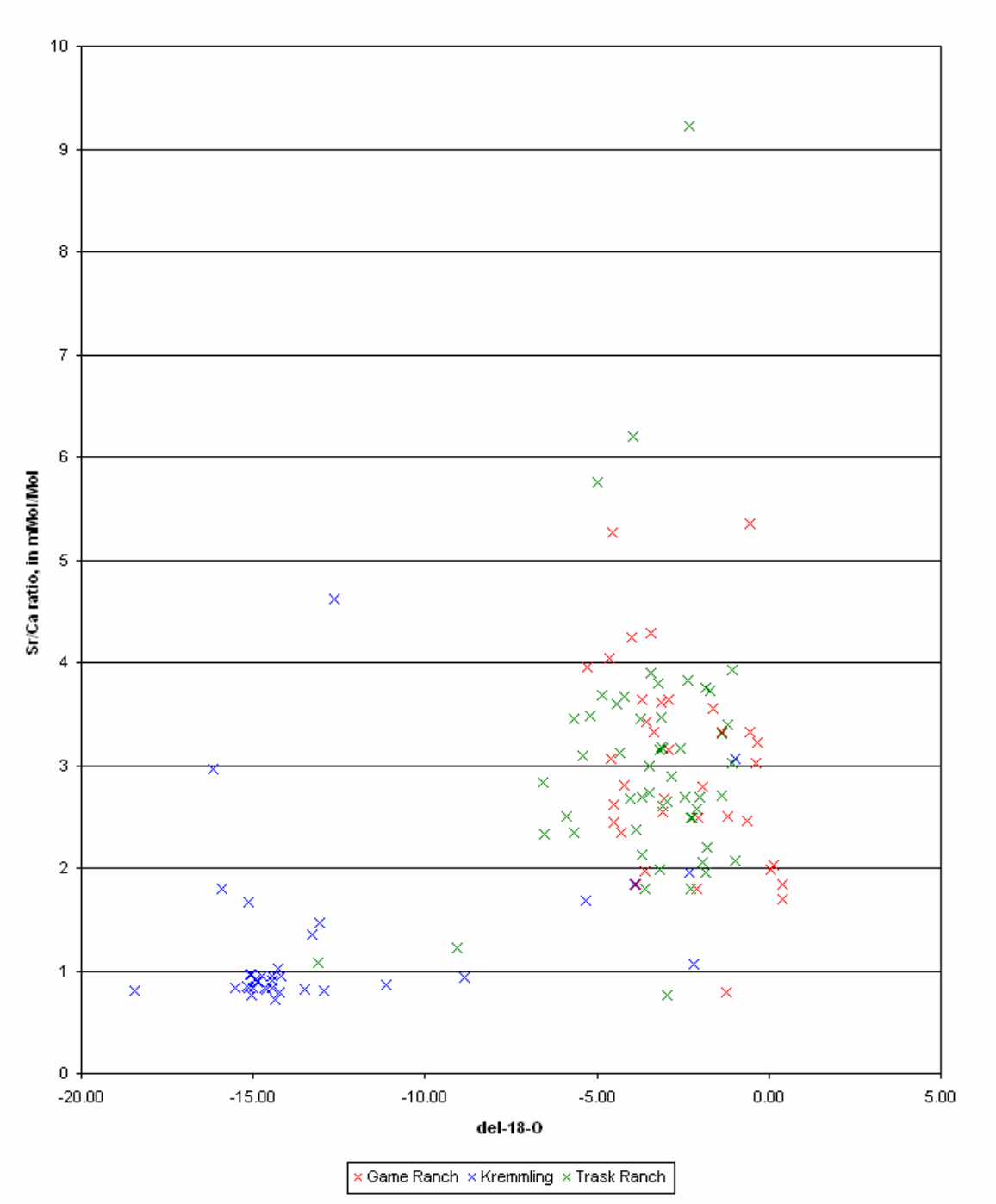

Below approximately 1.8 mMol/Mol Fe/Ca, very negative $\delta^{18}O$ values emerge for the Kremmling dataset. Isotopic outliers for Trask Ranch occur below 1.2 mMol/Mol.

FIGURE 16—Stable Isotope Cross Plot for All Shell Samples

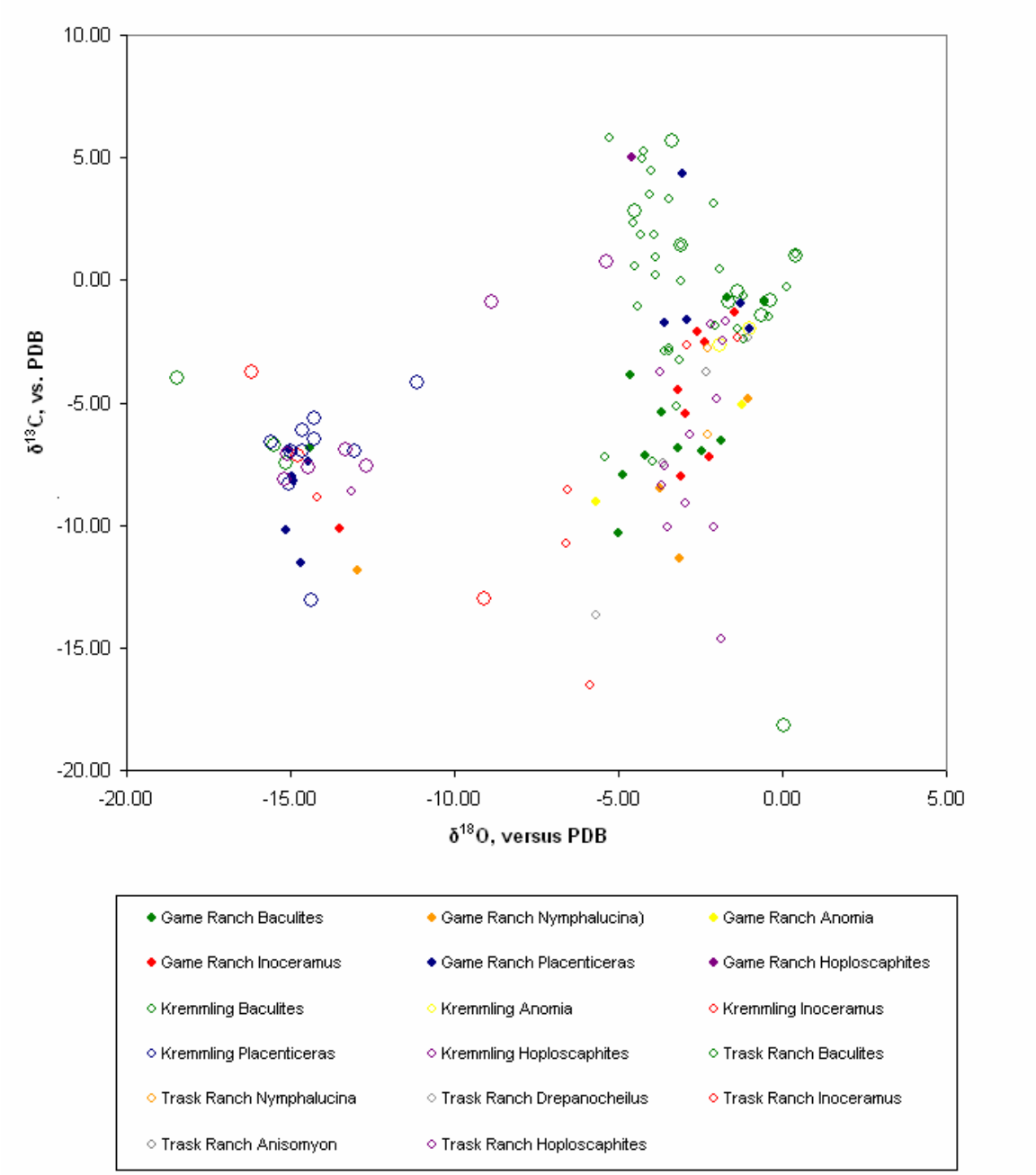

The unfiltered graph for the stable isotope data shows two clear clusters defined by their oxygen isotope ratios. There is also a high degree of variability in samples of the same genus with regards to carbon isotopes.

FIGURE 17—Isotope Cross-Plot For All Shell Samples, Filtered by Mg/Ca and Sr/Ca

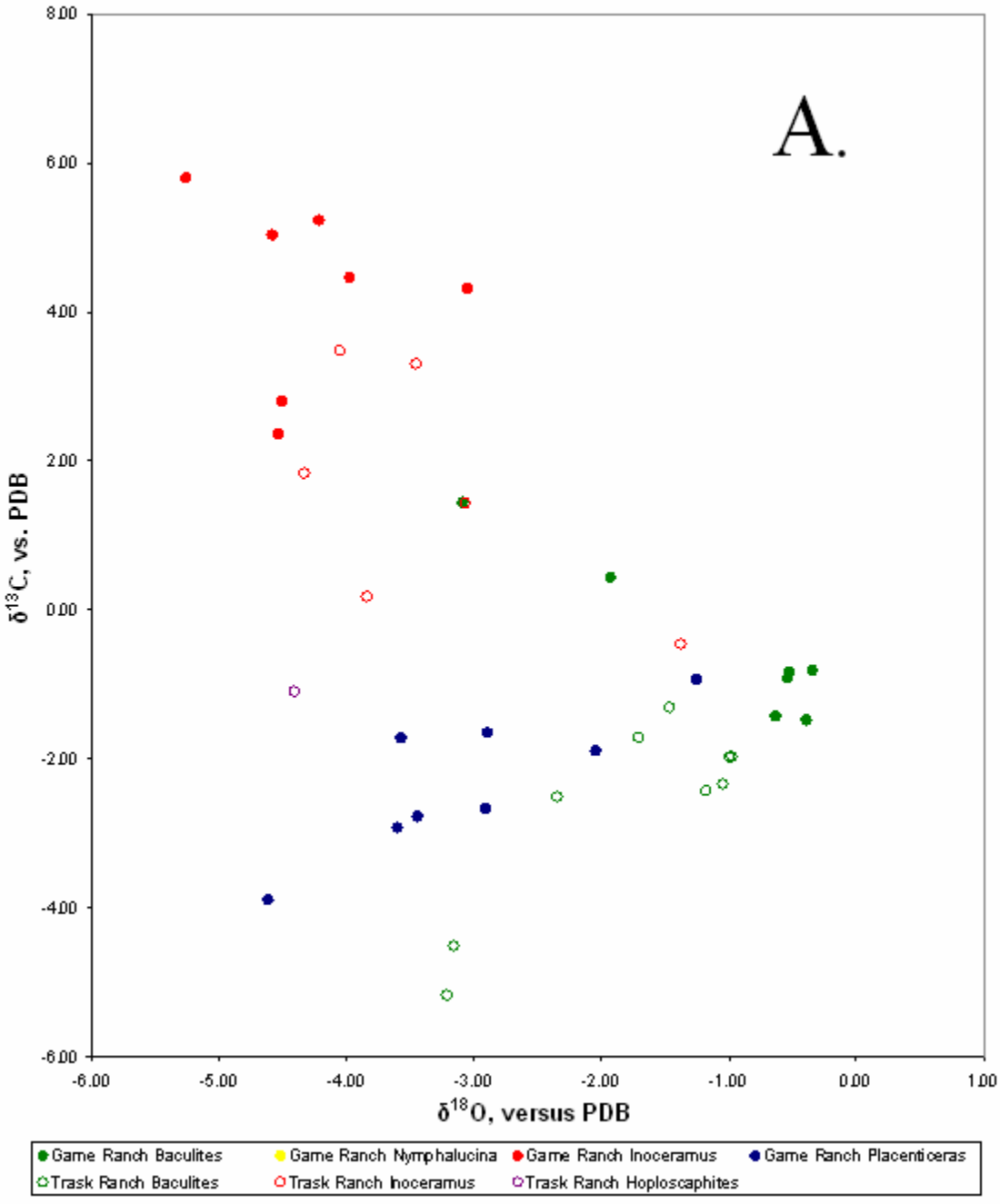

The stable isotope cross-plot of filtered data shows better-defined fields for each genus. The positioning of the fields relative to each other is consistent with prior research. The ammonites *Baculites* (green) and *Placenticeras* (blue) show a greater variability in oxygen isotopes, whereas the bivalve *Inoceramus* (red) shows more variation in carbon isotopes.

FIGURE 17—Isotope Cross-Plot For All Shell Samples, Filtered by Mg/Ca and Sr/Ca, With 90% Confidence Intervals

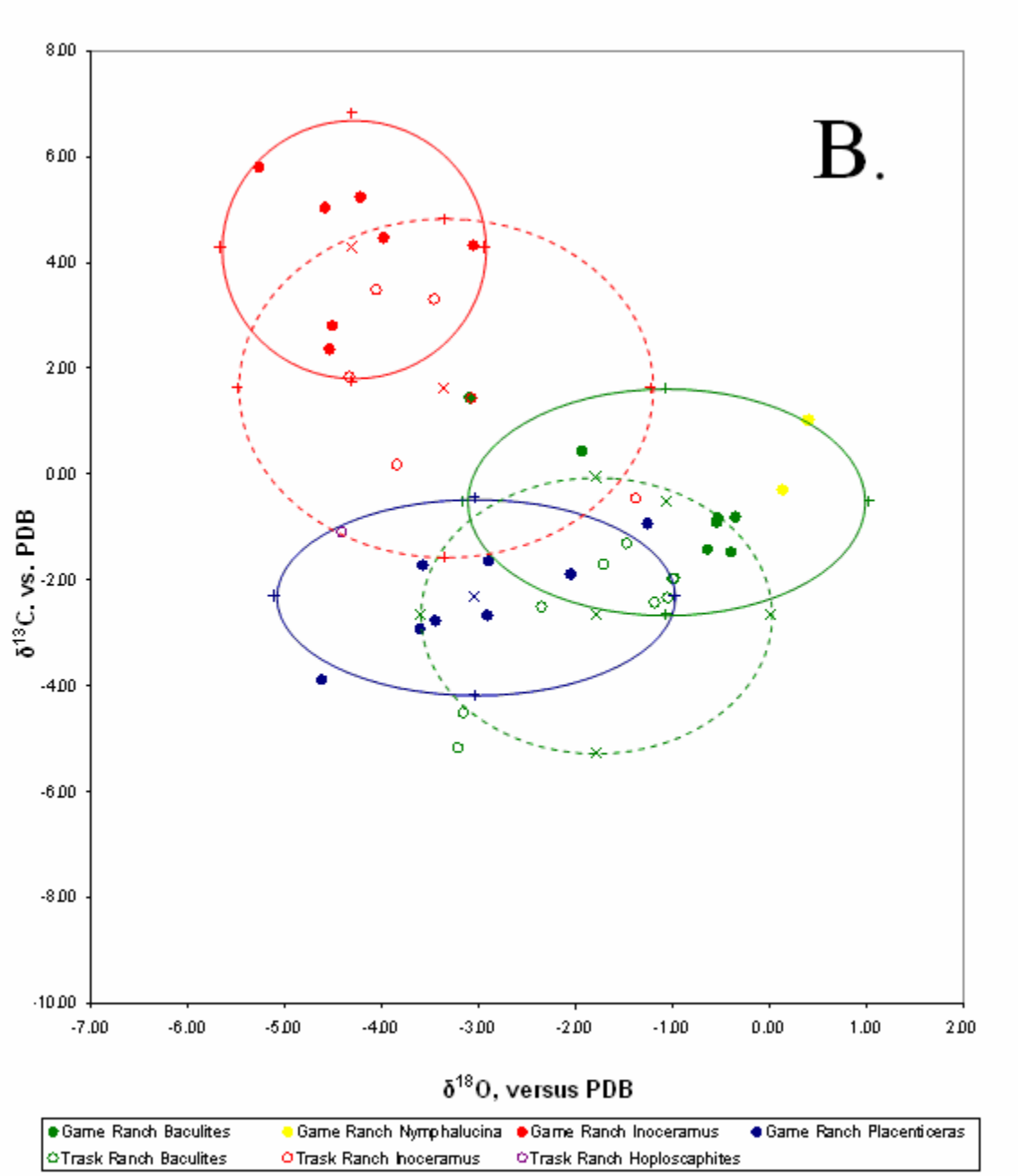

In this version of the isotope cross-plot for the filtered data, 90% confidence intervals are drawn from the mean data points. The 90% confidence interval means that if other samples of Western Interior Seaway fossils were taken from the sampling locations, the probability is 90% that they would fall within the confidence interval with the true population mean.

FIGURE 18—Oxygen Isotope Range Chart

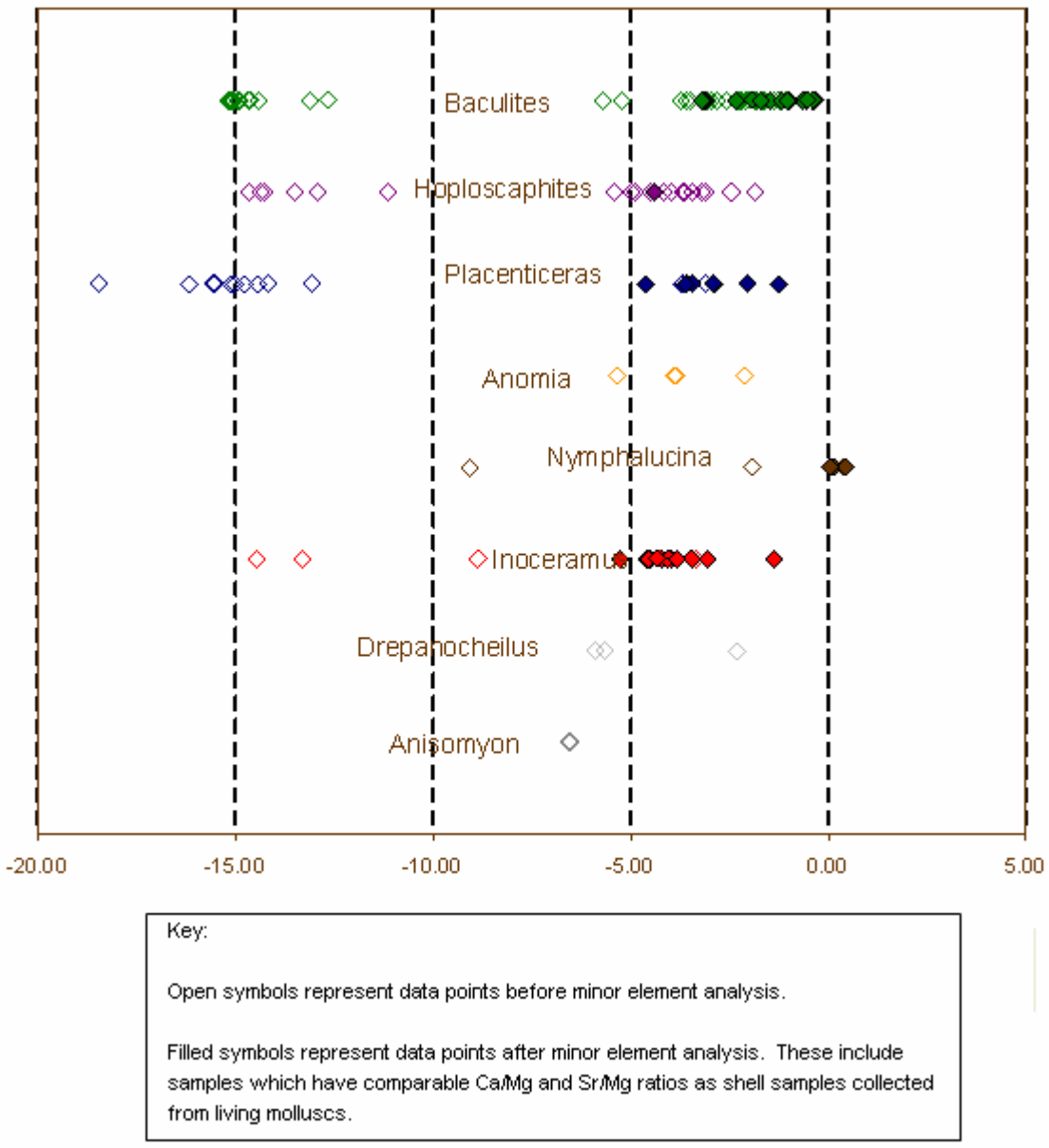

Elimination of the data points with Mg/Ca and Sr/Ca outside of the limits of the minor element filter decreases the range of the $\delta^{18}O$ values for each genus such that all points fall between 1‰ and -6‰. However, it also eliminates less common genera such as *Drepanocheilus* and *Anisomyon* from the dataset.

TABLE 16—Statistics Comparing $\delta^{18}O$ of Pre-filter and Post-filter Datasets

Alternate Hypothesis	Type of Test	N	Means, ± standard deviations	Calculated Value	Critical Value (0.05 signif.)	Result
Lighter $\delta^{18}O$ for Game Ranch *Baculites* after filter?	one-tailed t-test (ind.)	11u, 7f	u: -1.21 ± 0.84 f: -1.07 ± 1.05	t = -0.34	t = -1.75	Ho retained
Lighter $\delta^{18}O$ for Kremmling *Baculites* after filter?	one-tailed t-test (ind.)	12u, 0f	u: 11.56 ± 5.75 N/A	N/A	N/A	N/A
Lighter $\delta^{18}O$ for Trask Ranch *Baculites* after filter?	one-tailed t-test (ind.)	32u, 9f	u: -2.44 ± 1.14 f: -1.79 ± 0.90	t = -1.44	t = -1.69	Ho retained
Lighter $\delta^{18}O$ for Game Ranch *Hoploscaphites* after filter?	one-tailed t-test (ind.)	1u, 0f	u: -4.51 f: N/A	N/A	N/A	N/A
Lighter $\delta^{18}O$ for Kremmling *Hoploscaphites* after filter?	one-tailed t-test (ind.)	7u, 0f	u: -8.33 ± 3.37 f: N/A	N/A	N/A	N/A
Lighter $\delta^{18}O$ for Trask Ranch *Hoploscaphites* after filter?	one-tailed t-test (ind.)	13u, 1f	u: -3.79 ± 1.01 f: -4.41	N/A	N/A	N/A
Lighter $\delta^{18}O$ for Game Ranch *Placenticeras* after filter?	one-tailed t-test (ind.)	11u, 8f	u: -3.17 ± 0.90 f: -3.05 ± 1.03	t = -0.29	t = -1.74	Ho retained
Lighter $\delta^{18}O$ for Kremmling *Placenticeras* after filter?	one-tailed t-test (ind.)	10u, 0f	u: -15.23 ± 1.42 f: N/A	N/A	N/A	N/A
Lighter $\delta^{18}O$ for Game Ranch *Inoceramus* after filter?	one-tailed t-test (ind.)	9u, 7f	u: -4.20 ± 0.67 f: -4.27 ± 0.68	t = 0.48	t = -1.76	Ho retained
Lighter $\delta^{18}O$ for Kremmling *Inoceramus* after filter?	one-tailed t-test (ind.)	3u, 0f	u: -12.21 ± 2.96 f: N/A	N/A	N/A	N/A
Lighter $\delta^{18}O$ for Trask Ranch *Inoceramus* after filter?	one-tailed t-test (ind.)	6u, 6f	u: -3.36 ± 1.07 f: -3.36 ± 1.07	N/A	N/A	N/A
Lighter $\delta^{18}O$ for Game Ranch *Anomia* after filter?	one-tailed t-test (ind.)	2u, 0f	u: -2.99 ± 1.25 f: N/A	N/A	N/A	N/A
Lighter $\delta^{18}O$ for Kremmling *Anomia* after filter?	one-tailed t-test (ind.)	2u, 0f	u: -4.63 ± 1.01 f: N/A	N/A	N/A	N/A
Lighter $\delta^{18}O$ for Game Ranch *Nymphalucina* after filter?	one-tailed t-test (ind.)	4u, 4f	u: 0.25 ± 0.19 f: 0.25 ± 0.19	N/A	N/A	N/A
Lighter $\delta^{18}O$ for Trask Ranch *Nymphalucina* after filter?	one-tailed t-test (ind.)	2u, 0f	u: -5.50 ± 5.05 f: N/A	N/A	N/A	N/A
Lighter $\delta^{18}O$ for Trask Ranch *Drepanocheilus* after filter?	one-tailed t-test (ind.)	3u, 0f	u: -4.62 ± 2.00 f: N/A	N/A	N/A	N/A
Lighter $\delta^{18}O$ for Trask Ranch *Anisomyon* after filter?	one-tailed t-test (ind.)	2u, 0f	u: -6.56 ± 0.03 f: N/A	N/A	N/A	N/A

FIGURE 19—Carbon Isotope Range Chart

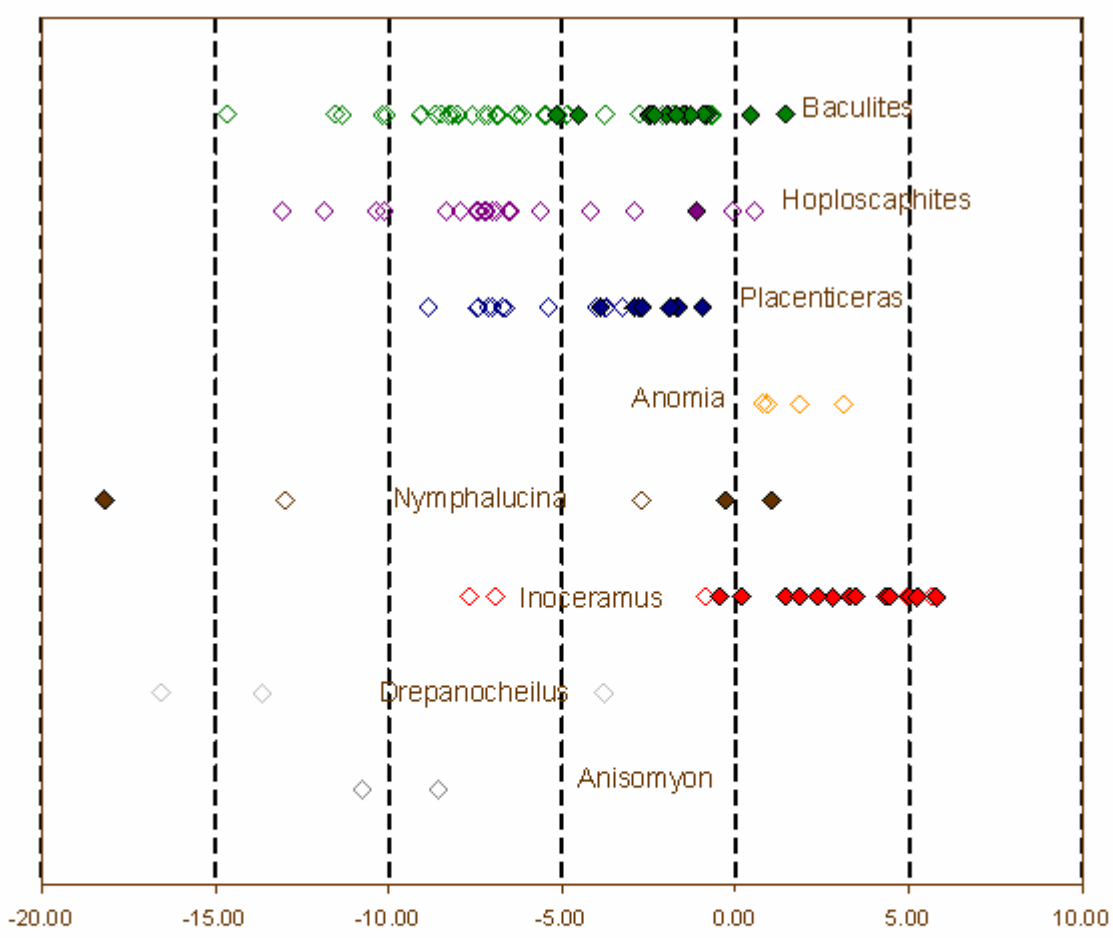

The minor element filter likewise eliminates light $\delta^{13}C$ values from the dataset. Ammonites are then distributed between 2‰ and -5‰, and bivalves 6‰ to -1‰, except for an apparent outlier in *Nymphalucina*.

TABLE 17—Statistics Comparing $\delta^{13}C$ of Pre-filter and Post-filter Datasets

Alternate Hypothesis	Type of Test	N	Means, ± standard deviations	Calculated Value	Critical Value (0.05 signif.)	Result
Lighter $\delta^{13}C$ for Game Ramch *Baculites* after filter?	one-tailed t-test (ind.)	11u, 7f	u: -0.71 ± 0.94 f: -0.51 ± 1.07	t = -0.43	t = -1.75	Ho retained
Lighter $\delta^{13}C$ for Kremmling *Baculites* after filter?	one-tailed t-test (ind.)	12u, of	u: -8.13 ± 1.50 N/A	N/A	N/A	N/A
Lighter $\delta^{13}C$ for Trask Ranch *Baculites* after filter?	one-tailed t-test (ind.)	32u, 9f	u: -5.41 ± 3.37 f: -2.67 ± 1.30	t = -0.78	t = -1.69	Ho retained
Lighter $\delta^{13}C$ for Game Ranch *Hoploscaphites* after filter?	one-tailed t-test (ind.)	1u, 0f	u: 0.544 f: N/A	N/A	N/A	N/A
Lighter $\delta^{18}O$ for Kremmling *Hoploscaphites* after filter?	one-tailed t-test (ind.)	7u, 0f	u: -13.59 ± 1.23 f: N/A	N/A	N/A	N/A
Lighter $\delta^{13}C$ for Trask Ranch *Hoploscaphites* after filter?	one-tailed t-test (ind.)	13u, 1f	u: -6.13 ± 2.97 f: -1.10	N/A	N/A	N/A
Lighter $\delta^{13}C$ for Game Ranch *Placenticeras* after filter?	one-tailed t-test (ind.)	11u, 8f	u: -2.81 ± 0.93 f: -2.31 ± 0.93	t = -0.83	t = -1.74	Ho retained
Lighter $\delta^{13}C$ for Kremmling *Placenticeras* after filter?	one-tailed t-test (ind.)	10u, 0f	u: -6.593 ± 1.564 f: N/A	N/A	N/A	N/A
Lighter $\delta^{13}C$ for Game Ranch *Inoceramus* after filter?	one-tailed t-test (ind.)	9u, 7f	u: 4.52 ± 1.20 f: 4.29 ± 1.27	t = 0.30	t = -1.76	Ho retained
Lighter $\delta^{13}C$ for Kremmling *Inoceramus* after filter?	one-tailed t-test (ind.)	3u, 0f	u: -5.16 ± 3.72 f: N/A	N/A	N/A	N/A
Lighter $\delta^{13}C$ for Trask Ranch *Inoceramus* after filter?	one-tailed t-test (ind.)	6u, 6f	u: 1.63 ± 1.60 f: 1.63 ± 1.60	N/A	N/A	N/A
Lighter $\delta^{13}C$ for Game Ranch *Anomia* after filter?	one-tailed t-test (ind.)	2u, 0f	u: -2.02 ± 1.56 f: N/A	N/A	N/A	N/A
Lighter $\delta^{13}C$ for Kremmling *Anomia* after filter?	one-tailed t-test (ind.)	2u, 0f	u: 1.31 ± 0.76 f: N/A	N/A	N/A	N/A
Lighter $\delta^{13}C$ for Game Ranch *Nymphalucina* after filter?	one-tailed t-test (ind.)	4u, 4f	u: -4.11 ± 9.42 f: N/A	N/A	N/A	N/A
Lighter $\delta^{13}C$ for Trask Ranch *Nymphalucina* after filter?	one-tailed t-test (ind.)	2u, 0f	u: -7.84 ± 7.30 f: N/A	N/A	N/A	N/A
Lighter $\delta^{13}C$ for Trask Ranch *Drepanocheilus* after filter?	one-tailed t-test (ind.)	3u, 0f	u: -11.33 ± 6.69 f: N/A	N/A	N/A	N/A
Lighter $\delta^{13}C$ for Trask Ranch *Anisomyon* after filter?	one-tailed t-test (ind.)	2u, 0f	u: -9.67 ± 1.54 f: N/A	N/A	N/A	N/A

TABLE 18—Paleoenvironmental Parameters Derived from Filtered Data

	Mean $\delta^{18}O_{(shell)}$, ‰,± Standard Deviation	Mean Salinity, ‰, ± Standard Deviation	Mean $\delta^{18}O_{(WIS)}$, ‰, ± Standard Deviation	Mean Paleotemperature, °C,± Standard Deviation
Game Ranch *Baculites*	-1.07 ± 1.04	30.6 ± 0.8	-1.26 ± 0.08	20.9 ± 4.9
Trask Ranch *Baculites*	-1.79 ± 0.91	29.9 ± 2.0	-1.26 ± 0.02	24.8 ± 4.2
Game Ranch *Placenticeras*	-3.05 ± 1.03	28.1 ± 1.1	-1.28 ± 0.01	30.1 ± 4.9
Trask Ranch *Hoplo-scaphites*	-4.41 (n = 1)	27.3 (n = 1)	-1.29 (n = 1)	36.5 (n = 1)
Game Ranch *Inoceramus*	-4.27 ± 0.68	31.1 ± 1.9	-1.25 ± 0.02	36.1 ± 3.2
Trask Ranch Inoceramus	-3.36 ± 1.07	27.7 ± 9.6	-1.28 ± 0.09	31.5 ± 4.9
Game Ranch *Nympha-lucina*	0.25 ± 0.19	31.7 ± 0.6	-1.25 ± 0.01	14.8 ± 1.2

The salinity, calculated using the strontium and sodium concentrations in the shell, was used to determine the mean $\delta^{18}O$ for the Western Interior Seaway. Taking $\delta^{18}O$ of freshwater to be equal to the mean $\delta^{18}O$ of Kremmling, Colorado concretions (because the western coastline was the likely source of more freshwater input to the seaway), the mean paleotemperature for each organism at each location was calculated. The data support the notion of lower than normal salinity in the upper-intermediate waters of the seaway and verify the unrealistically high paleotemperatures for benthic epifaunal bivalves.

FIGURE 20—Stable Isotope Ranges for Genera in this Study and Prior Research

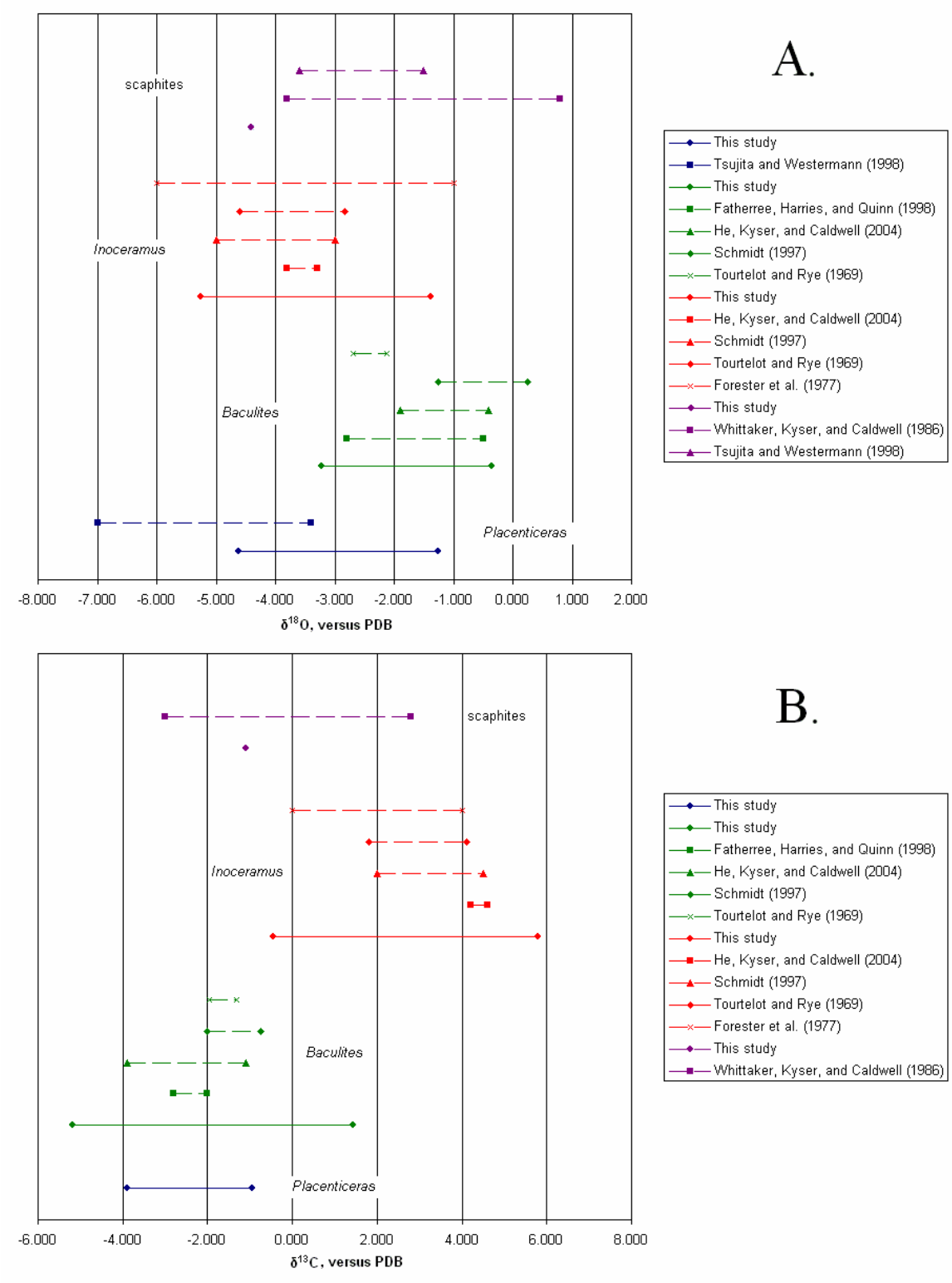

Results of this study showed comparable light stable isotope signatures with data found by previous studies in the Western Interior Seaway.

CHAPTER 3. SCLEROCHRONOLOGY

3.1 Previous Investigations of Molluscan Sclerochronology

3.1.1 Advantages of Molluscan Sclerochronology: Sclerochronology is the study of changes in the chemical composition of a shell over an organism's lifespan, taken along the growth axis. Chemical composition in this context can be stable isotopic or minor element data. Molluscs are ideal for sclerochronology be cause they grow accretionally, and most have well-defined growth bands that may be used to evaluate the relative age of different parts of the shell and orient the growth axis. For most mollusks, growth is non-destructive; in order to precipitate additional shell, a mollusk does not need to dissolve previously precipitated shell material. Therefore, all shell deposition from embryonic to gerontic stages is generally recorded in a single shell. The record of a single shell contains chemical information with respect to time on the order of months, years, or decades, a resolution generally not available by comparing specimens from different stratigraphic horizons or even within a stratigraphic horizon, which is necessarily time-averaged due to depositional processes. Although mollusks strongly discriminate with respect to elements such as magnesium and strontium found in seawater, they precipitate oxygen and carbon at isotopic ratios close to equilibrium with seawater (e.g., Dodd, 1967; Landman et al., 1994; Elliot et al., 2003).

3.1.2 Cessation of Growth: One limitation in evaluating paleotemperature using molluscan shell is that mollusks do not grow throughout the year (Ivany et al., 2003), although this may have been less of a factor during more equable greenhouse conditions.

Bivalves cease deposting shell when the temperature becomes too hot or too cold, or when the mollusk is spawning. These cessations distort the temperature curve derived from $\delta^{18}O$. Fatherree (1995) documented this effect for winter cessation of growth for the Western Interior Seaway bivalve *Arctica ovata,* so it is possible even in the more equable climate of the Cretaceous. Whether this cessation is related to temperature or spawning is unknown, as the spawning cycle of the bivalve is unknown. In their study of Recent *Mercenaria mercenaria*, Elliot et al. (2003) note that the bivalve, which spawns in March-June, grew more slowly in summer months than in winter, and grew more slowly overall in inlets with highly variable salinity. *Sepia* showed slowed growth when it was in periods of starvation (Bettencourt and Guerra, 1999).

3.1.3 Metabolism: Another challenge of molluscan sclerochronology is the "vital effect," or metabolic signature. All mollusks display a kinetic effect with regards to minor elements, precipitating shell with less strontium and magnesium than seawater (Dodd, 1982). However, the amount of discrimination differs based on shell mineralogy; calcitic bivalves discriminate less against magnesium and more against strontium as compared to aragonitic bivalves (Dodd, 1967). Sodium discrimination also varies, with higher sodium concentrations found in cephalopods than in bivalves or gastropods (Dodd, 1967; Brand, 1983). Mollusks, while not discriminating against heavy isotopes in the manner that plants and bacteria do, display a metabolic effect with regards to oxygen and carbon isotopes. When a correlation between $\delta^{18}O$ and $\delta^{13}C$ is positive, it may be due to alteration or to metabolism. At higher metabolic rates, mollusks incorporate more elements contained in their food supply, rather than from seawater, into their shells (e.g., Barrerra et al., 1990; Ivany et al., 2003). Because all molluscan food sources are

isotopically lighter than seawater, the net effect is an isotopically lighter shell. Barrerra et al. (1990) found positive correlations between stable isotopes in the bivalve *Admussium colbecki* along the metabolically active, fastest-growing parts of the shell. The positive correlations for the early ontogeny of *Eutrephoceras* (Landman et al., 1983), *Baculites* (Fatherree et al., 1998), and the bivalve *Cucullaea* (Dutton et al., 2002) may represent a rapid initial growth rate. When studying another Recent bivalve, *Mercenaria mercenaria*, Elliot et al. (2003) found direct relationships between stable isotopes for specimens living in ideal habitats but inverse relationships between the variables where the environment was less conducive to growth and had a shorter summer growth period.

3.1.4 Analogs for Mollusks of Western Interior Seaway: Ammonites and inoceramids are extinct organisms with no close relatives, so the interpretation of their sclerochronology must rely on more distantly related analogs. The most common analog used for ammonites is the shelled cephalopod *Nautilus*, of which there are four extant species (Mann, 1992). The cuttlefish *Sepia*, which may be phylogenetically more closely related to ammonites than *Nautilus*, has also been examined. *Sepia* $\delta^{13}C$ values increase as individuals mature and migrate from inlets with high freshwater input (and highly negative $\delta^{13}C$ of dissolved inorganic carbon) into the open ocean, though the change in $\delta^{13}C$ ratio may also reflect changing diet. Temperature values obtained by oxygen-isotope paleothermometry fall between 14 ^{o}C and 22 ^{o}C and slightly overestimate the actual temperature of the inlets in which the *Sepia* lived, as well as the temperature of aquaria where *Sepia* were experimentally raised (Bettencourt and Guerra, 1999). Though the authors explain this mismatch as evidence of a slight vital effect, it could also be the result of the temperature-based shell secretion rates they observed for the organism. As

Ivany et al. (2003) established for the surf clam *Spisula*, if more shell is deposited in warmer temperatures, the oxygen-isotope paleothermometry values will be biased towards the warmer seasons (2003). However, *Nautilus belauensis* individuals raised in an aquarium at 15-24 ^{o}C did not show any evidence of temperature-determined growth cessation, or any variation in the oxygen isotopic signature that could not be explained by equilibrium precipitation of aragonite (Landman et al., 1994). This finding suggests that the shift in $\delta^{18}O$ documented for wild *Nautilus* and potentially other shelled cephalopods after hatching is temperature-dependent rather than physiological.

Certain bivalves, such as *Anomia*, may be compared directly with Recent counterparts, with the caveat that over 73 million years, taxonomic uniformitarianism may not hold for such factors as salinity tolerances and habitat preferences. There are no close relatives to *Inoceramus*, so Wright (1987) applied paleotemperature and paleosalinity equations derived for *Mytilus* on the basis of benthic habitat and similar shell mineralogies. However, with generic-level controls exerting a substantial influence on Mg/Ca and Sr/Ca ratios in Recent bivalves (Turekian and Armstrong, 1960), the comparison could be flawed.

3.2 Methods

3.2.1 Sampling Locations: Specimens for sclerochronology were selected based on the results of the shell alteration investigation. A suite of specimens that possessed both thick, contiguous shell and Sr/Ca and Mg/Ca ratios similar to Recent aragonitic (or, in the case of *Anomia*, calcitic) mollusks was assembled. The samples included seven *Baculites* of differing diameters, two *Eutrephoceras*, two *Hoploscaphites*, three *Inoceramus*, one *Anomia*, and one *Nymphalucina*.

These shells were sampled using a Dremel® variable-speed drill along ontogenetic growth at 2.5 mm intervals starting from the ontogenetically oldest part of shell available. Samples were taken from the part of the shell where growth lines were spaced the furthest apart to maximize the precision. The surface layer of shell was initially excavated into using a flat-bottomed, 3–mm bit to clear away surface contaminants and avoid the light isotopic ratios seen by Mitchell et al. (1994). The internal shell layers were sampled with a 1-mm bit at a consistent depth that, whenever possible, did not penetrate to the inner layer of the shell, where isotopes could be enriched by metabolic CO_2 as noted by Auclair et al. (2004) for *Nautilus*. When shell material was limited, as in the *Eutrephoceras*, every other sample was taken for ICP-OES analysis and the even increments (0 mm, 5 mm, etc.) reserved for mass spectrometer analysis. In other cases, each odd sample (2.5 mm, 7.5 mm, etc.) was collected such that it could be run for both analyses. For each shell, samples were also taken 2.5 or 5.0 mm apart along specific growth lines, to serve as comparision to the range of values in the ontogenetic sequence.

3.2.2 Treatment and Analysis of Samples: Treatment and analysis of samples followed the same ICP-OES and mass spectrometer protocol as discussed in Chapter 2. The ICP-OES samples (see Appendix C) were run first so that their data could be used as a minor-element filter for the mass spectrometer. From these candidates, three specimens (depicted in Figure 20) were selected for isotopic analysis (see Appendix D).

3.2.3 Data Processing: Minor element data, reported in ppm, was once again translated into mMol/Mol Ca. These data were then subjected to the Sr/Ca-Mg/Ca minor element filter as discussed in Chapter 2. Sclerochronology candidates which fulfilled the

requirements of the minor element filter for at least 80% of their data points were then examined in terms of other minor element ratios that had been linked to altered $\delta^{18}O$ values, namely Fe/Ca, Mn/Ca, Sr/Ca, and Na/Ca. The three candidates with the minor element ratios least likely to be diagenetically altered were selected for isotopic analysis.

As in the shell alteration investigation, paleoceanographic parameters were calculated from the $\delta^{18}O$ and $\delta^{13}C$ ratios, as well as the concentrations of strontium and sodium. Paleosalinity was calculated using the equation of Brand (1986):

$$S = -5.769\ln(A) + 28.380 \quad (2)$$

Salinity S is given in parts per thousand ± 0.5, and A is the ratio of ppm Sr / ppm Na, or the geometric mean of such ratios. The salinity values for each point were then substituted into an equation (Wright, 1987) for the $\delta^{18}O$ of the Western Interior Seaway water mass in which the organisms were living:

$$S_{(WIS)} = [1 - (\delta_{w(WIS)} - \delta_{w(ocean)}))/(\delta_f - \delta_{w(ocean)})] \times S_{(ocean)} \quad (3)$$

Models of the Earth without polar ice caps provided the constants for $\delta^{18}O$ of the open ocean, $\delta_{w(ocean)} = -1.22‰$ PDB, and salinity of the open ocean, $S_{(ocean)} = 34.3‰$ (Schmidt, 1997). Lastly, the $\delta_{w(WIS)}$ value and $\delta^{18}O$ for each sample of shell material were substituted into Grossman and Ku's molluscan aragonite paleothermometry equation:

$$T = 21.8 - 4.69(\delta^{18}O_{arag} - \delta^{18}O_w) \quad (1)$$

where $\delta^{18}O_{arag}$ is the isotopic signature of the shell material.

FIGURE 21—Specimens Used in Sclerochronology

A. *Inoceramus* Specimen I2

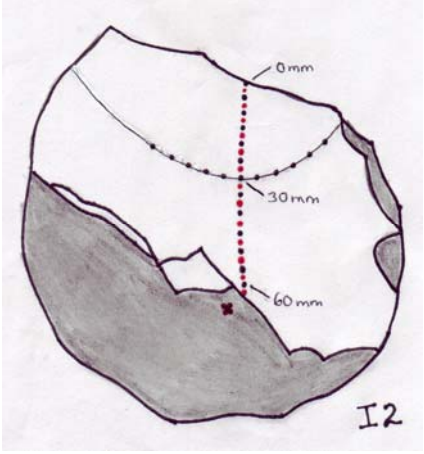

B. *Baculites* Specimen B7

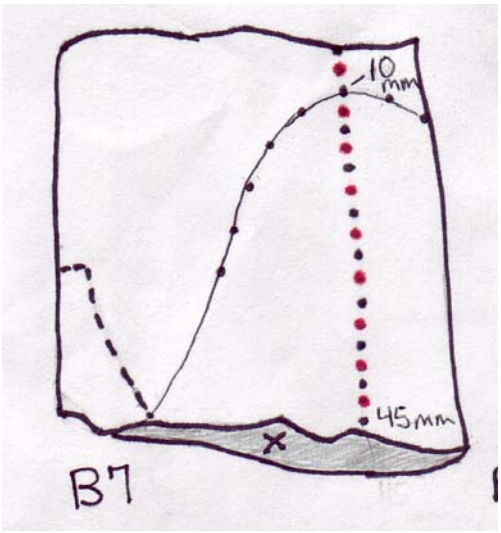

FIGURE 21—Specimens Used in Sclerochronology (Continued)

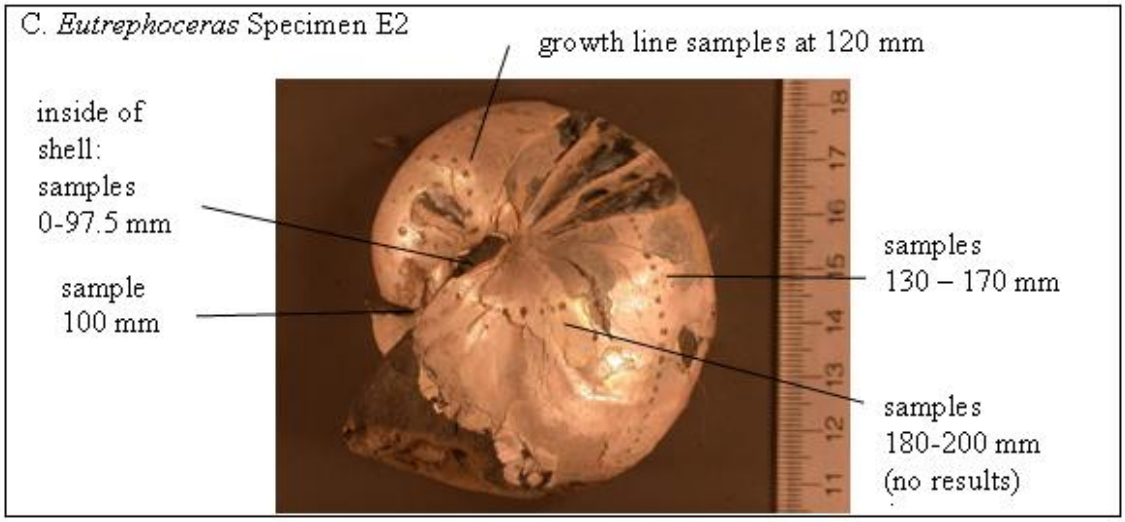

Based on minor element concentrations, three specimens were selected to be examined with the mass spectrometer. *Inoceramus* specimen I2 was from the Game Rach locality, and was infilled with, but not enclosed by, concretionary material. Baculites specimen B7 was also from the Game Ranch locality, preserved directly in the shale. *Eutrephoceras* E2 was recovered from a concretion at the Trask Ranch locality.

3.3 Results

3.3.1 Inoceramus: Of the bivalve specimens, I2 was selected because of its relatively uniform minor element concentrations (Figure 22). The *Nymphalucina* specimen N1 was excluded because of peaks in Fe/Ca, the *Inoceramus* specimen I3 was not considered because of peaks in Mg/Ca, Mn/Ca, and Fe/Ca, and the *Anomia* specimen A1 and *Inoceramus* specimen I1 were dismissed because of numerous peaks in multiple minor elements. The mean minor element ratios in the I2 shell material, in mMol/Mol, were Fe/Ca = 0.86 ± 1.49, K/Ca = 0.522 ± 0.142, Mg/Ca = 1.12 ± 0.42, Mn/Ca = 0.049 ± 0.046, Na/Ca = 19.8 ± 0.7, and Sr/Ca = 2.25 ± 0.93. Therefore, the specimen is considered favorable under the Sr/Ca-Mg/Ca minor element filter, and all other possible minor-element filters examined in Chapter 2. The Al/Ca dataset was incomplete so is omitted in this analysis. No general trends in minor element ratios were observed through ontogeny. Noticable deviations in minor element ratios occurred only at the last data point, taken closest to the aperature of the shell. At this point, the Mg/Ca and Fe/Ca ratios increased. The increases, however, do not correspond with changes in isotopic composition (Figure 23).

In general, the $\delta^{18}O$ and $\delta^{13}C$ ratios for the *Inoceramus* specimen are inversely related. A plot of these isotopes against each other (Figure 24), however, does not produce a significant correlation. The exception to this pattern occurs in shell samples taken from 0-7.5 mm in distance from the umbo. Ontogenetically, these are the earliest shell samples. In addition, the point at 12.5 mm, displays minima for both isotopic ratios. For the four $\delta^{18}O$ maxima that occur after 7.5 mm, labeled in Figure n+1, three are coincident with $\delta^{13}C$ minima, while the other preceded the $\delta^{13}C$ minima by one sampling

interval. The $\delta^{18}O$ minima also broadly correlate with salinity minima calculated from Brand's Sr/Na equation (1986). For the *Inoceramus*, the $\delta^{18}O$ represented in the data ranges from -2.21‰ to -7.02‰, and salinity from 32.2‰ to 33.6‰, corresponding to paleotemperatures of 26.4 ^{o}C to a very unlikely paleotemperature of 48.9 ^{o}C. The paleosalinity curve approximately parallels the $\delta^{18}O$ curve, with the exceptions of the ontogenetically earliest sample and the two $\delta^{18}O$ maxima (temperature minima). These temperature minima are spaced ~40 mm apart and are of approximately the same amplitude. The ontogenetically earlier minimum is ~7 ^{o}C warmer than the ontogenetically later minimum, while the ontogenetically earliest data point is ~8 ^{o}C warmer than the ontogenetically latest data point. However, the ranges in temperature and salinity for the *Inoceramus* do not necessarily represent the total range possible for the organism's lifespan. The accretion of the inner nacreous layer of aragonite is such that a sample taken in a given location will contain not only the paleoceanographic signature of the conditions during formation, but, below that, the signatures of shell formed later. Therefore, the sclerochronologic record of the *Inoceramus* is greatly time-averaged. Depending on the relative thickness of the layers secreted along the inside of the shell, the salinity and temperature profiles (Figure 25) that are produced may or may not be proportional to time.

Comparing the ontogenetic variability in $\delta^{18}O$ and $\delta^{13}C$ (n = 25) to the variability present in a single growth line at distance = 20 mm (n = 9), a lower standard deviation is present for the growth line than for the ontogenetic sequence. The standard deviation of the ontogenetic sequence is 0.97‰ for $\delta^{18}O$ and 0.67‰ for $\delta^{13}C$, whereas these values are 0.68‰ for $\delta^{18}O$ and 0.49‰ for $\delta^{13}C$ for the growth line. Based on one-tailed t-tests

with a 0.05 level of significance, there is no statistically significant difference between the mean $\delta^{18}O$ value of -5.46 ± 0.97‰ for the ontogenetic sequence and -5.39 ± 0.68‰ for the growth line, or between the mean $\delta^{13}C$ value of 5.48 ± 0.67‰ for the ontogenetic sequence and 5.62 ± 0.49‰ for the growth line. The sample taken from the I2 concretion produced no data due to mass spectrometer error.

FIGURE 22—Minor Element Ratios for Sclerochronology: Bivalves

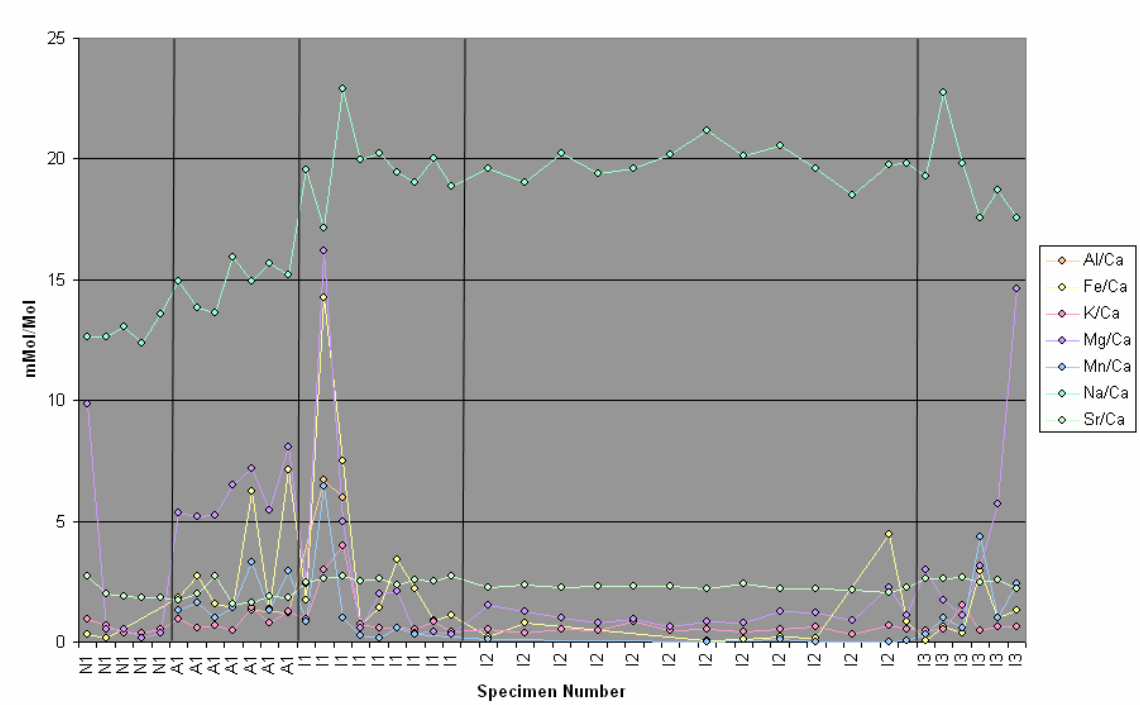

The inoceramid bivalve I2 shows the most consistent, low Fe/Ca, Mg/Ca, and Mn/Ca values. With twelve values for the minor element analysis, representing six centimeters, it is also the longest record for the sclerochronology candidate bivalves. Therefore, this specimen was selected for isotopic analysis. N1 = *Nymphalucina*, A1 = *Anomia*, I1-I3 = *Inoceramus*.

FIGURE 23—Sclerochronology of *Inoceramus* Specimen I2

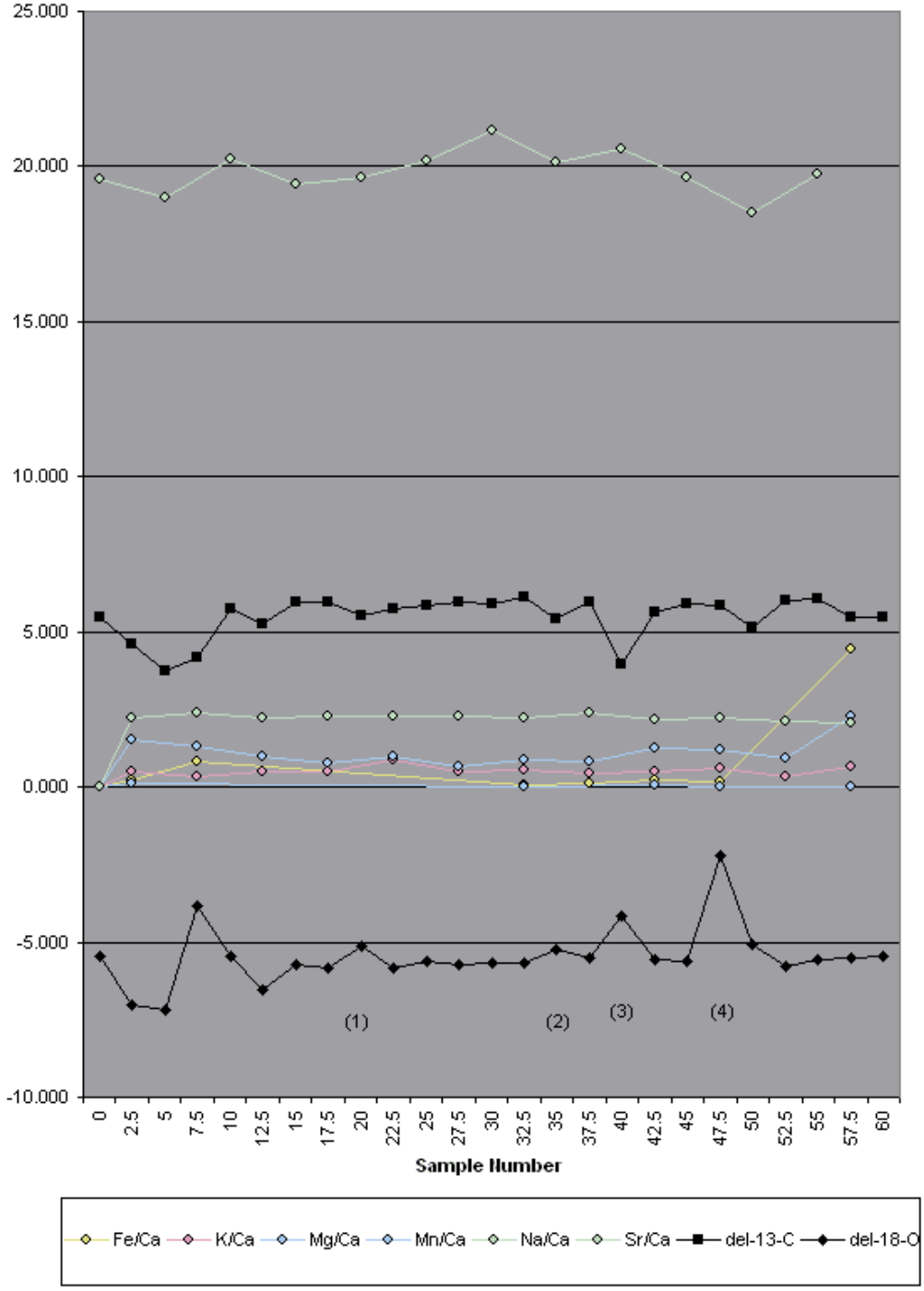

FIGURE 24—$\delta^{18}O$ Versus $\delta^{13}C$ for *Inoceramus* Specimen I2

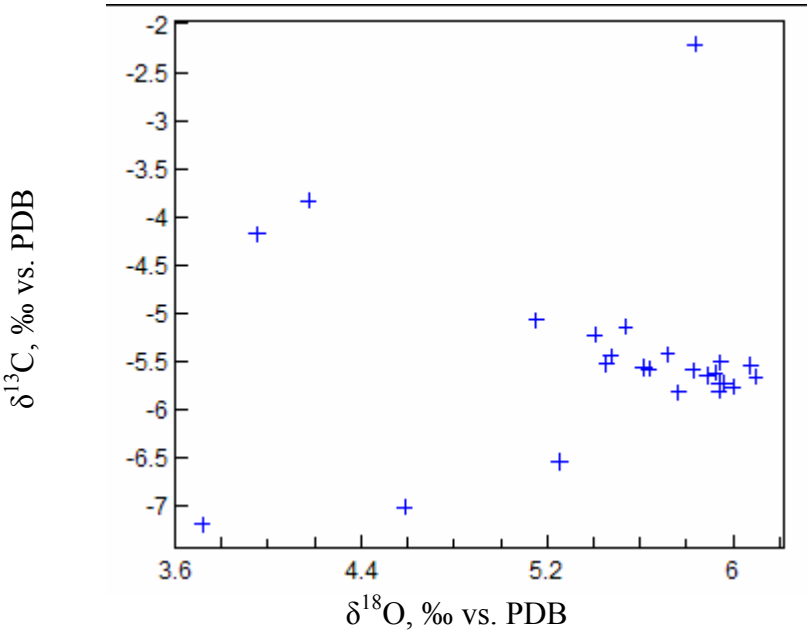

Although most relative maxima in the $\delta^{18}O$ curve correspond to relative minima in the $\delta^{13}C$ curve, a statistically significant linear correlation cannot be fit to the data. The data points below $\delta^{18}O = 5.2‰$ do not appear to fit any pattern; it is possible to see a slight negative trend to the clustered data of $\delta^{18}O$ values heavier than 5.2‰.

FIGURE 25—Calculated Paleotemperature through "Ontogeny" for *Inoceramus* Specimen I2

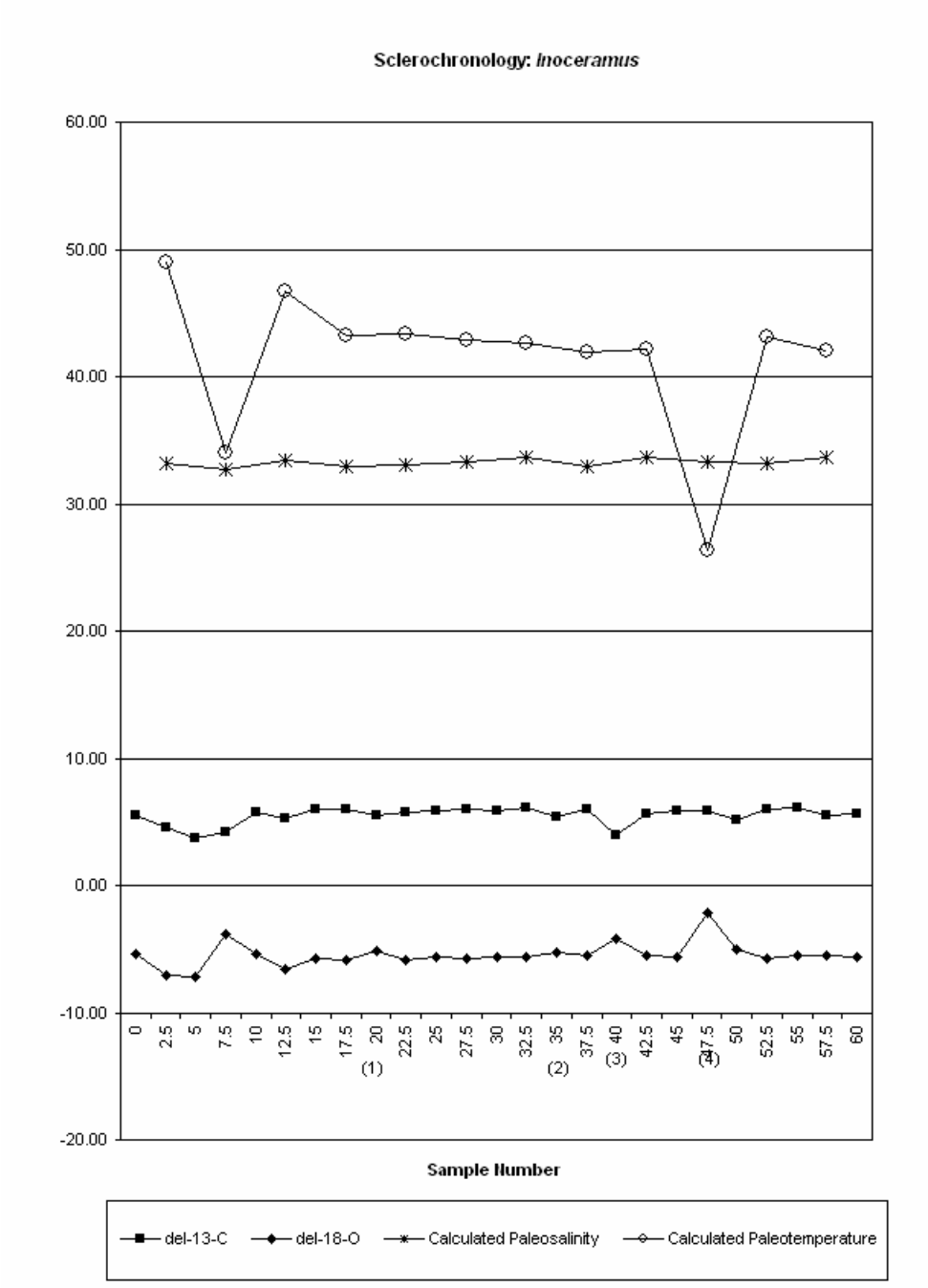

Although the "ontogenetic" sequence for the *Inoceramus* is time-averaged, a sine curve fits the temperature data reasonably well.

3.3.2. Baculites: Of the six *Baculites* specimens, B7 was selected because of its relatively uniform minor element concentrations (Figure 26), which satisfied all possible minor element filters. The mean minor element ratios in the shell, in mMol/Mol, were Fe/Ca = 0.389 ± 0.218, K/Ca = 0.86 ± 0.26, Mg/Ca = 1.31 ± 0.91, Na/Ca = 21.4 ± 3.4 (19.8 ± 0.9 without outlier), and Sr/Ca = 2.72 ± 0.29. The Al/Ca and Mn/Ca datasets were incomplete so are omitted in this analysis. No general trends in minor element ratios were observed over ontogeny. Noticable deviations in minor element ratios occurred at 12.5 mm from the ontogenetically youngest point on the specimen, where Mg/Ca increased from 1.14 to 3.04 mMol/Mol, and 17.5 mm, where the Na/Ca ratio changed from 19.9 to 28.2 mMol/Mol. In both cases, the sampling location directly following the deviation showed minor element ratios returning approximately to the pre-deviation value. As in the *Inoceramus* specimen, the increases in Na/Ca and Mg/Ca do not correspond with changes in isotopic composition (Figure 27).

In general, the $\delta^{18}O$ and $\delta^{13}C$ ratios for the *Baculites* specimen are directly related (Figure 28). A plot of these isotopes against each other (Figure 29) does not produce a statistically significant trendline. The sclerochronologic variations for the *Baculites* likewise show similar trends, albeit with vastly different magnitude fluctuations, between $\delta^{18}O$ and $\delta^{13}C$ data curves. For every $\delta^{18}O$ maximum, there is an equivalent $\delta^{13}C$ maximum at the same location, or one sampling location later in time/distance. Relative maxima occur at 5.0, 12.5, and 17.5 mm from the ontogenetically earliest sample. Relative minima occur at 0.0, 10.0, 15.0, and 25.0 mm. Through ontogeny, the amplitude of the $\delta^{18}O$ and $\delta^{13}C$ excursions decreases. There does not appear to be any relationship between the $\delta^{18}O$ and $\delta^{13}C$ maxima and the salinity data curve (Figure 30) derived from

Brand's Sr/Na equation (1986). For the *Baculites*, $\delta^{18}O$ ranged from -0.97‰ to -1.84‰, and salinity from 31.7‰ to 35.5‰, corresponding to paleotemperatures of 20.9 ^{o}C to 22.6 ^{o}C. The highest salinity value corresponds to the Na/Ca peak, and if this point is disregarded as a statistical outlier, the maximum salinity is 32.4‰ and the minimum paleotemperature is unaffected. There is a possible general decrease in $\delta^{18}O$ over ontogeny as well as the aforementioned trend in the amplitude of minima and maxima.

Comparing the ontogenetic variability in $\delta^{18}O$ and $\delta^{13}C$ (n = 11) to the variability present in a single growth line at distance = 15 mm (n = 8), a lower standard deviation is present for the ontogenetic sequence than for the growth line. The standard deviation of the ontogenetic sequence is 0.24‰ for $\delta^{18}O$ and 0.81‰ for $\delta^{13}C$, whereas these values are 1.23‰ for $\delta^{18}O$ and 0.72‰ for $\delta^{13}C$ for the growth line. Based on one-tailed t-tests with a 0.05 level of significance, there is no statistically significant difference between the mean $\delta^{18}O$ value of -1.28 ± 0.24‰ for the ontogenetic sequence and -1.65 ± 0.72‰ for the growth line, or between the mean $\delta^{13}C$ value of -3.25 ± 0.81‰ for the ontogenetic sequence and -3.62 ± 0.42‰ for the growth line. The sample taken from the B7 concretion returned a $\delta^{18}O$ value of -2.10‰ and a $\delta^{13}C$ value of -23.65‰.

FIGURE 26—Minor Elements Used for Sclerochronology: *Baculites*

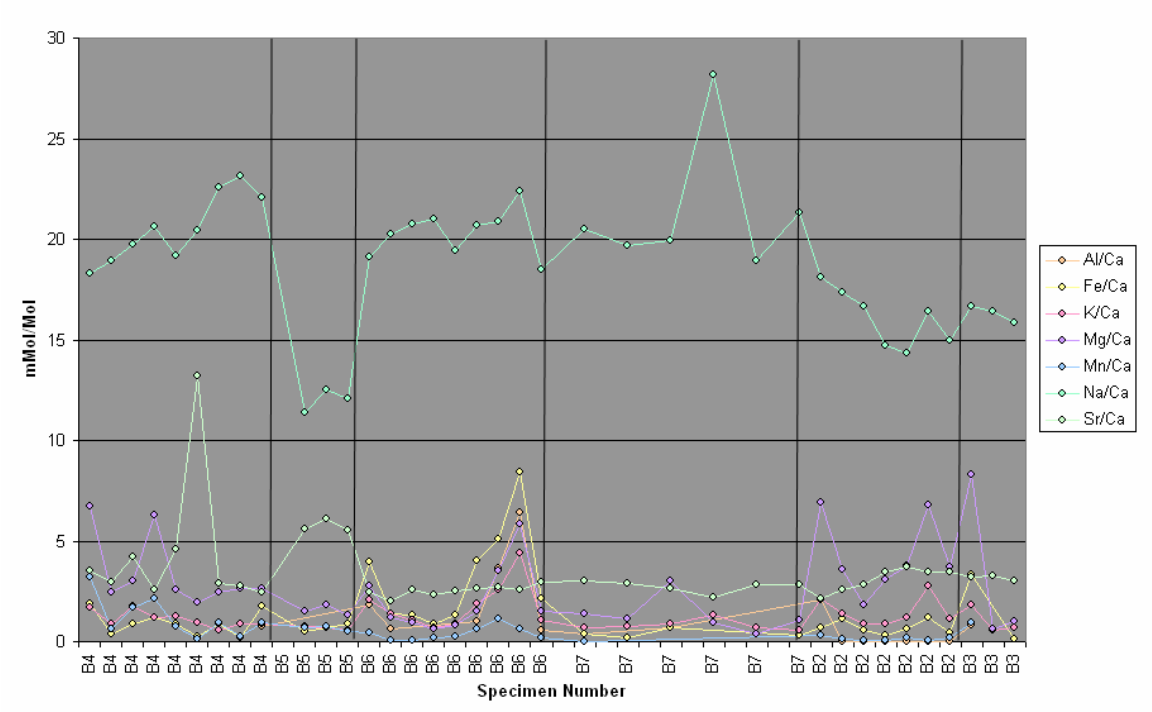

Among six *Baculites* specimens (B2-B7) screened, B7 had the most consistent K/Ca, Mg/Ca, Mn/Ca, and Sr/Ca values. Peaks in Mg/Ca and Na/Ca do exist at the middle of the ontogenetic sequence.

FIGURE 27—Sclerochronology of *Baculites* Specimen B7

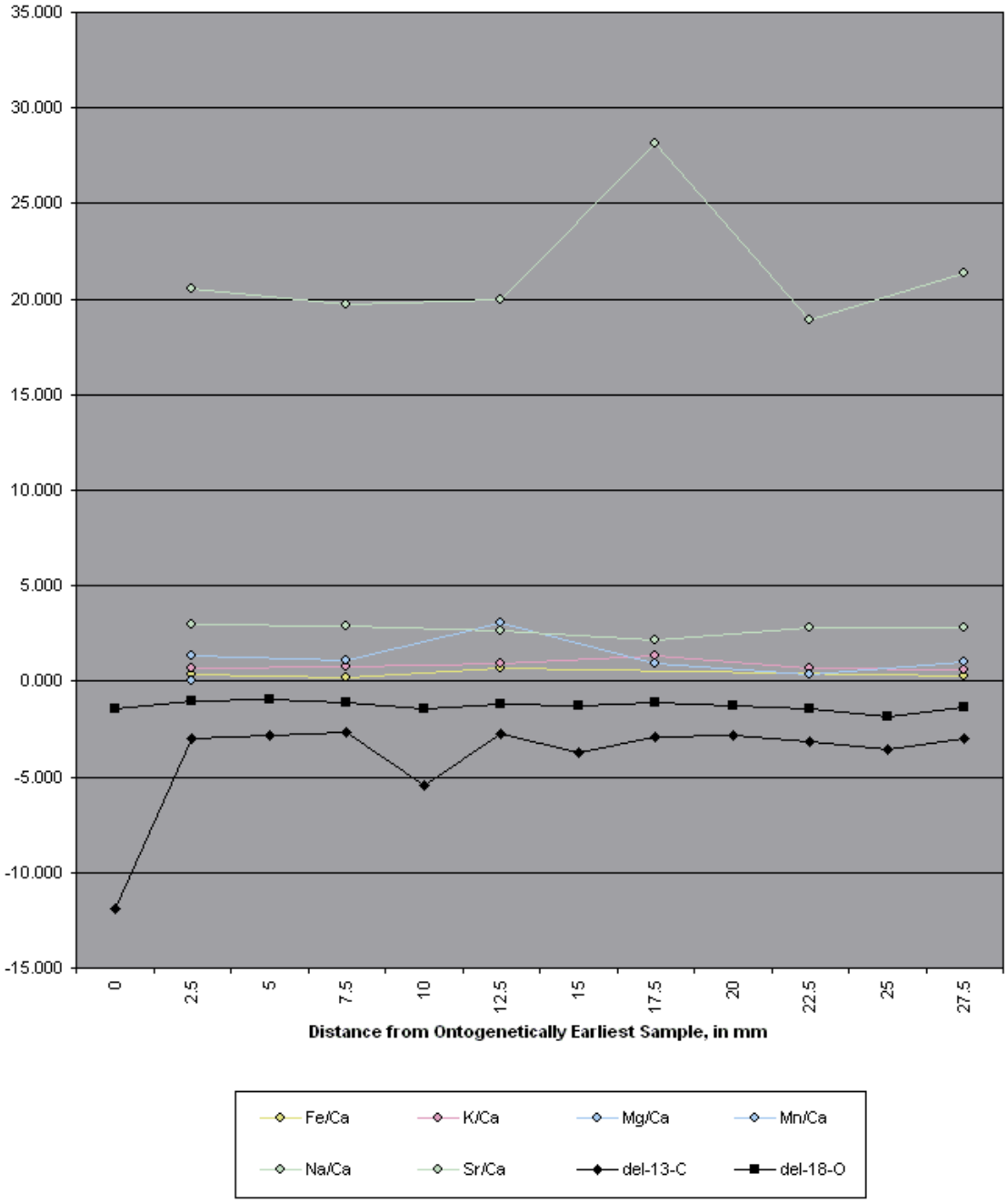

While the deviation in Na/Ca ratio seen at 17.5 mm from the ontogenetically earliest sample influenced the calculated salinity of *Baculites* specimen B7, it did not coincide with a change in $\delta^{18}O$ or $\delta^{13}C$. There was also no associated change in $\delta^{18}O$ or $\delta^{13}C$ associated with the Mg/Ca peak at distance = 12.5 mm.

FIGURE 28—Stable Isotope Sclerochronology of *Baculites* Specimen B7

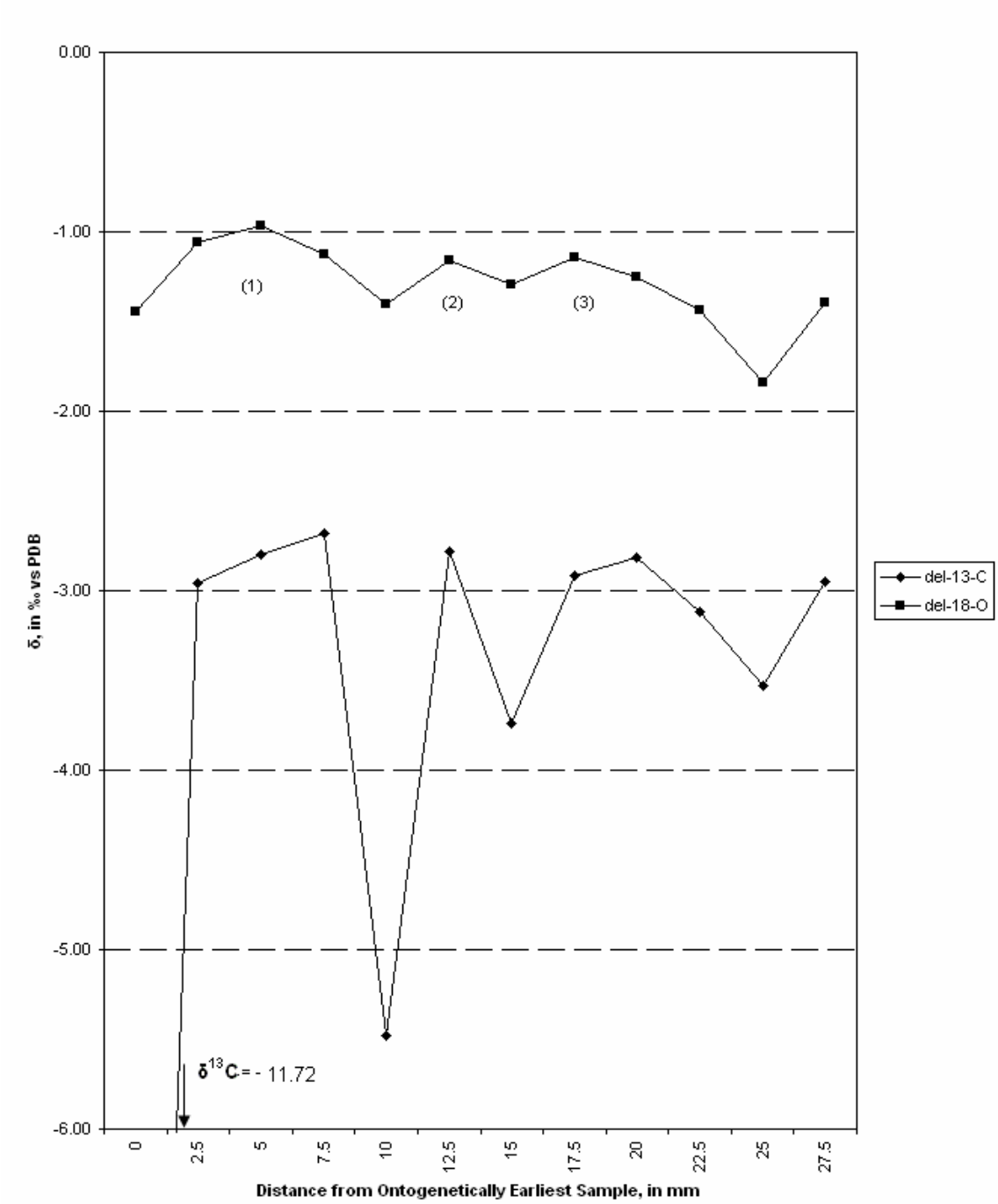

In general, the $\delta^{18}O$ or $\delta^{13}C$ curves for *Baculites* specimen B7 parallel each other. The three labeled maxima in the $\delta^{18}O$ curve match with three maxima in the $\delta^{13}C$ curve, though the amplitude of the variations in the $\delta^{13}C$ curve is much greater.

FIGURE 29—$\delta^{18}O$ Versus $\delta^{13}C$ for *Baculites* Specimen B7

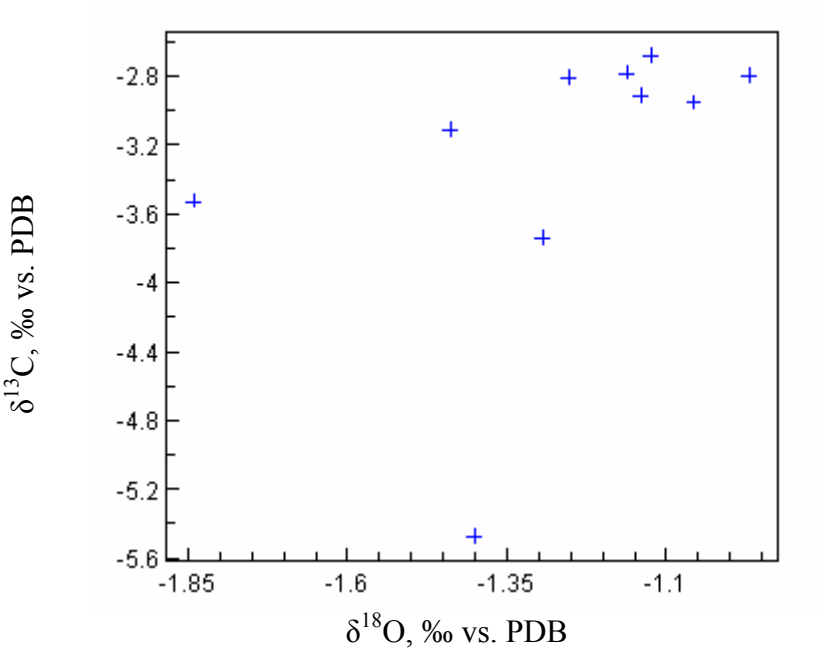

The $\delta^{18}O$ and $\delta^{13}C$ of *Baculites* specimen B7 do not produce a statistically significant linear fit. There does, however, appear to be a general trend of increasing $\delta^{18}O$ with increasing $\delta^{13}C$.

FIGURE 30—Calculated Paleotemperature and Paleosalinity for *Baculites* Specimen B7

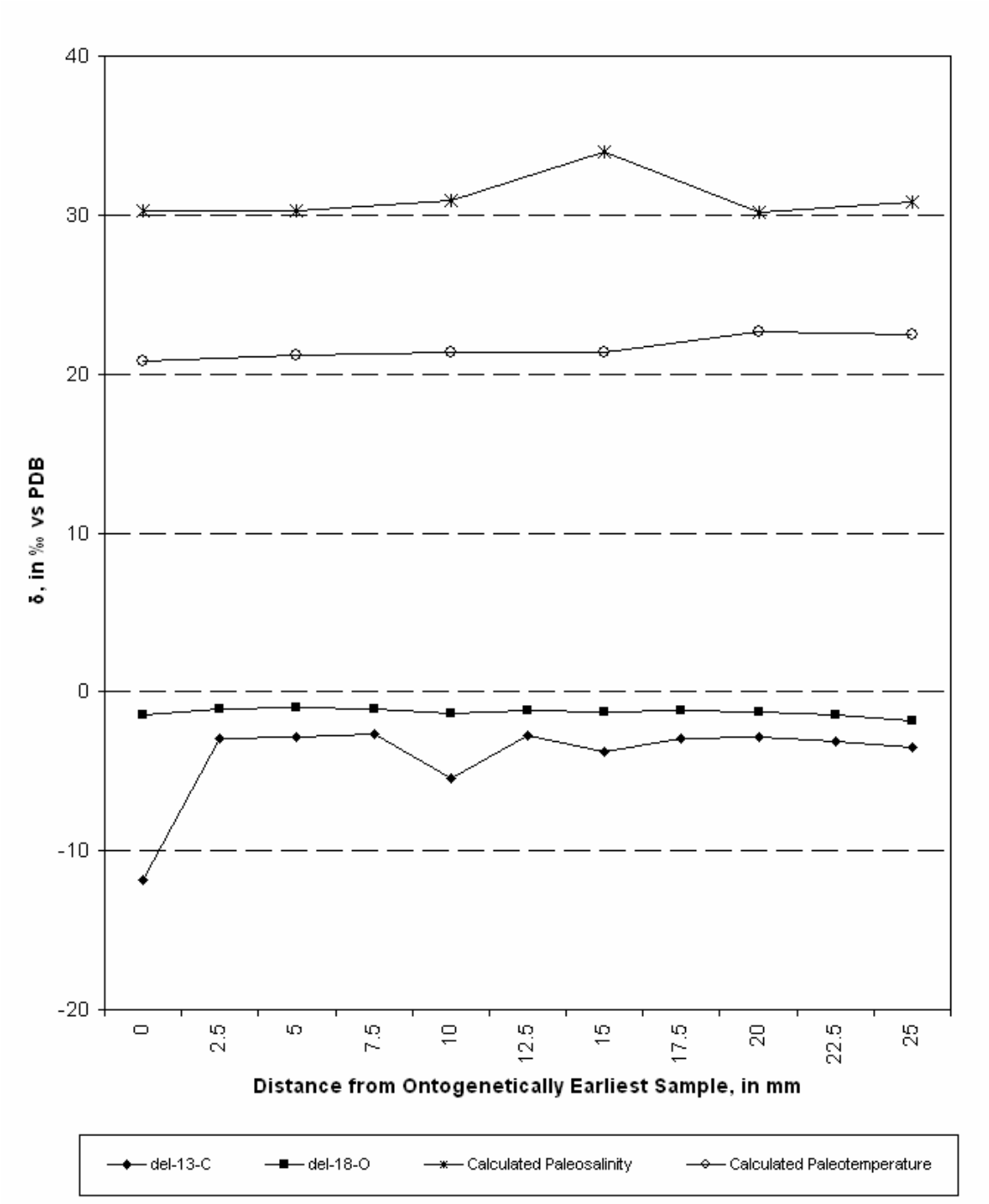

3.3.3 *Eutrephoceras*: Of the *Eutrephoceras* specimens, E2 was selected because it offered the most expansive dataset. Minor element ratios for the two specimens were comparable. The E2 dataset included more samples taken from the inner whorls of the shell, including two samples from the neanoconch, the early developmental stage characterized in *Eutrephoceras* by cancellate ornamentation (Landman et al, 1983). E2 also had fewer mass spectrometer errors or underweight samples. While the minor element ratios vary more than in the *Inoceramus* or *Baculites* specimens, the Sr/Ca ratio is reasonable with respect to the filter limits. The Mg/Ca ratio peaks above 6.5 mMol/Mol at 12.5, 32.5, and 62.5 mm from the ontogenetically earliest point (Figure 31). All of these points are coincident with the appearance of cement upon the septa. The cement is highly enriched in Mg, with Mg/Ca values of 71.9 mMol/Mol and 32.7 mMol/Mol. Fe/Ca and Mn/Ca ratios, also higher in the cement than in the shell, peak at these locations as well. Na/Ca minima coincide with these maxima. The cement nearest to the protoconch coincides with a slight increase in both $\delta^{18}O$ and $\delta^{13}C$, although this could be circumstantial.

The $\delta^{18}O$ and $\delta^{13}C$ curves in *Eutrephoceras* specimen E2 appear to parallel each other (Figure 32), and when the stable isotopes are plotted against each other as in Figure 33, a positive, statistically significant linear fit emerges. This trendline has a strong r^2 value of 0.673 and a p-value of 4.52×10^{-4}. The isotopes share relative minima at 40, 55, 75, 85, 105, and 170 mm from the protoconch. The largest deviations are those at 55, 105, and 175, and may represent a periodic trend. There does not appear to be any trend in the amplitude of these minima, nor any overall trend in $\delta^{18}O$ and $\delta^{13}C$. Another relationship which emerges from the sclerochronologic investigation of *Eutrephoceras*

specimen E2 is, as in *Baculites* specimen B7, a general positive correlation between $\delta^{18}O$ and salinity (Figure 34). This relationship is stronger for the interior portion of the shell. Clearly, the datapoints latest in ontogeny show anomalous $\delta^{13}C$ and Na/Ca.

Comparing the ontogenetic variability in $\delta^{18}O$ and $\delta^{13}C$ (n = 28) to the variability present in a single growth line at distance = 125 mm (n = 8), a higher standard deviation is present for the ontogenetic sequence than for the growth line. The standard deviation of the ontogenetic sequence is 0.80 ‰ for $\delta^{18}O$ and 2.40 ‰ for $\delta^{13}C$, while these values are 0.29 ‰ for $\delta^{18}O$ and 0.55 for $\delta^{13}C$ for the growth line. Based on one-tailed t-tests with a 0.05 level of significance, there is a statistically significant difference between the mean $\delta^{18}O$ value of -1.28 ± 0.80 ‰ for the ontogenetic sequence and -0.73 ± 0.29 ‰ for the growth line, and between the mean $\delta^{13}C$ value of -1.28 ± 2.40 ‰ for the ontogenetic sequence and -0.31 ± 0.55 ‰ for the growth line. The sample taken from the E2 concretion returned a $\delta^{18}O$ value of -1.18 ‰ and a $\delta^{13}C$ value of 0.18 ‰. Three cement samples also returned values, shown on Figure 35.

FIGURE 31—Sclerochronology of *Eutrephoceras* Specimen E2

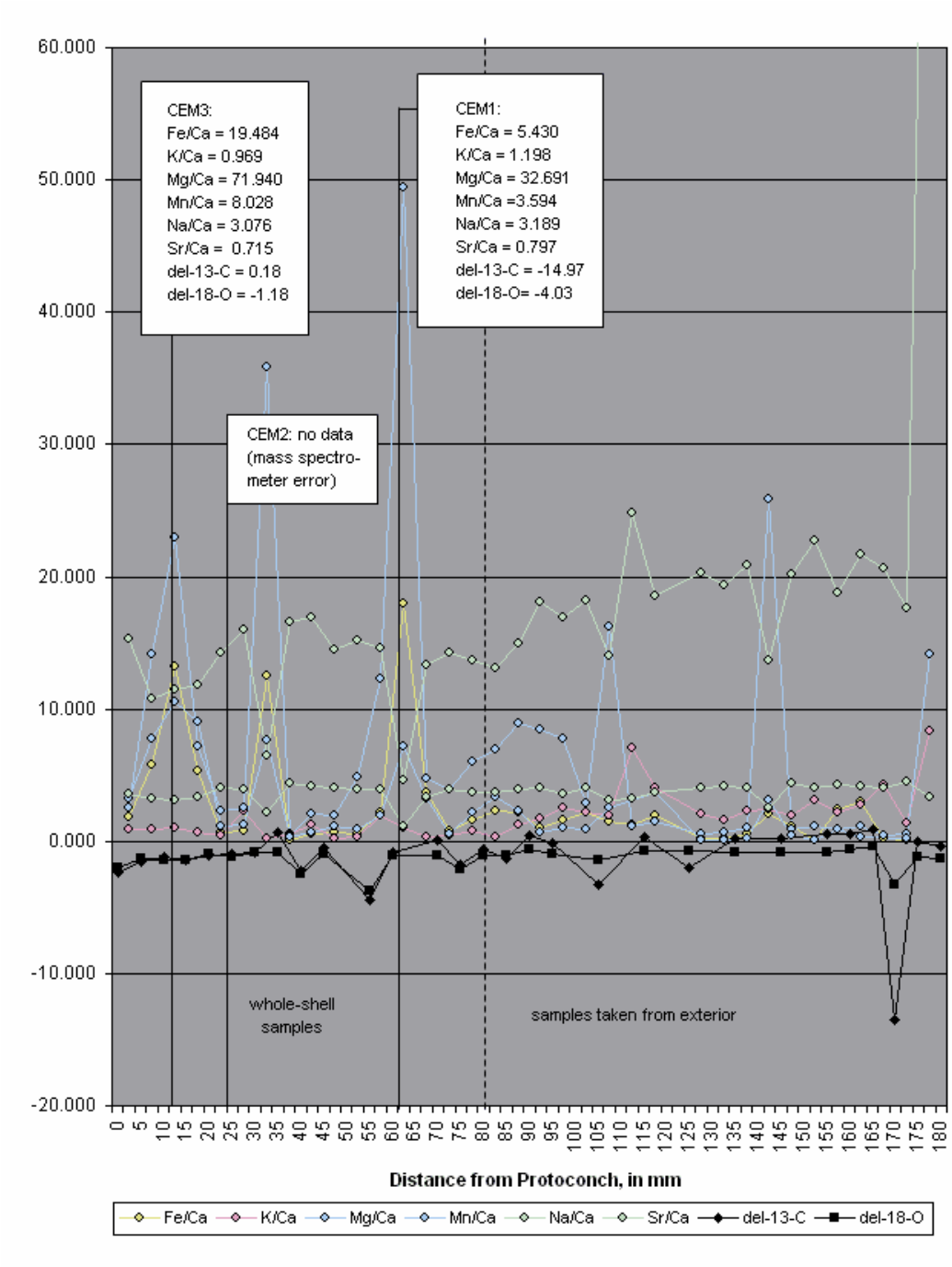

The minor element sclerochronology of *Eutrephoceras* specimen E2 shows clearly the relationship between diagenetic alteration of shell and cementation. Solid vertical lines, indicating the presence of cement, coincide with relative maxima in Fe/Ca, Mg/Ca, and Mn/Ca, which are minima in Na/Ca.

FIGURE 32—Stable Isotope Sclerochronology of Eutrephoceras Specimen E2

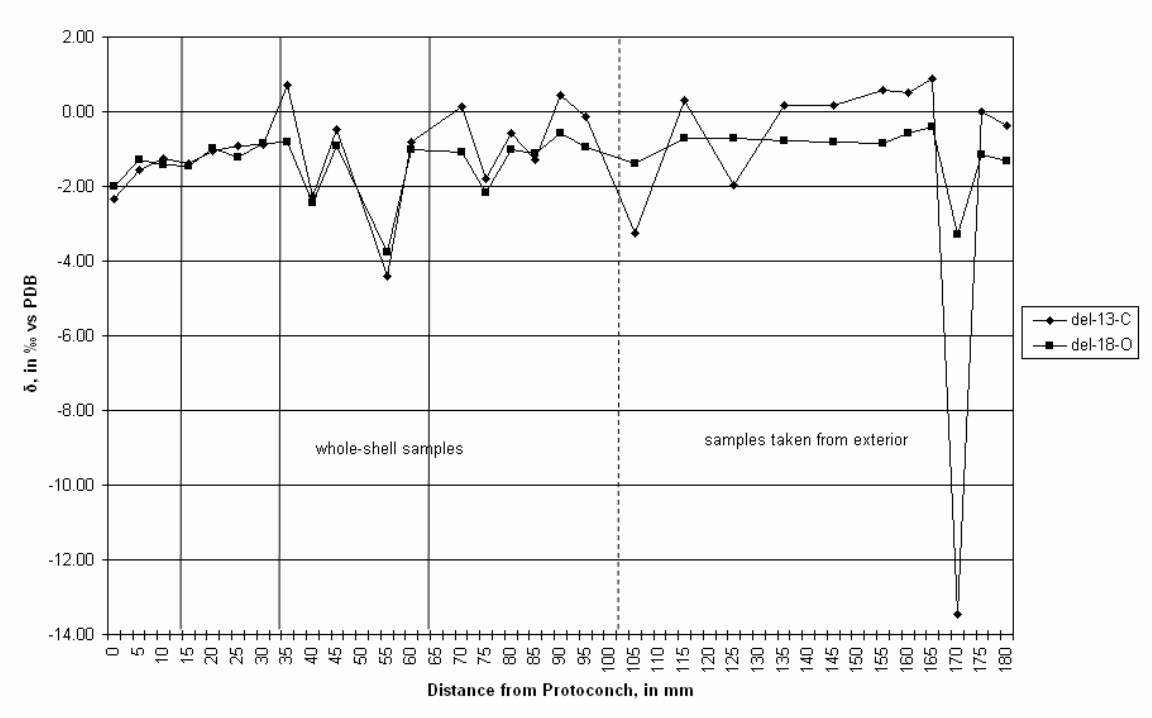

The stable isotope sclerochronology of the Eutrephoceras specimen shows parallel curves for $\delta^{18}O$ and $\delta^{13}C$, with nearly all minima and maxima coinciding. Both curves show greater fluctuations before distance = 30 mm. Once again, solid vertical lines indicate the location of cement.

FIGURE 33—$\delta^{18}O$ Versus $\delta^{13}C$ for *Eutrephoceras* Specimen E2

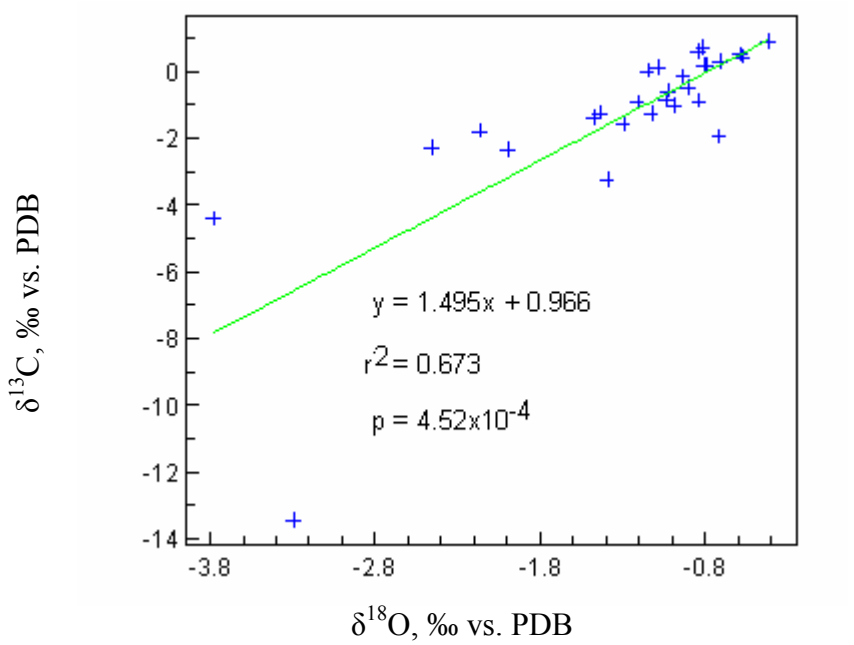

The relationship between $\delta^{18}O$ and $\delta^{13}C$ is positive, with an r^2 value of 0.673 and a p value of 4.52×10^{-4},. The majority of data points cluster from -2‰ to 0.5‰ for $\delta^{13}C$ and -0.5‰ to -1.5‰ for $\delta^{18}O$.

FIGURE 34—Calculated Paleotemperature and Paleosalinity for *Eutrephoceras* Specimen E2

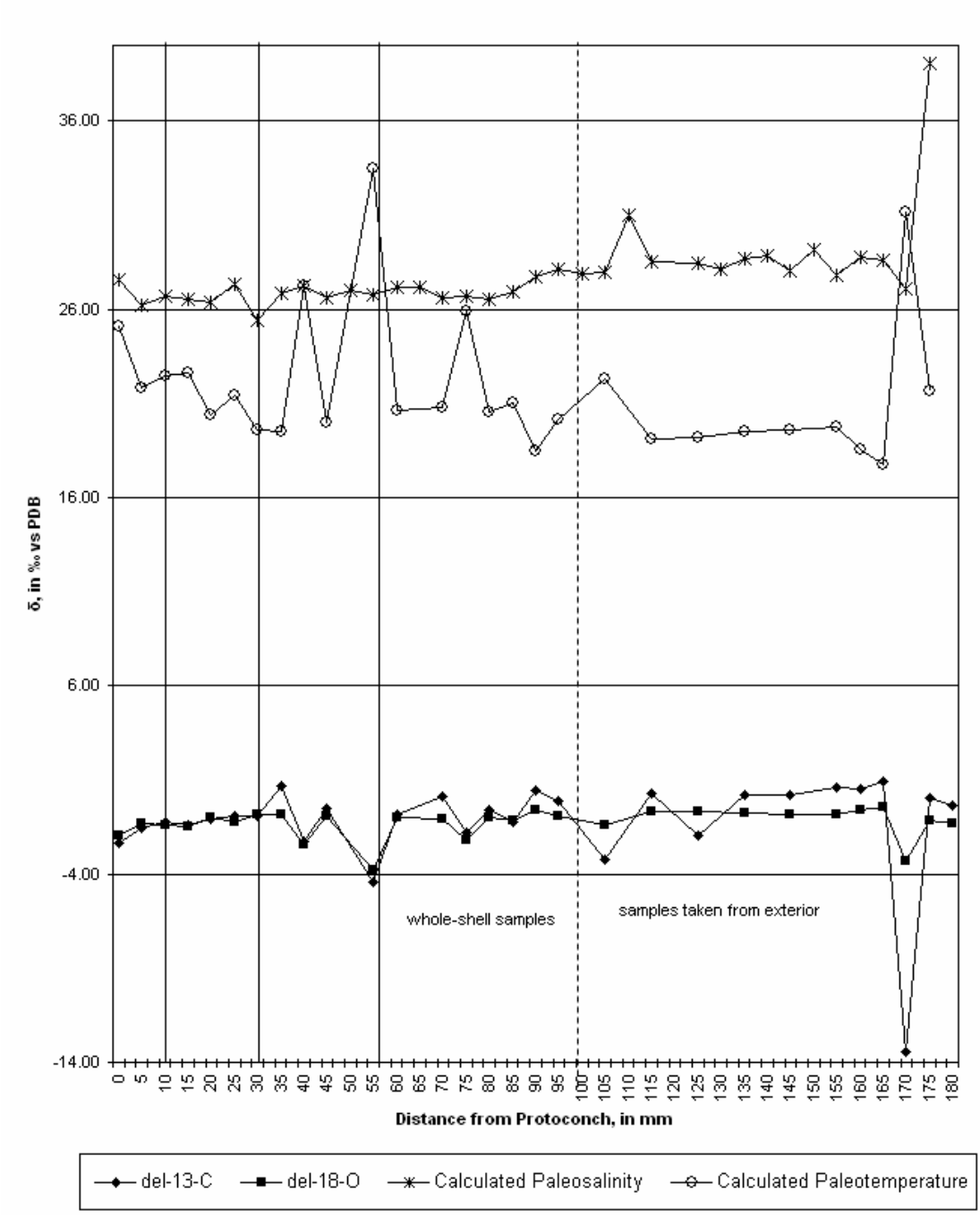

Calculated paleotemperature shows several fluctuations, with the largest being spaced at 55, 105, and 170 mm from the protoconch. Paleosalinity coincides with the isotopic trends for the first half of the ontogenetic sequence.

3.4 Discussion

3.4.1. Inoceramus: The slight negative correlation between $\delta^{18}O$ and $\delta^{13}C$ in *Inoceramus* specimen I2 (Figure 24) is characteristic of bivalves with a slow rate of metabolism (Ivany et al., 2003). Instead of reflecting metabolism, the isotopic signature in such mollusks reflects environmental parameters such as salinity and temperature. In the Western Interior Seaway, a specimen of the bivalve *Artica ovata* (Fatherree, 1995) also showed a negative correlation between stable isotopes. This pattern was noted for the Recent bivalve *Adamussium colbecki*, an Antarctic scallop (Barrerra et al., 1990). The Recent *Mercenaria mercenaria* specimen from the Long Island Sound examined by Elliot et al. (2003) also showed such a correlation, as did the Eocene *Cucullaea raea* after 6 mm of ontogenetic growth (Dutton et al., 2002). In contrast, *Mercenaria mercenaria* specimens found farther south showed a positive correlation between $\delta^{18}O$ and $\delta^{13}C$ (Elliot et. al., 2003), as did the *Cucullaea raea* before 6 mm growth. Previous studies of *Inoceramus* also revealed positive correlations between $\delta^{18}O$ and $\delta^{13}C$. Tourtelot and Rye (1969) found a positive correlation between stable isotopes in both the aragonitic and calcitic layers of an *Inoceramus* specimen, though their sequences for aragonite and calcite were limited to only had nine and ten data points, respectively. The ontogenetically earliest three of eight samples taken by Fatheree (1995) showed a positive relationship $\delta^{18}O$ and $\delta^{13}C$, whereas the ontogenetically latest four showed a negative correlation. Whittaker et al. (1988) showed a similar pattern for a contemporaneous (but farther north) *Inoceramus*. Of the 25 samples taken from *Inoceramus* specimen I2, the first six to eight show a positive relationship between $\delta^{18}O$ and $\delta^{13}C$ (Figure 23). This is likely the signature of a metabolic rate that decreases with

age, which is common in bivalves as energy in adulthood is redirected to reproductive maturation and spawning (Ivany et al., 2003). The inoceramid used in Fatheree et al. (1995) was from the *Baculites compressus* biozone in South Dakota, as was the *Inoceramus* specimen I2 used in this study. Both show $\delta^{18}O$ and $\delta^{13}C$ related positively for the first ~ 15 cm of (time-averaged) growth, suggesting that metabolic rate decreases at approximately the same time in each specimen.

Interpretations of ontogenetic trends in $\delta^{18}O$, $\delta^{13}C$, and calculated temperature are hampered by the time-averaging present in the data. The 22.5-degree total temperature range of 26.3 to 48.8 ^{o}C (Figure 25) is clearly unrealistic for a shallow ocean during a warm greenhouse climate interval. However, two more realistic temperatures can be found on the paleotemperature curve for the *Inoceramus*, 34.0 and 26.4 ^{o}C, at the two relative minima. While it should be remembered that these temperatures are influenced time-averaging inherent in the slowly deposited nacreous structure, they are clearly different from the remainder of the temperature data points. These points appear to represent marine conditions typical of the overlying water mass. These could be initiated by seasonal changes in oceanic circulation which produce a mixing of the water column. The length of such an interval with respect to the length of intervals with bottom-water isotopic signatures is unknown, because the *Inoceramus* could slow shell precipitation at such times and therefore produce an isotopic record biased towards bottom-water conditions.

While intervals of bottom-water can be identified in the sclerochronology of *Inoceramus* specimen I2, they cannot be readily explained. The heavy $\delta^{13}C$ and light $\delta^{18}O$ values are typical of Western Interior Seaway epifauna, with $\delta^{13}C$ and $\delta^{18}O$ values of 0.77 to 3.12‰ and -2.10 to -5.34, respectively, found for *Anomia*. On the other hand, *Inoceramus* remains found outside of the Western Interior Seaway do not show such isotopic ratios. For instance, those found in Mid-Late Campananian deep-ocean environments in the South Atlantic produced average $\delta^{13}C$ and $\delta^{18}O$ values of 1.38 ± 0.05‰ and 0.70 ± 0.14‰, respectively (Saltzman and Barron, 1982). Therefore, it is unlikely that the isotopic ratios in the *Inoceramus* represent biological factors peculiar to *Inoceramus*. Therefore, the bottom-water represents an isotopically unique environment.

An interesting observation with regards is that the salinity recorded by *Inoceramus* I2 stays close to normal marine conditions (~33‰) throughout ontogeny. However, using the $\delta^{18}O$ value of -1.27‰ for the Western Interior Seaway and assuming a decrease of 1‰ in δ_w for every 5‰ increase in salinity (Epstein and Mayeda, 1953), in order to bring the *Inoceramus* paleotemperature down the ~30 ^{o}C necessary for shell precipitation. Even if the salinity equation used in this study is discarded, however, using the $\delta^{18}O$ value of -1.27‰ for the Western Interior Seaway to reach realistic paleotemperatures for the *Inoceramus*, salinities in excess of 58‰ are needed, which would be inhospitable to *Anomia*. Therefore, salinity is likely not the cause for the disparity between bottom-water and the overlying water mass. If instead, the salinity value is accepted, $\delta^{18}O$ of the bottom-water would have to be -3.70‰ to produce realistic paleotemperatures. An absurdly depleted freshwater input of -78‰ is needed to produce this value, and this would surely leave a signature on the Sr/Na ratios of the shells.

Another mechanism for reaching this value is unknown, as changing the signal of freshwater between -5 and -25‰ does not significantly affect the $\delta^{18}O$ result for seawater, and increasing the quantity of freshwater input would lower the $\delta^{18}O$ but also change salinity and provide light $\delta^{13}C$. The $\delta^{13}C$ values of the epifauna are equally difficult to explain. Escape of methane present in the sediments would contribute $\delta^{13}C$ on the order of -15 to -20‰, consistent with the $\delta^{13}C$ values of shells for infaunal organisms but not those for epifaunal organisms. Addition of freshwater would likewise contribute negative $\delta^{13}C$ isotopes. Ocean anoxia is know to correlate with heavy $\delta^{13}C$ values in the unoxidized organic carbon, but how these values could be incorporated in molluscan shell is unknown. Therefore, at this time, it must be concluded that the light $\delta^{18}O$ and heavy $\delta^{13}C$ of the molluscan epifauna represent a distinct geochemical environment, without explanation, that may at times be mixed or replaced by water from the overlying water mass.

The length of cycles present in $\delta^{18}O$, $\delta^{13}C$, and calculated temperature are impossible to interpret numerically as it is unknown how many sub-layers within the thin aragonitic shell each sampling penetrated and the amount of time each layer represents (which may differ between layers). These ambiguities could be circumvented if a specimen could be sampled, using a microscope-mounted drill, at a fine enough scale. Considering that the entire aragonitic layer for specimen I2 is ~1 mm thick, this does not seem feasible. A better alternative is to find *Inoceramus* specimens with intact outer calcitic layers, which accreted along the growth axis, and therefore can be sampled throughout ontogeny. The prismatic calcite layer can unfortunately be fragile, as it is usually separated from the aragonitic layer and fragmented, but sampling a reasonably

large calcitic shell piece (that can be readily oriented with respect to ontogeny) would resolve many questions about the bivalve.

3.4.2. Baculites: The slight positive correlation between $\delta^{18}O$ and $\delta^{13}C$ (Figures 28 and 29) is characteristic of a mollusk that is secreting shell that is influenced by metabolic CO_2, usually implying a rapid metabolic rate (Ivany et al., 2003). A negative correlation between these two variables was also present for *Baculites* specimens from the Western Interior Seaway examined by Tourtelot and Rye (1969) and Forester et al. (1977). However, Whittaker et al. (1988) found well-defined negative correlations between stable isotopes in *Baculites*. It is also present in the first few samples of the *Baculites* studied by Fatherree et al. (1998). Their samples taken later in the ontogeny of *Baculites* showed a negative correlation, which most likely indicates a decrease in the baculitid's rate of growth. A useful follow-up study would be examining the relationship between $\delta^{18}O$ and $\delta^{13}C$ with respect to the diameter of the baculite, preferably using fossils with longer contiguous shell records. The fluctuations in $\delta^{18}O$, salinity, and temperature do not appear to be significant, and imply that the baculitid was living in the upper/intermediate water mass for the time span represented in the shell precipitated. The minima in $\delta^{13}C$ are not associated with changes in salinity, so likely do not represent migration into bottom-water. These fluctuations could be due to fluctuations in dissolved inorganic carbon within the water column, seasonal changes in food source, or alteration that is not coincident with minor element alteration.

The temperature recorded by *Baculites* specimen B7, excluding the outlier of 24.2 ^{o}C at 25 mm from the ontogenetically earliest sample (a product of an unusually high Na/Ca ratio) ranges from 20.2 to 22.3 ^{o}C. This range represents reasonable living

conditions for a mollusk, and reasonable paleotemperatures for a shallow marine setting during a greenhouse climate interval. Forester et al. (1977) derived a temperature range from 17 to 25 ^{o}C for a 10-cm *Baculites compressus* var. *robinsoni* of the Western Interior Seaway. Fatherree et al. (1998) found an even greater temperature range, 19.7 to 29.7 ^{o}C, for their 44-cm ontogenetic sequence of a *Baculites compressus* found at Game Ranch. Because the temperature range for that specimen depends on the decrease in calculated temperature through ontogeny, within a 2.5-cm segment, however, the temperature difference is 0.4 to 5.8 ^{o}C, most often ~2.5^{o}C. This is comparable to the range for baculitid B7. Because of the truncated temperature range, the ontogenetic growth in the specimen likely represents less than one year, as is further suggestede by Fatherree et al.'s (1998) analysis. Recent *Nautilus* in the wild grows 9-44 mm/yr, with 24-44 mm/yr for adolescent individuals (Saunders, 1983). This should be considered a minimum growth rate for the *Baculites* because *Nautilus* must precipitate shell in a cold-water, high-pressure environment. Both of these physical factors are correlated with slower shell precipitation in Recent mollusks (Mann, 1992).

3.4.3. Eutrephoceras: Compared to the *Eutrephoceras* specimens studied by Landman et al. (1983), the *Eutrephoceras* in this study has a similar, but statistically significant, positive correlation between δ^{18}O and δ^{13}C (Figure 33). Recent *Nautilus* individuals raised in an aquarium instead show generally negative correlations, except for the first few millimeters of growth (Landman et al., 1984). This cannot be the effect of changes in feeding habits, as the majority of the ontogenetic sequence for the aquaria-raised specimens was represented by pre-hatching growth. Whether the δ^{13}C of the aquarium water changed over the period of study is unknown, as is the general health of

the organisms, who died shortly after hatching and precipitated abnormally-shaped shells. As in the *Nautilus* and in the *Eutrephoceras* studied by Landman et al. (1983), the *Eutrephoceras* specimen E2 shows an increase to heavier isotopes in the first few centimeters of growth. In addition, the variability in isotopes prior to a distance of 35 mm from the E2 protoconch is low. This suggests a protected environment for the young nautiloid, presumably the egg sac. Through ontogeny, the *Eutrephoceras* shell shows slowly decreasing paleosalinities, likely reflecting offshore migration, as in Recent *Sepia* (Bettencourt and Guerra, 1999). With paleosalinities of ~27‰ during the first 75 mm of phragmacone accretion, these are comparable to the salinities calculated for *Placenticeras,* so likely represent the uppermost waters of the Western Interior Seaway. The sharp temperature drop prior to 35 mm could represent the migration out of a near-planktic mode of life into one where the organism is living in colder water and swimming actively through the water column, where it accumulates both seawater carbonate and metabolic carbon with slightly varying isotopic signature.

If the three largest temperature peaks on Figure 34 represent an annual cycle, the *Eutrephoceras* is growing at 60-80 mm in a year, slightly higher than the average growth rate for adolescent *Nautilus*, and comparable to the growth rate for the cuttlefish *Sepia offinalis* living off the coast of Spain (Bettencourt and Guerra, 1999). Because the habitat of the *Eutrephoceras* is determined to be warm-water, the growth rate for *Sepia* is realistic.

The $\delta^{13}C$ curve for Eutrephoceras specimen E2 shows a $\delta^{13}C$ range of -4.2 to -0.4‰, comparable in values and range to the *Eutrephoceras* in Landman et al. (1983) and in range alone to *Nautilus* (Landman et al., 1994). There is a single very negative $\delta^{13}C$

excursion, late in ontogeny, which likely represents a migration into the bottom-water, because the salinity increases dramatically at the same time. Other excursions at 75 and 105 mm into this bottom water may be recorded by the $\delta^{13}C$ and salinity curves, with lower-amplitude $\delta^{13}C$ deviations. Why the *Eutrephoceras* would migrate into the bottom-water is a good question. It is possible that a preferred food source was present in the benthic sediments, and if this is the case, this research supports the notion of nektobenthic ammonites hovering above the seafloor when feeding. Another potential explanation is that the bottom-waters provided refuge from vertebrate predators during times of susceptibility, such as spawning or septal secretion. On the other hand, the signatures may instead record mixing events with the light- $\delta^{18}O$ bottom water.

4. CONCLUSIONS

When performing stable isotope sclerochronology, or when using stable isotopes in molluscan shell for paleoclimate proxies, diagenetically altered shell must be avoided. The results of this study suggest that for paleotemperature reconstruction based on the isotopic analysis of aragonite, one must be selective. Specimens preserved in shale are preferable, as shown by the "Mode of Preservation" suite and the higher standard deviations for paleotemperatures derived from fossils found in concretions (e.g., Trask Ranch *Inoceramus* versus Game Ranch *Inoceramus*). In ammonites, phragmacones rather than septa should be sampled, given the greater likelihood of alteration in the latter. Opalescent or non-opalescent shell is acceptable, but color appears to have a slight effect on $\delta^{18}O$ which may affect diagenetic alteration. For the most part, $\delta^{18}O$ values are fairly robust even in the presence of cement, although, as seen at the Trask Ranch, the cementation phase may be a crucial factor in that later, meteoric cements can have a substantial influence on $\delta^{18}O$. Based on the analysis, a series of minor-element filters were developed for aragonitic shell at the three sites. Anomalously low $\delta^{18}O$ values resulted from Sr/Ca ratios > 1.8 mMol/Mol, Na/Ca ratios > 10 mMol/Mol, Mn/Ca ratios < 11 mMol/Mol, Mg/Ca ratios < 6.5 mMol/Mol, and Fe/Ca ratios < 7 mMol/Mol. These limits were derived for the Kremmling sampling site, which had the greatest quantity of altered shell. Comparable values exist for the Trask Ranch site, but more data points of shell with altered $\delta^{18}O$ values are needed to define useful limits. The results for alteration of aragonitic $\delta^{18}O$ should not be extended to calcite without separate

investigation of calcitic mollusks, because the different crystal structure of calcitic shells will react differently to the influx of diagenetic waters.

To glean information about paleoproductivity, molluscan diet, or the presence of methane using $\delta^{13}C$ ratios, a different set of criteria apply. Shale or concretions may be used, so long as neither contains cement directly in the shells. Septa and phragmacone samples both provide useful information, as most of the difference in isotopes between septa and phragmacone samples was in $\delta^{18}O$. Opalescence and shell color had little bearing on $\delta^{13}C$ values for the sites investigated.

Furthermore, the concentrations of certain minor elements, such as K, Na, and Al, appear to be quite robust. Sr is also robust when meteoric water is not implicated in diagenesis. These elements are not readily altered by the same diagenetic processes that affect $\delta^{18}O$ and $\delta^{13}C$. Other minor elements, such as Fe, Mg, and Mn, are easily altered.

Implementation of an empirically-derived Sr/Ca-Mg/Ca filter eliminated isotopically light, altered specimens. When these data points were removed, fields emerged on stable isotope cross-plots for each genus investigated. The confidence limits for the benthic bivalve *Inoceramus* did not overlap the nektic ammonites *Baculites, Placenticeras,* and *Hoploscaphites*, implying that the environments were distinct. Calculations from the data support a very light $\delta^{13}C$, methane-rich benthic habitat. The salinity figure for the intermediate/upper water is below normal salinity and the salinity figure for the bottom-water is close to normal salinity. There is no evidence for a distinct surface water mass, as a gradational series of paleosalinities and paleotemperatures were derived for the genera present in the *Baculites compressus/cuneatus* biozones. These include:

(1) Game Ranch *Baculites*: S = 30.6 ± 0.8‰, T = 20.9 ± 4.9 °C

(2) Trask Ranch *Baculites:* S = 29.9 ± 2.0‰, T = 24.8 ± 4.2 °C

(3) Game Ranch *Placenticeras:* S = 28.1 ± 1.1‰, T = 30.1 ± 4.9 °C

(4) Game Ranch *Hoploscaphites*: S = 27.3‰ (n = 1), T = 36.5 (n = 1) °C

(5) Game Ranch *Inoceramus:* S = 31.1 ± 1.9‰, T = 36.1 ± 3.2 °C

(6) Trask Ranch *Inoceramus:* S = 27.7 ± 9.6‰, T = 31.5 ± 4.9 °C

(7) Game Ranch *Nymphalucina*: S = 31.7 ± 0.6‰, T = 14.8 ± 1.2 °C

The clearly unrealistic paleotemperatures for the benthic genera such as *Inoceramus* (and possibly the *Hoploscaphites* as well) cannot be explained at present. Methane seeps, a feature of the Western Interior Seaway during the Campanian, would contribute isotopically light $\delta^{13}C$ like the concretions and cements, not the heavy values seen in shell for this dataset and in prior research. Manipulation of the values for salinity and $\delta^{18}O_{(freshwater)}$ in order to produce reasonable paleotemperatures results in salinities and freshwater geochemistries that are as unrealistic as the paleotemperatures were.

Shale and concretions are both viable data sources for strontium and sodium data, as are both septa and phragmacone samples of ammonites. Opalescent shell should be selected, and color may have some influence on the depletion of Sr/Ca ratios. The presence of cementation, however, generally need not worry the paleosalinity investigator, at least at the localities investigated in this study.

$\delta^{18}O$ and $\delta^{13}C$ sclerochronology of mollusks screened by the minor element filter reveals that *Inoceramus* precipitates most of its shell in bottom waters of unusual isotopic composition. There are two excursions into more normal paleotemperatures, but these do not correlate with any changes in the $\delta^{13}C$ of the benthic organisms. Because *Inoceramus*

is sessile, these excursions must represent environmental changes. On the other hand, *Eutrephoceras* precipitates most of its shell in the upper/intermediate waters but shows excursions which likely reflect migration into the bottom waters. In the *Eutrephoceras*, changes in $\delta^{18}O$ are concurrent with and of the same magnitude as changes in $\delta^{13}C$. *Baculites* appears to remain in the upper/intermediate waters, but shows fluctuations in $\delta^{13}C$ that could represent oceanic productivity and/or the organism's food source.

REFERENCES

Abdel-Gawad, G. 1986, Maastrichtian non-cephalopod mollusks (Scaphopoda, Gastropoda, and Bivalvia) of the Middle Vistula Valley, central Poland: Acta Geologica Polonica, v. 36.

Auclair, A., Lecuyer, C., Bucher, H., and Sheppard, S., 2004, Carbon and oxygen isotope composition of *Nautilus macromphalus*: a record of thermocline waters off New Calendonia: Chemical Geology: v. 207, p. 91-100.

Barrerra, E., Tevesz, M., and Carter, J., 1990, Variations in oxygen and carbon isotopic compositions and microstructure of the shell of *Adamussium colbecki* (Bivalvia): PALAIOS, v. 5, p. 149-159.

Besnosov, N., and Michailova, I, 1991, Higher taxa of Jurassic and Cretaceous Ammonitida: Paleontological Journal, v. 25, p. 3-18.

Bettencourt, V., and Guerra, A., 1999, Carbon- and oxygen-isotope composition of the cuttlebone of *Sepia officinalis*: a tool for predicting ecological information?: Marine Biology, v. 133, p. 651-657.

Brand, U., 1983, Geochemical analysis of Nautilus pompilius from Fiji, South Pacific: Marine Geology, v. 53, p. M1-M5.

Brand, U., 1986, Paleoenvironmental analysis of Middle Jurassic (Callovian) ammonoids from Poland: trace elements and stable isotopes: Journal of Paleontology, v. 60, p. 293-301.

Brand, U., 1994, Morphochemical and replacement diagenesis of carbonates: in Wolf, K. and Chilingarian, G., eds., Diagenesis, IV: Elsevier Science, Amsterdam, p. 217-282.

Buchardt, B., 1977, Oxygen isotope ratios from shell material from the Danish Middle Paleocene (Selandian) deposits and their interpretation as paleotemperature indicators: Palaeogeography, Palaeoclimatology, Palaeoecology, v. 22, p. 209-230.

Buchardt, B., and Weiner, S, 1981, Diagenesis of aragonite from Upper Cretaceous ammonites: a geochemical case-study: Sedimentology, v. 28, p. 423-438.

Cochran, K., Kallenberg, K., Landman, N., Harries, P., and Cobban, W, 2004, Effect of the preservation of Late Cretaceous mollusks from the Western Interior Seaway of North America. Part I: Sr, O, and C Isotopes: poster presented at Geological Society of America Annual Meeting, Salt Lake City.

Cochran, J., Rye, D., and Landman, N., 1981, Growth rate and habitat of Nautilus pompilius inferred from radioactive and stable isotope studies: Paleobiology, v. 7, p. 469-480.

Constantz, B., 1986, The primary surface area of corals and variations in their susceptibility to diagenesis: *in* Schroeder, I. and Purser, B., eds., Reef Diagenesis: Springer-Verlag, Berlin.

Dodd, J., 1967, Magnesium and strontium in calcareous skeletons: a review: Journal of Paleontology, v. 41, p. 1313-1328.

Dodd, J., and Crisp, E., 1982, Non-linear variation with salinity of Sr/Ca and Mg/Ca ratios in water and aragonitic bivalve shells and implications for paleosalinity studies: Palaeoecology, v. 38, p. 45-46.

Dutton, A., Lohmann, K., and Zinsmeister, J., 2002, Stable isotope and minor element proxies for Eocene climate of Seymour Island, Antarctica: Paleoceanography, v. 17, p. 1-13.

Elorza, J., and García-Garmilla, F., 1996, Petrological and geochemical evidence for diagenesis of inoceramid bivalve shells in the Plentzia Formation (Upper Cretaceous, Basque-Cantabrian Region, northern Spain): Cretaceous Research, v. 17, p. 479-503.

Elliot, M., deMenocal, P., Linsley, B., and Howe, S., 2003, Environmental controls on the stable isotopic composition of *Mercenaria mercenaria*: Potential application to paleoenvironmental studies: Geochemistry, Geophysics, Geosystems, v. 4, p. 1-16.

Epstein, S., Buchsbaum, R., Lowenstam, H., and Urey, H., 1953, Revised carbonate-water isotopic temperature scale: Bulletin of the Geological Society of America, v. 64, p. 1315-1326.

Epstein, S., and Mayeda, T., 1953, Variation of O18 content of waters from natural sources: Geochimica et Cosmochimica Acta, v. 4, p. 213-224.

Fatheree, J., Harries, P., and Quinn, T., 1998, Oxygen and carbon isotope dissection of *Baculites compressus* (Mollusca: Cephalopoda) from the Pierre Shale (Upper Campanian) of South Dakota: implications for paleoenvironment reconstructions: PALAIOS, v. 13, p. 376-385.

Fatheree, J., 1995, Isotope Paleontology of Selected Molluscs from the Upper Pierre

Shale (Late Campanian - Early Maastrichtian) of the Cretaceous Western Interior Seaway of North America: MS Thesis, University of South Florida, Tampa, 70 p.

Forester, R., Caldwell, W., and Oro, F., 1977, Oxygen and carbon isotopic study of ammonites from the Late Cretaceous Bearpaw Formation in southwestern Saskatchewan: Canadian Journal of Earth Sciences, v. 14, p. 2086-2100.

Grossman, E., and Ku, T., 1986, Oxygen and carbon isotope fractionation in biogenic aragonite: temperature effects: Chemical Geology (Isotope Geoscience Section), v. 59, p. 59-74.

Hallam, A., and Price, N., 1966, Strontium contents of Recent and fossil aragonitic cephalopod shells: Nature, v. 212, p. 25-27.

Harries, P., 2004, personal communication.

Holmden, C., and Hudson, J., 2003, $^{87}Sr/^{86}Sr$ and Sr/Ca investigation of Jurassic mollusks from Scotland: implications for paleosalinities and the Sr/Ca ratio of seawater: GSA Bulletin, v. 115, p. 1249-1264.

Howard, R., Shultz, A., and Schroeder, W., 2005, Methane-induced cementation in a transgressive nearshore setting, northern Gulf of Mexico: Southeastern Geology, v. 43, p. 137-155.

Hughes, W., and Rosenberg, G., 1991, A metabolic model for the determination of shell composition in the bivalve mollusk, *Mytilus edulis*: Lethaia, v. 24, p. 83-96.

Ivany, L., Wilkinson, B., and Jones, D., 2003, Using stable isotopic data to resolve rate and duration of growth throughout ontogeny: an example from the surf clam, *Spisula solidissima*: PALAIOS, v. 18, p. 126-137.

Krause, F., Clark, J., Sayegh, S., Collom, C, and Johnston, P., 2003, Submarine carbonate diagenesis in a fossil methane-metabolizing community: Campanian coquinoid limestone in the Pierre Shale "Teepee Buttes," Western Interior Seaway, Pueblo region, Colorado, USA: Abstracts with Programs – Geological Society of America Annual Meeting, Nov. 2-5, Seattle, WA, USA.

Landman, N., 2005, personal communication.

Landman, N., Cochran, J., Rye, D., Tanabe, K., and Arnold, J., 1994, Early life history of *Nautilus*: evidence from isotopic analysis of aquarium-reared specimens: Paleobiology, v. 20, p. 40-51.

Landman, N., Rye, D., and Shelton, K., 1983, Early ontogeny of *Eutrephoceras* compared to Recent *Nautilus* and Mesozoic ammonites: evidence from shell morphology and light stable isotopes: Paleobiology, v. 9, p. 269-279.

Larson, N., Jorgensen, S., Farrar, R., and Larson, P., 1997, Ammonites and Other Cephalopods of the Pierre Seaway: Geoscience Press, Tucson, 148 p.

Mann, K., 1992, Physiological, environmental, and mineralogical controls on Mg and Sr concentrations in *Nautilus*: Journal of Paleontology, v. 66, p. 620-636.

McArthur, J., Kennedy, W., Chen, M., Thirlwall, M., and Gale, A., 1993, Strontium isotope stratigraphy for Late Cretaceous time: Direct numerical calibration of the Sr isotope curve based on the US Western Interior: Palaeogeography, Palaeoclimatology, Palaeoclimatology, v. 108, p. 95-119.

Mitchell, L., Fallick, A., and Curry, G., 1994, Stable carbon and oxygen isotope compositions of mollusc shells from Britain and New Zealand: Palaeogeography, Palaeoclimatology, Palaeoclimatology, v. 111, p. 207-216.

Pagani, M., and Arthur, M., 1998, Stable isotopic studies of Cenomanian-Turonian proximal marine fauna from the U.S. Western Interior Seaway. SEPM Concepts in Sedimentology and Paleontology Publiation 6 (Paleogeography and Paleoenvironments of the Cretaceous Western Interior Seaway, USA): SEPM, publication location, ## p.

Purton, L., Shields, G., Brasier, M., and Grine, G., 1999, Metabolism controls Sr/Ca ratios in fossil aragonitic mollusks: Geology, v. 27, p. 1083-1086.

Ragland, P., Pilkey, O., and Blackwelder, B., 1979, Diagenetic changes in the elemental composition of unrecrystallized mollusk shells: Chemical Geology, v. 25, p. 123-134.

Rucker, J., and Valentine, J., 1961, Salinity response of trace element concentration in *Crassostrea virginica*: Nature, v. 190, p. 1099-1100.

Saltzman, E., and Barron, E., 1982, Deep circulation in the Late Cretaceous: oxygen isotope paleotemperatures from *Inoceramus* remains in DSDP cores: Palaeogeography, Palaeoclimatology, Palaeoecology, v. 40, p. 167-181.

Saunders, W., 1983, Natural rates of growth and longevity of *Nautilus belauensis*: Paleobiology, v. 9, p. 280-288.

Schmidt, M., 1997, Paleoceanography of the North American Western Interior Seaway based on geochemical analysis of carbonate shell material: MS Thesis, University of South Florida, Tampa, 81 p.

Scott, G. R., and Cobban, W., 1986, Geologic and biostratigraphic map of the Pierre

Shale in the Colorado Springs – Pueblo area, Colorado: USGS Miscellaneous Investigations Series Map I-1627.

Slingerland, R., Kump, L., Arthur, M., Fawcett, P., Sageman, B., and Barron, E., 1996, Estuarine circulation in the Turonian Western Interior seaway of North America: GSA Bulletin, v. 108, p. 941-952.

Speden, I., 1970, Bulletin 33 of the Peabody Museum of Natural History, Yale University: The Type Fox Hills Formation, Cretaceous (Maestrichtian), South Dakota, Part 2, Systematics of the Bivalvia: New Haven, CT, ### p.

Stahl, W., and Jordan, R., 1969, General considerations on isotopic paleotemperature determinations and analyses on Jurassic ammonites: Earth and Planetary Science Letters, v. 6, p. 173-178.

Stanley, S., and Hardie, L., 1998, Secular oscillations in the carbonate mineralogy of reef-building and sediment-producing organisms driven by tectonically forced shifts in seawater chemistry: Palaeogeography, Palaeoclimatology, Palaeoecology, v. 144, p. 3-19.

Teys, R., Kiselevskiy, M., and Naydin, D., 1978, Oxygen and carbon isotopic compostion of organogenic carbonates and concretions in the Late Cretaceous rocks of northwestern Siberia: Geokhimiya (translation), v. 1, p. 111-118.

Timofeeff, M., Lowenstein, T., da Silva, M., and Harris, N., 2006, Secular variation in the major-ion chemistry of seawater: Evidence from fluid inclusions of Cretaceous halites: Geochimica et Cosmochimica Acta, v. 70, p.1977-1994.

Tsujita, C., and Westermann, G., 1998, Ammonoid habitats and habits in the Western Interior Seaway: a case study from the Upper Cretaceous Bearpaw Formation of southern Alberta, Canada: Palaeogeography, Palaeoclimatology, Palaeoecology, v. 144, p. 135-160.

Turekian, K., and Armstrong, R., 1960, Magnesium, strontium, and barium concentrations and calcite-aragonite ratios of some Recent molluscan shells: Journal of Marine Research, v. 18, p. 133-

Tourtelot, H., and Rye, R., 1969, Distribution of oxygen and carbon isotopes in fossils of Late Cretaceous age, Western Interior region of North America: GSA Bulletin, v. 80, p. 1903-1922.

Veizer, J., and Fritz, P., 1976, Possible control of post-depositional alteration in oxygen paleotemperature determination: Earth and Planetary Science Letters, v. 33, p. 255-260.

Walaszczyk, I., and Cobban, W., 2000, Special Papers in Paleontology: Inoceramid Faunas and Biostratigraphy of the Upper Turonian – Lower Coniacian of the Western Interior of the United States: Palaeontological Association, London, ## p.

Whittaker, S., Kyser, T., and Caldwell, W., 1986, Paleoenvironmental geochemistry of the Claggett marine cyclothem in south-central Saskatchewan: Canadian Journal of Earth Sciences, v. 24, p. 967-984.

Wright, E., 1987, Stratification and paleocirculation of the Late Cretaceous Western Interior Seaway of North America: GSA Bulletin, v. 99, p. 480-490.

Zakharov, Y., Smyshlyaeva, O., Tanabe,K., Shigeta, Y., Maeda, H., Ignatiev, A., Velivetskaya, T., Afanasyeva, T., Popov, A., Golozubov, V., Kolyada, A., Cherbadzhi, A., and Moriya, K., 2005, Seasonal temperature fluctuations int he high northern latitudes during the Cretaceous Period: isotopic evidence from Albian and Coniacian shallow-water invertebrates of the Talavka River Basin, Koryak Upland, Russian Far East: Cretaceous Research, v. 5, p. 1-20.

APPENDICES

APPENDIX A: SHELL ALTERATION MASS SPECTROMETER DATA

Mode of Preservation Suite

Preserved Directly in Shale:

Sample	Location	Genus	$\delta^{18}O$, vs. PDB	$\delta^{13}C$, vs. PDB
MP-1	Game Ranch, SD	*Placenticeras*	-3.58	-1.72
MP-2	Game Ranch, SD	*Placenticeras*	-1.26	-0.93
MP-3	Game Ranch, SD	*Placenticeras*	-2.90	-1.65
MP-4	Game Ranch, SD	*Inoceramus*	-3.05	4.32
MP-5	Game Ranch, SD	*Inoceramus*	-4.59	5.04
MP-6	Game Ranch, SD	*Baculites*	-0.35	-0.81
MP-7	Game Ranch, SD	*Baculites*	-3.09	1.44
MP-8	Game Ranch, SD	*Nymphalucina*	0.39	1.02
MP-9	Game Ranch, SD	*Nymphalucina*	0.04	-18.20

Preserved in Concretions:

Sample	Location	Genus	$\delta^{18}O$, vs. PDB	$\delta^{13}C$, vs. PDB
MP-10	Kremmling, CO	*Placenticeras*	-18.46	-3.99
MP-11	Kremmling, CO	*Placenticeras*	-15.51	-6.72
MP-12	Kremmling, CO	*Placenticeras*	-15.13	-7.44
MP-13	Game Ranch, SD	*Inoceramus*	-4.51	2.80
MP-14	Game Ranch, SD	*Inoceramus*	-3.35	-0.91
MP-15	Trask Ranch, SD	*Inoceramus*	-1.38	5.66
MP-16	Game Ranch, SD	*Baculites*	-1.61	-0.46
MP-17	Game Ranch, SD	*Baculites*	-0.64	-1.42
MP-18	Trask Ranch, SD	*Baculites*	-1.00	-1.98
MP-19	Trask Ranch, SD	*Nymphalucina*	-1.93	-2.68
MP-20	Trask Ranch, SD	*Nymphalucina*	-9.07	-13.00

Shell Testing Location Suite

Shell Taken from Septum:

Sample	**Location**	**Genus**	**$\delta^{18}O$, vs. PDB**	**$\delta^{13}C$, vs. PDB**
SC-1S	Game Ranch, SD	*Placenticeras*	-3.71	-3.74
SC-2S	Kremmling, CO	*Baculites*	-13.12	-8.64
SC-3S	Kremmling, CO	*Placenticeras*	N/A	N/A
SC-4S	Trask Ranch, SD	*Hoploscaphites*	-3.69	-8.36
SC-5S	Trask Ranch, SD	*Baculites*	-2.02	-4.85
SC-6S	Trask Ranch, SD	*Baculites*	-3.48	-10.07
SC-7S	Trask Ranch, SD	*Baculites*	-2.96	-9.09
SC-8S	Trask Ranch, SD	*Baculites*	-2.08	-10.08
SC-9S	Trask Ranch, SD	*Baculites*	-3.59	-7.58
SC-10S	Trask Ranch, SD	*Baculites*	-1.81	-2.47

Shell Taken from Phragmacone Adjacent to Septum:

Specimen	**Location**	**Genus**	**$\delta^{18}O$, vs. PDB**	**$\delta^{13}C$, vs. PDB**
SC-1P	Game Ranch, SD	*Placenticeras*	-2.91	-2.67
SC-2P	Kremmling, CO	*Baculites*	N/A	N/A
SC-3P	Kremmling, CO	*Placenticeras*	-8.86	-14.18
SC-4P	Trask Ranch, SD	*Hoploscaphites*	-3.64	-7.46
SC-5P	Trask Ranch, SD	*Baculites*	-2.31	-3.76
SC-6P	Trask Ranch, SD	*Baculites*	-2.19	-1.79
SC-7P	Trask Ranch, SD	*Baculites*	-1.85	-14.66
SC-8P	Trask Ranch, SD	*Baculites*	-1.71	-1.71
SC-9P	Trask Ranch, SD	*Baculites*	-2.82	-6.29
SC-10P	Trask Ranch, SD	*Baculites*	-1.36	-2.36

Shell Color Suite

Kremmling, Colorado, samples				
Sample	**Genus**	**Color Class**	**$\delta^{18}O$, vs. PDB**	**$\delta^{13}C$, vs. PDB**
SC-1	*Placenticeras*	Tan	-16.17	-3.74
SC-2	*Placenticeras*	Cream	*N/A*	*N/A*
SC-3	*Placenticeras*	Moccasin	-15.58	-6.63
SC-4	*Placenticeras*	Yellow	-13.06	-7.01
SC-5	*Placenticeras*	Opalescent White	-15.01	-6.99
SC-6	*Hoploscaphites*	Moccasin	-14.65	-7.01
SC-7	*Hoploscaphites*	Cream	-11.15	-4.17
SC-8	*Hoploscaphites*	Moccasin	-14.36	-13.07
SC-9	*Hoploscaphites*	Tan	-14.28	-6.48
SC-10	*Hoploscaphites*	Wheat	-14.25	-5.62
SC-11	*Baculites*	Cream	-14.63	-6.14
SC-12	*Baculites*	Brown	-15.06	-8.29
SC-13	*Baculites*	Cream	-15.17	-8.15
SC-14	*Baculites*	Wheat	*-12.66*	*-7.59*
SC-15	*Baculites*	Yellow	-15.09	-7.12
SC-16	*Inoceramus*	Tan	-8.87	-0.88
SC-17	*Inoceramus*	Wheat	*-13.30*	*-6.93*
SC-18	*Inoceramus*	Moccasin	-14.47	-7.67
SC-19	*Anomia*	Tan	-5.34	0.77
SC-20	*Anomia*	Seashell	-3.92	1.84

Shell Color Suite (Continued)

Game Ranch, South Dakota, samples				
Sample	**Genus**	**Color Class**	**$\delta^{18}O$, vs. PDB**	**$\delta^{13}C$, vs. PDB**
SC-21	*Placenticeras*	Opalescent White	N/A	N/A
SC-22	*Placenticeras*	Opalescent White	-3.45	-2.77
SC-23	*Placenticeras*	Linen	-3.61	-2.93
SC-24	*Placenticeras*	Opalescent White	-3.12	-3.27
SC-25	*Placenticeras*	Opalescent Yellow	-2.05	-1.89
SC-26	*Hoploscaphites*	Moccasin	-4.51	0.54
SC-27	*Baculites*	Seashell	-1.36	-1.97
SC-28	*Baculites*	Opalescent White	-0.39	-1.48
SC-29	*Baculites*	Opalescent White	-1.18	-0.65
SC-30	*Baculites*	Linen	-0.54	-0.91
SC-31	*Baculites*	Opalescent White	-1.93	0.44
SC-32	*Inoceramus*	Grey	-4.54	2.36
SC-33	*Inoceramus*	Brown	-4.22	5.24
SC-34	*Inoceramus*	Orange	-4.29	4.97
SC-35	*Inoceramus*	Linen	-5.26	5.80
SC-36	*Inoceramus*	Seashell	-3.98	4.47
SC-37	*Anomia*	Grey	-3.87	0.92
SC-38	*Anomia*	Grey	-2.10	3.12
SC-39	*Nymphalucina*	Seashell	0.14	-0.29
SC-40	*Nymphalucina*	Cream	0.42	1.03

Shell Color Suite (Continued)

Trask Ranch, South Dakota, samples				
Sample	**Genus**	**Color Class**	**$\delta^{18}O$, vs. PDB**	**$\delta^{13}C$, vs. PDB**
SC-41	*Hoploscaphites*	Tan	-4.41	-1.10
SC-42	*Hoploscaphites*	Moccasin	-5.41	-7.22
SC-43	*Hoploscaphites*	Linen	-3.45	-2.91
SC-44	*Hoploscaphites*	Orange	-3.97	-7.40
SC-45	*Hoploscaphites*	Opalescent Grey	-3.11	-0.05
SC-46	*Inoceramus*	Tan	-3.46	3.31
SC-47	*Inoceramus*	Opalescent White	-3.07	1.43
SC-48	*Inoceramus*	Moccasin	-4.06	3.48
SC-49	*Inoceramus*	Seashell	-3.84	0.18
SC-50	*Inoceramus*	Wheat	-4.34	1.84
SC-51	*Baculites*	Opalescent White	-1.18	-2.43
SC-52	*Baculites*	Opalescent Seashell	-3.22	-5.17
SC-53	*Baculites*	Seashell	-2.27	-2.76
SC-54	*Baculites*	Yellow	*-2.27*	*-6.33*
SC-55	*Baculites*	Brown	-1.05	-2.34
SC-56	*Drepanocheilus*	Wheat	-5.66	-13.65
SC-57	*Drepanocheilus*	Seashell	-2.31	-3.78
SC-58	*Drepanocheilus*	Grey	-5.89	-16.54
SC-59	*Anisomyon*	Orange	-6.58	-10.76
SC-60	*Anisomyon*	Seashell	-6.54	-8.58

Cementation Suite

Kremmling, Colorado, samples				
Sample	**Shell**	**Cement**	**Concretion**	**($\delta^{18}O$, $\delta^{13}C$), vs. PDB**
CEM-1	*Hoploscaphites*	Sparry yellow	Grey	(-12.93, -11.87) (-13.99, -5.92) (-10.64, -9.10)
CEM-2	*Hoploscaphites*	None	None	(-13.50, -11.87) None None
CEM-3	*Placenticeras*	Sparry clear	Tan	(-14.45, -7.40) (-17.02, -4.64) (-13.71, -6.63)
CEM-4	*Baculites*	None	Tan	(-14.94, -8.00) None (-14.33, -6.54)
CEM-5	*Baculites*	None	Tan	(-14.68, -11.54) None (-12.62, -11.17)
CEM-6	*Baculites*	Agate moccasin	Tan	N/A (-6.97, -2.97) (-12.50, -6.39)
CEM-7	*Baculites*	Sparry white	Grey	(-14.89, -8.19) (-10.90, -8.52) (-14.07, -11.30)
CEM-8	*Baculites*	Sparry yellow	Grey	(-15.15, -10.19) (-8.00, -7.57) (-12.87, -13.36)
CEM-9	*Baculites*	1. Blocky clear 2. Sparry clear	None	(-15.04, -6.90) 1. (-23.74, -3.59) 2. (-10.03, -7.55) None
CEM-10	*Baculites*	1. Agate yellow 2. Blocky clear	Tan	(-14.43, -6.83) 1. (-14.04, -4.94) 2. (-14.34, -3.17) None

Cementation Suite (Continued)

Game Ranch, South Dakota, samples				
Sample	**Shell**	**Cement**	**Concretion**	**($\delta^{18}O$, $\delta^{13}C$), vs. PDB**
CEM-11	*Placenticeras*	None	None	(-3.68, -5.40) None None
CEM-12	*Placenticeras*	None	Yellow-Brown	(-4.62, -3.89) None (-1.72, -7.81)
CEM-13	*Baculites*	None	Yellow-Brown	N/A None (-1.66, -11.00)
CEM-14	*Baculites*	None	None	(-1.67, -0.73) None None
CEM-15	*Baculites* (2 samples)	None	1. Red-Brown 2. Dark Grey	1. (-0.53, -0.83) 2. N/A None 1. (-1.19, -6.83) 2. N/A
Trask Ranch, South Dakota, samples				
Sample	**Shell**	**Cement**	**Concretion**	**($\delta^{18}O$, $\delta^{13}C$), vs. PDB**
CEM-16	*Hoploscaphites*	1. Sparry yellow 2. Sparry moccasin	Dark grey	(-1.85, -6.54) 1. (-9.24, -12.67) 2. (-4.24, -10.45) (-1.68, -17.75)
CEM-17	*Hoploscaphites* (2 samples)	1. Sparry yellow 2. Sparry tan	Dark grey	1. (-3.19, -6.88) 2. (-2.46, -6.98) 1. (-4.53, -10.47) 2. (-8.66,-12.84) (-1.80, -18.86)
CEM-18	*Hoploscaphites*	None	Dark grey	(-4.99, -10.34) None (-2.38, -19.14)

Cementation Suite (Continued)

Trask Ranch, South Dakota, samples (continued)				
Sample	**Shell**	**Cement**	**Concretion**	**($\delta^{18}O$, $\delta^{13}C$), vs. PDB**
CEM-19	*Hoploscaphites* (2 samples)	1. Sparry moccasin 2. Sparry moccasin	Dark grey	1. (-4.87, -7.95) 2. (-4.19, -7.18) 1. (-6.03, -10.58) 2. (-6.50, -10.21) (-1.86, -17.65)
CEM-20	*Hoploscaphites*	None	Grey	N/A None (-1.69, -25.09)
CEM-21	*Baculites*	1. Sparry tan 2. Blocky brown	Grey	(-1.06, -4.86) 1. (-1.05, -9.96) 2. (-4.38, -7.87) (-2.11, -19.21)
CEM-22	*Baculites* (2 samples)	1. Sparry yellow 2. Blocky yellow	Grey	1. N/A 2. (-1.25, -5.11) 1. (-5.73, -11.45) 2. (-4.04, -10.09) (-4.41, -19.91)
CEM-23	*Baculites*	1. Blocky mocc. 2. Blocky seashell	Grey	(-5.69, -9.05) 1. (-11.98, -14.37) 2. (-13.78, -16.34) (-3.50, -19.60)
CEM-24	*Baculites*	Sparry yellow	Dark Grey	(-3.15, -11.34) (-1.95, -12.73) (-1.70, -19.84)
CEM-25	*Baculites*	Blocky yellow	None	N/A (-1.82, -19.48) None
CEM-26	*Baculites*	Sparry grey-brown	Grey	(-3.73, -8.49) (-1.82, -19.48) (-6.21, -10.47)
CEM-27	*Baculites*	Sparry linen	Dark Grey	(-2.24, -7.23) (-1.10, -16.97) (-1.35, -24.54)

Cementation Suite (Continued)

Trask Ranch, South Dakota, samples (continued)				
Sample	**Shell**	**Cement**	**Concretion**	**($\delta^{18}O$, $\delta^{13}C$), vs. PDB**
CEM-28	*Baculites*	Blocky, yellow-moccasin	Dark grey	(-3.07, -8.01) (-4.81, -21.00) (-1.29, -24.70)
CEM-29	*Baculites*	None	Grey	(-1.47, -1.31) None (-2.29, -18.58)
CEM-30	*Baculites*	1. Sparry dark grey 2. Agate brown	Grey	(-2.96, -5.45) 1. (-1.72, -12.96) 2. (-8.55, -11.72) (-1.70, -18.64)
CEM-31	*Baculites*	Agate yellow	None	(-2.35, -2.51) (-10.20, -12.17) None
CEM-32	*Baculites*	Sparry seashell	None	(-5.21, -5.52) (-10.02, -12.67) None
CEM-33	*Baculites*	None	Dark Grey	(-2.58, -2.09) None (-4.02, -19.86)
CEM-34	*Baculites*	None	Dark Grey	(-3.16, -4.51) None (-1.24, -25.75)
CEM-35	*Baculites*	None	Dark Grey	(-0.98, -1.97) None (-1.62, -14.28)

APPENDIX B: SHELL ALTERATION ICP DATA

Mode of Preservation Suite

Preserved Directly in Shale

Specimen	[Ca] ppm	[Al] ppm	Al/Ca (mMol/Mol)
MP-1	349831.691	N/A	N/A
MP-2	175693.342	N/A	N/A
MP-3	373965.603	N/A	N/A
MP-4	341289.398	N/A	N/A
MP-5	322061.902	N/A	N/A
MP-6	334993.853	N/A	N/A
MP-7	370032.558	N/A	N/A
MP-8	391581.568	N/A	N/A
MP-9	321557.153	N/A	N/A

Preserved in Concretions

Specimen	[Ca] ppm	[Al] ppm	Al/Ca (mMol/Mol)
MP-10	342648.817	N/A	N/A
MP-11	357578.327	1591.860	0.178
MP-12	396504.370	165.661	0.017
MP-13	313047.021	N/A	N/A
MP-14	384331.947	N/A	N/A
MP-15	357487.581	N/A	N/A
MP-16	290491.855	106.879	0.015
MP-17	329805.680	N/A	N/A
MP-18	387999.920	N/A	N/A
MP-19	348750.500	467.572	0.054
MP-20	286764.750	4507.980	0.629

*weight percents normalized to 40% Ca

Mode of Preservation Suite (Continued)

Preserved Directly in Shale

Specimen	[Fe] ppm	Fe/Ca (mMol/Mol)	[K] ppm	K/Ca (mMol/Mol)
MP-1	164.295	0.337	338.309	0.992
MP-2	N/A	N/A	167.558	0.978
MP-3	286.090	0.549	245.962	0.675
MP-4	N/A	N/A	139.411	0.419
MP-5	1916.905	4.270	179.928	0.573
MP-6	307.577	0.659	302.695	0.927
MP-7	340.507	0.660	276.961	0.768
MP-8	N/A	N/A	185.102	0.485
MP-9	108.322	0.242	238.344	0.760

Preserved in Concretions

Specimen	[Fe] ppm	Fe/Ca (mMol/Mol)	[K] ppm	K/Ca (mMol/Mol)
MP-10	3589.299	7.514	153.669	0.460
MP-11	3426.162	6.873	183.978	0.528
MP-12	4207.602	7.612	310.269	0.803
MP-13	610.069	1.398	437.089	1.432
MP-14	115.773	0.216	310.451	0.828
MP-15	3721.623	7.468	186.998	0.536
MP-16	12977.510	32.047	461.101	1.628
MP-17	139.936	0.304	194.419	0.605
MP-18	N/A	N/A	194.544	0.514
MP-19	5955.417	12.250	257.469	0.757
MP-20	3092.760	7.737	591.085	2.114

*weight percents normalized to 40% Ca

Mode of Preservation Suite (Continued)

Preserved Directly in Shale

Specimen	[Mg] ppm	Mg/Ca (mMol/Mol)	[Mn] ppm	Mn/Ca (mMol/Mol)
MP-1	106.439	0.502	199.801	0.417
MP-2	46.272	0.435	147.254	0.612
MP-3	161.308	0.712	404.205	0.789
MP-4	82.343	0.398	N/A	N/A
MP-5	95.359	0.489	285.207	0.647
MP-6	166.258	0.819	3239.452	7.063
MP-7	120.008	0.535	307.190	0.606
MP-8	804.598	3.391	N/A	N/A
MP-9	121.945	0.626	N/A	N/A

Preserved in Concretions

Specimen	[Mg] ppm	Mg/Ca (mMol/Mol)	[Mn] ppm	Mn/Ca (mMol/Mol)
MP-10	2308.430	11.117	1762.292	3.757
MP-11	1500.110	6.923	7216.334	14.741
MP-12	1579.443	6.573	3931.915	7.243
MP-13	192.618	1.015	2249.453	5.249
MP-14	114.152	0.490	110.404	0.210
MP-15	744.114	3.435	2575.970	5.263
MP-16	1030.181	5.852	1184.273	2.978
MP-17	95.991	0.480	85.498	0.189
MP-18	264.723	1.126	26.294	0.049
MP-19	2546.293	12.048	6814.483	14.272
MP-20	3351.211	19.285	969.246	2.469

*weight percents normalized to 40% Ca

Mode of Preservation Suite (Continued)

Preserved Directly in Shale

Specimen	[Na] ppm	Na/Ca (mMol/Mol)	[Sr] ppm	Sr/Ca (mMol/Mol)
MP-1	3902.407	19.449	2409.576	3.153
MP-2	1801.963	17.882	1237.669	3.225
MP-3	3410.736	15.901	3499.546	4.284
MP-4	3940.044	20.128	1823.674	2.446
MP-5	3636.226	19.685	2335.145	3.319
MP-6	3528.756	18.365	2212.174	3.023
MP-7	4009.190	18.890	2029.169	2.510
MP-8	2814.216	12.530	1449.045	1.694
MP-9	2142.852	11.619	1399.016	1.992

Preserved in Concretions

Specimen	[Na] ppm	Na/Ca (mMol/Mol)	[Sr] ppm	Sr/Ca (mMol/Mol)
MP-10	577.991	2.941	1093.216	1.460
MP-11	344.619	1.680	651.877	0.835
MP-12	3103.771	13.648	1838.879	2.123
MP-13	3347.031	18.641	1833.716	2.681
MP-14	4178.667	18.956	2574.603	3.067
MP-15	3266.041	15.929	2584.284	3.309
MP-16	3350.219	20.107	9318.315	14.684
MP-17	3792.947	20.051	2397.838	3.328
MP-18	4238.460	19.046	2111.923	2.492
MP-19	1248.359	6.241	932.789	1.224
MP-20	2728.575	16.589	1290.938	2.061

*weight percents normalized to 40% Ca

Shell Testing Location Suite (Continued)

Shell Taken from Septum:

Specimen	[Ca] ppm	[Al] ppm	Al/Ca (mMol/Mol)
1S	397800.760	N/A	N/A
2S	302918.706	586.552	0.077
3S	275462.981	2783.478	0.404
4S	339307.629	1144.141	0.135
5S	293972.437	1158.966	0.158
6S	323656.561	870.411	0.108
7S	353154.550	N/A	N/A
8S	379448.012	99.169	0.010
9S	328225.280	224.715	0.027
10S	304005.309	597.682	0.079

Shell Taken from Phragmacone Adjacent to Septum:

Specimen	[Ca] ppm	[Al] ppm	Al/Ca (mMol/Mol)
1P	323301.687	353.076	0.044
2P	394523.767	486.131	0.049
3P	13893.955	190.225	0.548
4P	307581.549	1735.389	0.226
5P	289798.190	891.545	0.123
6P	303252.508	645.480	0.085
7P	318913.955	537.746	0.067
8P	310820.113	736.899	0.095
9P	314319.917	231.145	0.029
10P	293918.604	1086.639	0.148

*weight percents normalized to 40% Ca

Shell Testing Location Suite (Continued)

Shell Taken from Septum:

Specimen	[Fe] ppm	Fe/Ca (mMol/Mol)	[K] ppm	K/Ca (mMol/Mol)
1S	337.061	0.608	241.893	0.624
2S	4216.932	9.986	745.807	2.525
3S	14485.545	37.723	756.209	2.815
4S	1402.202	2.964	650.465	1.966
5S	408.654	0.997	458.002	1.598
6S	1445.960	3.205	675.592	2.141
7S	596.196	1.211	272.637	0.792
8S	294.276	0.556	326.919	0.884
9S	702.057	1.534	547.704	1.711
10S	811.700	1.915	536.863	1.811

Shell Taken from Phragmacone Adjacent to Septum:

Specimen	[Fe] ppm	Fe/Ca (mMol/Mol)	[K] ppm	K/Ca (mMol/Mol)
1P	5953.316	13.209	689.200	2.186
2P	4679.821	8.509	566.304	1.472
3P	534.425	27.593	196.770	14.525
4P	3701.232	8.632	998.568	3.330
5P	1833.183	4.538	360.167	1.275
6P	1243.161	2.941	658.346	2.226
7P	3108.675	6.993	546.688	1.758
8P	3081.612	7.112	470.134	1.551
9P	913.828	2.086	376.295	1.228
10P	1756.955	4.288	701.014	2.446

*weight percents normalized to 40% Ca

Shell Testing Location Suite (Continued)

Shell Taken from Septum:

Specimen	[Mg] ppm	Mg/Ca (mMol/Mol)	[Mn] ppm	Mn/Ca (mMol/Mol)
1S	165.999	0.689	164.926	0.303
2S	1573.935	8.574	5820.233	14.034
3S	3102.620	18.587	5411.270	14.349
4S	4785.934	23.276	3524.525	7.587
5S	1428.219	8.017	113.901	0.283
6S	1602.254	8.169	410.622	0.927
7S	10471.826	48.932	983.656	2.034
8S	465.993	2.027	66.291	0.128
9S	2525.540	12.698	844.126	1.878
10S	2497.084	13.555	398.261	0.957

Shell Taken from Phragmacone Adjacent to Septum:

Specimen	[Mg] ppm	Mg/Ca (mMol/Mol)	[Mn] ppm	Mn/Ca (mMol/Mol)
1P	1292.838	6.599	3199.795	7.229
2P	3127.006	13.080	6612.912	12.243
3P	216.894	25.761	174.509	9.174
4P	3838.157	20.592	3650.128	8.668
5P	2335.732	13.300	341.210	0.860
6P	5492.704	29.890	571.669	1.377
7P	8059.765	41.705	3192.408	7.312
8P	4881.985	25.919	1311.369	3.082
9P	3011.749	15.812	1636.809	3.804
10P	2041.629	11.463	492.919	1.225

*weight percents normalized to 40% Ca

Shell Testing Location Suite (Continued)

Shell Taken from Septum:

Specimen	[Na] ppm	Na/Ca (mMol/Mol)	[Sr] ppm	Sr/Ca (mMol/Mol)
1S	3690.897	16.176	2975.639	3.424
2S	628.338	3.616	523.399	0.791
3S	670.099	4.241	512.388	0.851
4S	3067.143	15.760	3425.384	4.621
5S	3264.908	19.363	1964.570	3.059
6S	5959.577	32.103	2099.138	2.969
7S	2431.042	12.002	1535.904	1.991
8S	4064.048	18.673	2228.468	2.688
9S	6641.447	35.278	2721.898	3.796
10S	7111.696	40.786	1783.532	2.686

Shell Taken from Phragmacone Adjacent to Septum:

Specimen	[Na] ppm	Na/Ca (mMol/Mol)	[Sr] ppm	Sr/Ca (mMol/Mol)
1P	3019.709	16.284	11566.121	16.376
2P	920.300	4.067	931.567	1.081
3P	284.505	35.701	604.503	19.917
4P	3295.050	18.677	1940.755	2.888
5P	3517.415	21.161	1997.610	3.155
6P	5232.188	30.081	2606.202	3.934
7P	7940.190	43.408	1531.817	2.199
8P	2746.384	15.405	2707.685	3.988
9P	2187.071	12.131	2827.012	4.117
10P	5139.491	30.487	2212.709	3.446

*weight percents normalized to 40% Ca

Shell Color Suite (Continued)

Kremmling, Colorado, samples			
Sample	**[Ca] ppm**	**[Al] ppm**	**Al/Ca (mMol/Mol)**
SC-1	349374.665	N/A	N/A
SC-2	210798.358	428.866	0.081
SC-3	307749.064	N/A	N/A
SC-4	324906.964	N/A	N/A
SC-5	388851.043	N/A	N/A
SC-6	336077.139	231.945	0.028
SC-7	233388.744	2414.911	0.414
SC-8	256015.593	284.786	0.044
SC-9	296636.139	1137.917	0.153
SC-10	346784.033	N/A	N/A
SC-11	255766.478	1426.706	0.223
SC-12	391821.330	N/A	N/A
SC-13	309157.385	N/A	N/A
SC-14	196443.855	2467.386	0.502
SC-15	327370.577	314.596	0.038
SC-16	179071.433	1857.479	0.415
SC-17	120771.796	2009.081	0.665
SC-18	272407.339	1657.166	0.243
SC-19	245129.445	2012.211	0.328
SC-20	338296.486	N/A	N/A

Shell Color Suite (Continued)

Game Ranch, South Dakota, samples			
Sample	**[Ca] ppm**	**[Al] ppm**	**Al/Ca (mMol/Mol)**
SC-21	295002.574	779.089	0.106
SC-22	380815.313	N/A	N/A
SC-23	377794.156	N/A	N/A
SC-24	285378.708	493.717	0.069
SC-25	375552.472	N/A	N/A
SC-26	350602.189	88.597	0.010
SC-27	286893.057	N/A	N/A
SC-28	348429.480	N/A	N/A
SC-29	307341.279	1147.963	0.149
SC-30	368493.489	N/A	N/A
SC-31	346095.016	N/A	N/A
SC-32	379592.814	N/A	N/A
SC-33	346144.010	N/A	N/A
SC-34	303721.408	234.436	0.031
SC-35	350303.529	N/A	N/A
SC-36	351040.497	N/A	N/A
SC-37	354576.098	229.018	0.026
SC-38	338869.682	176.870	0.021
SC-39	370022.686	N/A	N/A
SC-40	333044.179	268.238	0.032

Shell Color Suite (Continued)

Trask Ranch, South Dakota, samples			
Sample	**[Ca] ppm**	**[Al] ppm**	**Al/Ca (mMol/Mol)**
SC-41	383656.252	N/A	N/A
SC-42	314802.951	120.130	0.015
SC-43	336563.754	272.687	0.032
SC-44	327926.765	431.806	0.053
SC-45	344621.864	183.885	0.021
SC-46	367743.402	N/A	N/A
SC-47	368017.078	N/A	N/A
SC-48	382577.145	N/A	N/A
SC-49	349892.589	N/A	N/A
SC-50	384139.477	N/A	N/A
SC-51	346954.297	247.461	0.029
SC-52	374739.380	N/A	N/A
SC-53	292900.718	921.493	0.126
SC-54	354750.549	440.163	0.050
SC-55	369232.955	N/A	N/A
SC-56	322742.995	928.338	0.115
SC-57	306012.390	1902.768	0.249
SC-58	363062.012	1239.145	0.137
SC-59	592092.486	1893.634	0.128
SC-60	310263.392	1487.702	0.192

Shell Color Suite (Continued)

Kremmling, Colorado, samples				
Sample	**[Fe] ppm**	**Fe/Ca (mMol/Mol)**	**[K] ppm**	**K/Ca (mMol/Mol)**
SC-1	6736.994	13.833	119.007	0.349
SC-2	3903.263	13.283	446.898	2.174
SC-3	2759.682	6.433	176.120	0.587
SC-4	9989.496	22.056	181.576	0.573
SC-5	4047.950	7.468	163.946	0.432
SC-6	4666.698	9.961	352.146	1.075
SC-7	5025.051	15.445	1215.893	5.343
SC-8	4336.310	12.150	264.814	1.061
SC-9	7274.074	17.591	807.516	2.792
SC-10	11367.810	23.515	174.042	0.515
SC-11	4837.432	13.568	838.281	3.361
SC-12	4392.651	8.042	226.923	0.594
SC-13	4055.587	9.410	216.167	0.717
SC-14	5199.664	18.988	1221.966	6.380
SC-15	5293.590	11.600	398.537	1.249
SC-16	3264.076	13.076	983.965	5.635
SC-17	3826.494	22.728	1014.966	8.619
SC-18	5829.126	15.350	957.701	3.606
SC-19	1465.171	4.288	502.938	2.104
SC-20	182.013	0.386	180.520	0.547

Shell Color Suite (Continued)

Game Ranch, South Dakota, samples				
Sample	**[Fe] ppm**	**Fe/Ca (mMol/Mol)**	**[K] ppm**	**K/Ca (mMol/Mol)**
SC-21	11119.928	27.040	1085.274	3.773
SC-22	377.728	0.712	288.124	0.776
SC-23	67.176	0.128	281.042	0.763
SC-24	11255.772	28.293	774.921	2.785
SC-25	1138.393	2.174	301.653	0.824
SC-26	951.777	1.947	549.251	1.607
SC-27	54990.386	137.499	358.482	1.281
SC-28	429.027	0.883	430.792	1.268
SC-29	13124.393	30.633	1283.895	4.284
SC-30	136.915	0.267	295.726	0.823
SC-31	399.480	0.828	323.004	0.957
SC-32	348.335	0.658	480.928	1.299
SC-33	396.158	0.821	545.087	1.615
SC-34	8802.022	20.789	569.099	1.922
SC-35	269.467	0.552	387.858	1.136
SC-36	61.635	0.126	330.524	0.966
SC-37	2319.393	4.692	532.004	1.539
SC-38	1191.225	2.522	420.055	1.271
SC-39	994.297	1.928	413.204	1.145
SC-40	473.524	1.020	525.450	1.618

Shell Color Suite (Continued)

Trask Ranch, South Dakota, samples				
Sample	**[Fe] ppm**	**Fe/Ca (mMol/Mol)**	**[K] ppm**	**K/Ca (mMol/Mol)**
SC-41	878.332	1.642	343.065	0.917
SC-42	560.224	1.277	510.236	1.662
SC-43	1040.026	2.217	348.456	1.062
SC-44	3153.780	6.899	519.968	1.626
SC-45	907.823	1.890	416.701	1.240
SC-46	375.105	0.732	352.882	0.984
SC-47	350.843	0.684	383.760	1.069
SC-48	250.910	0.470	293.720	0.787
SC-49	484.413	0.993	484.836	1.421
SC-50	154.620	0.289	350.884	0.937
SC-51	621.354	1.285	559.584	1.654
SC-52	267.156	0.511	395.679	1.083
SC-53	1651.748	4.045	1057.093	3.701
SC-54	5099.743	10.312	624.870	1.806
SC-55	144.526	0.281	333.893	0.927
SC-56	6788.838	15.089	833.530	2.649
SC-57	2378.588	5.576	902.531	3.025
SC-58	1655.949	3.272	1000.435	2.826
SC-59	10936.007	13.250	1526.556	2.644
SC-60	5306.503	12.269	820.833	2.713

Shell Color Suite (Continued)

Kremmling, Colorado, samples				
Sample	**[Mg] ppm**	**Mg/Ca (mMol/Mol)**	**[Mn] ppm**	**Mn/Ca (mMol/Mol)**
SC-1	1972.721	9.318	2945.413	6.158
SC-2	2026.530	15.864	3988.699	13.821
SC-3	1270.365	6.812	6230.504	14.788
SC-4	2581.117	13.110	4049.314	9.103
SC-5	1672.626	7.098	5448.521	10.235
SC-6	1582.790	7.772	7306.718	15.880
SC-7	2956.605	20.905	2494.407	7.807
SC-8	2453.366	15.814	4032.559	11.505
SC-9	2325.221	12.935	4855.124	11.955
SC-10	2141.687	10.191	4314.775	9.088
SC-11	1993.891	12.865	5579.722	15.935
SC-12	1911.589	8.051	8319.078	15.508
SC-13	1383.786	7.386	6944.814	16.408
SC-14	2935.301	24.658	3169.419	11.785
SC-15	1797.564	9.061	6779.449	15.126
SC-16	4074.614	37.549	1342.895	5.478
SC-17	2616.606	35.753	2074.170	12.544
SC-18	2865.714	17.360	5512.545	14.781
SC-19	2396.181	16.131	1418.026	4.225
SC-20	2667.130	13.010	526.068	1.136

Shell Color Suite (Continued)

Game Ranch, South Dakota, samples				
Sample	**[Mg] ppm**	**Mg/Ca (mMol/Mol)**	**[Mn] ppm**	**Mn/Ca (mMol/Mol)**
SC-21	1326.876	7.422	2942.568	7.286
SC-22	126.981	0.550	180.025	0.345
SC-23	161.861	0.707	78.945	0.153
SC-24	5449.457	31.512	3517.102	9.002
SC-25	183.582	0.807	2635.794	5.126
SC-26	994.923	4.683	1260.325	2.626
SC-27	2497.682	14.367	5775.334	14.704
SC-28	298.577	1.414	347.127	0.728
SC-29	1190.107	6.390	1739.087	4.133
SC-30	84.588	0.379	302.604	0.600
SC-31	98.034	0.467	152.352	0.322
SC-32	309.860	1.347	4919.315	9.466
SC-33	270.770	1.291	3134.235	6.614
SC-34	11160.331	60.637	942.549	2.267
SC-35	276.651	1.303	45.970	0.096
SC-36	452.250	2.126	73.290	0.152
SC-37	1860.869	8.661	1747.161	3.599
SC-38	1306.539	6.362	783.941	1.690
SC-39	648.516	2.892	329.873	0.651
SC-40	216.444	1.072	N/A	N/A

Shell Color Suite (Continued)

Trask Ranch, South Dakota, samples				
Sample	**[Mg] ppm**	**Mg/Ca (mMol/Mol)**	**[Mn] ppm**	**Mn/Ca (mMol/Mol)**
SC-41	575.944	2.477	2145.707	4.085
SC-42	2240.993	11.747	475.724	1.104
SC-43	2782.707	13.644	972.733	2.111
SC-44	6031.295	30.351	2779.305	6.191
SC-45	1216.740	5.826	974.129	2.065
SC-46	1021.474	4.584	460.717	0.915
SC-47	1458.854	6.542	582.723	1.157
SC-48	348.164	1.502	232.611	0.444
SC-49	904.993	4.268	455.948	0.952
SC-50	394.804	1.696	130.099	0.247
SC-51	321.873	1.531	N/A	N/A
SC-52	804.157	3.541	244.546	0.477
SC-53	3537.012	19.928	759.422	1.894
SC-54	12247.372	56.972	3563.514	7.337
SC-55	628.403	2.809	246.420	0.487
SC-56	5729.899	29.297	5775.688	13.071
SC-57	6623.041	35.715	1543.848	3.685
SC-58	2741.765	12.462	1749.631	3.520
SC-59	13388.800	37.316	7764.048	9.578
SC-60	2694.561	14.332	4623.775	10.885

Shell Color Suite (Continued)

Kremmling, Colorado, samples				
Sample	**[Na] ppm**	**Na/Ca (mMol/Mol)**	**[Sr] ppm**	**Sr/Ca (mMol/Mol)**
SC-1	706.544	3.526	1493.954	1.957
SC-2	3390.397	28.041	384.189	0.834
SC-3	306.451	1.736	544.015	0.809
SC-4	374.077	2.007	754.795	1.063
SC-5	1734.972	7.779	1422.817	1.675
SC-6	345.030	1.790	576.458	0.785
SC-7	4594.785	34.324	369.622	0.725
SC-8	369.586	2.517	467.831	0.836
SC-9	420.889	2.474	657.507	1.015
SC-10	254.623	1.280	656.443	0.867
SC-11	1212.344	8.264	456.583	0.817
SC-12	448.175	1.994	819.504	0.957
SC-13	285.333	1.609	511.231	0.757
SC-14	2246.541	19.938	384.357	0.896
SC-15	358.141	1.907	600.895	0.840
SC-16	3531.446	34.383	529.702	1.354
SC-17	809.730	11.689	221.732	0.840
SC-18	803.904	5.145	554.923	0.933
SC-19	1735.618	12.345	982.662	1.835
SC-20	2457.735	12.666	1240.698	1.679

Shell Color Suite (Continued)

Game Ranch, South Dakota, samples				
Sample	**[Na] ppm**	**Na/Ca (mMol/Mol)**	**[Sr] ppm**	**Sr/Ca (mMol/Mol)**
SC-21	3084.444	18.229	2567.832	3.985
SC-22	3718.036	17.022	3027.965	3.640
SC-23	3937.584	18.172	3002.582	3.638
SC-24	2470.400	15.093	2518.660	4.040
SC-25	3165.385	14.695	3544.326	4.320
SC-26	3828.344	19.038	2000.966	2.613
SC-27	3498.948	21.263	2083.027	3.324
SC-28	4338.181	21.707	1937.749	2.546
SC-29	3608.656	20.471	2389.502	3.559
SC-30	4533.102	21.448	2597.124	3.226
SC-31	4128.452	20.797	1863.390	2.465
SC-32	3924.948	18.027	2324.538	2.803
SC-33	3546.025	17.861	3980.821	5.264
SC-34	3646.641	20.933	2623.239	3.954
SC-35	4065.437	20.234	1799.189	2.351
SC-36	4150.104	20.612	3250.576	4.239
SC-37	2970.007	14.604	1424.169	1.839
SC-38	3362.519	17.300	1336.423	1.805
SC-39	2839.399	13.379	1493.068	1.847
SC-40	2508.917	13.134	1473.977	2.026

Shell Color Suite (Continued)

Trask Ranch, South Dakota, samples				
Sample	**[Na] ppm**	**Na/Ca (mMol/Mol)**	**[Sr] ppm**	**Sr/Ca (mMol/Mol)**
SC-41	3504.255	15.925	3265.464	3.896
SC-42	4861.709	26.926	4260.665	6.196
SC-43	8975.105	46.493	2648.529	3.602
SC-44	1760.631	9.361	2212.598	3.089
SC-45	4285.288	21.680	2388.933	3.173
SC-46	3941.349	18.686	1908.415	2.376
SC-47	5417.316	25.664	2154.871	2.680
SC-48	4112.303	18.741	2179.679	2.608
SC-49	3601.184	17.944	2286.626	2.992
SC-50	3804.437	17.267	2615.512	3.117
SC-51	3864.684	19.420	2577.314	3.400
SC-52	3568.098	16.601	3130.853	3.824
SC-53	4957.611	29.510	1734.128	2.710
SC-54	2300.133	11.304	592.935	0.765
SC-55	3944.085	18.624	2813.711	3.488
SC-56	2382.854	12.872	1656.773	2.350
SC-57	8502.651	48.443	1671.584	2.501
SC-58	2169.675	10.419	7309.292	9.216
SC-59	9058.639	26.674	3659.690	2.829
SC-60	2842.429	15.973	1575.591	2.325

Cementation Suite

Kremmling, Colorado, samples			
Sample	**[Ca] ppm**	**[Al] ppm**	**Al/Ca (mMol/Mol)**
CEM-1S	255432.82	771.18	4.484
CEM-1Ce	303879.50	N/A	N/A
CEM-1Co	220810.48	1711.05	11.509
CEM-2S	358874.98	276.10	1.143
CEM-2Co	251093.16	1847.62	10.928
CEM-3S	265065.62	727.46	4.076
CEM-3Ce	475948.97	N/A	N/A
CEM-3Co	179162.98	1766.72	14.645
CEM-4S	625305.54	2580.28	6.129
CEM-4Co	211100.68	4971.60	34.977
CEM-5S	350061.94	N/A	N/A
CEM-5Ce	278865.48	N/A	N/A
CEM-5Co	222344.01	1680.37	11.224
CEM-6S	52036.78	296.93	8.475
CEM-6Ce	339589.59	N/A	N/A
CEM-6Co	190857.76	2513.65	19.560
CEM-7S	339329.61	534.68	2.340
CEM-7Ce	372392.56	N/A	N/A
CEM-7Co	324670.05	1038.23	4.749
CEM-8S	335406.50	N/A	N/A
CEM-8Ce	341787.32	N/A	N/A
CEM-8Co	227985.95	2069.69	13.483
CEM-9S	378031.27	289.17	1.136
CEM-9Ce1	356061.91	N/A	N/A
CEM-9Ce2	266343.28	631.94	3.524
CEM-9Co	362867.17	122.50	0.501
CEM-10S	361903.30	N/A	N/A
CEM-10Ce1	388303.55	N/A	N/A
CEM-10Ce2	379821.80	N/A	N/A
CEM-10Co	299197.88	2180.76	10.825

Cementation Suite (Continued)

Game Ranch, South Dakota, samples			
Sample	**[Ca] ppm**	**[Al] ppm**	**Al/Ca (mMol/Mol)**
CEM-11S	261172.41	1819.58	10.347
CEM-11Co	90588.34	3288.19	53.909
CEM-11Cr1	237395.84	394.69	2.469
CEM-11Cr2	226000.39	100.90	0.663
CEM-12S	388705.07	N/A	N/A
CEM-12Co	245278.19	1463.17	8.860
CEM-12Cr1	225573.17	615.60	4.053
CEM-12Cr2	169693.24	111.13	0.973
CEM-13S	380419.54	106.25	0.415
CEM-13Co	237231.41	2053.75	12.858
CEM-13Cr	236948.73	286.25	1.794
CEM-14S	290700.00	840.43	4.294
CEM-14Ce1	103306.32	221.48	3.184
CEM-14Ce2	17070.41	135.15	11.759
CEM-14Cr1	25103.31	876.95	51.883
CEM-14Cr2	40110.25	1261.28	46.702
CEM-15S	391032.82	N/A	N/A
CEM-15Co1	268303.24	2156.22	11.936
CEM-15Co2	92163.79	3094.03	49.859

Cementation Suite (Continued)

Trask Ranch, South Dakota, samples			
Sample	**[Ca] ppm**	**[Al] ppm**	**Al/Ca (mMol/Mol)**
CEM-16S	372319.20	308.46	1.230
CEM-16Ce1	348010.29	N/A	N/A
CEM-16Ce2	367833.26	259.47	1.048
CEM-16Co	300039.42	2645.31	13.094
CEM-17S1	284559.41	586.30	3.060
CEM-17S2	349902.11	359.28	1.525
CEM-17Ce1	317855.38	568.15	2.655
CEM-17Ce2	381884.20	102.89	0.400
CEM-17Co	298747.21	2399.52	11.929
CEM-18S	393776.54	N/A	N/A
CEM-18Ce	399144.37	259.38	0.965
CEM-18Co	260098.66	6439.27	36.769
CEM-19S1	317955.32	226.61	1.058
CEM-19S2	351780.35	371.10	1.567
CEM-19Ce1	521438.36	456.92	1.301
CEM-19Ce2	323274.26	101.27	0.465
CEM-19Co	302066.99	2586.47	12.717
CEM-20S	382850.85	654.04	2.537
CEM-20Co	263178.45	6559.99	37.020
CEM-21S	293049.19	1095.25	5.551
CEM-21Ce1	317672.23	N/A	N/A
CEM-21Co	274184.03	2495.04	13.515
CEM-22S1	281796.30	1014.27	5.346
CEM-22S2	336458.65	1515.34	6.689
CEM-22Ce1	280626.69	1540.34	8.152
CEM-22Ce2	370888.45	N/A	N/A
CEM-22Co	264976.38	3974.43	22.277
CEM-23S	277337.00	2329.73	12.476
CEM-23Ce1	394020.73	279.22	1.052
CEM-23Ce2	379758.14	N/A	N/A
CEM-23Co	292270.67	2905.92	14.767

Cementation Suite (Continued)

Trask Ranch, South Dakota, samples (continued)			
Sample	**[Ca] ppm**	**[Al] ppm**	**Al/Ca (mMol/Mol)**
CEM-24S	272964.37	426.63	2.321
CEM-24Ce	374382.05	186.00	0.738
CEM-24Co	267054.50	3016.73	16.777
CEM-25S	404485.34	N/A	N/A
CEM-25Ce	370380.16	3651.09	14.640
CEM-25Co	288819.66	3618.82	18.609
CEM-26S	370368.96	823.22	3.301
CEM-26Ce	294838.84	3018.75	15.206
CEM-26Co	370133.19	436.05	1.750
CEM-27S	313509.45	1406.78	6.664
CEM-27Ce	360938.20	N/A	N/A
CEM-27Co	293772.24	2021.58	10.220
CEM-28S	367916.87	330.63	1.335
CEM-28Ce	227586.99	141.91	0.926
CEM-28Co	227852.24	1858.50	12.114
CEM-29S	333660.53	970.36	4.319
CEM-29Co	289763.65	2262.83	11.598
CEM-29Cr	338142.89	591.50	2.598
CEM-30S	342594.96	1264.37	5.481
CEM-30Ce1	274004.45	N/A	N/A
CEM-30Ce2	279716.77	1045.67	5.552
CEM-30Co	278435.07	3013.68	16.075
CEM-31S	349977.93	N/A	N/A
CEM-31Ce	350808.53	N/A	N/A
CEM-32S	368450.73	N/A	N/A
CEM-32Ce	335529.56	N/A	N/A
CEM-33S	333255.24	1848.23	8.237
CEM-33Co	252382.59	2369.31	13.943
CEM-34S	241088.47	N/A	N/A
CEM-34Co	297050.08	2770.89	13.854

APPENDIX B (CONTINUED)

Cementation Suite (Continued)

Kremmling, Colorado, samples				
Sample	**[Fe] ppm**	**Fe/Ca (mMol/Mol)**	**[K] ppm**	**K/Ca (mMol/Mol)**
CEM-1S	4952.44	13.908	582.62	0.091
CEM-1Ce	3752.21	8.858	222.65	0.029
CEM-1Co	4490.18	14.587	1192.48	0.216
CEM-2S	13500.74	26.987	270.92	0.030
CEM-2Co	10301.29	29.430	1270.91	0.202
CEM-3S	2344.41	6.345	372.91	0.056
CEM-3Ce	9026.85	13.605	224.80	0.019
CEM-3Co	5168.33	20.694	1211.73	0.271
CEM-4S	6919.87	7.938	315.07	0.020
CEM-4Co	35258.23	119.813	1974.82	0.374
CEM-5S	6224.77	12.756	256.35	0.029
CEM-5Ce	5358.11	13.783	184.99	0.027
CEM-5Co	5655.22	18.246	1160.82	0.209
CEM-6S	1608.08	22.168	283.20	0.218
CEM-6Ce	11414.49	24.112	292.68	0.034
CEM-6Co	9809.57	36.870	1131.19	0.237
CEM-7S	3839.88	8.118	539.74	0.064
CEM-7Ce	4255.77	8.198	260.99	0.028
CEM-7Co	7070.92	15.623	749.87	0.092
CEM-8S	4197.52	8.977	273.64	0.033
CEM-8Ce	4372.52	9.177	188.24	0.022
CEM-8Co	4748.04	14.940	1315.89	0.231
CEM-9S	3942.20	7.481	320.97	0.034
CEM-9Ce1	1483.53	2.989	224.33	0.025
CEM-9Ce2	2690.76	7.247	521.19	0.078
CEM-9Co	1401.35	2.770	276.86	0.031
CEM-10S	6058.57	12.009	280.20	0.031
CEM-10Ce1	9109.87	16.830	234.90	0.024
CEM-10Ce2	1074.91	2.030	241.38	0.025
CEM-10Co	13218.88	31.693	1063.35	0.142

Cementation Suite (Continued)

Game Ranch, South Dakota, samples				
Sample	**[Fe] ppm**	**Fe/Ca (mMol/Mol)**	**[K] ppm**	**K/Ca (mMol/Mol)**
CEM-11S	10183.93	27.972	1442.34	0.221
CEM-11Co	22768.73	180.301	2461.97	1.087
CEM-11Cr1	4073.17	12.308	423.42	0.071
CEM-11Cr2	1644.17	5.219	346.32	0.061
CEM-12S	773.39	1.427	322.47	0.033
CEM-12Co	28657.81	83.814	1541.98	0.251
CEM-12Cr1	15255.76	48.515	625.00	0.111
CEM-12Cr2	1516.00	6.409	308.19	0.073
CEM-13S	553.87	1.044	479.80	0.050
CEM-13Co	8455.51	25.568	2086.71	0.352
CEM-13Cr	851.55	2.578	385.02	0.065
CEM-14S	18157.46	44.807	853.81	0.117
CEM-14Ce1	251512.43	1746.486	437.05	0.169
CEM-14Ce2	5458.01	229.363	293.87	0.689
CEM-14Cr1	299573.59	8560.619	916.13	1.460
CEM-14Cr2	36920.99	660.314	1493.93	1.490
CEM-15S	1062.48	1.949	398.01	0.041
CEM-15Co1	11014.53	29.449	1498.51	0.223
CEM-15Co2	19198.16	149.428	2612.06	1.134

Cementation Suite (Continued)

Trask Ranch, South Dakota, samples				
Sample	**[Fe] ppm**	**Fe/Ca (mMol/Mol)**	**[K] ppm**	**K/Ca (mMol/Mol)**
CEM-16S	1249.06	2.407	435.43	0.047
CEM-16Ce1	2447.17	5.044	345.91	0.040
CEM-16Ce2	5213.36	10.167	428.40	0.047
CEM-16Co	4763.16	11.388	1275.58	0.170
CEM-17S1	1483.17	3.739	451.16	0.063
CEM-17S2	3249.96	6.663	401.03	0.046
CEM-17Ce1	4655.32	10.506	408.06	0.051
CEM-17Ce2	1818.36	3.416	321.83	0.034
CEM-17Co	4593.61	11.030	1259.95	0.169
CEM-18S	565.11	1.029	285.96	0.029
CEM-18Ce	4260.18	7.657	500.78	0.050
CEM-18Co	6202.89	17.108	1431.01	0.220
CEM-19S1	1015.03	2.290	393.22	0.049
CEM-19S2	974.03	1.986	336.07	0.038
CEM-19Ce1	10597.98	14.580	885.75	0.068
CEM-19Ce2	3362.32	7.461	733.11	0.091
CEM-19Co	4800.10	11.399	1326.01	0.176
CEM-20S	500.36	0.938	552.24	0.058
CEM-20Co	7025.35	19.149	1602.90	0.244
CEM-21S	1508.37	3.692	475.97	0.065
CEM-21Ce1	47.19	0.107	277.22	0.035
CEM-21Co	4781.54	12.510	1379.76	0.201
CEM-22S1	2047.93	5.213	815.19	0.116
CEM-22S2	1250.87	2.667	744.25	0.088
CEM-22Ce1	3883.43	9.927	892.39	0.127
CEM-22Ce2	1072.54	2.074	213.98	0.023
CEM-22Co	7773.58	21.045	2059.93	0.311
CEM-23S	4351.04	11.254	1102.74	0.159
CEM-23Ce1	4112.30	7.487	399.04	0.041
CEM-23Ce2	5012.99	9.469	211.90	0.022
CEM-23Co	6507.38	15.972	1712.64	0.234

Cementation Suite (Continued)

Trask Ranch, South Dakota, samples (Continued)				
Sample	**[Fe] ppm**	**Fe/Ca (mMol/Mol)**	**[K] ppm**	**K/Ca (mMol/Mol)**
CEM-24S	2006.90	5.274	557.65	0.082
CEM-24Ce	1309.88	2.510	323.60	0.035
CEM-24Co	5344.90	14.357	1596.19	0.239
CEM-25S	103.24	0.183	283.57	0.028
CEM-25Ce	1665.79	3.226	301.08	0.033
CEM-25Co	5375.24	13.351	1241.12	0.172
CEM-26S	2497.39	4.837	448.43	0.048
CEM-26Ce	5861.85	14.262	1416.74	0.192
CEM-26Co	6339.45	12.286	468.31	0.051
CEM-27S	5588.00	12.786	1044.63	0.133
CEM-27Ce	2114.49	4.202	191.74	0.021
CEM-27Co	4139.04	10.107	1259.02	0.171
CEM-28S	1116.53	2.177	461.56	0.050
CEM-28Ce	2327.46	7.336	312.40	0.055
CEM-28Co	4255.89	13.399	1245.74	0.219
CEM-29S	737.26	1.585	382.61	0.046
CEM-29Co	5663.25	14.020	1304.50	0.180
CEM-29Cr	3382.42	7.176	562.29	0.067
CEM-30S	2736.93	5.731	805.32	0.094
CEM-30Ce1	1276.86	3.343	71.29	0.010
CEM-30Ce2	6931.16	17.775	464.26	0.066
CEM-30Co	4968.02	12.799	1256.27	0.180
CEM-31S	1661.88	3.406	956.27	0.109
CEM-31Ce	4575.42	9.356	803.24	0.092
CEM-32S	4423.38	8.612	185.87	0.020
CEM-32Ce	11133.99	23.804	59.69	0.007
CEM-33S	1501.39	3.232	343.47	0.041
CEM-33Co	5290.24	15.037	1413.63	0.224
CEM-34S	N/A	N/A	287.84	0.048
CEM-34Co	4690.15	11.326	1352.09	0.182

APPENDIX B (CONTINUED)

Cementation Suite (Continued)

Kremmling, Colorado, samples				
Sample	**[Mg] ppm**	**Mg/Ca (mMol/Mol)**	**[Mn] ppm**	**Mn/Ca (mMol/Mol)**
CEM-1S	1925.60	12.440	4209.74	12.038
CEM-1Ce	2204.28	11.970	2338.66	5.621
CEM-1Co	3500.28	26.159	3284.83	10.866
CEM-2S	2642.51	12.151	4333.35	8.820
CEM-2Co	7586.01	49.856	9212.94	26.800
CEM-3S	1086.86	6.766	5189.71	14.301
CEM-3Ce	1766.71	6.126	2497.75	3.833
CEM-3Co	2208.73	20.344	3135.77	12.784
CEM-4S	2657.12	7.012	10423.82	12.176
CEM-4Co	3684.14	28.799	3798.09	13.142
CEM-5S	2258.40	10.646	5992.27	12.503
CEM-5Ce	1573.58	9.312	2454.61	6.429
CEM-5Co	3735.79	27.727	3675.51	12.074
CEM-6S	577.62	18.318	246.42	3.459
CEM-6Ce	3695.40	17.957	647.83	1.393
CEM-6Co	3180.86	27.503	3887.91	14.879
CEM-7S	2411.34	11.727	4917.09	10.584
CEM-7Ce	3709.39	16.438	2710.49	5.316
CEM-7Co	3036.54	15.434	5409.66	12.170
CEM-8S	1713.13	8.429	7196.78	15.673
CEM-8Ce	2476.26	11.956	2338.92	4.998
CEM-8Co	4684.42	33.907	3881.35	12.435
CEM-9S	2789.99	12.179	2781.31	5.374
CEM-9Ce1	503.97	2.336	2059.01	4.224
CEM-9Ce2	970.86	6.015	929.51	2.549
CEM-9Co	619.93	2.819	2212.32	4.453
CEM-10S	1909.15	8.705	7771.08	15.684
CEM-10Ce1	1700.05	7.225	2001.87	3.766
CEM-10Ce2	448.86	1.950	3297.99	6.342
CEM-10Co	2928.45	16.152	5831.75	14.237

Cementation Suite (Continued)

Game Ranch, South Dakota, samples				
Sample	**[Mg] ppm**	**Mg/Ca (mMol/Mol)**	**[Mn] ppm**	**Mn/Ca (mMol/Mol)**
CEM-11S	11234.98	70.988	4048.30	11.322
CEM-11Co	4141.76	75.449	5173.71	41.716
CEM-11Cr1	436.46	3.034	1856.76	5.713
CEM-11Cr2	185.38	1.354	348.50	1.126
CEM-12S	265.57	1.127	264.06	0.496
CEM-12Co	6878.74	46.279	7669.42	22.839
CEM-12Cr1	1208.51	8.841	2079.96	6.735
CEM-12Cr2	161.56	1.571	1385.51	5.964
CEM-13S	339.54	1.473	484.53	0.930
CEM-13Co	5107.06	35.525	4783.73	14.729
CEM-13Cr	311.36	2.168	903.60	2.785
CEM-14S	2292.85	13.016	1515.90	3.809
CEM-14Ce1	15911.84	254.174	13506.79	95.499
CEM-14Ce2	557.98	53.940	372.86	15.954
CEM-14Cr1	13037.18	857.020	23881.43	694.867
CEM-14Cr2	2910.27	119.734	16724.11	304.551
CEM-15S	188.58	0.796	756.39	1.413
CEM-15Co1	8167.99	50.237	3238.25	8.816
CEM-15Co2	4782.25	85.627	10352.44	82.045

APPENDIX B (CONTINUED)

Cementation Suite (Continued)

Trask Ranch, South Dakota, samples				
Sample	**[Mg] ppm**	**Mg/Ca (mMol/Mol)**	**[Mn] ppm**	**Mn/Ca (mMol/Mol)**
CEM-16S	2746.05	12.171	783.25	1.537
CEM-16Ce1	925.28	4.388	1522.48	3.195
CEM-16Ce2	3115.91	13.979	2982.59	5.923
CEM-16Co	13260.39	72.932	5819.61	14.167
CEM-17S1	3621.42	21.001	1411.27	3.622
CEM-17S2	8289.60	39.095	2397.31	5.004
CEM-17Ce1	3066.32	15.919	2473.52	5.684
CEM-17Ce2	1846.18	7.978	1344.48	2.572
CEM-17Co	15531.84	85.794	3813.52	9.324
CEM-18S	926.51	3.883	527.06	0.978
CEM-18Ce	4185.72	17.305	2549.51	4.666
CEM-18Co	16163.31	102.549	3596.46	10.100
CEM-19S1	2394.59	12.428	1539.06	3.536
CEM-19S2	4131.37	19.380	1493.92	3.102
CEM-19Ce1	3203.42	10.138	9155.12	12.824
CEM-19Ce2	1099.64	5.613	2387.06	5.393
CEM-19Co	12223.09	66.775	13683.93	33.089
CEM-20S	2263.66	9.757	425.34	0.811
CEM-20Co	15983.06	100.218	2752.25	7.639
CEM-21S	5109.22	28.771	1101.75	2.746
CEM-21Ce1	12088.74	62.797	1371.51	3.153
CEM-21Co	12978.97	78.115	2763.75	7.363
CEM-22S1	6911.16	40.472	794.24	2.059
CEM-22S2	6727.02	32.994	691.14	1.500
CEM-22Ce1	7815.29	45.957	1728.23	4.498
CEM-22Ce2	9454.39	42.066	1911.97	3.765
CEM-22Co	13359.77	83.201	3337.65	9.200
CEM-23S	4629.41	27.546	2878.12	7.580
CEM-23Ce1	2241.49	9.388	5662.31	10.497
CEM-23Ce2	654.48	2.844	8617.82	16.575
CEM-23Co	14039.63	79.270	3287.83	8.217

APPENDIX B (CONTINUED)

Cementation Suite (Continued)

Trask Ranch, South Dakota, samples (continued)				
Sample	**[Mg] ppm**	**Mg/Ca (mMol/Mol)**	**[Mn] ppm**	**Mn/Ca (mMol/Mol)**
CEM-24S	5749.52	34.759	1635.41	4.376
CEM-24Ce	10506.80	46.312	1647.69	3.215
CEM-24Co	15756.35	97.363	4240.37	11.598
CEM-25S	597.62	2.438	225.38	0.407
CEM-25Ce	18500.89	82.430	3719.73	7.336
CEM-25Co	12874.94	73.563	3473.57	8.785
CEM-26S	4046.24	18.028	3240.42	6.391
CEM-26Ce	15324.63	85.772	6730.28	16.673
CEM-26Co	2889.94	12.885	3591.80	7.088
CEM-27S	7527.14	39.620	3907.32	9.103
CEM-27Ce	13019.12	59.523	7352.15	14.878
CEM-27Co	17161.91	96.404	3598.44	8.947
CEM-28S	2813.35	12.619	523.58	1.039
CEM-28Ce	7824.72	56.736	1484.89	4.766
CEM-28Co	13351.52	96.698	2170.49	6.958
CEM-29S	1115.73	5.518	55.99	0.123
CEM-29Co	13707.01	78.062	6269.72	15.804
CEM-29Cr	1873.37	9.142	3474.58	7.505
CEM-30S	4141.72	19.950	1576.25	3.361
CEM-30Ce1	13108.56	78.947	2087.25	5.564
CEM-30Ce2	2959.39	17.459	6204.11	16.201
CEM-30Co	16865.85	99.959	3175.60	8.331
CEM-31S	1302.99	6.144	2656.91	5.545
CEM-31Ce	798.18	3.755	7422.87	15.455
CEM-32S	2185.38	9.788	8619.19	17.087
CEM-32Ce	1927.36	9.479	20595.20	44.834
CEM-33S	3068.71	15.196	594.38	1.303
CEM-33Co	11965.39	78.236	3103.77	8.983
CEM-34S	231.95	1.588	32.20	0.098
CEM-34Co	19755.00	109.745	2059.04	5.063

Cementation Suite

Kremmling, Colorado, samples				
Sample	**[Na] ppm**	**Na/Ca (mMol/Mol)**	**[Sr] ppm**	**Sr/Ca (mMol/Mol)**
CEM-1S	608.14	4.151	446.82	0.801
CEM-1Ce	388.22	2.227	304.26	0.458
CEM-1Co	608.65	4.806	339.70	0.704
CEM-2S	546.98	2.657	647.58	0.826
CEM-2Co	1713.64	11.899	1028.78	1.876
CEM-3S	696.95	4.584	546.90	0.944
CEM-3Ce	481.71	1.765	624.18	0.600
CEM-3Co	654.92	6.373	202.35	0.517
CEM-4S	655.23	1.827	1325.49	0.970
CEM-4Co	929.55	7.677	317.10	0.688
CEM-5S	492.22	2.452	725.64	0.949
CEM-5Ce	533.66	3.336	94.09	0.154
CEM-5Co	649.28	5.091	409.40	0.843
CEM-6S	416.39	13.951	1171.13	10.302
CEM-6Ce	526.52	2.703	279.10	0.376
CEM-6Co	581.35	5.311	337.13	0.809
CEM-7S	2052.37	10.545	707.50	0.954
CEM-7Ce	683.35	3.199	381.89	0.469
CEM-7Co	567.91	3.050	549.30	0.774
CEM-8S	547.09	2.844	663.57	0.906
CEM-8Ce	398.67	2.034	286.08	0.383
CEM-8Co	606.63	4.639	368.25	0.739
CEM-9S	636.25	2.934	763.94	0.925
CEM-9Ce1	377.19	1.847	356.28	0.458
CEM-9Ce2	512.19	3.353	N/A	N/A
CEM-9Co	387.33	1.861	137.54	0.174
CEM-10S	476.94	2.298	663.14	0.839
CEM-10Ce1	427.46	1.919	468.24	0.552
CEM-10Ce2	918.71	4.217	142.32	0.172
CEM-10Co	477.01	2.780	435.87	0.667

Cementation Suite (Continued)

Game Ranch, South Dakota, samples				
Sample	**[Na] ppm**	**Na/Ca (mMol/Mol)**	**[Sr] ppm**	**Sr/Ca (mMol/Mol)**
CEM-11S	1699.97	11.348	1123.33	1.969
CEM-11Co	1876.77	36.121	426.30	2.154
CEM-11Cr1	848.81	6.234	1182.29	2.280
CEM-11Cr2	725.21	5.595	1072.97	2.173
CEM-12S	3882.54	17.415	3061.82	3.606
CEM-12Co	1981.10	14.082	919.51	1.716
CEM-12Cr1	959.66	7.417	1077.21	2.186
CEM-12Cr2	501.68	5.154	1059.68	2.859
CEM-13S	4203.02	19.263	2069.59	2.490
CEM-13Co	2242.68	16.482	1530.01	2.952
CEM-13Cr	607.09	4.467	653.35	1.262
CEM-14S	3579.83	21.470	3398.15	5.351
CEM-14Ce1	993.15	16.761	470.24	2.084
CEM-14Ce2	446.20	45.573	3578.30	95.956
CEM-14Cr1	582.63	40.465	13.02	0.237
CEM-14Cr2	896.45	38.966	309.72	3.535
CEM-15S	4865.36	21.693	2384.12	2.791
CEM-15Co1	1218.55	7.918	906.31	1.546
CEM-15Co2	2040.53	38.601	444.73	2.209

Cementation Suite (Continued)

Trask Ranch, South Dakota, samples				
Sample	**[Na] ppm**	**Na/Ca (mMol/Mol)**	**[Sr] ppm**	**SrCa (mMol/Mol)**
CEM-16S	3658.19	10.436	11408.96	4.498
CEM-16Ce1	160.44	2.481	5896.43	0.211
CEM-16Ce2	243.88	3.432	12967.74	0.304
CEM-16Co	551.83	7.658	29633.70	0.842
CEM-17S1	2332.95	12.648	11950.54	3.753
CEM-17S2	1499.76	9.382	18079.87	1.962
CEM-17Ce1	211.38	18.433	14743.31	0.304
CEM-17Ce2	209.58	7.262	7233.90	0.251
CEM-17Co	577.64	7.265	29420.97	0.885
CEM-18S	4946.09	11.721	9898.06	5.750
CEM-18Ce	291.11	4.985	13187.86	0.334
CEM-18Co	554.10	17.648	37019.87	0.975
CEM-19S1	2561.37	14.381	10752.52	3.688
CEM-19S2	2818.05	10.309	12204.53	3.667
CEM-19Ce1	444.79	3.763	25869.54	0.390
CEM-19Ce2	290.94	9.574	9749.54	0.412
CEM-19Co	638.93	8.170	36674.08	0.968
CEM-20S	3114.51	16.133	11052.71	3.724
CEM-20Co	587.00	7.976	35714.57	1.021
CEM-21S	1591.71	17.893	13889.75	2.486
CEM-21Ce1	712.77	7.870	15931.48	1.027
CEM-21Co	474.55	8.543	26217.09	0.792
CEM-22S1	1949.98	43.450	20555.48	3.168
CEM-22S2	1945.49	28.435	18361.48	2.647
CEM-22Ce1	875.22	45.712	24092.61	1.428
CEM-22Ce2	426.24	4.688	14076.35	0.526
CEM-22Co	442.71	14.503	33152.26	0.765
CEM-23S	1288.43	17.179	19312.15	2.127
CEM-23Ce1	263.68	9.402	15082.80	0.306
CEM-23Ce2	255.65	1.470	15073.05	0.308
CEM-23Co	529.26	7.867	30301.44	0.829

Cementation Suite (Continued)

Trask Ranch, South Dakota, samples (continued)				
Sample	**[Na] ppm**	**Na/Ca (mMol/Mol)**	**[Sr] ppm**	**SrCa (mMol/Mol)**
CEM-24S	3739.38	23.884	1538.88	2.581
CEM-24Ce	1238.99	5.770	1205.27	1.474
CEM-24Co	1914.21	12.497	583.39	1.000
CEM-25S	3408.53	14.692	3061.08	3.464
CEM-25Ce	926.39	4.361	721.52	0.892
CEM-25Co	959.09	5.790	565.92	0.897
CEM-26S	2252.36	10.603	2561.66	3.166
CEM-26Ce	1207.39	7.140	707.12	1.098
CEM-26Co	874.07	4.117	602.84	0.746
CEM-27S	6268.12	34.858	1842.73	2.691
CEM-27Ce	551.09	2.662	452.77	0.574
CEM-27Co	1330.67	7.897	618.02	0.963
CEM-28S	4233.60	20.062	2772.22	3.449
CEM-28Ce	623.57	4.777	283.21	0.570
CEM-28Co	1494.71	11.437	493.74	0.992
CEM-29S	4056.19	21.195	1506.57	2.067
CEM-29Co	1452.21	8.738	582.05	0.920
CEM-29Cr	3006.70	15.503	243.90	0.330
CEM-30S	3000.70	15.271	1346.21	1.799
CEM-30Ce1	682.00	4.340	539.89	0.902
CEM-30Ce2	680.85	4.244	299.99	0.491
CEM-30Co	1085.38	6.796	673.87	1.108
CEM-31S	5300.72	26.406	2090.25	2.734
CEM-31Ce	786.07	3.907	358.32	0.468
CEM-32S	2828.21	13.383	1443.49	1.793
CEM-32Ce	492.66	2.560	417.26	0.569
CEM-33S	4640.90	24.280	2195.65	3.016
CEM-33Co	1453.32	10.040	543.67	0.986
CEM-34S	2081.65	15.054	2043.12	3.879
CEM-34Co	1047.47	6.148	708.97	1.093
CEM-24S	3739.38	23.884	1538.88	2.581

APPENDIX C: MINOR ELEMENTS FOR SCLEROCHRONOLOGY CANDIDATES

Baculites candidates				
Sample		**[Al] ppm**	**Al/Ca (mMol/Mol)**	**[Ca] ppm**
B2	2.5	365.81	2.063	264065.56
B2	7.5	N/A	N/A	321462.40
B2	12.5	N/A	N/A	343369.70
B2	17.5	N/A	N/A	294905.20
B2	22.5	N/A	N/A	335379.87
B2	27.5	N/A	N/A	284469.30
B2	32.5	N/A	N/A	326394.41
B3	2.5	188.00	0.846	330841.49
B3	7.5	N/A	N/A	355309.16
B3	12.5	N/A	N/A	369106.63
B4	2.5	N/A	N/A	170565.47
B4	7.5	N/A	N/A	364469.94
B4	12.5	N/A	N/A	305218.85
B4	17.5	N/A	N/A	367046.51
B4	22.5	N/A	N/A	362235.49
B4	27.5	N/A	N/A	344474.10
B4	32.5	N/A	N/A	381711.31
B4	37.5	N/A	N/A	346901.60
B4	42.5	278.85	0.764	543356.45
B5	2.5	N/A	N/A	N/A
B5	7.5	N/A	N/A	366027.98
B5	12.5	N/A	N/A	763881.69
B5	17.5	N/A	N/A	413460.84
B6	12.5	409.97	1.809	337424.10
B6	17.5	125.86	0.598	313332.14
B6	22.5	N/A	N/A	330895.94
B6	27.5	N/A	N/A	368588.90
B6	32.5	N/A	N/A	339138.45
B6	37.5	231.32	1.030	334370.43
B7	2.5	223.58	0.397	838018.58
B7	7.5	N/A	N/A	406809.47
B7	12.5	156.61	0.688	339064.25
B7	17.5	N/A	N/A	53845.91
B7	22.5	N/A	N/A	210883.79
B7	27.5	N/A	N/A	478341.92

APPENDIX C: MINOR ELEMENTS FOR SCLEROCHRONOLOGY CANDIDATES (CONTINUED)

Baculites candidates					
Sample		**[Fe] ppm**	**Fe/Ca (mMol/Mol)**	**[K] ppm**	**K/Ca (mMol/Mol)**
B2	2.5	253.38	0.688	542.61	2.107
B2	7.5	512.75	1.144	427.00	1.362
B2	12.5	285.70	0.597	300.75	0.898
B2	17.5	138.77	0.338	246.24	0.856
B2	22.5	288.98	0.618	397.57	1.216
B2	27.5	467.20	1.178	771.03	2.780
B2	32.5	203.63	0.448	365.25	1.148
B3	2.5	1549.54	3.360	594.00	1.841
B3	7.5	N/A	N/A	202.63	0.585
B3	12.5	58.80	0.114	251.90	0.700
B4	2.5	455.94	1.918	277.64	1.669
B4	7.5	198.24	0.390	316.33	0.890
B4	12.5	365.87	0.860	519.55	1.746
B4	17.5	624.25	1.220	422.99	1.182
B4	22.5	456.92	0.905	443.68	1.256
B4	27.5	133.28	0.278	319.08	0.950
B4	32.5	476.06	0.895	204.51	0.549
B4	37.5	100.25	0.207	290.00	0.857
B4	42.5	1329.01	1.755	452.25	0.854
B5	2.5	N/A	N/A	N/A	N/A
B5	7.5	260.38	0.510	268.07	0.751
B5	12.5	729.59	0.685	514.90	0.691
B5	17.5	493.78	0.857	228.26	0.566
B6	12.5	1864.20	3.963	679.94	2.067
B6	17.5	604.98	1.385	429.89	1.407
B6	22.5	596.92	1.294	340.73	1.056
B6	27.5	458.02	0.891	248.77	0.692
B6	32.5	632.02	1.337	294.57	0.891
B6	37.5	1867.93	4.007	624.41	1.915
B7	2.5	411.079	0.352	571.386	0.699
B7	7.5	112.121	0.198	305.127	0.769
B7	12.5	331.526	0.701	299.098	0.905
B7	17.5	N/A	N/A	69.551	1.325
B7	22.5	N/A	N/A	138.953	0.676
B7	27.5	203.877	0.306	272.128	0.583

APPENDIX C: MINOR ELEMENTS FOR SCLEROCHRONOLOGY CANDIDATES (CONTINUED)

Baculites candidates					
Sample		**[Mg] ppm**	**Mg/Ca (mMol/Mol)**	**[Mn] ppm**	**Mn/Ca (mMol/Mol)**
B2	2.5	1103.28	6.895	121.96	0.337
B2	7.5	692.85	3.557	61.34	0.139
B2	12.5	377.51	1.814	16.95	0.036
B2	17.5	554.67	3.104	26.15	0.065
B2	22.5	769.82	3.788	99.04	0.216
B2	27.5	1166.87	6.769	35.76	0.092
B2	32.5	736.39	3.723	87.52	0.196
B3	2.5	1662.20	8.291	415.16	0.917
B3	7.5	140.79	0.654	N/A	N/A
B3	12.5	225.82	1.010	N/A	N/A
B4	2.5	696.56	6.739	745.32	3.192
B4	7.5	539.15	2.441	301.33	0.604
B4	12.5	553.86	2.994	696.80	1.668
B4	17.5	1403.97	6.312	1076.20	2.142
B4	22.5	560.25	2.552	365.53	0.737
B4	27.5	403.32	1.932	46.49	0.099
B4	32.5	567.06	2.451	490.47	0.939
B4	37.5	551.40	2.623	123.12	0.259
B4	42.5	874.62	2.656	686.58	0.923
B5	2.5	N/A	N/A	N/A	N/A
B5	7.5	338.17	1.525	339.01	0.677
B5	12.5	852.53	1.842	772.40	0.739
B5	17.5	325.04	1.297	293.41	0.518
B6	12.5	569.22	2.784	202.87	0.439
B6	17.5	227.85	1.200	33.72	0.079
B6	22.5	192.82	0.962	39.96	0.088
B6	27.5	133.89	0.599	96.75	0.192
B6	32.5	173.27	0.843	106.28	0.229
B6	37.5	309.15	1.526	294.99	0.644
B7	2.5	689.49	1.358	20.46	0.018
B7	7.5	279.84	N/A	N/A	N/A
B7	12.5	624.12	1.135	N/A	N/A
B7	17.5	29.91	N/A	N/A	N/A
B7	22.5	48.37	3.038	N/A	N/A
B7	27.5	300.82	N/A	N/A	N/A

APPENDIX C: MINOR ELEMENTS FOR SCLEROCHRONOLOGY CANDIDATES (CONTINUED)

Baculites candidates					
Sample		**[Na] ppm**	**Na/Ca (mMol/Mol)**	**[Sr] ppm**	**Sr/Ca (mMol/Mol)**
B2	2.5	2745.51	18.127	1250.82	2.168
B2	7.5	3195.37	17.330	1814.69	2.584
B2	12.5	3280.43	16.657	2139.38	2.852
B2	17.5	2489.63	14.719	2248.10	3.490
B2	22.5	2753.32	14.313	2713.46	3.704
B2	27.5	2677.46	16.410	2143.82	3.450
B2	32.5	2803.36	14.975	2455.55	3.444
B3	2.5	3161.26	16.659	2336.08	3.232
B3	7.5	3347.26	16.425	2550.73	3.286
B3	12.5	3356.28	15.853	2458.28	3.049
B4	2.5	1789.78	18.295	1301.99	3.494
B4	7.5	3953.98	18.914	2360.86	2.965
B4	12.5	3451.79	19.717	2824.90	4.237
B4	17.5	4339.64	20.613	2089.54	2.606
B4	22.5	3984.04	19.176	3629.91	4.587
B4	27.5	4034.24	20.418	9932.54	13.199
B4	32.5	4945.77	22.590	2419.72	2.902
B4	37.5	4605.32	23.146	2106.24	2.779
B4	42.5	6871.01	22.047	2930.35	2.469
B5	2.5	N/A	N/A	N/A	N/A
B5	7.5	2386.76	11.369	4491.82	5.618
B5	12.5	5477.84	12.503	10180.48	6.101
B5	17.5	2857.64	12.050	4980.93	5.515
B6	12.5	3694.64	19.090	1809.70	2.455
B6	17.5	3643.65	20.274	1388.38	2.028
B6	22.5	3936.76	20.743	1843.46	2.550
B6	27.5	4443.74	21.020	1854.99	2.304
B6	32.5	3776.52	19.415	1856.95	2.506
B6	37.5	3968.67	20.694	1911.85	2.617
B7	2.5	9865.91	20.526	5495.74	3.002
B7	7.5	4594.97	19.693	2547.85	2.867
B7	12.5	3876.55	19.933	1946.12	2.627
B7	17.5	870.24	28.178	255.58	2.173
B7	22.5	2287.59	18.913	1297.76	2.817
B7	27.5	9865.91	21.350	5495.74	2.825

APPENDIX C: MINOR ELEMENTS FOR SCLEROCHRONOLOGY CANDIDATES (CONTINUED)

Hoploscaphites candidates				
Sample		**[Al] ppm**	**Al/Ca (mMol/Mol)**	**[Ca] ppm**
S1	2.5	267.506	1.921	207305.573
S1	7.5	221.982	0.800	413260.421
S1	12.5	463.827	1.842	374873.236
S1	17.5	181.901	0.670	404235.535
S1	32.5	1233.915	4.842	379420.193
S1	37.5	845.684	2.757	456738.989
S1	42.5	335.825	1.441	346888.808
S1	47.5	302.080	1.447	310867.078
S1	62.5	783.004	3.873	300981.475
S1	67.5	1312.810	4.583	426500.180
S2	2.5	N/A	N/A	363074.242
S2	7.5	501.274	2.114	353040.889
S2	12.5	285.278	1.234	344306.458
S2	17.5	219.309	1.132	288390.323
S2	22.5	140.032	0.560	372052.545
S2	27.5	352.531	1.426	368066.327

Sample		**[Fe] ppm**	**Fe/Ca (mMol/Mol)**	**[K] ppm**	**K/Ca (mMol/Mol)**
S1	2.5	1037.694	3.591	673.166	3.330
S1	7.5	991.069	1.720	884.817	2.196
S1	12.5	653.155	1.250	841.025	2.301
S1	17.5	526.465	0.934	1265.433	3.210
S1	32.5	1296.603	2.451	707.980	1.914
S1	37.5	1640.322	2.576	872.473	1.959
S1	42.5	701.613	1.451	731.966	2.164
S1	47.5	1241.730	2.865	859.870	2.837
S1	62.5	1420.432	3.385	773.337	2.635
S1	67.5	1473.389	2.478	1918.705	4.614
S2	2.5	373.206	0.737	534.245	1.509
S2	7.5	1310.532	2.663	613.555	1.782
S2	12.5	2192.516	4.568	473.918	1.412
S2	17.5	676.055	1.682	623.382	2.217
S2	22.5	634.111	1.223	460.938	1.271
S2	27.5	3331.153	6.492	1165.538	3.248

APPENDIX C: MINOR ELEMENTS FOR SCLEROCHRONOLOGY CANDIDATES (CONTINUED)

Hoploscaphites candidates					
Sample		**[Mg] ppm**	**Mg/Ca (mMol/Mol)**	**[Mn] ppm**	**Mn/Ca (mMol/Mol)**
S1	2.5	929.445	7.399	477.264	1.682
S1	7.5	2262.391	9.034	919.957	1.626
S1	12.5	1407.234	6.195	568.949	1.109
S1	17.5	895.423	3.655	464.788	0.840
S1	32.5	2468.561	10.736	954.553	1.838
S1	37.5	3976.392	14.367	1830.487	2.927
S1	42.5	1935.495	9.207	593.163	1.249
S1	47.5	1452.461	7.710	753.260	1.770
S1	62.5	2940.578	16.122	1473.613	3.576
S1	67.5	1995.245	7.720	1668.781	2.858
S2	2.5	747.733	3.399	333.517	0.671
S2	7.5	1382.136	6.460	1219.453	2.523
S2	12.5	3328.246	15.952	2018.030	4.281
S2	17.5	971.218	5.557	666.030	1.687
S2	22.5	801.759	3.556	489.688	0.961
S2	27.5	3972.158	17.809	2750.446	5.458
Sample		**[Na] ppm**	**Na/Ca (mMol/Mol)**	**[Sr] ppm**	**Sr/Ca (mMol/Mol)**
S1	2.5	1680.081	14.130	2097.634	4.632
S1	7.5	3447.681	14.545	4458.938	4.939
S1	12.5	2998.697	13.946	4022.630	4.912
S1	17.5	3274.164	14.122	4434.066	5.021
S1	32.5	3435.729	15.788	3551.256	4.285
S1	37.5	5545.564	21.169	4098.000	4.107
S1	42.5	2998.499	15.071	3625.386	4.784
S1	47.5	2647.014	14.846	3056.276	4.500
S1	62.5	2667.383	15.451	2545.437	3.871
S1	67.5	4227.225	17.280	3902.494	4.189
S2	2.5	2812.526	13.506	4496.015	5.669
S2	7.5	2428.104	11.991	4250.387	5.511
S2	12.5	1970.739	9.979	3389.025	4.506
S2	17.5	2199.829	13.299	3635.913	5.771
S2	22.5	2612.656	12.243	4590.141	5.648
S2	27.5	2749.112	13.022	3636.406	4.523

APPENDIX C: MINOR ELEMENTS FOR SCLEROCHRONOLOGY CANDIDATES (CONTINUED)

Eutrephoceras candidates				
Sample		**[Al] ppm**	**Al/Ca (mMol/Mol)**	**[Ca] ppm**
E2	2.5	N/A	N/A	357989.515
E2	7.5	N/A	N/A	392733.687
E2	12.5	N/A	N/A	316045.993
E2	17.5	N/A	N/A	343872.149
E2	22.5	N/A	N/A	379829.797
E2	27.5	N/A	N/A	339860.586
E2	32.5	N/A	N/A	358598.942
E2	37.5	N/A	N/A	386914.337
E2	42.5	N/A	N/A	415595.254
E2	47.5	N/A	N/A	321592.717
E2	52.5	N/A	N/A	268579.797
E2	57.5	N/A	N/A	371053.678
E2	62.5	N/A	N/A	333722.987
E2	67.5	N/A	N/A	344491.441
E2	72.5	N/A	N/A	302795.163
E2	77.5	N/A	N/A	386660.944
E2	82.5	N/A	N/A	719557.827
E2	87.5	281.205	1.999	209487.467
E2	92.5	N/A	N/A	262396.338
E2	97.5	N/A	N/A	295143.927
E2	102.5	124.799	0.710	261856.053
E2	107.5	N/A	N/A	315942.621
E2	112.5	N/A	N/A	426532.824
E2	117.5	N/A	N/A	380409.148
E2	122.5	N/A	N/A	N/A
E2	127.5	N/A	N/A	358731.534
E2	132.5	N/A	N/A	381276.879
E2	137.5	N/A	N/A	389496.894
E2	142.5	N/A	N/A	307078.777
E2	147.5	N/A	N/A	355207.188
E2	152.5	N/A	N/A	329934.782
E2	157.5	N/A	N/A	321906.769
E2	162.5	N/A	N/A	350568.683
E2	167.5	N/A	N/A	344855.345
E2	172.5	N/A	N/A	370882.865
E2	177.5	N/A	N/A	119064.165

APPENDIX C: MINOR ELEMENTS FOR SCLEROCHRONOLOGY CANDIDATES (CONTINUED)

Eutrephoceras candidates					
Sample		**[Fe] ppm**	**Fe/Ca (mMol/Mol)**	**[K] ppm**	**K/Ca (mMol/Mol)**
E2	2.5	938.191	1.880	323.853	0.928
E2	7.5	3131.102	5.719	365.827	0.955
E2	12.5	5840.093	13.256	306.323	0.994
E2	17.5	2553.503	5.327	242.078	0.722
E2	22.5	327.995	0.619	172.459	0.466
E2	27.5	368.158	0.777	765.244	2.309
E2	32.5	6239.827	12.482	66.705	0.191
E2	37.5	43.613	0.081	208.561	0.553
E2	42.5	303.957	0.525	492.421	1.215
E2	47.5	277.377	0.619	74.623	0.238
E2	52.5	218.064	0.582	80.698	0.308
E2	57.5	1126.252	2.177	696.592	1.925
E2	62.5	8376.820	18.006	330.674	1.016
E2	67.5	1781.972	3.711	92.997	0.277
E2	72.5	328.411	0.778	126.692	0.429
E2	77.5	884.107	1.640	294.667	0.782
E2	82.5	2249.656	2.243	240.859	0.343
E2	87.5	634.189	2.172	254.076	1.244
E2	92.5	351.399	0.961	438.625	1.714
E2	97.5	674.868	1.640	713.208	2.478
E2	102.5	775.879	2.126	550.986	2.158
E2	107.5	675.692	1.534	587.231	1.906
E2	112.5	766.888	1.290	2956.035	7.108
E2	117.5	1037.426	1.956	1507.606	4.064
E2	122.5	N/A	N/A	N/A	N/A
E2	127.5	122.770	0.246	714.571	2.043
E2	132.5	111.700	0.210	602.870	1.622
E2	137.5	323.470	0.596	869.781	2.290
E2	142.5	893.415	2.087	719.905	2.404
E2	147.5	536.647	1.084	665.591	1.922
E2	152.5	63.138	0.137	1001.761	3.114
E2	157.5	1080.845	2.409	687.522	2.190
E2	162.5	1450.485	2.968	943.150	2.759
E2	167.5	121.729	0.253	1431.286	4.257
E2	172.5	39.575	0.077	494.127	1.366
E2	177.5	N/A	N/A	968.986	8.346

APPENDIX C: MINOR ELEMENTS FOR SCLEROCHRONOLOGY CANDIDATES (CONTINUED)

Eutrephoceras candidates					
Sample		**[Mg] ppm**	**Mg/Ca (mMol/Mol)**	**[Mn] ppm**	**Mn/Ca (mMol/Mol)**
E2	2.5	558.708	2.575	1596.912	3.258
E2	7.5	3359.352	14.115	4139.469	7.699
E2	12.5	4393.909	22.942	4555.007	10.527
E2	17.5	1501.208	7.204	4232.184	8.990
E2	22.5	525.503	2.283	564.516	1.086
E2	27.5	529.075	2.569	564.660	1.214
E2	32.5	7783.962	35.820	3775.783	7.691
E2	37.5	90.974	0.388	171.050	0.323
E2	42.5	525.259	2.086	371.867	0.654
E2	47.5	380.864	1.954	518.794	1.178
E2	52.5	792.042	4.866	327.559	0.891
E2	57.5	2761.972	12.283	992.663	1.954
E2	62.5	9996.105	49.429	3297.253	7.217
E2	67.5	987.714	4.731	1497.412	3.175
E2	72.5	712.695	3.884	213.278	0.514
E2	77.5	1412.707	6.029	1144.864	2.163
E2	82.5	3027.117	6.942	3259.342	3.309
E2	87.5	1130.262	8.903	659.651	2.300
E2	92.5	1348.895	8.483	249.326	0.694
E2	97.5	1396.050	7.806	401.265	0.993
E2	102.5	451.286	2.844	311.868	0.870
E2	107.5	3108.621	16.237	1080.125	2.497
E2	112.5	289.345	1.119	N/A	N/A
E2	117.5	346.270	1.502	1932.354	3.710
E2	122.5	N/A	N/A	N/A	N/A
E2	127.5	126.928	0.584	34.516	0.070
E2	132.5	151.922	0.658	22.586	0.043
E2	137.5	229.721	0.973	94.090	0.176
E2	142.5	4813.707	25.868	1292.276	3.074
E2	147.5	203.056	0.943	205.688	0.423
E2	152.5	215.164	1.076	38.379	0.085
E2	157.5	167.241	0.857	398.627	0.905
E2	162.5	240.580	1.132	178.241	0.371
E2	167.5	91.297	0.437	N/A	N/A
E2	172.5	136.143	0.606	96.542	0.190
E2	177.5	1023.247	14.182	N/A	N/A

(CONTINUED)

Eutrephoceras candidates					
Sample		**[Na] ppm**	**Na/Ca (mMol/Mol)**	**[Sr] ppm**	**Sr/Ca (mMol/Mol)**
E2	2.5	3143.566	15.310	2815.277	3.600
E2	7.5	2433.356	10.802	2745.420	3.200
E2	12.5	2074.545	11.444	2159.821	3.128
E2	17.5	2337.642	11.852	2497.766	3.325
E2	22.5	3097.241	14.217	3382.274	4.076
E2	27.5	3127.369	16.043	2890.340	3.893
E2	32.5	1328.274	6.458	1727.350	2.205
E2	37.5	3673.192	16.552	3718.224	4.399
E2	42.5	4029.576	16.905	3791.570	4.176
E2	47.5	2677.898	14.518	2817.560	4.011
E2	52.5	2331.152	15.133	2297.579	3.916
E2	57.5	3101.720	14.574	3186.961	3.932
E2	62.5	891.246	4.656	854.129	1.172
E2	67.5	2635.394	13.338	2502.775	3.326
E2	72.5	2479.422	14.276	2627.486	3.972
E2	77.5	3043.543	13.724	3157.269	3.738
E2	82.5	5390.879	13.062	5796.172	3.687
E2	87.5	1792.081	14.915	1788.658	3.908
E2	92.5	2718.365	18.062	2343.992	4.089
E2	97.5	2872.468	16.968	2338.568	3.627
E2	102.5	2732.672	18.195	2296.197	4.014
E2	107.5	2539.856	14.016	2118.883	3.070
E2	112.5	6065.631	24.794	2974.800	3.193
E2	117.5	4048.767	18.556	3071.339	3.696
E2	122.5	N/A	N/A	N/A	N/A
E2	127.5	4169.405	20.264	3173.310	4.049
E2	132.5	4231.817	19.351	3415.773	4.101
E2	137.5	4656.530	20.844	3430.437	4.032
E2	142.5	2415.989	13.717	1728.667	2.577
E2	147.5	4109.150	20.169	3364.547	4.336
E2	152.5	4303.299	22.740	2895.533	4.017
E2	157.5	3467.890	18.782	2972.524	4.227
E2	162.5	4367.932	21.723	3176.304	4.148
E2	167.5	4073.746	20.596	3040.137	4.035
E2	172.5	3739.776	17.580	3621.499	4.470
E2	177.5	7042.681	103.127	863.113	3.318

APPENDIX C: MINOR ELEMENTS FOR SCLEROCHRONOLOGY CANDIDATES (CONTINUED)

Nymphalucina and *Anomia* candidates									
Sample		**[Al] ppm**		**Al/Ca (mMol/Mol)**		**[Ca] ppm**			
N1	2.5	N/A		N/A		383590.021			
N1	7.5	N/A		N/A		362891.188			
N1	12.5	N/A		N/A		398020.200			
N1	17.5	N/A		N/A		392288.327			
N1	32.5	N/A		N/A		323092.385			
A1	2.5	N/A		N/A		358872.790			
A1	7.5	N/A		N/A		384260.889			
A1	12.5	N/A		N/A		374301.768			
A1	17.5	N/A		N/A		353644.015			
A1	32.5	313.512		1.336		349475.836			
A1	37.5	N/A		N/A		373988.796			
A1	42.5	278.264		1.208		342863.817			
Sample		**[Fe] ppm**	**Fe/Ca (mMol/Mol)**	**[K] ppm**	**K/Ca (mMol/Mol)**				
N1	2.5	170.106	0.318	362.403	0.969				
N1	7.5	67.622	0.134	234.074	0.662				
N1	12.5	N/A	N/A	148.942	0.384				
N1	17.5	N/A	N/A	131.907	0.345				
N1	32.5	N/A	N/A	171.604	0.545				
A1	2.5	918.146	1.835	323.444	0.924				
A1	7.5	1451.142	2.709	209.154	0.558				
A1	12.5	829.541	1.590	241.885	0.663				
A1	17.5	709.174	1.439	156.098	0.453				
A1	32.5	3036.520	6.233	486.185	1.427				
A1	37.5	710.092	1.362	290.445	0.796				
A1	42.5	3401.292	7.116	421.545	1.261				

APPENDIX C: MINOR ELEMENTS FOR SCLEROCHRONOLOGY CANDIDATES (CONTINUED)

Nymphalucina and *Anomia* candidates					
Sample		**[Mg] ppm**	**Mg/Ca (mMol/Mol)**	**[Mn] ppm**	**Mn/Ca (mMol/Mol)**
N1	2.5	2285.270	9.831	N/A	N/A
N1	7.5	118.549	0.539	N/A	N/A
N1	12.5	121.402	0.503	N/A	N/A
N1	17.5	41.921	0.176	N/A	N/A
N1	32.5	71.621	0.366	N/A	N/A
A1	2.5	1163.814	5.352	645.626	1.314
A1	7.5	1212.179	5.206	868.040	1.650
A1	12.5	1190.934	5.251	508.333	0.992
A1	17.5	1388.580	6.480	679.623	1.404
A1	32.5	1525.369	7.203	1569.174	3.280
A1	37.5	1236.942	5.458	662.344	1.294
A1	42.5	1677.122	8.072	1378.195	2.936
Sample		**[Na] ppm**	**Na/Ca (mMol/Mol)**	**[Sr] ppm**	**Sr/Ca (mMol/Mol)**
N1	2.5	2778.774	12.630	2293.196	2.737
N1	7.5	2632.913	12.650	1591.672	2.008
N1	12.5	2977.844	13.044	1645.657	1.893
N1	17.5	2781.541	12.362	1558.266	1.818
N1	32.5	2513.402	13.563	1289.327	1.827
A1	2.5	3073.618	14.932	1344.809	1.715
A1	7.5	3051.470	13.845	1681.350	2.003
A1	12.5	2922.953	13.615	2210.529	2.703
A1	17.5	3226.778	15.908	1198.267	1.551
A1	32.5	2992.887	14.931	1227.686	1.608
A1	37.5	3358.447	15.657	1528.931	1.871
A1	42.5	2985.336	15.181	1362.495	1.819

APPENDIX C: MINOR ELEMENTS FOR SCLEROCHRONOLOGY CANDIDATES (CONTINUED)

Inoceramus candidates				
Sample		**[Al] ppm**	**Al/Ca (mMol/Mol)**	**[Ca] ppm**
I1	2.5	N/A	N/A	311233.753
I1	7.5	6.710	6.710	315723.669
I1	12.5	5.967	5.967	298556.713
I1	17.5	N/A	N/A	354651.599
I1	22.5	N/A	N/A	366202.379
I1	27.5	N/A	N/A	314031.888
I1	32.5	N/A	N/A	371512.081
I1	37.5	N/A	N/A	377823.081
I1	42.5	N/A	N/A	350025.256
I2	2.5	N/A	N/A	405596.204
I2	7.5	N/A	N/A	386228.463
I2	12.5	N/A	N/A	341148.399
I2	17.5	N/A	N/A	387708.491
I2	22.5	N/A	N/A	386007.936
I2	27.5	N/A	N/A	393150.593
I2	32.5	N/A	N/A	368654.959
I2	37.5	N/A	N/A	390735.564
I2	42.5	N/A	N/A	376613.059
I2	47.5	N/A	N/A	380720.871
I2	52.5	N/A	N/A	404350.446
I2	57.5	N/A	N/A	381163.831
I3		N/A	N/A	352842.797
I3		N/A	N/A	374635.577
I3		N/A	N/A	354491.942
I3		N/A	N/A	356544.725
I3		N/A	N/A	358457.535
I3		N/A	N/A	378183.506

APPENDIX C: MINOR ELEMENTS FOR SCLEROCHRONOLOGY CANDIDATES (CONTINUED)

Inoceramus candidates					
Sample		**[Fe] ppm**	**Fe/Ca (mMol/Mol)**	**[K] ppm**	**K/Ca (mMol/Mol)**
I1	2.5	740.784	1.707	280.234	0.923
I1	7.5	6273.967	14.255	918.821	2.985
I1	12.5	3114.574	7.483	1159.364	3.983
I1	17.5	372.069	0.753	260.439	0.753
I1	22.5	728.480	1.427	209.828	0.588
I1	37.5	1491.288	3.407	171.881	0.561
I1	32.5	1128.745	2.179	193.222	0.533
I1	37.5	481.342	0.914	306.752	0.833
I1	42.5	548.592	1.124	134.286	0.393
I2	2.5	132.397	0.234	200.077	0.506
I2	7.5	431.041	0.801	129.950	0.345
I2	12.5	N/A	N/A	169.841	0.511
I2	17.5	N/A	N/A	178.982	0.473
I2	22.5	N/A	N/A	325.233	0.864
I2	27.5	N/A	N/A	179.307	0.468
I2	32.5	24.808	0.048	188.606	0.525
I2	37.5	48.559	0.089	166.232	0.436
I2	42.5	108.046	0.206	191.277	0.521
I2	47.5	86.389	0.163	229.989	0.620
I2	52.5	N/A	N/A	122.324	0.310
I2	57.5	2366.774	4.454	253.962	0.683
I3	2.5	17.547	0.036	168.466	0.490
I3	7.5	341.205	0.653	194.376	0.532
I3	12.5	193.455	0.391	523.458	1.514
I3	17.5	1465.781	2.949	170.131	0.489
I3	22.5	485.473	0.972	215.001	0.615
I3	27.5	692.303	1.313	223.124	0.605
I1	2.5	740.784	1.707	280.234	0.923

APPENDIX C: MINOR ELEMENTS FOR SCLEROCHRONOLOGY CANDIDATES (CONTINUED)

Inoceramus candidates					
Sample		**[Mg] ppm**	**Mg/Ca (mMol/Mol)**	**[Mn] ppm**	**Mn/Ca (mMol/Mol)**
I1	2.5	452.468	2.399	367.301	0.862
I1	7.5	3102.098	16.214	2778.576	6.428
I1	12.5	902.069	4.986	410.499	1.004
I1	17.5	124.178	0.578	133.729	0.275
I1	22.5	441.142	1.988	65.877	0.131
I1	37.5	401.973	2.112	258.259	0.601
I1	32.5	81.242	0.361	154.267	0.303
I1	37.5	99.908	0.436	N/A	N/A
I1	42.5	62.324	0.294	N/A	N/A
I2	2.5	373.383	1.519	68.772	0.124
I2	7.5	300.494	1.284	N/A	N/A
I2	12.5	204.998	0.992	N/A	N/A
I2	17.5	183.920	0.783	N/A	N/A
I2	22.5	224.038	0.958	N/A	N/A
I2	27.5	153.988	0.646	N/A	N/A
I2	32.5	192.483	0.862	6.257	0.012
I2	37.5	188.492	0.796	N/A	N/A
I2	42.5	283.073	1.240	40.911	0.079
I2	47.5	272.151	1.180	4.696	0.009
I2	52.5	221.544	0.904	N/A	N/A
I2	57.5	524.688	2.272	9.651	0.018
I3	2.5	636.499	2.977	162.376	0.336
I3	7.5	389.245	1.715	506.590	0.988
I3	12.5	241.137	1.123	290.843	0.599
I3	17.5	680.197	3.148	2131.878	4.367
I3	22.5	1239.602	5.707	498.207	1.015
I3	27.5	3348.280	14.610	1256.739	2.427
I1	2.5	636.499	2.399	162.376	0.862

APPENDIX C: MINOR ELEMENTS FOR SCLEROCHRONOLOGY CANDIDATES (CONTINUED)

Inoceramus candidates					
Sample		**[Na] ppm**	**Na/Ca (mMol/Mol)**	**[Sr] ppm**	**Sr/Ca (mMol/Mol)**
I1	2.5	3494.366	19.575	1685.724	2.479
I1	7.5	3106.635	17.155	1816.394	2.634
I1	12.5	3924.016	22.915	1787.118	2.740
I1	17.5	4065.831	19.988	1933.915	2.496
I1	22.5	4246.498	20.217	2114.187	2.643
I1	37.5	3499.893	19.431	1632.272	2.379
I1	32.5	4059.590	19.051	2098.192	2.585
I1	37.5	4337.164	20.014	2058.813	2.494
I1	42.5	3785.824	18.857	2102.860	2.750
I2	2.5	4558.486	19.595	1987.458	2.243
I2	7.5	4213.404	19.020	2010.075	2.382
I2	12.5	3960.495	20.241	1660.538	2.228
I2	17.5	4316.053	19.409	1951.055	2.304
I2	22.5	4343.952	19.620	1939.585	2.300
I2	27.5	4546.847	20.164	1959.102	2.281
I2	32.5	4472.340	21.151	1786.193	2.218
I2	37.5	4511.545	20.131	2049.885	2.402
I2	42.5	4440.401	20.556	1794.189	2.181
I2	47.5	4283.955	19.618	1830.258	2.201
I2	52.5	4288.871	18.493	1887.894	2.137
I2	57.5	4317.318	19.748	1713.865	2.058
I3	2.5	3907.010	19.305	2010.343	2.608
I3	7.5	4882.861	22.724	2139.548	2.614
I3	12.5	4029.178	19.816	2077.490	2.683
I3	17.5	3586.001	17.535	1907.647	2.449
I3	22.5	3842.407	18.689	2011.537	2.569
I3	27.5	3803.934	17.537	1818.348	2.201

APPENDIX D: STABLE ISOTOPE SCLEROCHRONOLOGY

Sample		del-13-C	del-18-O
I2	L05	5.23	-5.32
I2	L10	5.72	-5.87
I2	L15	5.54	-5.55
I2	L20	5.89	-5.59
I2	L25	N/A	N/A
I2	R05	5.63	-5.35
I2	R10	5.96	-5.77
I2	R15	6.10	-5.66
I2	R20	6.02	-5.72
I2	R25	4.52	-3.62
I2	MTX	N/A	N/A
I2	0	5.47	-5.44
I2	2.5	4.59	-7.02
I2	5	3.72	-7.19
I2	7.5	4.17	-3.83
I2	10	5.72	-5.43
I2	12.5	5.25	-6.55
I2	15	5.96	-5.73
I2	17.5	5.94	-5.81
I2	20	5.54	-5.14
I2	22.5	5.76	-5.82
I2	25	5.83	-5.60
I2	27.5	5.94	-5.73
I2	30	5.89	-5.65
I2	32.5	6.10	-5.66
I2	35	5.40	-5.23
I2	37.5	5.95	-5.52
I2	40	3.95	-4.18
I2	42.5	5.61	-5.57
I2	45	5.92	-5.63
I2	47.5	5.84	-2.21
I2	50	5.15	-5.07
I2	52.5	6.00	-5.77
I2	55	6.07	-5.55
I2	57.5	5.45	-5.53
I2	60	5.64	-5.58

Sample		del-13-C	del-18-O
B7	L2.5	-3.40	-1.44
B7	L5.0	N/A	N/A
B7	L7.5	-2.68	-1.06
B7	L10.0	-3.08	-1.54
B7	L12.5	-2.51	-1.07
B7	R2.5	-2.98	-1.35
B7	R5.0	N/A	N/A
B7	R7.5	-3.17	-1.54
B7	R10.0	-5.61	-3.47
B7	R12.5	-5.50	-1.72
B7	MTX	-23.65	-2.10
B7	0	-11.8716	-1.44463
B7	2.5	-2.95515	-1.05585
B7	5	-2.80042	-0.96956
B7	7.5	-2.67933	-1.12274
B7	10	-5.47786	-1.40391
B7	12.5	-2.78312	-1.16152
B7	15	-3.74223	-1.29338
B7	17.5	-2.91671	-1.13923
B7	20	-2.81291	-1.25169
B7	22.5	-3.11564	-1.43784
B7	25	-3.52696	-1.84117

Sample		del-13-C	del-18-O
E2	L05	N/A	N/A
E2	L10	1.26	-0.34
E2	L25	0.33	-0.48
E2	L30	0.03	-0.78
E2	R05	0.74	-0.81
E2	R10	0.59	-0.66
E2	R15	0.40	-0.60
E2	R20	-0.66	-1.37
E2	R25	-0.20	-0.76
E2	MTX	-22.15	-1.69
E2	CEM1	-14.97	-4.03
E2	CEM2	N/A	N/A
E2	CEM3	0.18	-1.18

Sample		del-13-C	del-18-O
E2	0	-2.34	-1.99
E2	5	-1.57	-1.29
E2	10	-1.24	-1.43
E2	15	-1.38	-1.47
E2	20	-1.04	-0.99
E2	25	-0.93	-1.21
E2	30	-0.89	-0.84
E2	35	0.70	-0.81
E2	40	-2.28	-2.46
E2	45	-0.48	-0.90
E2	50	N/A	N/A
E2	55	-4.41	-3.78
E2	60	-0.83	-1.03
E2	65	N/A	N/A
E2	70	0.12	-1.08
E2	75	-1.79	-2.16
E2	80	-0.59	-1.02
E2	85	-1.28	-1.12
E2	90	0.43	-0.57
E2	95	-0.15	-0.93
E2	95	-0.15	-0.93
E2	100	N/A	N/A
E2	105	-3.24	-1.39
E2	110	N/A	N/A
E2	115	0.31	-0.71
E2	120	N/A	N/A
E2	125	-1.96	-0.72
E2	130	N/A	N/A
E2	135	0.17	-0.79
E2	140	N/A	N/A
E2	145	0.16	-0.81
E2	150	N/A	N/A
E2	155	0.59	-0.84
E2	160	0.51	-0.58
E2	165	0.89	-0.42
E2	170	-13.47	-3.29
E2	175	0.01	-1.15